Testrapporter

Bilaga 2

Elforsk rapport 14:58

Pia Borg

Oktober 2014

Innehåll

1 Inledning

Dokumentet innehåller samtliga testrapporter som har ingått i projektet Test och utvärdering av energilager, Elforsk rapport 32146. Testmetodiken i de genomförda testen har sitt ursprung i *Rational Unified Process* (RUP).

PRACTICAL GRID BENEFITS OF BATTERY ENERGY STORAGE SYSTEM IN FALKÖPING DISTRIBUTION GRID

Carlos MARTINEZ, ABB – Estonia, carlos.nieto@ee.abb.com
Erik HANSEN, ABB – Denmark, erik.hansen@dk.abb.com
Tomas TENGNER, ABB – Sweden, tomas.tengner@se.abb.com
Willy HERMANSON, ABB - Sweden, willy.hermansson@se.abb.com
Jimmy EHNBERG, FEAB – Sweden, Jimmy.Ehnberg@poyry.com

ABSTRACT

This paper describes the research that has been conducted as a part of a real project commissioned by Falbygdens Energi in the Falköping distribution network consisting of a battery energy storage system. The main overall project set-up, main components and their relation to the performance of the system as well as the control system have been analysed. Practical measurements and the impact of the system in the grid have been studied and analysed.

I. INTRODUCTION

In the coming years, energy storage is becoming a key component of smart grids, since the power landscape has shifted towards greater use of renewable energy in the form of wind and solar. These installations generate power only intermittently and with a highly variable output. Excess power generated, when the wind is blowing or the sun is shining, should be stored and made available during suboptimal generating conditions or during peak demand [1]-[5]. This requires the storage of energy at appropriate time and locations, both to balance generation with consumption and to maintain grid stability [3].

The 15th of December 2011 the first pilot installation of a Battery Energy Storage System (BESS) in a Swedish distribution system commissioned by Falbygdens Energi was energized in the city of Falköping. A BESS (see Fig. 1) is a packaged solution of power equipment such as coupling transformer and sensing transformer, medium and low voltage switchgear together with automation equipment such as inverters in a complete segregated enclosure. The energy is stored in batteries for use at a later time or to effectively optimize cost. This solution can store electrical energy and supply it to the loads as a primary or supplementary source [2]. It provides a stable and continuous power supply regardless of the supply source status and voltage. Moreover, generation smoothing and transient support for renewable energies are feasible with this solution [1], [5].

In Fig. 1 a typical BESS enclosure is shown. This design provides quick, simple installation and/or relocation, with a high level of safety for the equipment as well as for operators or people around it in case of an internal fault.

The main applications for this BESS installation are load shifting, peak shaving, power factor correction and harmonic mitigation [1]. Regarding the load shifting capability, the pattern of energy use can be shifted from high day time load to low night time load [2]. With the elimination of short term peaks in the energy consumption pattern achieved by the peak shaving, the customer's power fee can be reduced. With the overcapacity in the converter, the reactive power compensation and the harmonic mitigation features of the BESS, the capacity of the distribution substation transformer can be increased and the losses in the transformer and in the medium voltage (MV) grid can be reduced. These practical grid benefits of the BESS in the Falköping distribution grid, with a significant portion of wind power, are presented in section III.

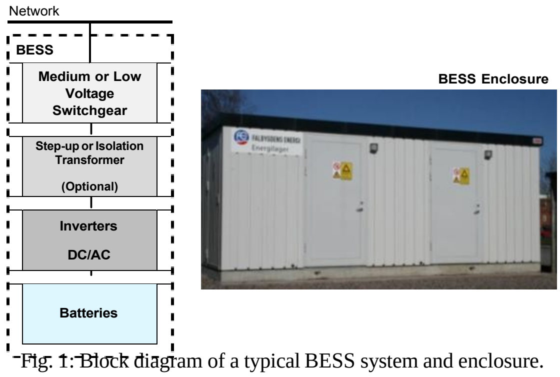

Fig. 1: Block diagram of a typical BESS system and enclosure.

II. PROJECT SET-UP

The BESS is designed to output 75 kW of power for 1 hour, during the discharging period, for its entire lifetime (10 years for the battery system). Charging of the batteries is scheduled during the night while the discharging is planned during the high-consumption periods, when it will be necessary. The BESS will perform one such cycle per day.

The BESS pilot installation also supports the grid on the low voltage side of the distribution substation (20 / 0,4 kV) (see Fig. 2), by regulating of the reactive power and improve the power quality, by the filtration of the desired higher harmonics of current. These functions are provided constantly during the normal operation conditions of the system regardless the state of charge (SOC) of the batteries. In this case, the BESS solution will operate as an active filter for the grid.

The specifications for the BESS in the Falköping distribution grid are summarized in Table I and the single-line diagram is shown in Fig. 2.

TABLE I. SPECIFICATIONS OF THE BESS SYSTEM

Parameter	Value
Maximum Stored Energy	75kWh
Maximum charging/discharging rate per hour (1C)	75kW
Maximum capacity of the converter	100kVA
Voltage (via 110 kVA 400/230 V coupling transformer)	400V
Battery life span	10 years

A) System components

Having a look to the single-line diagram of the BESS shown in Fig. 2, some components can be distinguished in addition to the existing compact secondary substation (CSS) and the control system, which will be explained later.

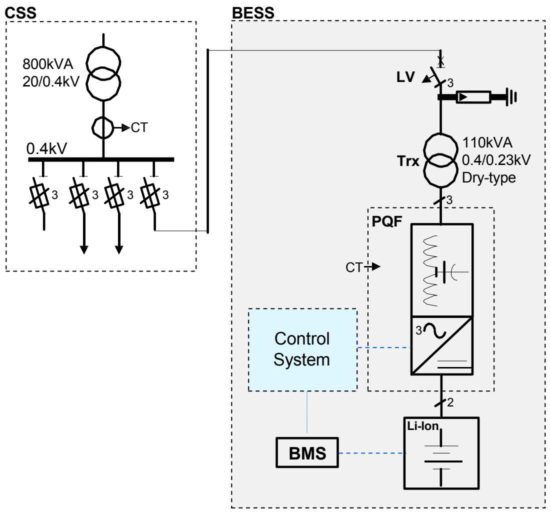

Fig. 2: Single-line diagram of the BESS.

Low voltage distribution and control switchboard:

The low voltage distribution and control switchboard (see LV in Fig. 2) include incoming AC circuit breaker, BESS station local control system's components and other protection and control equipment needed for the operation of the facility.

Coupling transformer:

In order to connect the required battery system to the 400 VAC grid, a 110kVA dry-type coupling transformer (see Trx in Fig. 2) has been used, due to the low voltage present in the battery array.

Power electronic bi-directional converter:

The bi-directional power electronic converter (see PQF in Fig. 2) is one of the main components of the BESS. It acts as a rectifier during the charging of the batteries and as an inverter during the supplying of the energy from the batteries to the grid.

For this application, the selected converter is the PQFI - V1- M25 - IP21 from the ABB [6] manufacturer.

The internal control, with a closed loop strategy, is able to generate for each harmonic frequency a compensation current in perfect phase opposition to the polluting current taking into account the high frequency rejection filter which is included in this solution. The current transformers (CTs) are installed on the incoming busbars of the LV Switchboard inside the existing CSS (CT in Fig. 2) in order to monitor the power flow on the grid.

Battery Management System (BMS):

The BMS performs the measurement necessary to manage the batteries (voltage, temperature, current) in order to extend the battery life and increase the safety of the system.

Batteries:

The batteries have been selected according to the power and energy requirements. The LiFePO4 battery array has a nominal voltage of 547Vdc (428 Vdc – 616 Vdc), 80.5kW nominal power and 85kWh nominal energy. The deviation in the nominal power from 75kW is to compensate the losses inside the converter and the coupling transformer and the degradation in the batteries during their lifetime.

Enclosure:

A "Walk-In" type outdoor enclosure with thermally insulated walls, made from sheet steel, and a climate control inside the station to keep the temperature under operation limits have been developed.

B) Control system

The BESS station presents a local control system that is able to initiate charging/discharging process according to the time-based algorithm programmed within the station controller. The control system architecture is presented in Fig. 3.

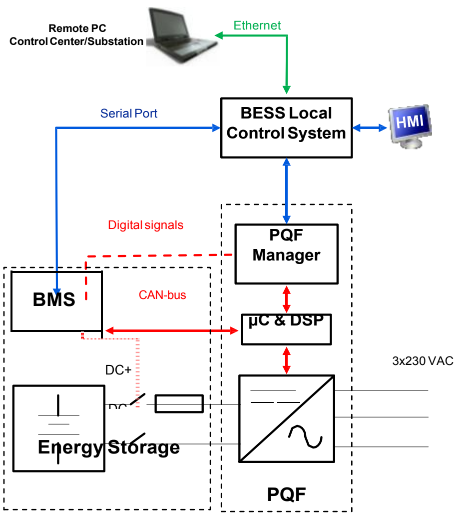

Fig. 3: BESS station control system.

In Fig. 3, the local control system is connected to the PQF manager control and to the BMS. These two connections are intended to operate the converter based on the time-based algorithm taking into account all the information received from the PQF converter performance and the battery status through the BMS.

As it can be observed, there is a communication between the local control system and a remote PC, so the BESS can be operated locally or remotely. Also a human machine interface (HMI) is included in the control architecture, so in that case the operating values can be set locally and the system status can be visualized.

The control system logs events, such as change in operational mode, commands sent to the PQF converter, received commands, faults, and shutdowns. Also, time based performance data are logged in a time-stamped format, including: power converter real power and reactive power flow, AC voltages and currents, battery state of charge, battery voltages and currents, temperatures and internal control variables.

All data logs are stored locally and can be retrieved locally or remotely via a standard computer port. With the Ethernet communication, the BESS control system is able to transmit all the performance parameters to the control and monitoring centre with a defined frequency.

The local control system presents two possibilities regarding the control strategy: automatic control, in which a simple algorithm, based on the time of the day, has been implemented; and the manual control, which allows the manual control of the charging/discharging process of the system.

Automatic control:

- **Discharging mode:** The BESS control system will initiate the discharging process at the predefined time of the day if the batteries SOC is more than some predefined value (for example 20 %), by sending the signal to the PQF Manager to start the discharging of the batteries with the predefined level of an active power (75kW) for the predefined period of time (1 hour).

During the active power discharging mode the BESS supports the grid by reactive power compensation (up to 66kVAr) and by filtering some of the higher order current harmonics. After the total discharge of the batteries (this information is sent from the PQF Manager to the BESS control system), the system switches into another mode ("Battery stand-by mode").

- **Battery stand-by mode:** The system operates in this mode during the time of the day between the discharging and the charging modes with all the available capacity of the converter used for the reactive power compensation (up to 100kVAr) and higher order current harmonics filtration. During this mode there is not needed any activity from the BESS local control system related to the active power dispatch.

- **Charging mode:** The BESS local control system initiates the charging process at the predefined time of the day if the batteries SOC is not higher than some predefined value (for example 99.5 %), by sending the signal to the PQF Manager to start the charging of the batteries with the predefined level of an active power (25kW) for the predefined period of time (3 hours).

During this mode the system is compensating reactive power with a capacity up to 96kVAr. When the battery system is fully charged the BESS control system initiates the ("Battery stand-by mode") again.

Manual control:

The BESS system allows the manual control of the charging/discharging process of the system. The manual/automatic switch in the HMI panel is used for this purpose. It is possible to stop the initiated process (charging- or discharging) and start it again later.

III. PRACTICAL GRID BENEFITS

Due to the inclusion of a BESS in a distribution grid, some benefits may be achieved in terms of energy quality (power factor correction and harmonic mitigation) and transformer losses.

In Fig. 4 the loading of the distribution transformer in the Falköping grid during one typical day is shown considering two scenarios (taking into account the control strategy mentioned before): when the system is operating with and without energy storage system.

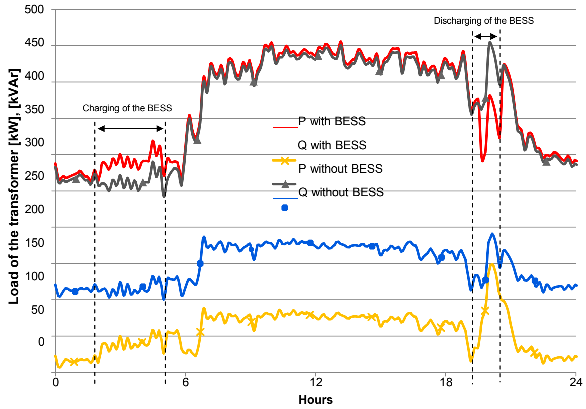

Fig. 4: Loading of the transformer for load shifting operation.

The first benefit that can be observed is the load shifting that the BESS is able to provide. The difference in the active power (around 5kW) is caused of the power consumption of the BESS, due to the losses in the inverter, filter, coupling transformer and the cooling system, in order to provide and benefit the grid with reactive power compensation and harmonic mitigation.

The transformer is affected in terms of losses and harmonic content by the operation of the BESS solution. The transformer losses are given by the load term and the no load term losses, as expressed in equation (1), where x is the utilization factor which has been defined in (2).

$$P_{losses} = x^2 P_{load\ losses} + P_{noload\ losses} \qquad (1)$$

$$x = \frac{\sqrt{P^2 + Q^2}}{S_n} \qquad (2)$$

Under nominal conditions, 800kVA, the load losses are 6.5kW and the no load losses are 1kW. With these values, the losses estimation can be obtained using expressions (1) and (2) for the data contained in Fig. 4. Fig. 5 shows the losses with and without BESS solution, as well as the achieved losses reduction.

It is important to remark that attending to (1) only copper losses (load losses) are affected by the BESS operation due to the charge/discharge of the batteries and the harmonic filtering and current balancing provided by the system. In this study the core losses (no load losses) term is constant, but in fact, the core losses are reduced as well, since the voltage harmonic distortion is related directly with the current distortion by means of the network impedance.

Regarding the achieved load shifting, it can be concluded that the distribution transformer operates in better conditions during this time due to the losses reduction and harmonic mitigation. During the charging of the batteries it can be observed a slightly increase in the transformer losses. This is caused by the increase of power due to the battery charging and the BESS losses mentioned before.

With the load shifting, the maximum power peak can be eliminated. Therefore, the transformer does not need to be oversized. In the present study it is obvious that this is not the case, due to the fact that the peak power is in the order of magnitude of the power at normal load, but it is important to remark that this BESS is a pilot installation and so, it is a small unit in the grid.

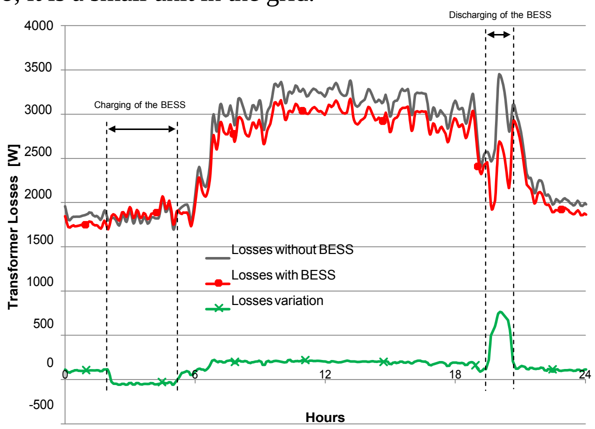

Fig. 5: Transformer losses with and without BESS solution and variation in the transformer losses for load shifting operation.

At the moment, the BESS solution is only working as load shifting and with the control algorithm described before, but the peak shaving operation can be also achieved by means of a different charging/discharging algorithm.

Fig. 6 shows the operation of the BESS under a peak shaving algorithm taking into account a round trip battery energy efficiency of 92% and average BESS losses of 5kW. The algorithm has been established in order to obtain the flatter power profile as possible in the transformer.

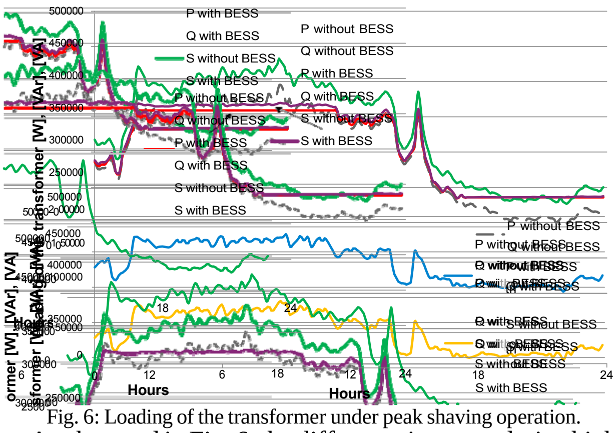

Fig. 6: Loading of the transformer under peak shaving operation.

As observed in Fig. 6, the difference in power during high load and low load has been reduced. With this achievement the power profile is flatter and so, the consumer's power fee would not be penalized. The transformer losses reduction is not the aim of the peak shaving operation, but as it can be observed in Fig. 7, they are slightly reduced.

It is important to notice that, for both control algorithms, the overall system efficiency has been reduced with the BESS solution due to the losses in the equipment (this is a small unit and so a bigger one would provide better efficiency). With this solution, the transformer is benefited with a reduction in losses and harmonic content. These two achievements are related with the transformer heating and therefore the life span; overloaded transformer or with high harmonic content can reach unacceptable levels in the temperatures of the windings, insulation, oil, etc.

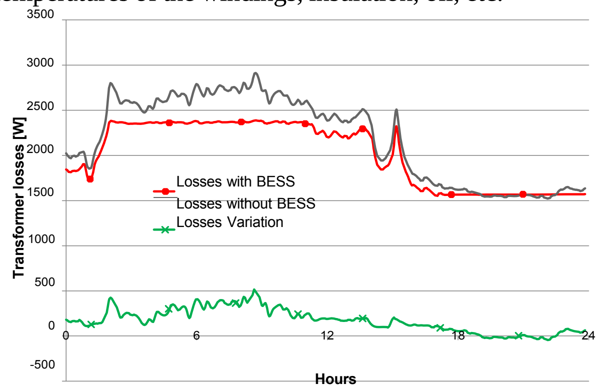

Fig. 7: Transformer losses for the peak shaving operation.

CONCLUSIONS

In this paper a BESS solution has been presented and tested in a real distribution grid. All the main components as well as the control system have been also presented. The main grid benefits achieved with the energy storage system can be summarized in the load shifting with high reduction in transformer losses when the batteries are discharging.

The peak shaving operation has been presented through an estimation taking into account a new algorithm focused on this purpose. With this operation the transformer losses and the consumer's power fee are not penalised.

Although the system overall efficiency has been penalised, the BESS solution provides a more stable voltage available for the end users of the grid, and benefits for the transformer in terms of life span.

REFERENCES

[1] TANG, S., YANG, H., ZHAO, R., GENG, X. "Influence of battery storage system on steady state stability of power system". Proceedings of Int. Conference on Electrical Machines and Systems, 2009, pp.1-4.

[2] OUDALOV, A., CHERKAOUI, R., BEGUIN, A. "Sizing and Optimal Operation of Battery Energy storage system for Peak Shaving Application". Proceedings of the IEEE Power Tech, 2007, pp. 621-625.

[3] SVENSSON, J., JONES, P., HALVARSSON, P. "Improved Power System Stability and Reliability using Innovative Energy storage Technologies". Proceedings of the 8th Int. Conf. on AC and DC Power Transmission, 2006, pp. 220-224.

[4] ROSENFELD, P.. "Battery energy storage optimizes integration of renewable energy to the grid". Proceedings of Int. Conf. CONCAPAN XXXI, 2011.

[5] ZENG, J. et al. "Use of BESS to Improve the Power Quality and Stability of Wind Farms". Proceedings of Int. Conf. on Power System Technology, 2006, pp.1-6.

[6] ABB Energy Storage Modules. [on line].< http://abblibrary.abb.com/global/scot/scot235.nsf/veritydisplay/f09413974e2f041cc12579e3004fa562/$file/energy_storage_modules_brochure_rev_e.pdf> [Consulted: December, 12, 2012].

Practical Grid Benefits of Battery Energy Storage System in Falköping Distribution Grid

Carlos MARTINEZ, Erik HANSEN, Tomas TENGNER, Willy HERMANSON, Jimmy EHNBERG

Outline

CUSTOMER NEEDS

ABB's SOLUTION

PRACTICAL GRID BENEFITS

CONCLUSIONS

Outline

CUSTOMER NEEDS

ABB's SOLUTION

PRACTICAL GRID BENEFITS

CONCLUSIONS

CUSTOMER NEEDS
Background

FALBYGDENS ENERGI

Falköping distribution grid

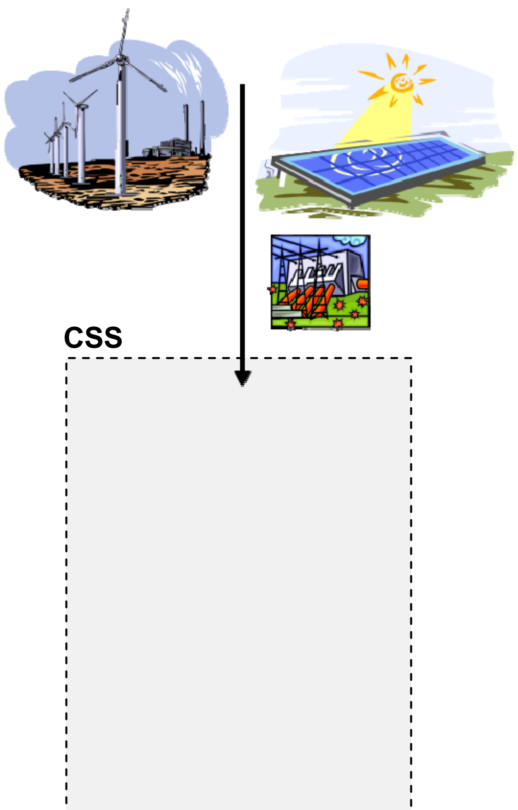

- Distribution grid with **high portion of renewable energy**

CUSTOMER NEEDS
Background

FALBYGDENS ENERGI

Falköping distribution grid

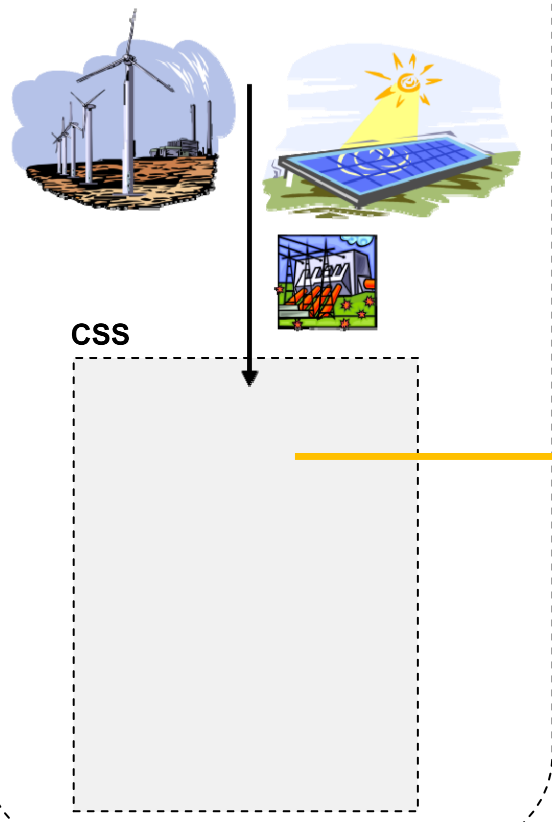

- Distribution grid with **high portion of renewable energy**
- **Uneven transformer load profile** with high demand in the evening
- **Power factor below 0.93**

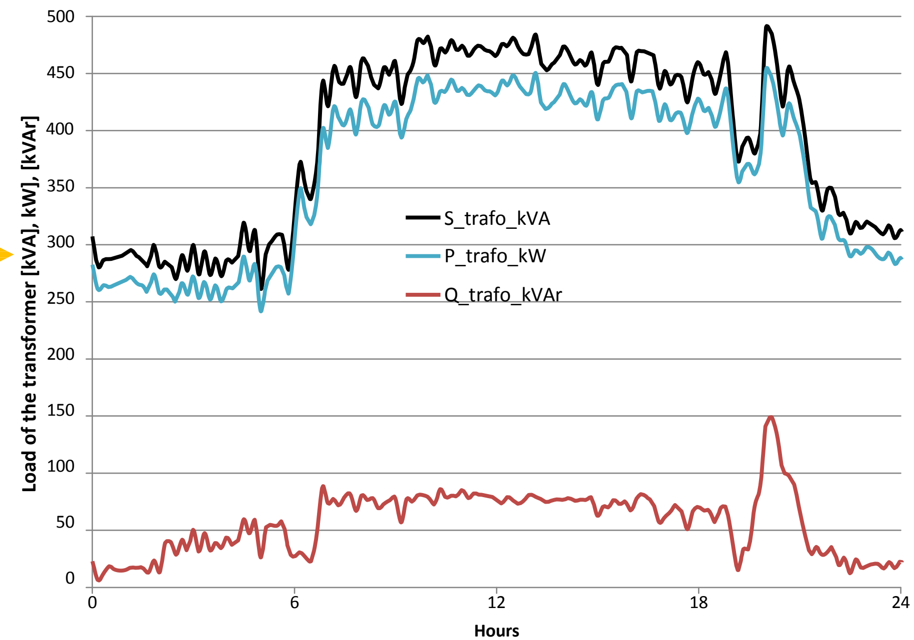

CUSTOMER NEEDS
Requirements

FALBYGDENS ENERGI

Falköping distribution grid

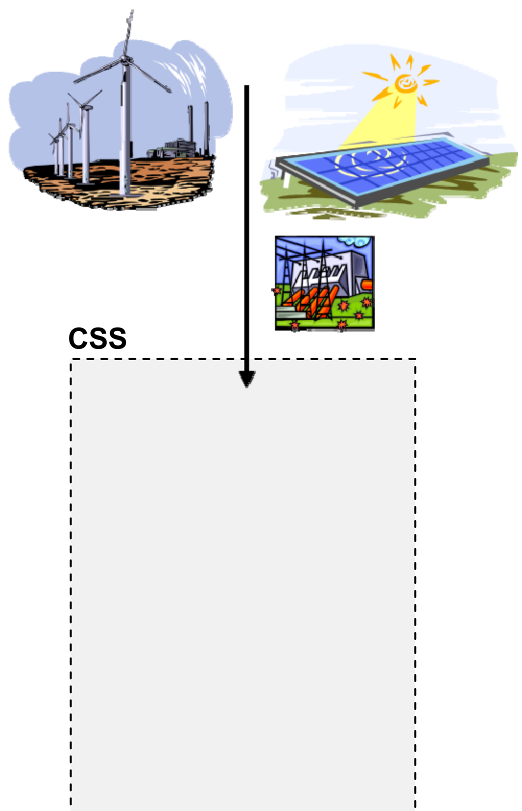

- **Peak shaving** => reduction in the customer's power fee
- **Load shifthing** => trafo's load shifted from high to low energy demand
- **Power factor correction**
- **Harmonic mitigation**

=> trafo's capacity may be increased

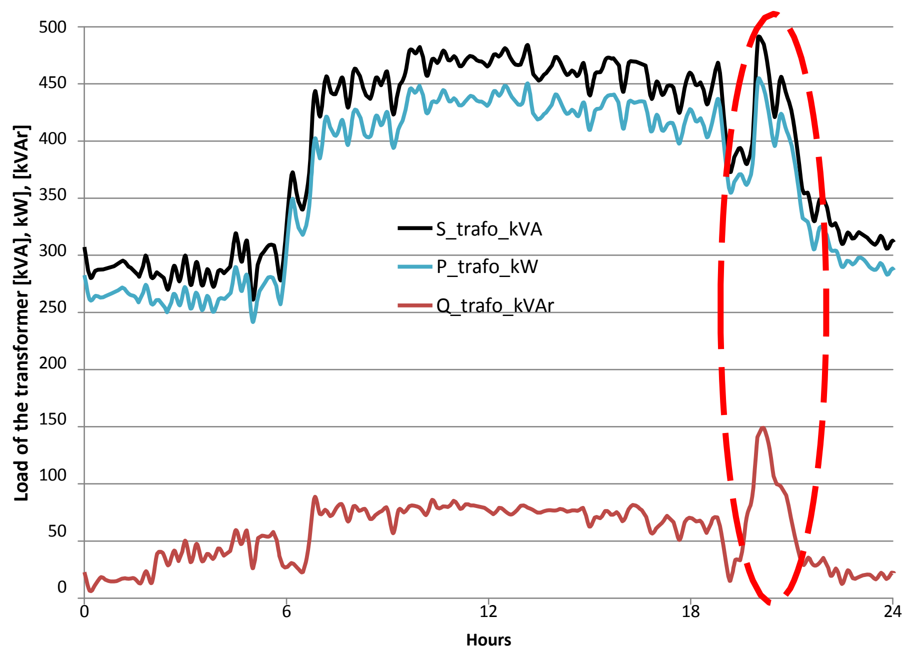

Outline

CUSTOMER NEEDS

ABB's SOLUTION

PRACTICAL GRID BENEFITS

CONCLUSIONS

ABB's solution
Battery Energy Storage System (BESS)

FALBYGDENS ENERGI

Falköping distribution grid

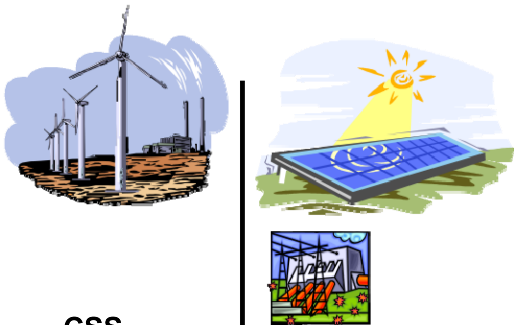

CSS

BESS

BESS

Medium or Low Voltage Switchgear

Step-up or Isolation Transformer

(Optional)

Inverters

DC/AC

Batteries

Segregated enclosure

ABB's solution
Battery Energy Storage System (BESS)

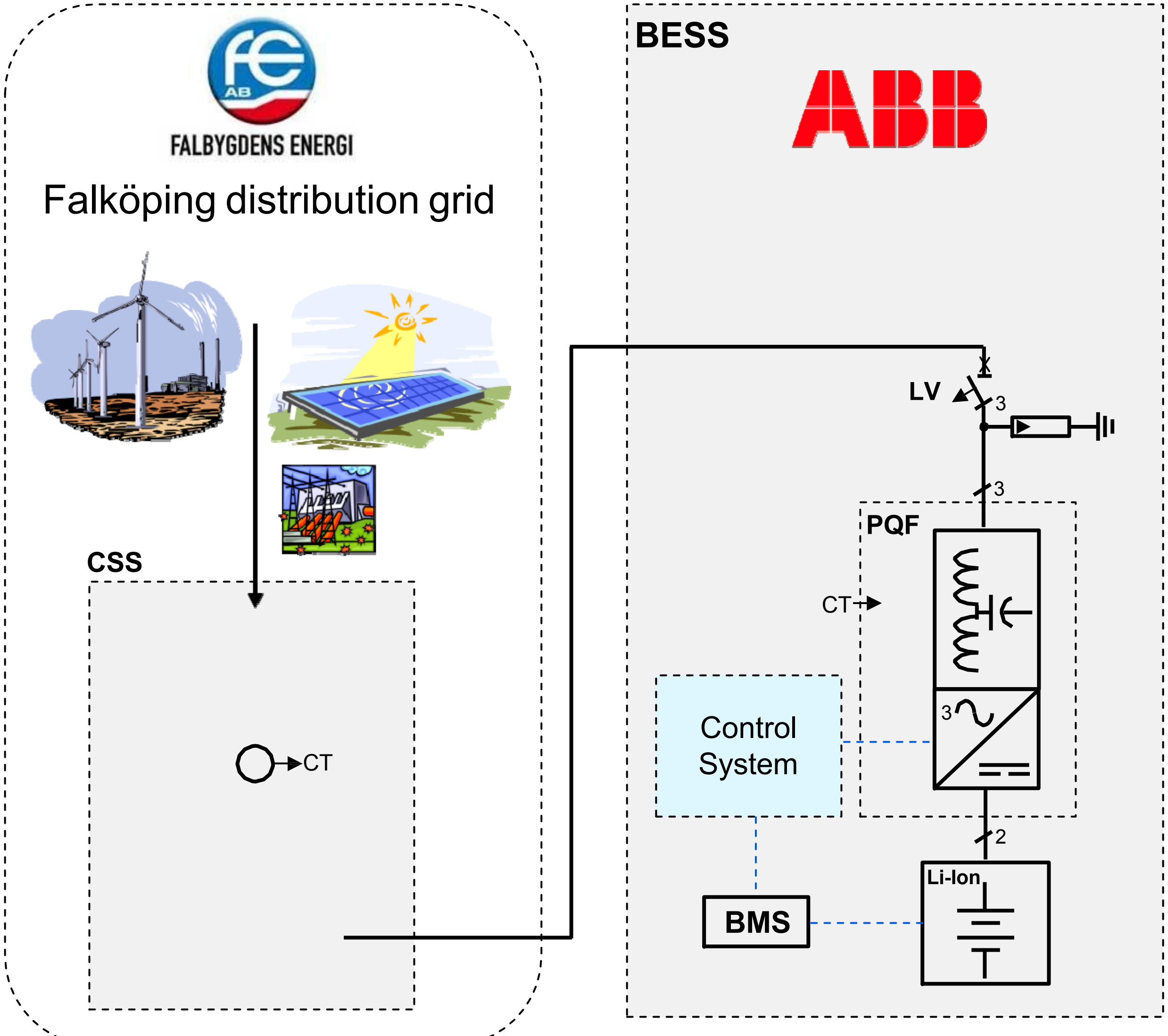

Specifications for the BESS

Parameter	Value
Maximum Stored Energy	75kWh
Maximum charging/discharging rate per hour (1C)	75kW
Maximum capacity of the converter	100kVA
Connection voltage	400V
Battery life span	10 years

ABB's solution
BESS' System Components

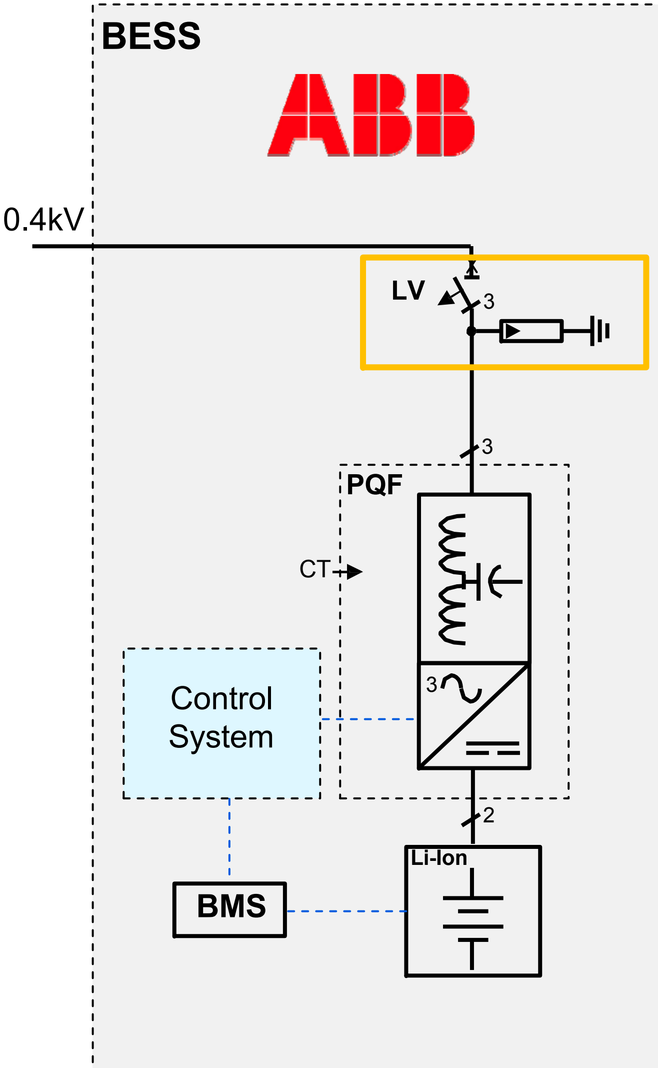

- **LV distribution and control switchboard.**

  AC breaker, Station local control system, protection and control

ABB's solution
BESS' System Components

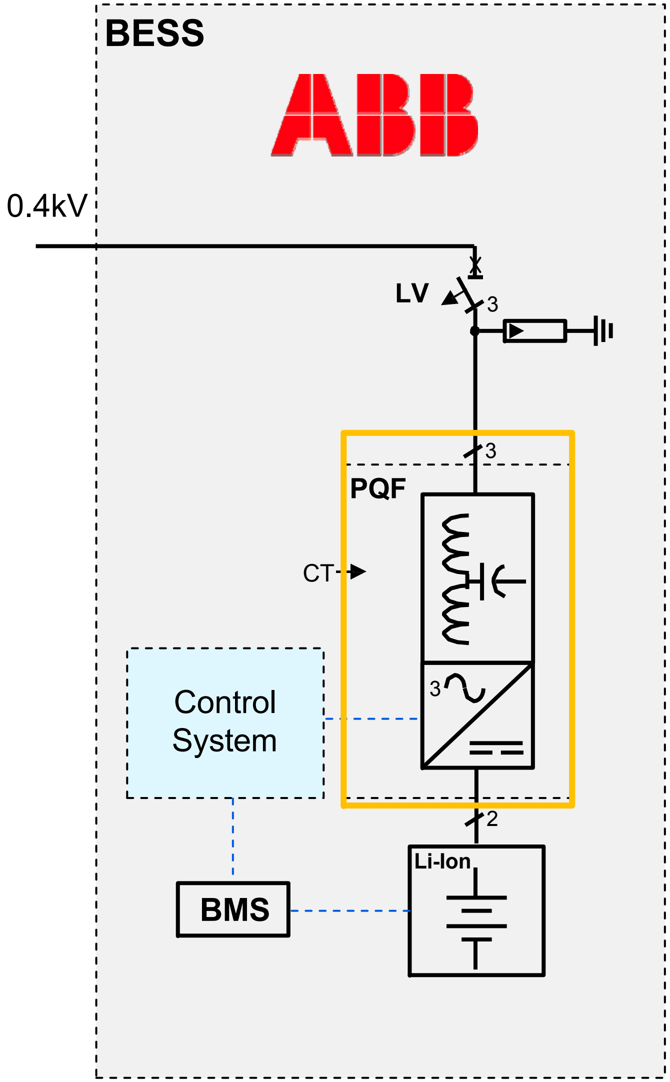

- **LV distribution and control switchboard.**

  AC breaker, Station local control system, protection and control
- **Power electronic bi-directional converter**
  - ABB's PQFI-I-V1-M25
  - Rectifier (charging) and inverter (discharging)
  - Closed loop strategy for harmonic compensation => CTs

ABB's solution
BESS' System Components

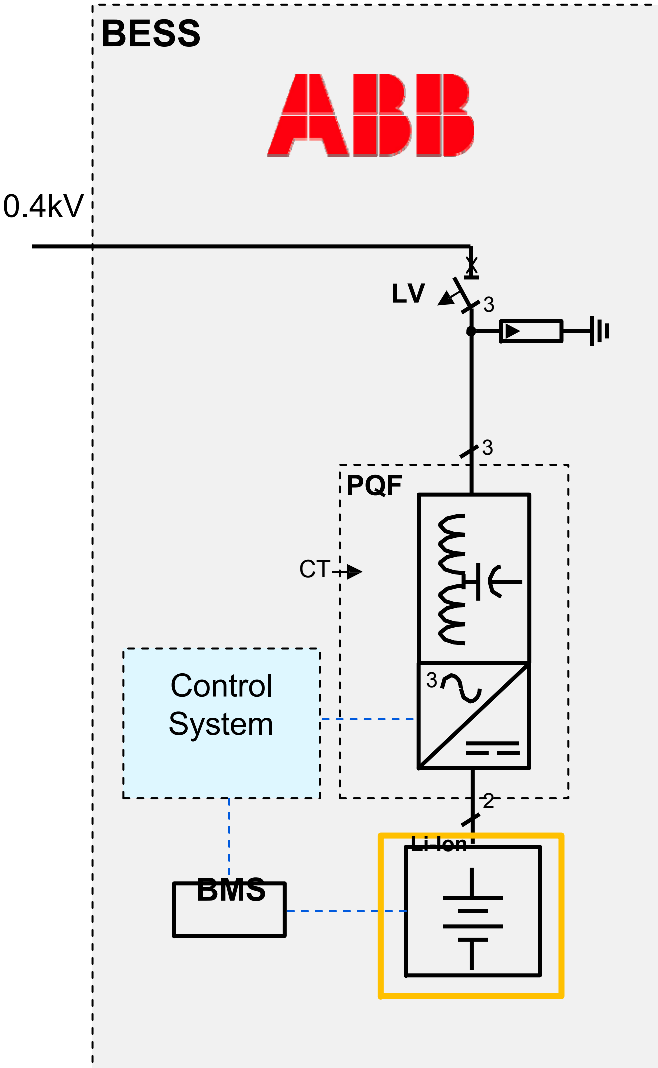

- **LV distribution and control switchboard.**
  AC breaker, Station local control system, protection and control
- **Power electronic bi-directional converter**
  - ABB's PQFI-I-V1-M25
  - Rectifier (charging) and inverter (discharging)
  - Closed loop strategy for harmonic compensation
- **Batteries (LG Chem)**
  - 3 Racks LG Chem R800 with LiFePO4 chemistry

Specifications for 3 R800 Racks

Parameter	Value
Maximum Stored Energy	135kWh
Maximum charging/discharging rate per hour (1C)	135kW
Voltage span	588V-826V
Round trip efficiency	>94%
Battery life span	10 years

ABB's solution
BESS' System Components

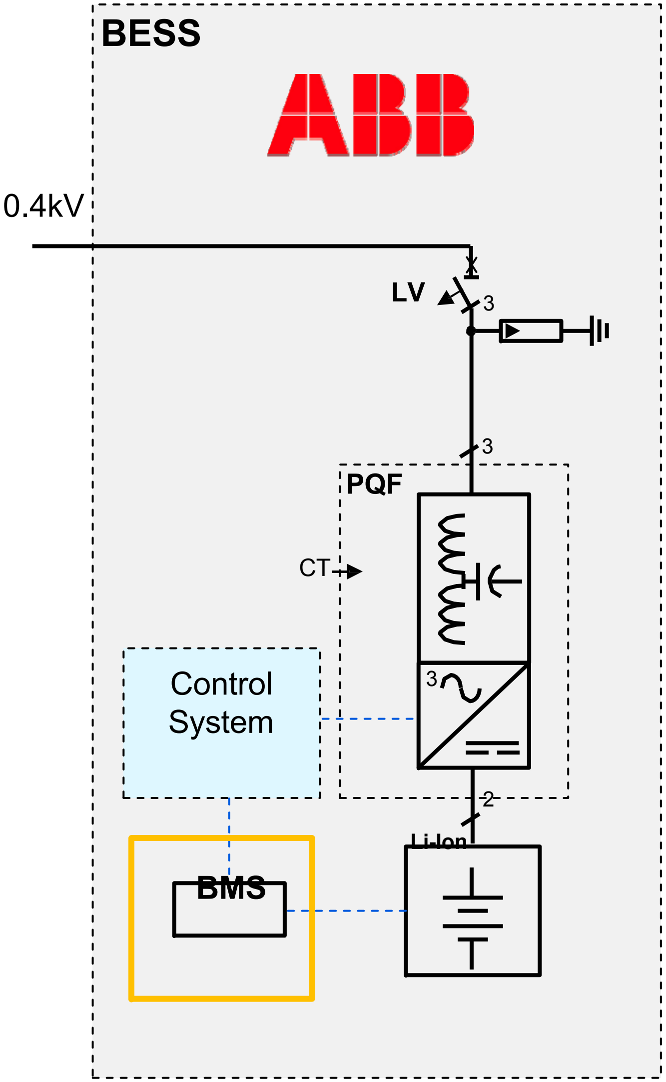

- **LV distribution and control switchboard.**

  AC breaker, Station local control system, protection and control

- **Power electronic bi-directional converter**
  - ABB's PQFI-I-V1-M25
  - Rectifier (charging) and inverter (discharging)
  - Closed loop strategy for harmonic compensation
- **Batteries (LG Chem)**
  - 3 Racks LG Chem R800 with LiFePO4 chemistry
- **Battery Management System (BMS) (LG Chem)**
  - Manages the batteries by monitoring, reporting data, balancing modules and protection

ABB's solution
BESS' System Components

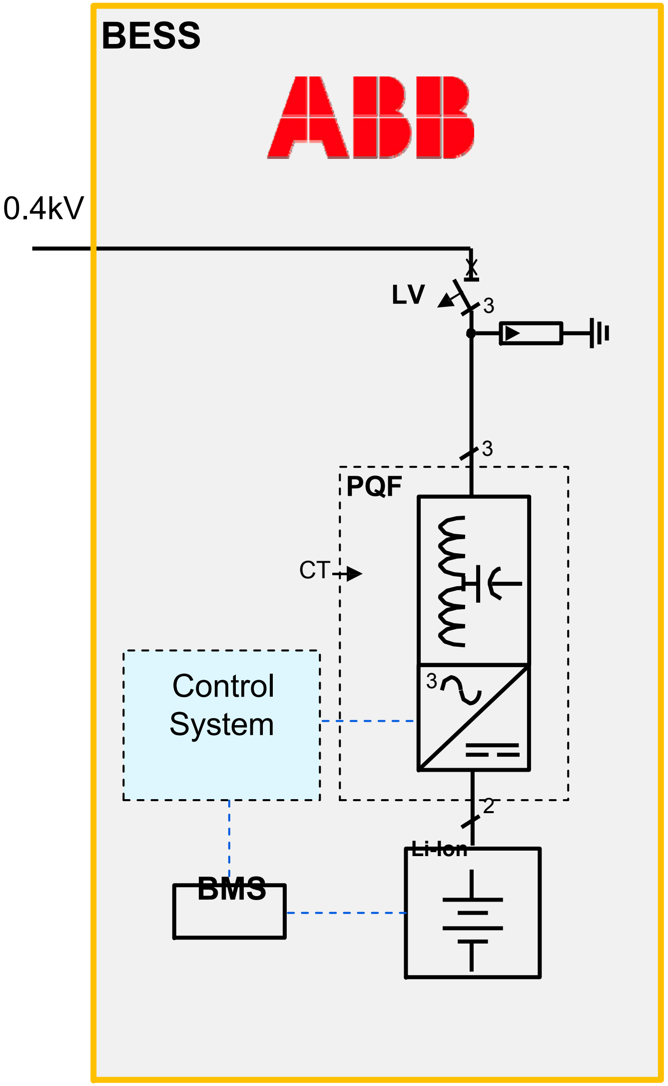

- **LV distribution and control switchboard.**

  AC breaker, Station local control system, protection and control

- **Power electronic bi-directional converter**
  - ABB's PQFI-I-V1-M25
  - Rectifier (charging) and inverter (discharging)
  - Closed loop strategy for harmonic compensation
- **Batteries (LG Chem)**
  - 3 Racks LG Chem R800 with LiFePO4 chemistry
- **Battery Management System (BMS) (LG Chem)**
  - Manages the batteries by monitoring, reporting data, balancing modules and protection
- **Enclosure**

  "Walk-in" with thermal insulted steel walls provided with climate control

ABB's solution
BESS' System Components

Battery Room

Inverter Room

ABB's solution
BESS' Control System

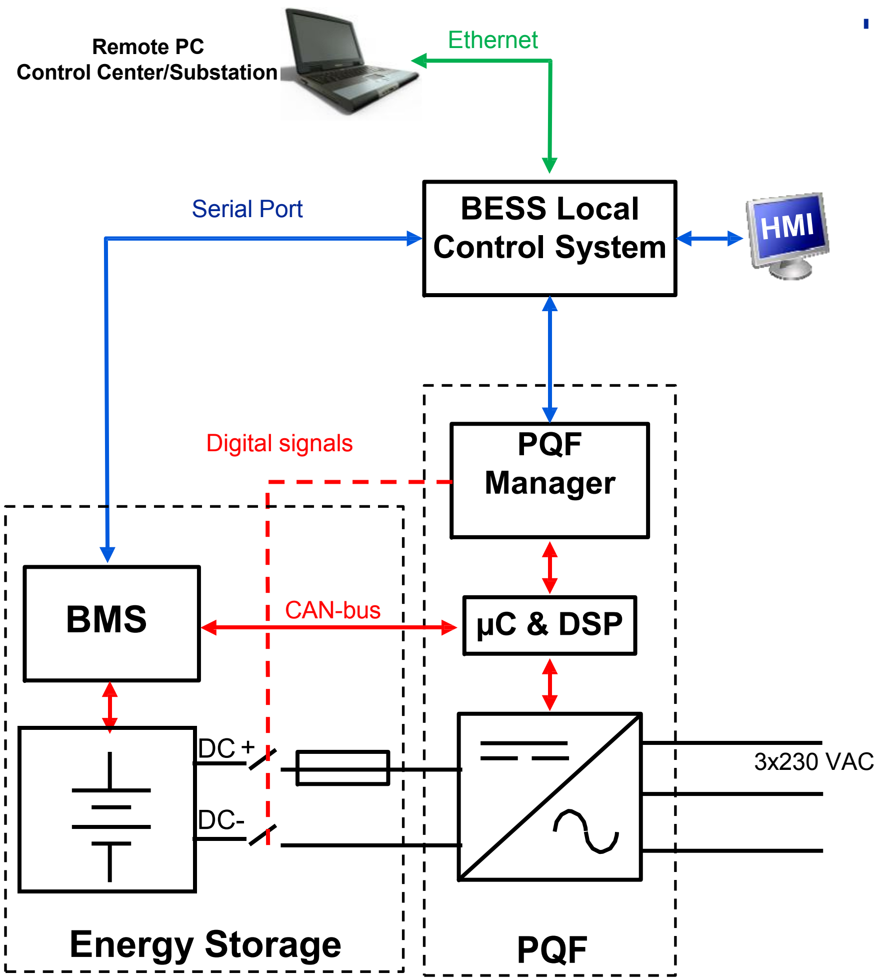

- **Main Features**
  - Initiates charging/discharging according to a time-based algorithm
  - Receives data from PQF and the BMS
  - Local and remote operation:
    - HMI located inside the enclosure
    - Remote PC located in control center (Ethernet)
  - Data logging (locally stored):
    - Time-stamped data from PQF and BMS
    - Faults
    - Shutdowns
    - Sent and received commands
  - Data can be retrieved locally or remotely
  - Two control modes available:
    - Automatic
    - Manual

ABB's solution
BESS' Control System

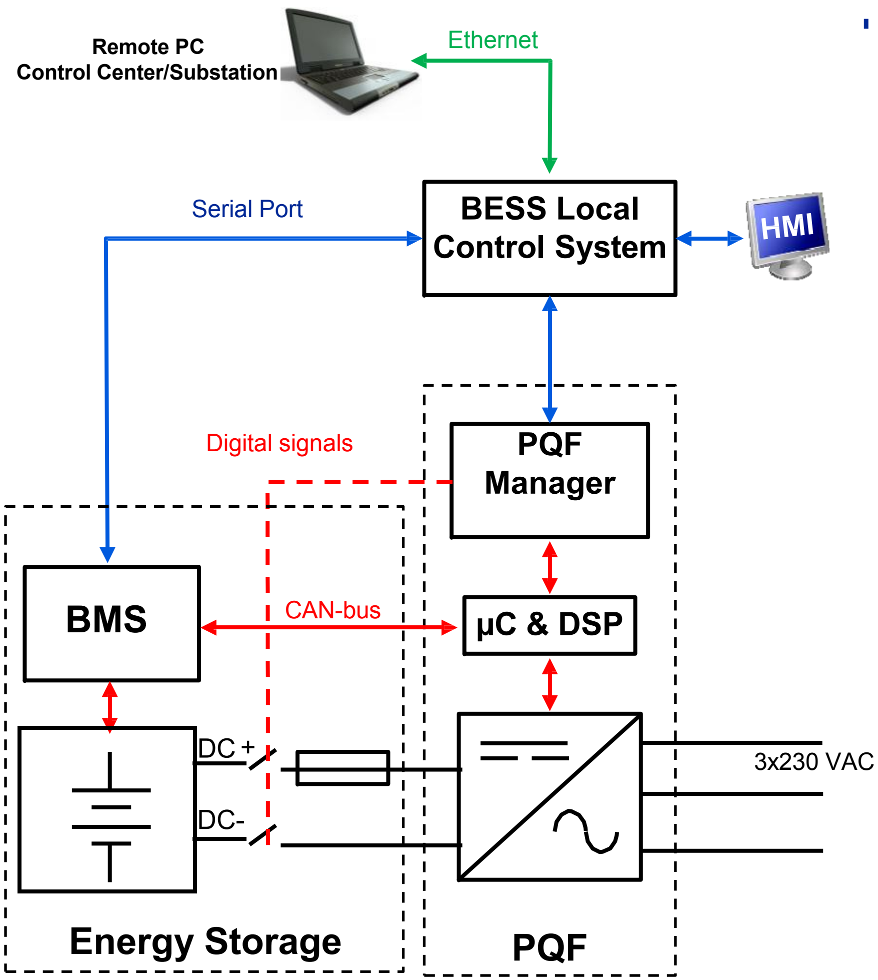

Main Features

- Initiates charging/discharging according to a time-based algorithm
- Receives data from PQF and the BMS
- Local and remote operation:
  - HMI located inside the enclosure
  - Remote PC located in control center (Ethernet)
- Data logging (locally stored):
  - Time-stamped data from PQF and BMS
  - Faults
  - Shutdowns
  - Sent and received commands
- Data can be retrieved locally or remotely
- **Two control modes available:**
  - **Automatic**
  - **Manual**

ABB's solution
BESS' Control System

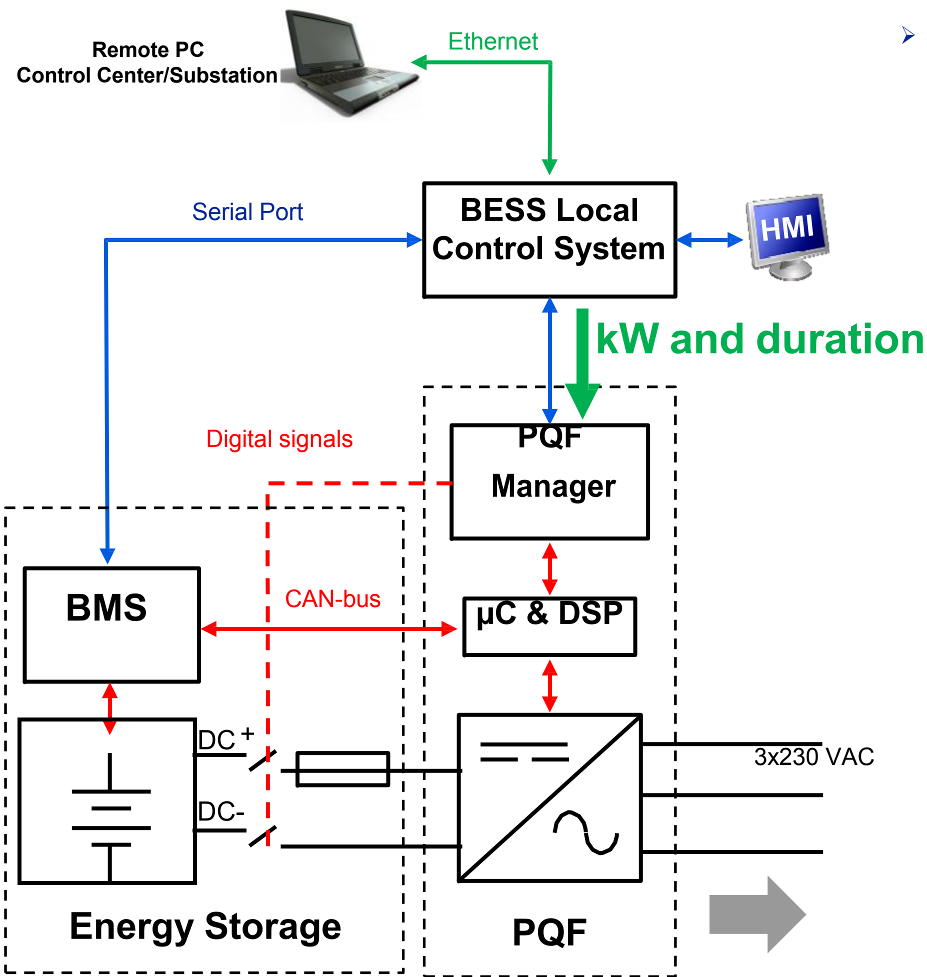

- **Automatic Control (BESS local control)**
  - **Discharging Mode @ predefined time:**
    - **Power and duration of discharge sent to the PQF manager (80kW – 1 hour)**
    - **Depth of discharge 60% (15%SOC – 75%SOC)**

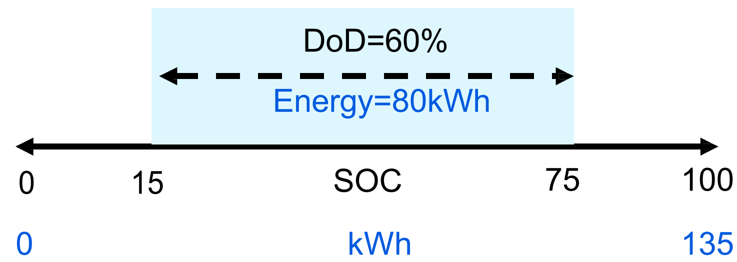

ABB's solution
BESS' Control System

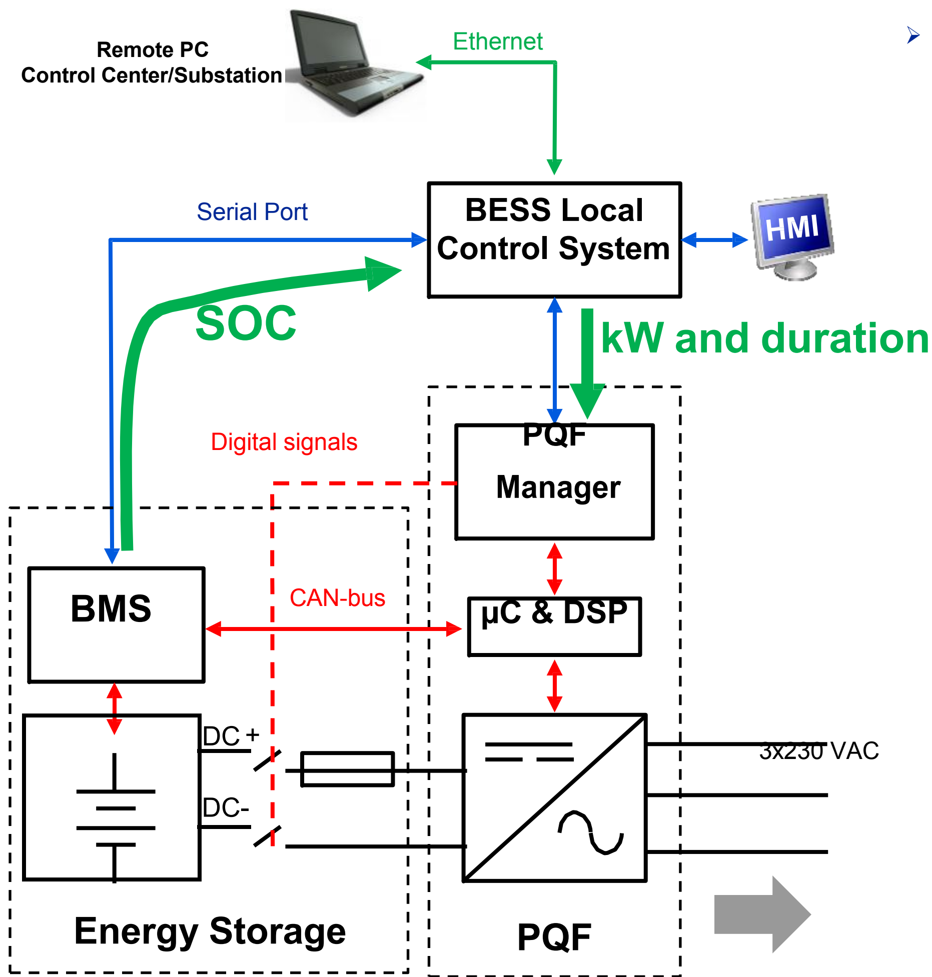

- **Automatic Control (BESS local control)**
  - **Discharging Mode @ predefined time:**
    - **Power and duration of discharge sent to the PQF manager (80kW – 1 hour)**
    - **Depth of discharge 60% (15%SOC – 75%SOC)**

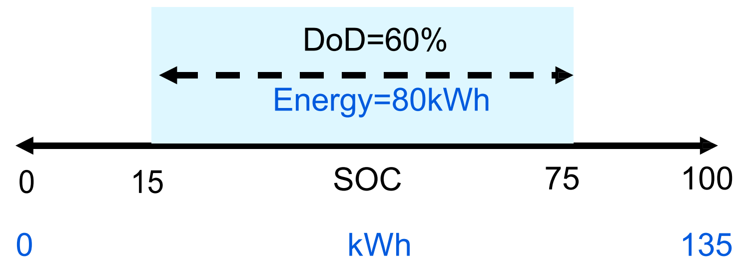

  - **SOC>5%? => Protection purposes**
    - **Below 5% the discharge current is limited by the BMS**
  - **In the case the estimated SOC by the system differs from the real one at the end of the cycle, the control system compensates the deviation with a maximum power up to 5kW.**

ABB's solution
BESS' Control System

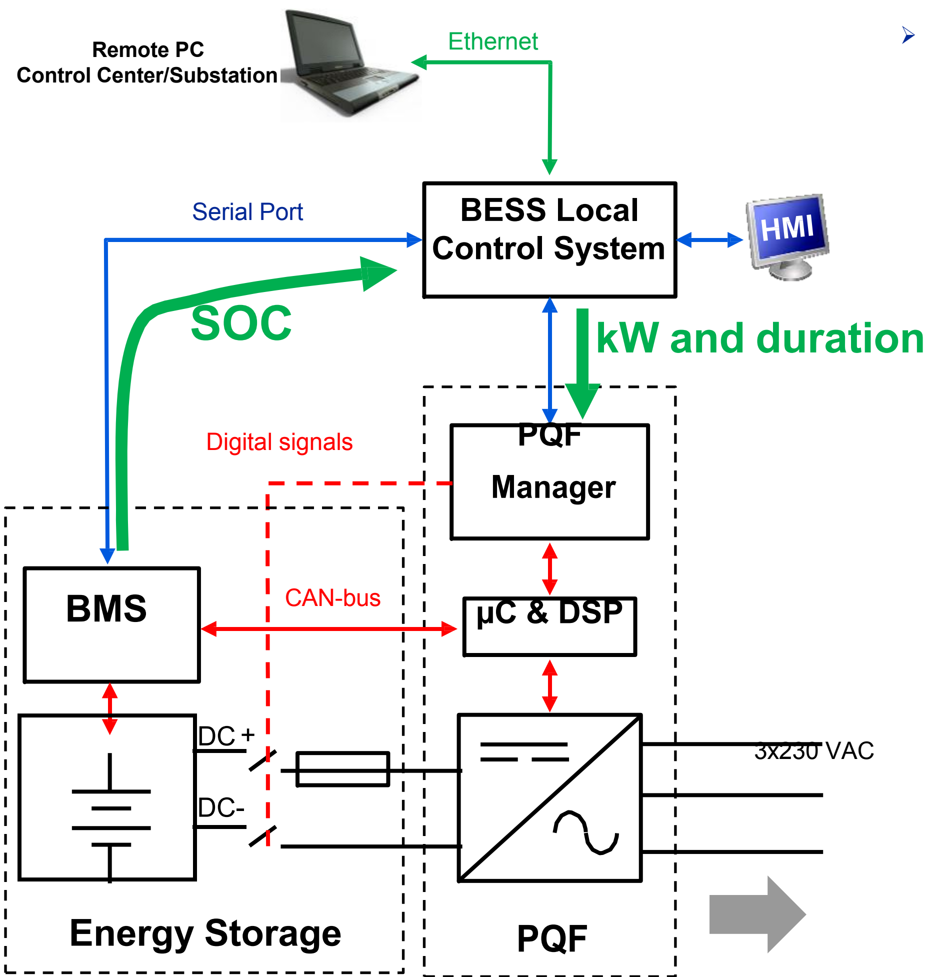

- **Automatic Control (BESS local control)**
  - **Discharging Mode @ predefined time:**
    - **Power and duration of discharge sent to the PQF manager (80kW – 1 hour)**
    - **Depth of discharge 60% (15%SOC – 75%SOC)**

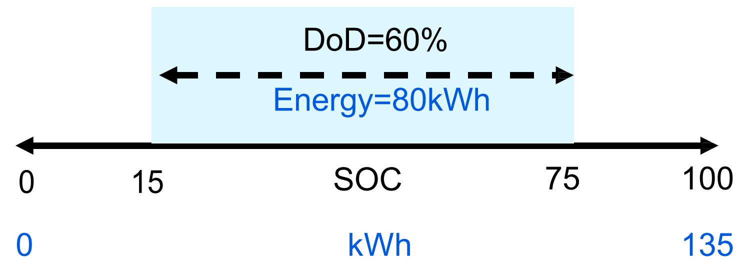

- **SOC>5%? => Protection purposes**
  - **Below 5% the discharge current is limited by the BMS**
- **In the case the estimated SOC by the system differs from the real one at the end of the cycle the control system compensates the deviation with a maximum power of 5kW.**
- **Supporting the grid with up to 66kVar and filtering harmonics**
- **When batteries discharged => stand-by mode**

ABB's solution
BESS' Control System

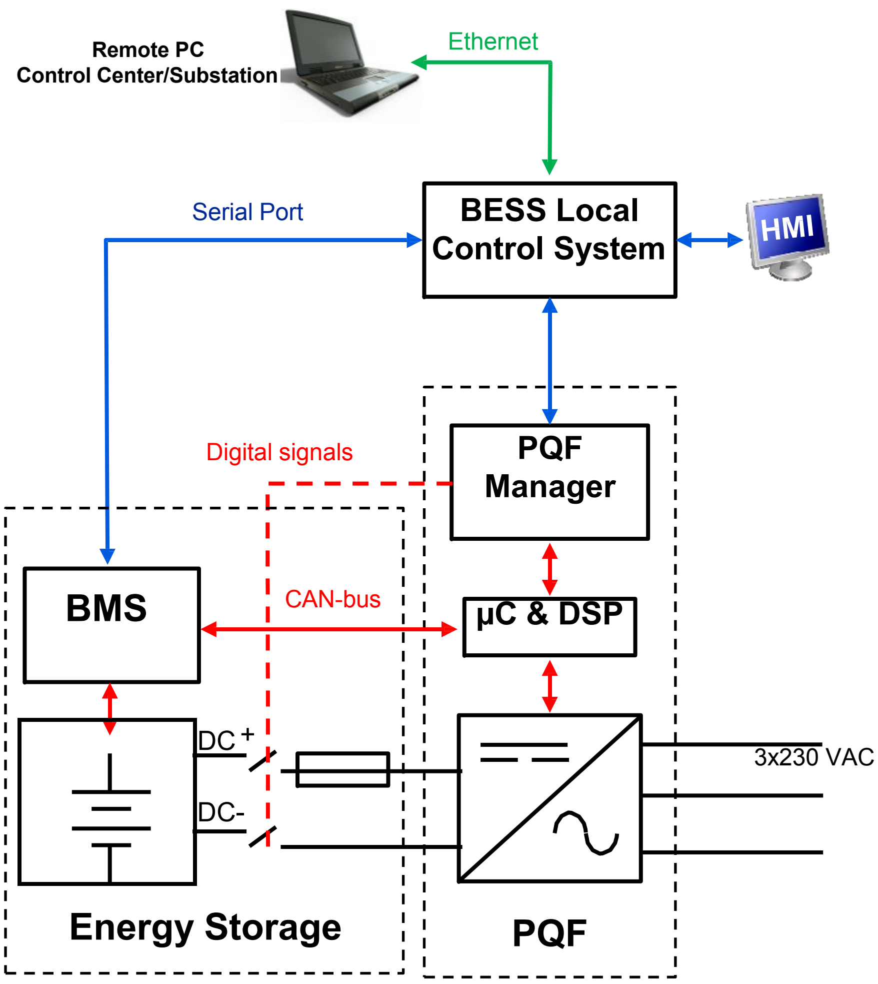

- **Automatic Control (BESS local control)**
  - **Discharging Mode @ predefined time:**
  - **Stand-by Mode:**
    - **Supporting the grid with up to 100kVar and filtering harmonics**
    - **No further actions form the local control system**

ABB's solution
BESS' Control System

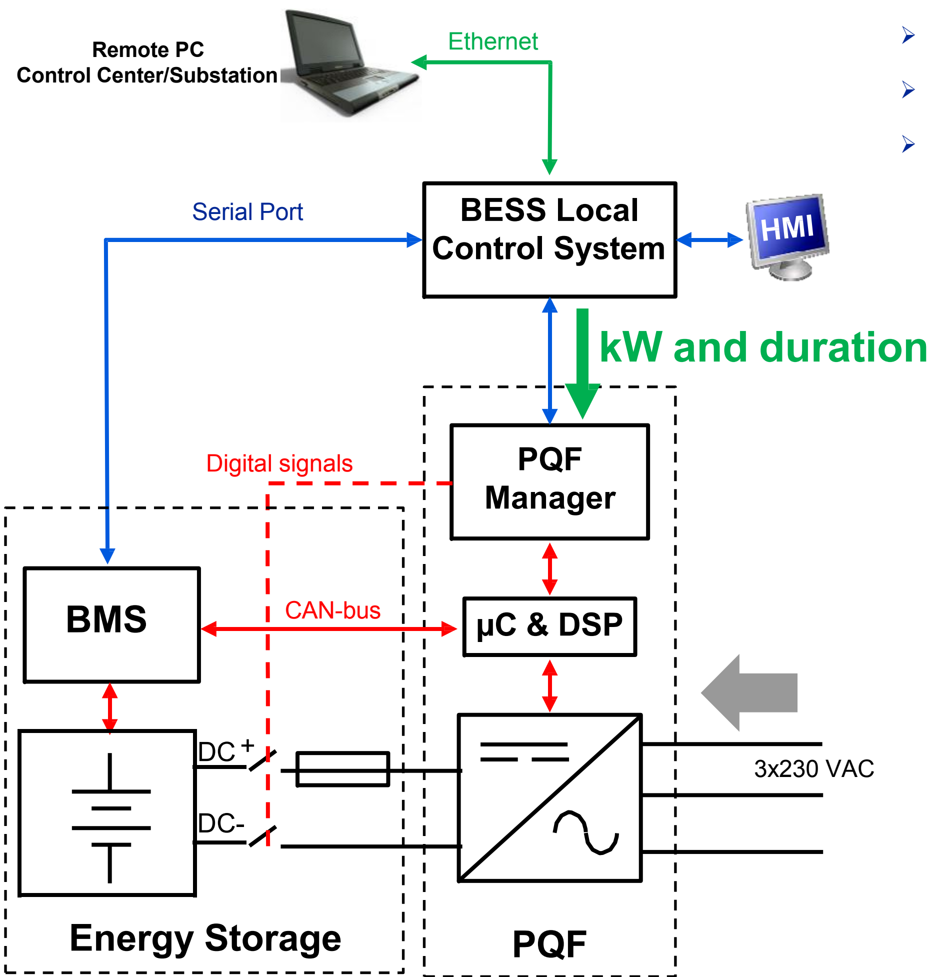

- **Automatic Control (BESS local control)**
  - **Discharging Mode @ predefined time:**
  - **Stand-by Mode:**
  - **Charging Mode @ predefined time:**
    - **Power and duration of charge sent to the PQF manager (40kW – 2 hour and 8 minutes).**
    - **8 more minutes needed to compensate losses in the batteries**
    - **Charging from 15%SOC till 75%SOC**

ABB's solution
BESS' Control System

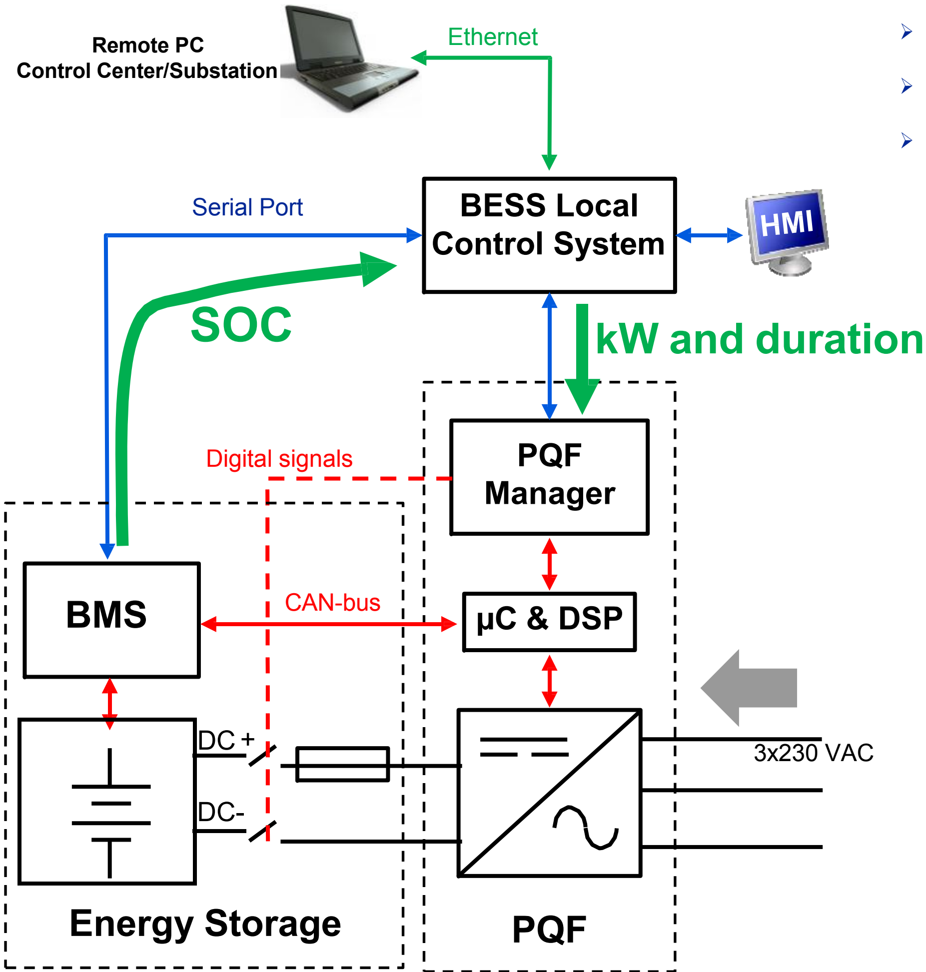

- **Automatic Control (BESS local control)**
  - **Discharging Mode @ predefined time:**
  - **Stand-by Mode:**
  - **Charging Mode @ predefined time:**
    - **Power and duration of charge sent to the PQF manager (40kW – 2 hour and 8 minutes).**
    - **8 more minutes needed to compensate losses in the batteries**
    - **Charging from 15%SOC till 75%SOC**
    - **SOC<95%? => Protection purposes**
      - **Above 95% the discharge current is limited by the BMS**
    - **In the case the estimated SOC by the system differs from the real one at the end of the cycle the control system compensates the deviation with a maximum power of 5kW.**

ABB's solution
BESS' Control System

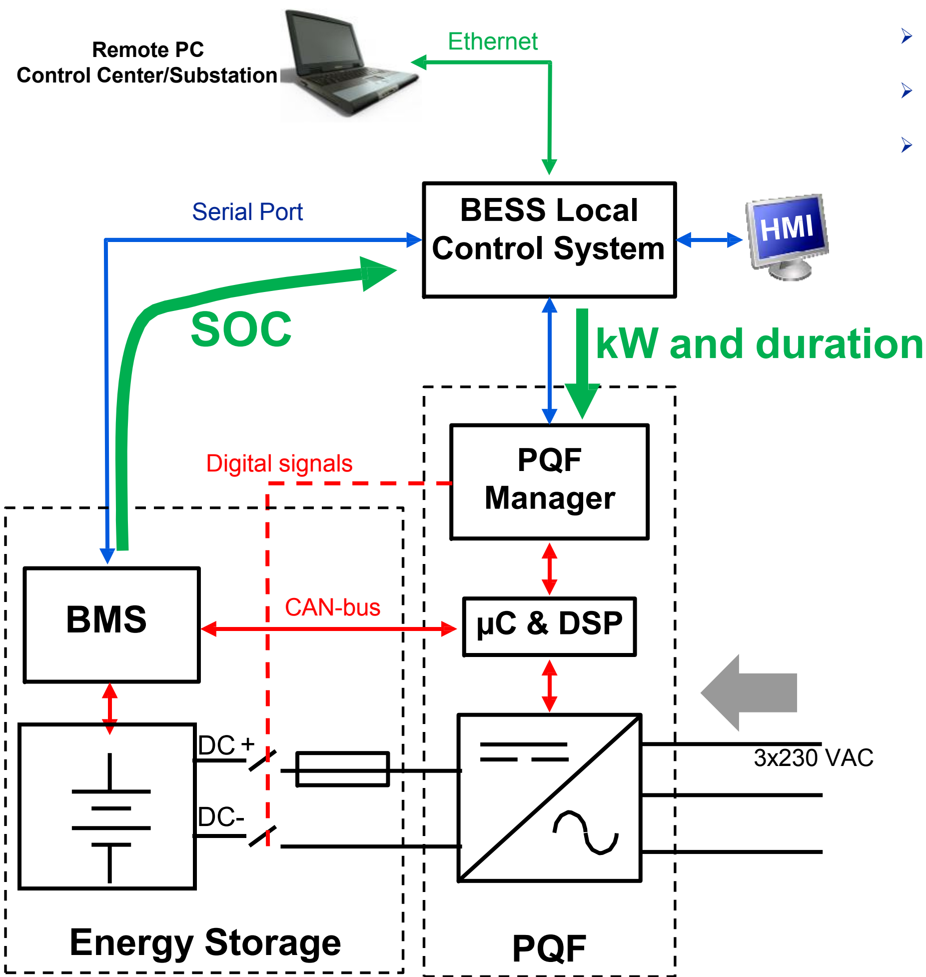

Automatic Control (BESS local control)

- Discharging Mode @ predefined time:
- Stand-by Mode:
- Charging Mode @ predefined time:
  - Power and duration of charge sent to the PQF manager (40kW – 2 hour and 8 minutes).
  - 8 more minutes needed to compensate losses in the batteries
  - Charging from 15%SOC till 75%SOC
  - SOC<95%? => Protection purposes
    - Above 95% the discharge current is limited by the BMS
  - In the case the estimated SOC by the system differs from the real one at the end of the cycle the control system compensates the deviation with a maximum power of 5kW.
  - Supporting the grid with up to 90kVar and filtering harmonics
  - When batteries charged => stand-by mode

ABB's solution
BESS' Control System

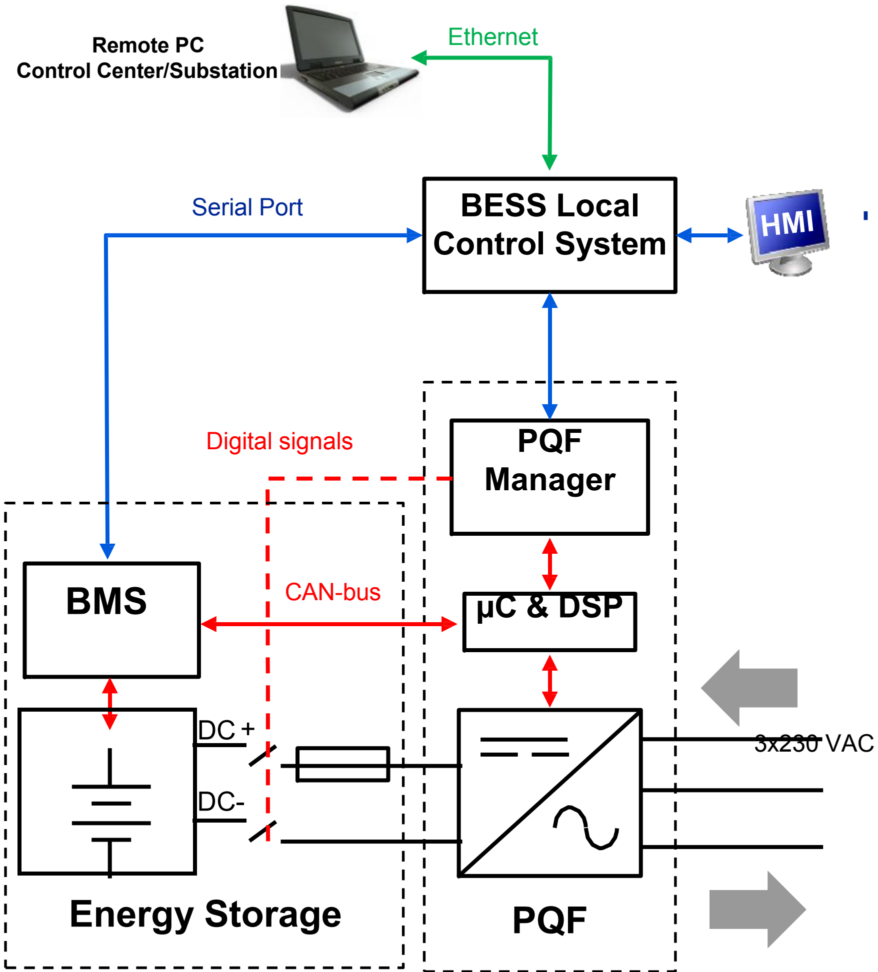

- **Automatic Control (BESS local control)**
  - **Discharging Mode @ predefined time:**
  - **Stand-by Mode:**
  - **Charging Mode @ predefined time:**
- **Manual Control (BESS local control)**
  - **Charging and discharging process set up in the HMI panel**

ABB's solution
System Performance

ABB's solution
System Performance

Outline

CUSTOMER NEEDS

ABB's SOLUTION

PRACTICAL GRID BENEFITS

CONCLUSIONS

Practical Grid Benefits
Load Shifting

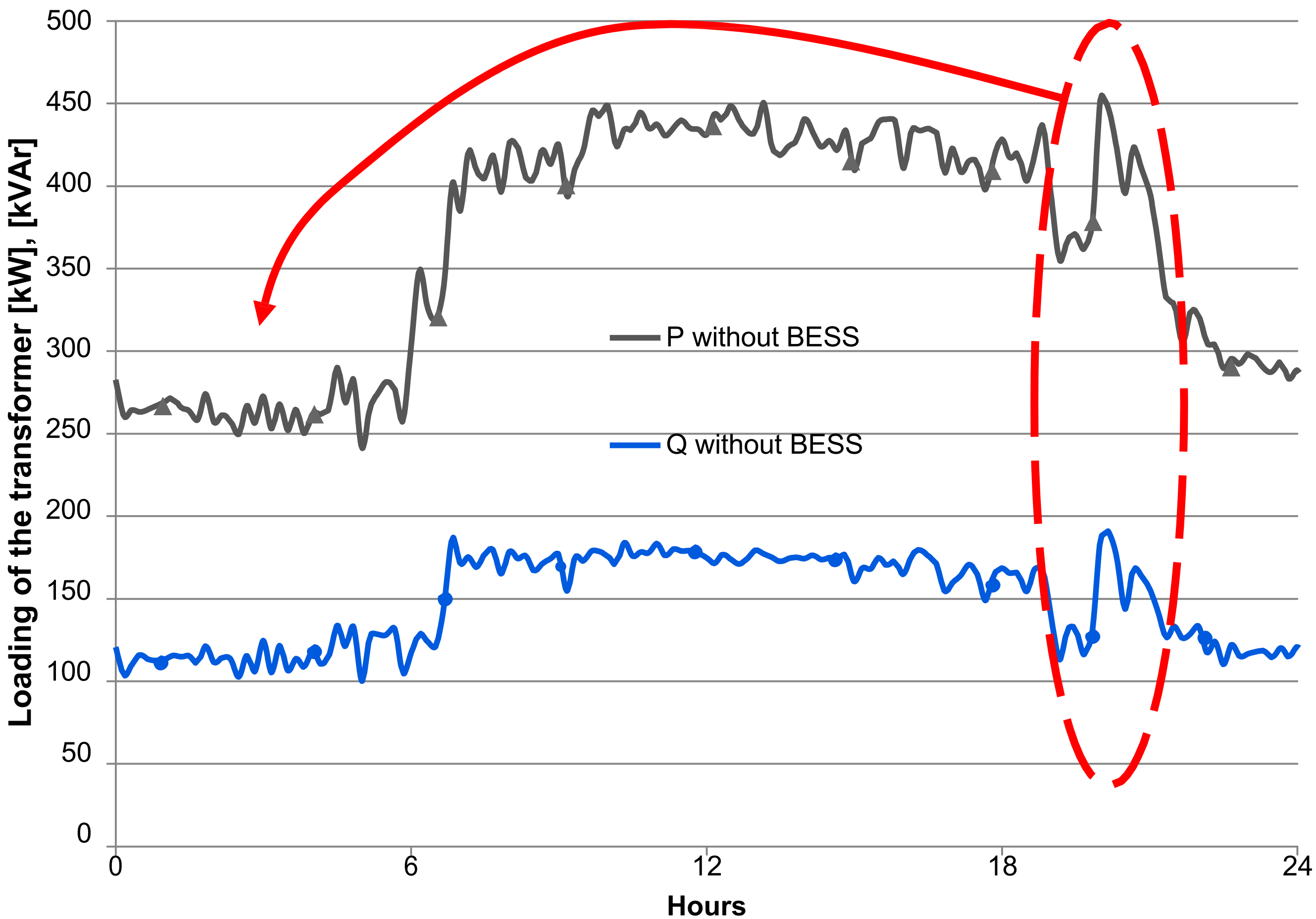

- **Load shifting**
  - High consumption shifted to low demand period
  - The transformer would not be overloaded

Practical Grid Benefits
Load Shifting

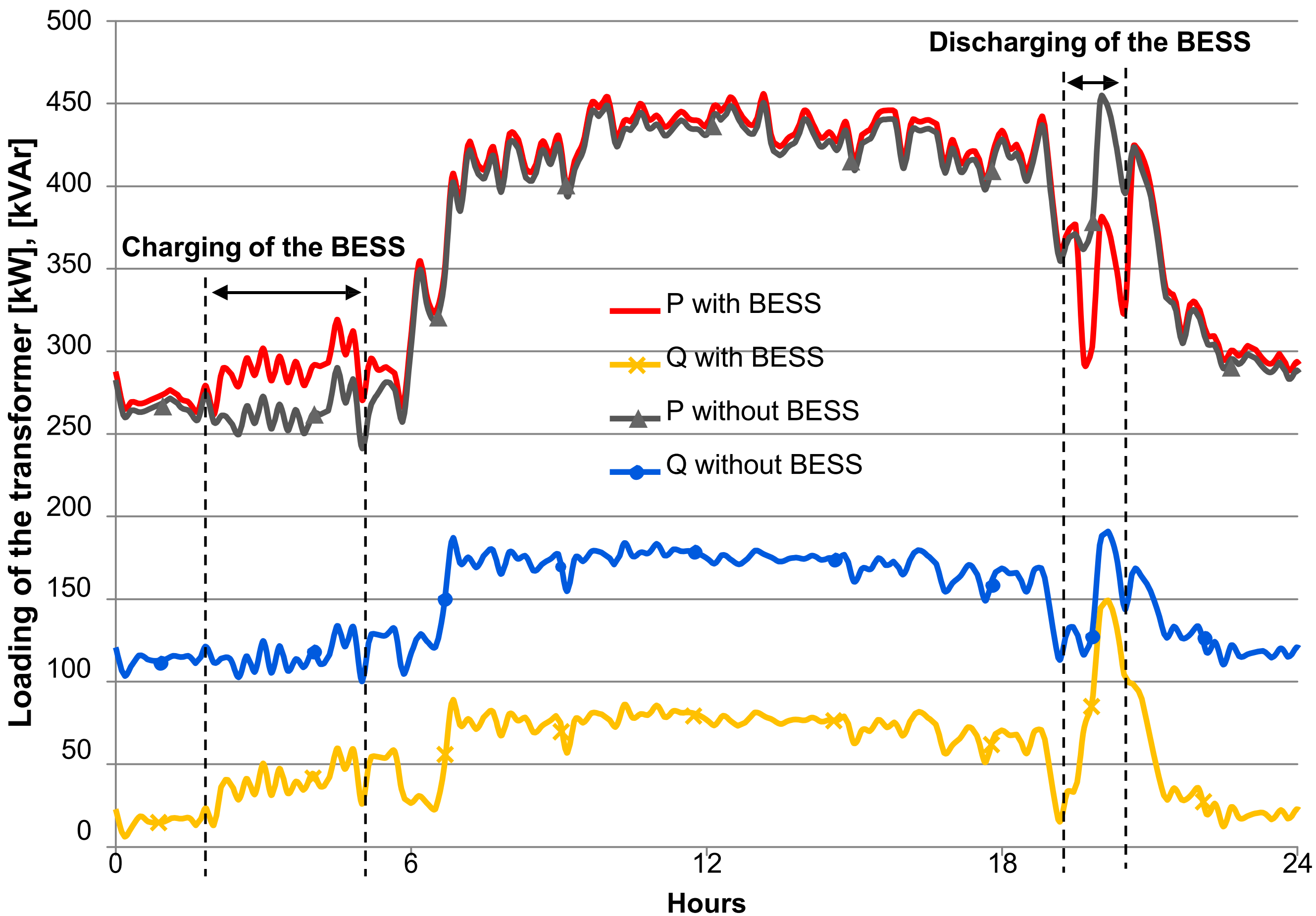

- **Load shifting**
  - High consumption shifted to low demand period
  - The transformer would not be overloaded
  - Difference in Active Power due to losses in the system **(5kW)**

Practical Grid Benefits
Load Shifting

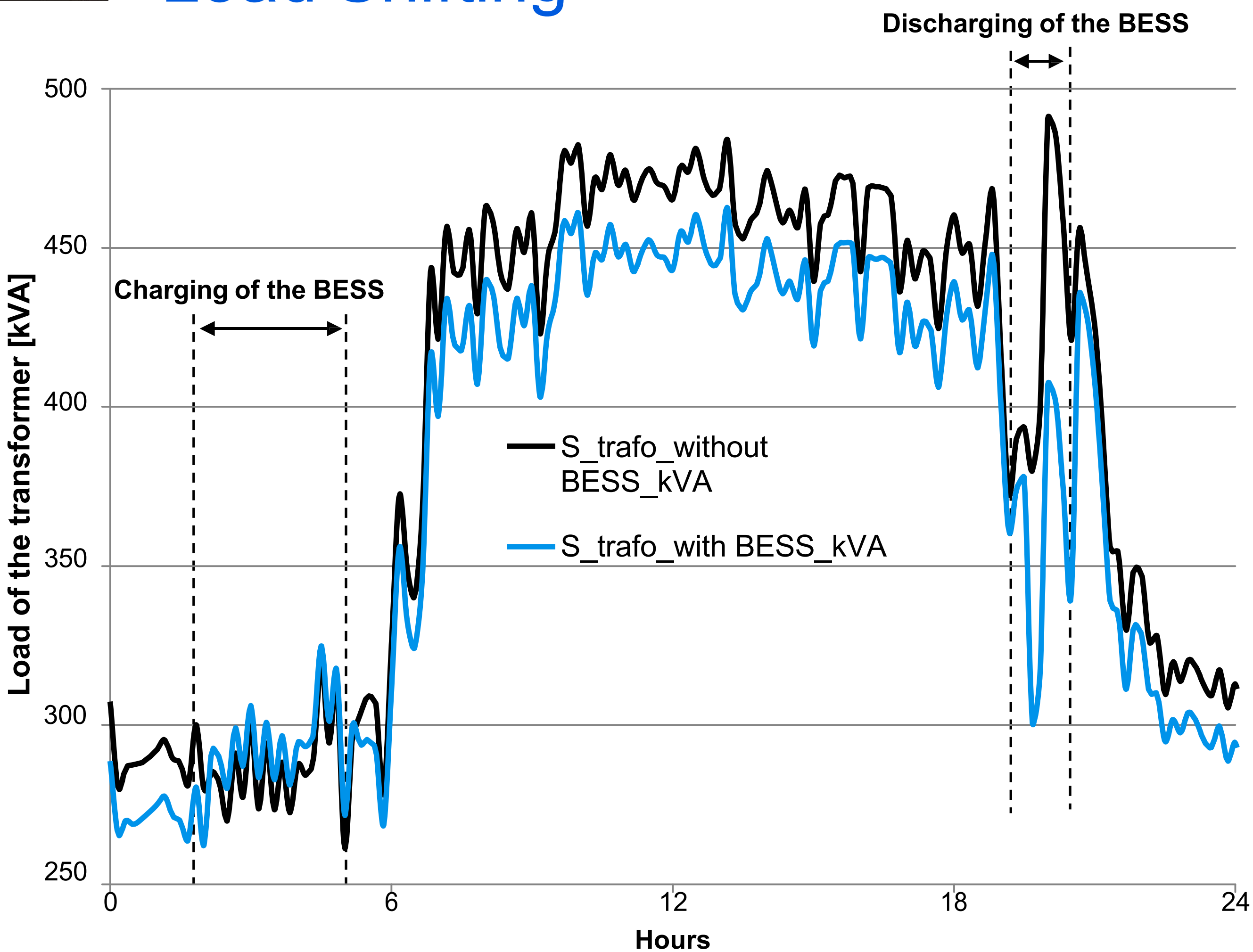

- **Load shifting**
  - High consumption shifted to low demand period
  - The transformer would not be overloaded
  - **Aparent Power:**
    - Lower when BESS is running except when this is charging.
    - **Transformer load has been reduced**

Practical Grid Benefits
Load Shifting

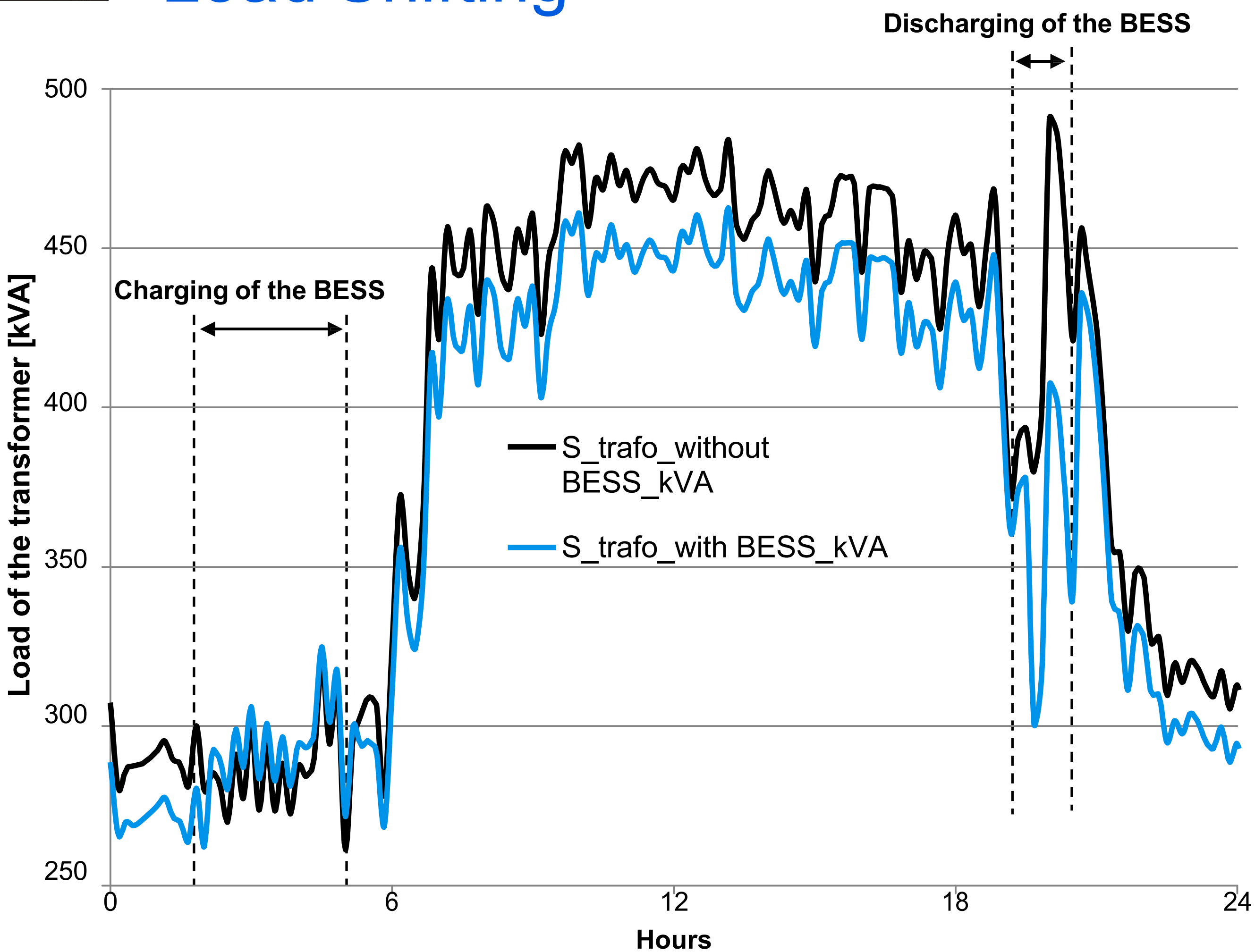

- **Load shifting**
  - High consumption shifted to low demand period
  - The transformer would not be overloaded
  - **Aparent Power:**
    - Lower when BESS is running except when this is charging.
    - **Transformer load has been reduced**

Impact on Trafo Losses

Practical Grid Benefits
Load Shifting: Transformer Losses

CSS

$$P_{losses} = x^2 P_{load\ losses} + P_{noload\ losses}$$

$$x = \frac{\sqrt{P^2 + }}{S_n}$$

Pload_losses@S_n=6.5kW

Pnoload_losses@S_n=1kW

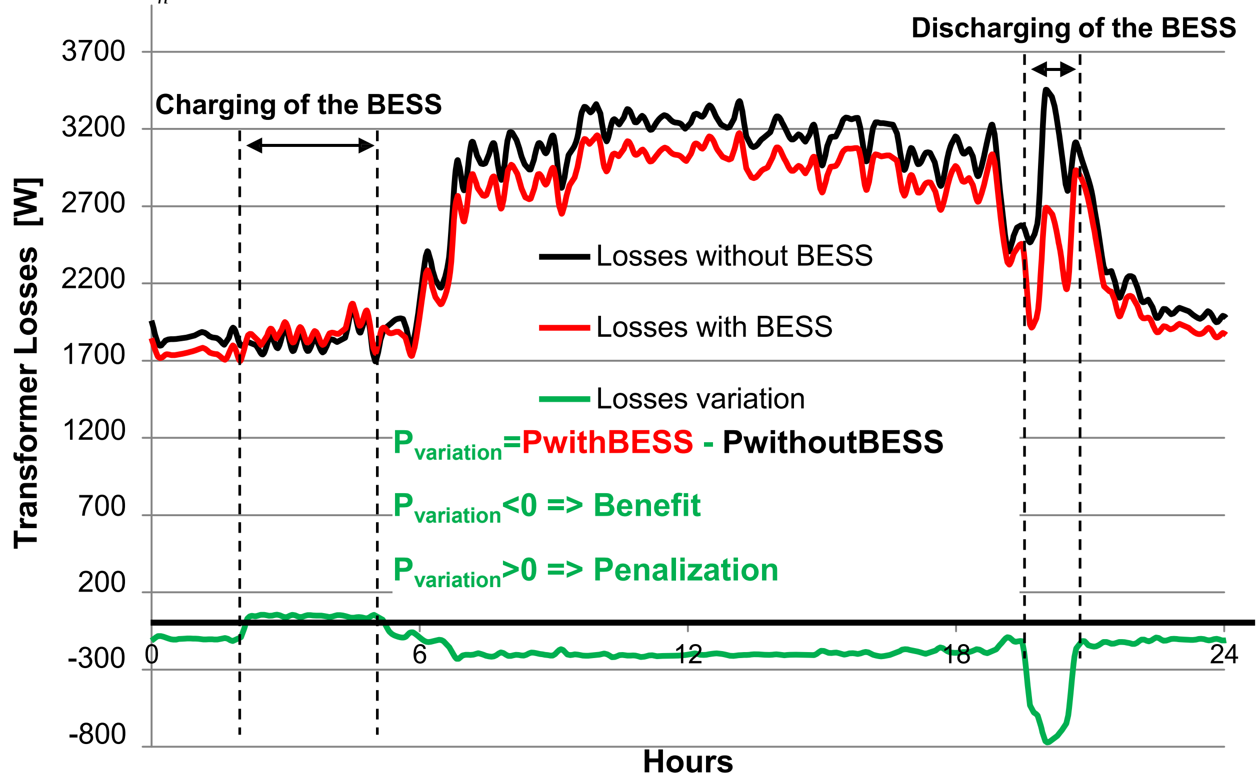

Practical Grid Benefits
Load Shifting: Power Factor

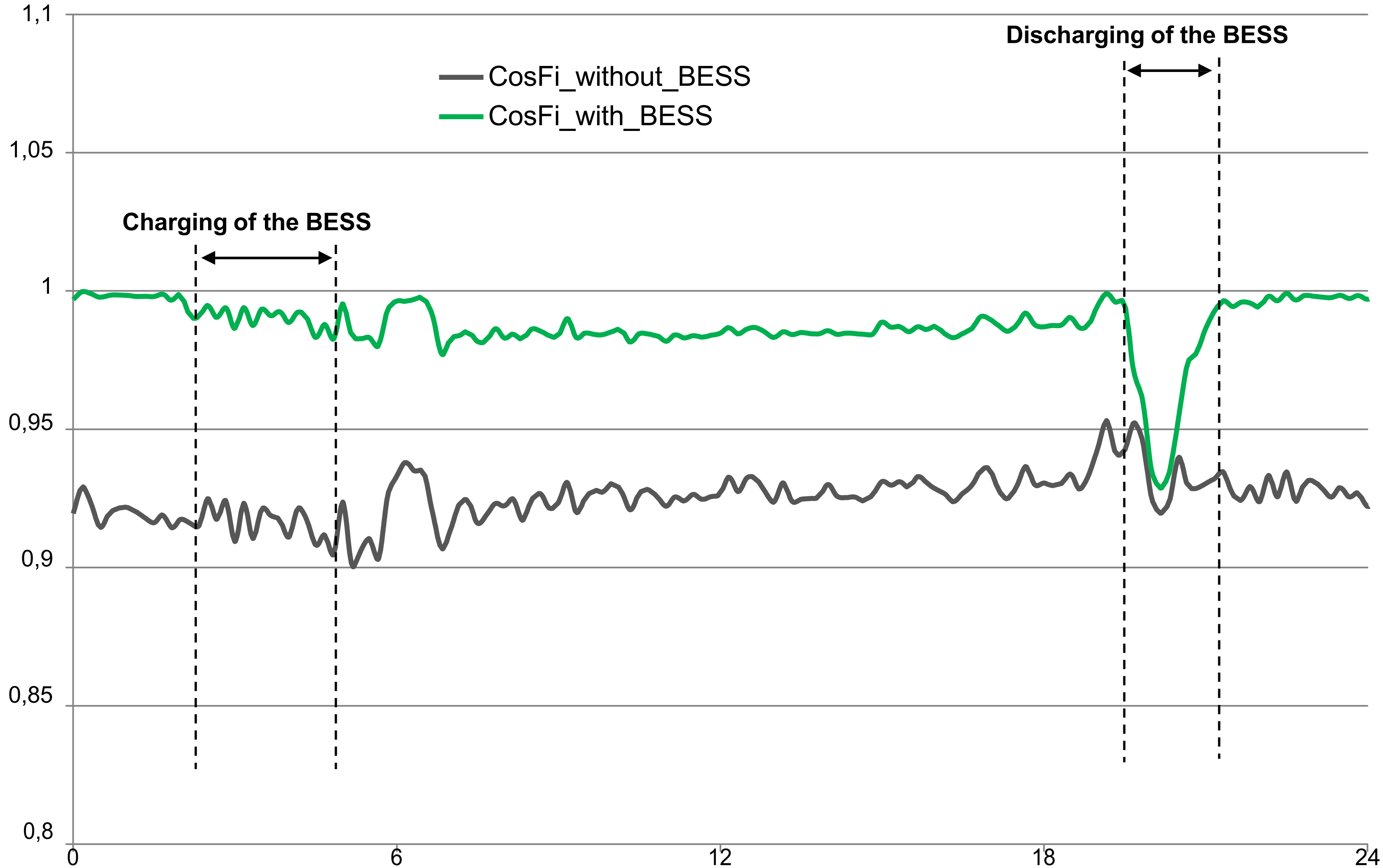

Practical Grid Benefits
Load Shifting: Power Factor

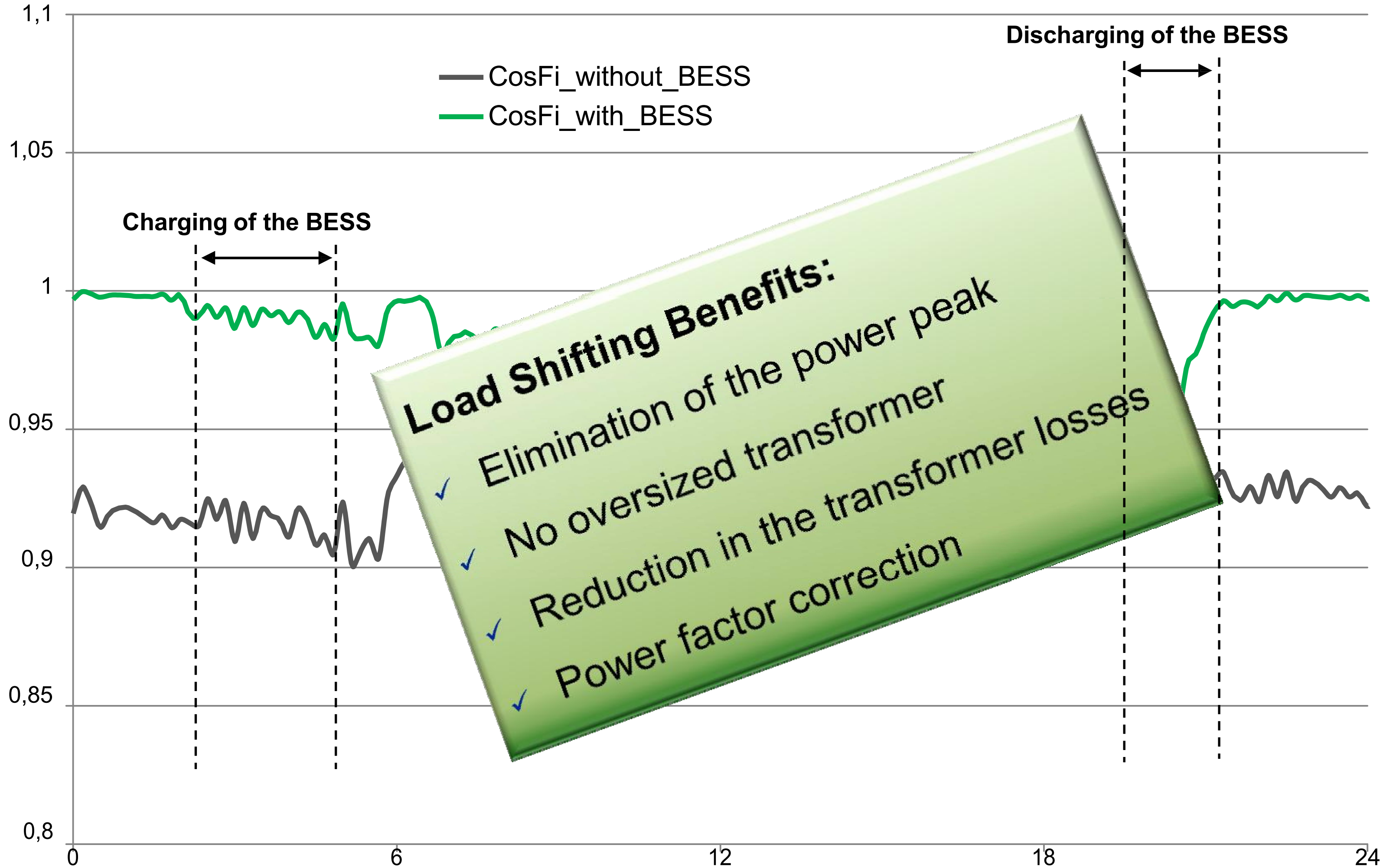

Practical Grid Benefits
Peak Shaving

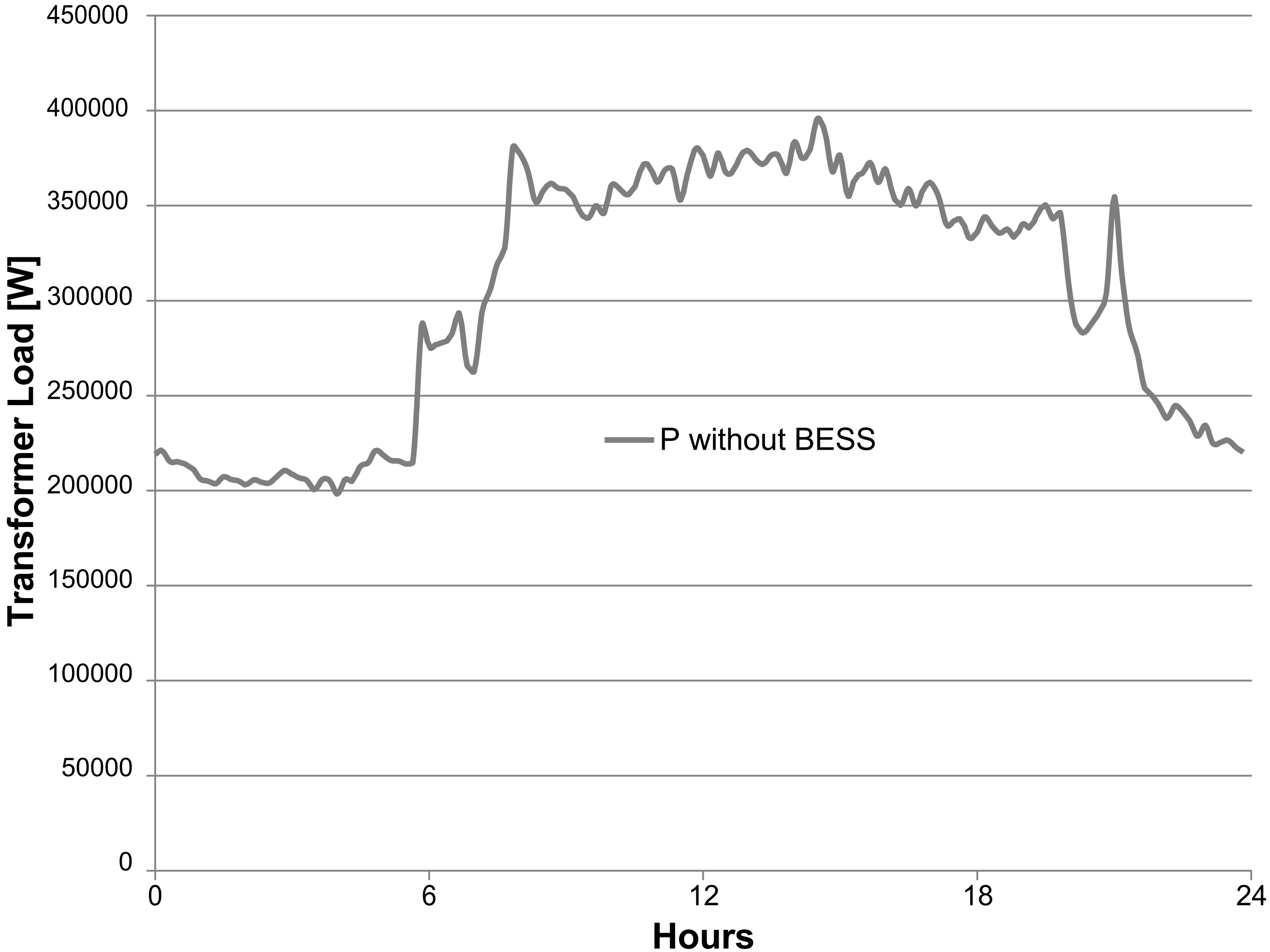

- **Peak Shaving**
  - As flat load profile in the transformer as possible.
  - NO penalization in the cosumer’s power fee

Practical Grid Benefits
Peak Shaving

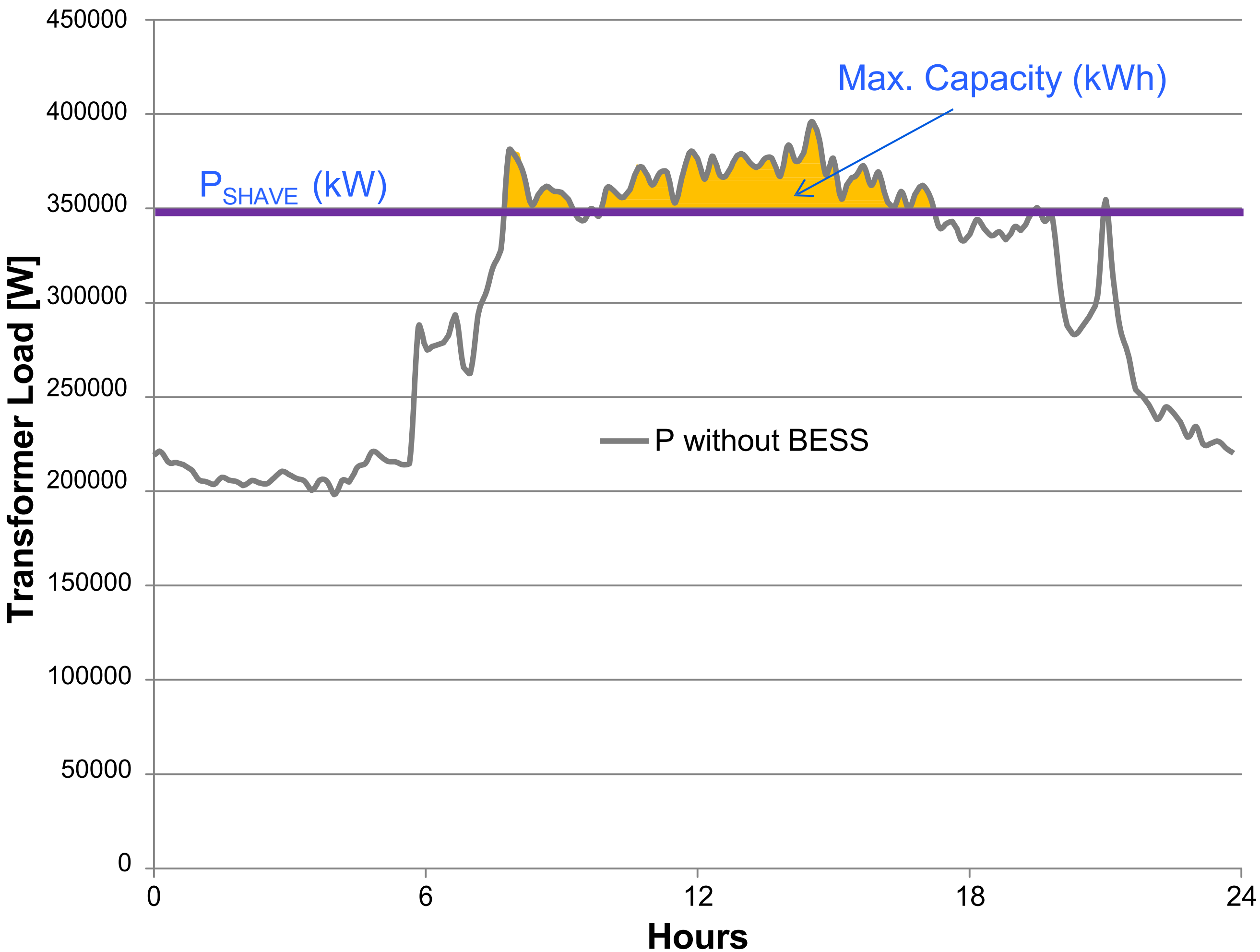

- **Peak Shaving**
  - As flat load profile in the transformer as possible.
  - NO penalization in the cosumer's power fee
  - Algorithm NEEDS:
    - **Load profile**
    - **P_{SHAVE}** (no over passsed)
    - Max. Capacity of the BESS

Practical Grid Benefits
Peak Shaving

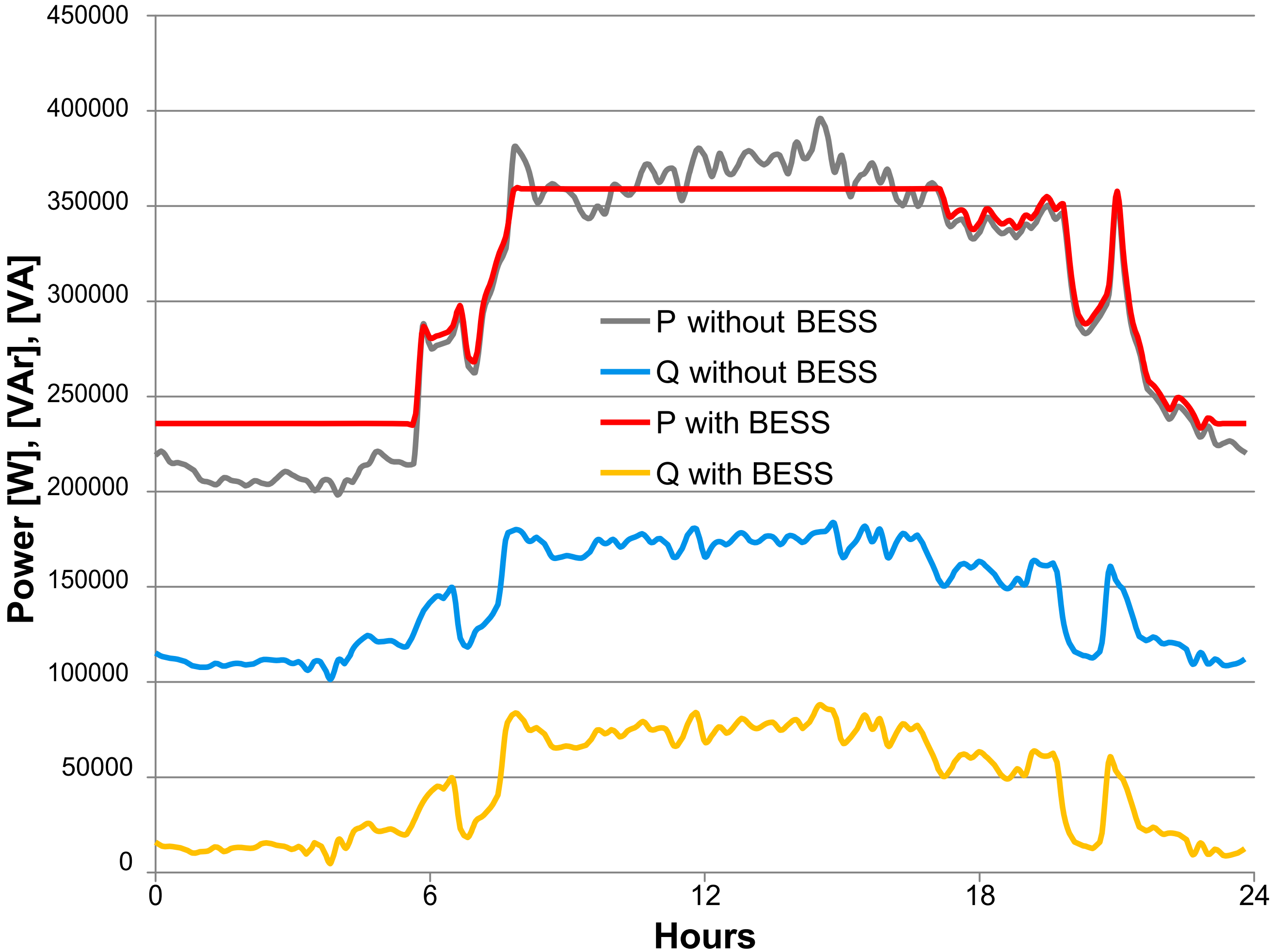

- Peak Shaving
  - **Benefits achieved:**
    - Flatter Power Profile
    - Reactive power compensation
    - Transformer load has been reduced

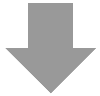

Impact on Trafo Losses

Carlos Martinez - ABB Estonia - Session 4 – Paper 1172

Practical Grid Benefits
Peak Shaving: Transformer losses

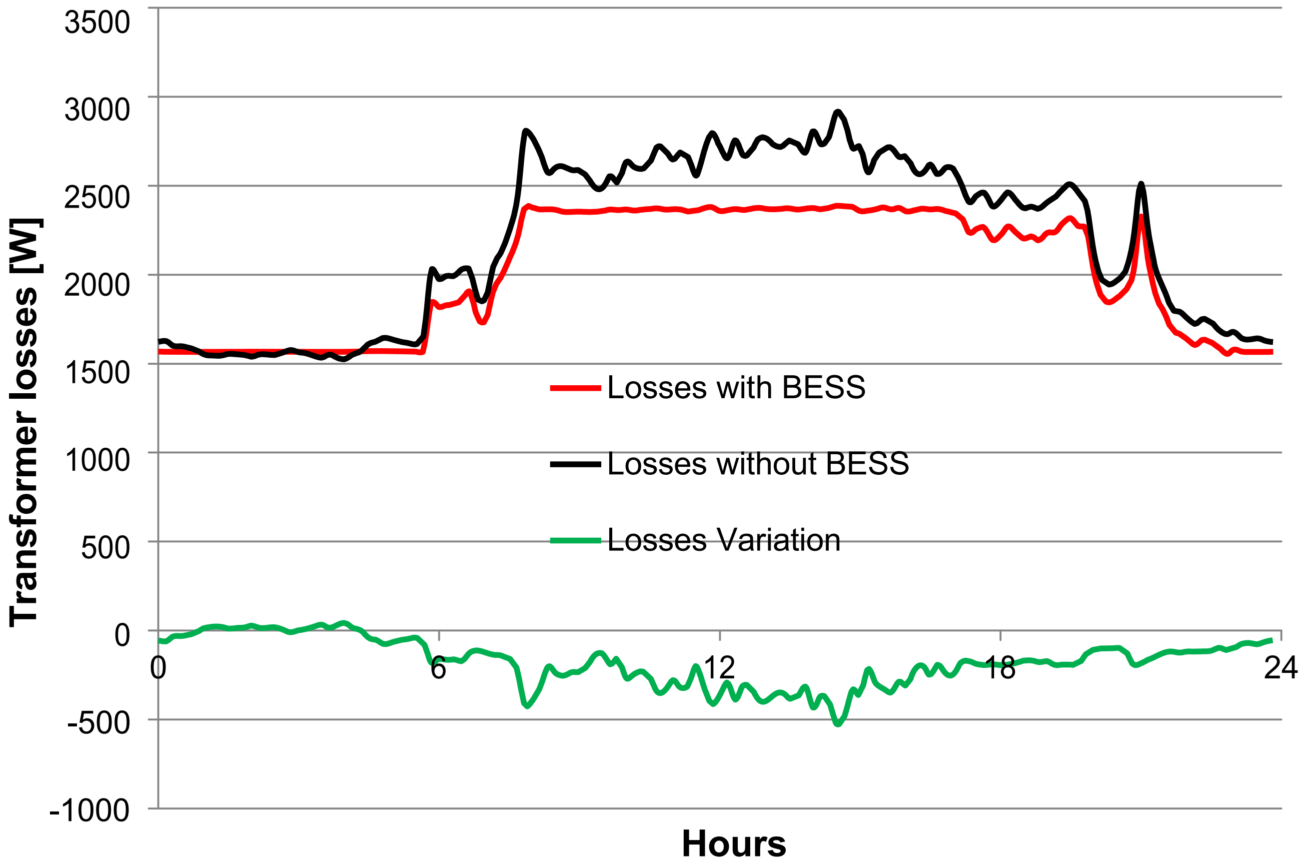

- **Peak Shaving**
  - **Benefits achieved:**
    - Flatter Power Profile
    - Reactive power compensation
    - Transformer load has been reduced

Impact on Trafo Losses

Practical Grid Benefits
Peak Shaving: Transformer losses

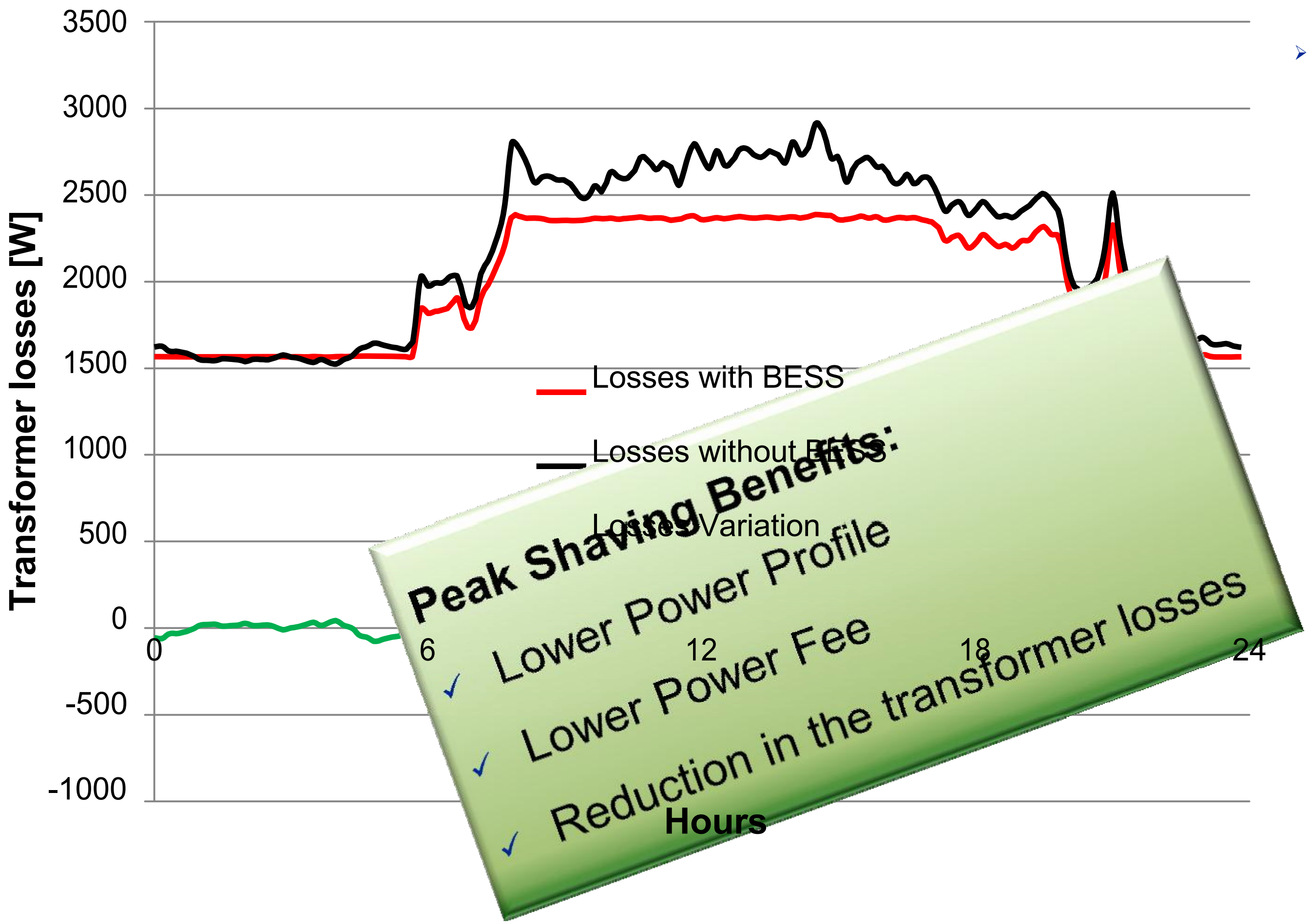

- **Peak Shaving**
  - **Benefits achieved:**
    - Flatter Power Profile
    - Reactive power compensation
    - Transformer load has been reduced

Impact on Trafo Losses

Outline

CUSTOMER NEEDS

ABB's SOLUTION

PRACTICAL GRID BENEFITS

CONCLUSIONS

Conclusions

BESS Solution 75kW/75kWh to accomplish customer's requirements

- Peak shaving, load shifting, reactive and harmonic compensation

Main components and control system have been presented.

System Losses of 5kW and **Round trip efficiency** > 94%.

GRID BENEFITS:

- **Load shifting** from high peak demand to off-peak period with high reduction in the transformer losses.
- **Peak shaving** in order to reduce consumer's power fee with reduction in the transformer losses
- **Reactive compensation (cosfi=0.99)** and **harmonic mitigation** independent from the status of the batteries
- **Main transformer** working in better conditions. No overloaded is needed
- **Pilot installation**: it has not been sized to obtain the full benefits on the grid where it is installed. It has been installed for testing purposes.

Thank you for you attention!!!

Power and productivity
for a better world™

ABB

Document number: 1VPD110001A0158	**Energy Storage Module** **Voltage control by energy storage reactive power compensation**				
Dept.	Project	Status Date	Author	Status	Revision
PPMV	FEAB	05.03.2014	Carlos Nieto	Released	1

ABB Document number: 1VPD110001A0158	**Energy Storage Module** **Voltage control by energy storage reactive power compensation**				
Dept. PPMV	Project FEAB	Status Date 5.03.2014	Author Carlos Nieto	Status Released	Revision 1

Rev.	Description	Modified by	Date/Initial
1	First version	Carlos Nieto	05.03.2014

Table of Contents

1 Introduction

1.1 Scope, purpose and extent

The scope of this document is to present a technical report about the evaluation of the capability of the Energy storage Module (ESM) property of FEAB installed in Falköping (Sweden) to control the voltage due to the reactive power compensation.

The schematic of the FEAB ESM power circuit can be seen in the Figure 1. The main components of the power circuit are:

- Li-Ion battery system (+C);
- DC power breaker (+Q2);
- DC contactor (+K1);
- PQFI BESS converter (+TA);
- Isolation transformer (+T)
- AC power breaker (+Q1).

Definition of the indicated on Figure 1.1 measured parameters could be found in Appendix 1.

For carrying out the tests, several combinations of active power and reactive power compensation and higher order current harmonics filtration have been tested in order to analyse the influence in the voltage control. These measurements were carried out during the data acquisition for Test 5: Evaluation in Losses in Energy Storage.

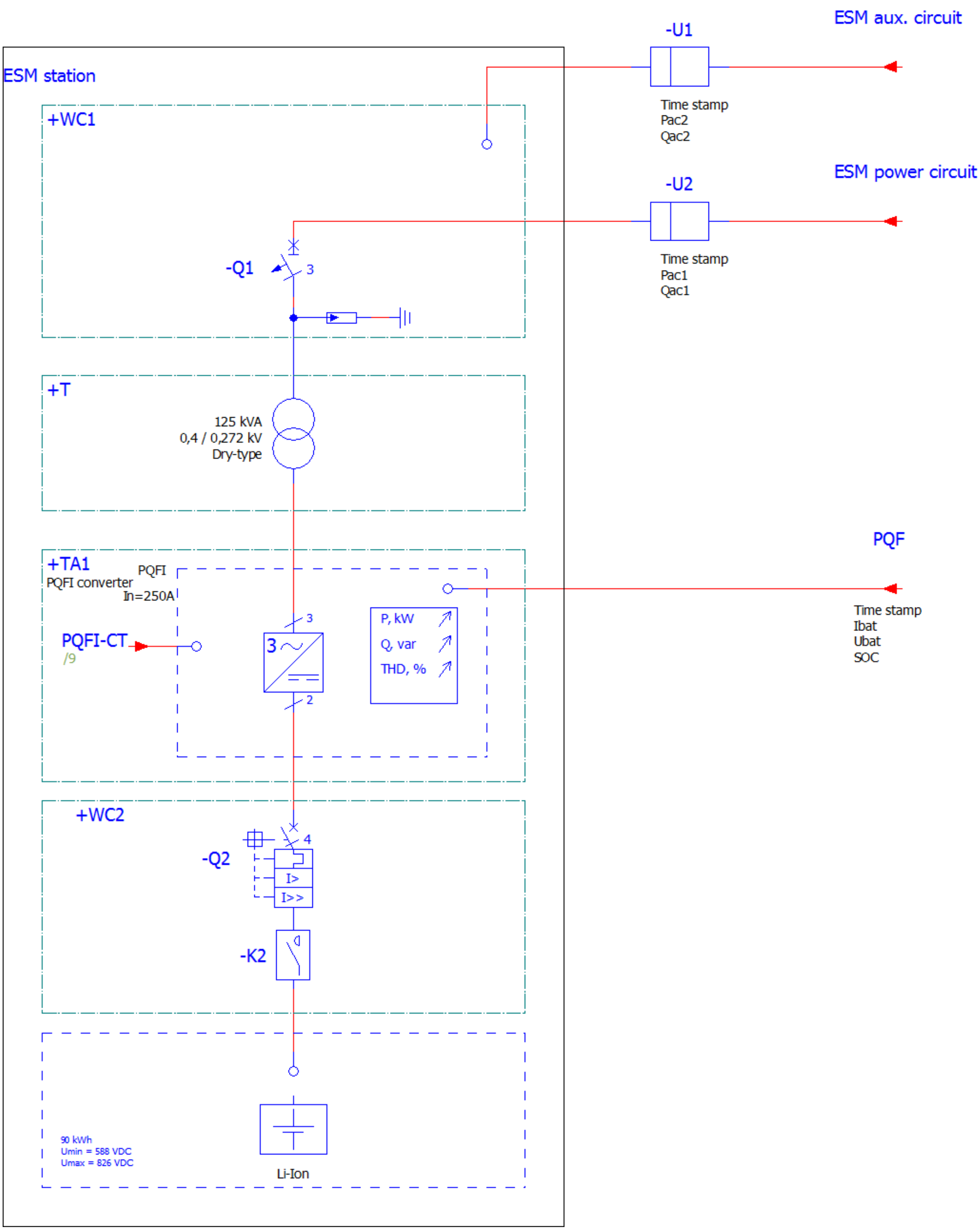

Figure 1. Energy storage system overall diagram and measured paramenters

1.2 References

[Ref 1] Test Specification for evaluation in losses in energy storage.

1.3 Abbreviations

BESS Battery Energy Storage System

PQF Power Quality Filter (an active power quality filters platform based on which the power converter for energy storage system has been realized)

BMS Battery Management System

FEAB Falbygdens Energi AB

ESM Energy Storage Module

AC Alternating Current

DC Direct Current

2 General

2.1 Hardware

The hardware used to develop the test is the Energy storage Module (ESM) property of FEAB installed in Falköping (Sweden) and the meters from Metrum which monitors the operation of the ESM. All the configurations tested were described for the case of Test 5: Evaluation in Losses in Energy Storage.

2.2 System Settings

The following settings have been modified during the tests:

- Active power, kW;
- Reactive power, kVar;
- Higher order harmonics filtration current, A.

2.2.1 Measurements and calculations

The time synchronization between the PQFI- and Metrum measuring system has been done after the tests when all the data were put together.

All the data analysed were measured in the moment of the test carried out for the evaluation of losses of the system (Test 5)

For this case, the most relevant parameters measured are the voltage in the output of inverter, the amount of reactive power and the presence of harmonic filtration or not.

The votlage in the inverter output does not take into consideration the transformer, so in order to express the results in terms of the grid voltage, the turns ratio of the transformer has been applied.

3 Tests

The aim of the following tests is to identify how the influence of the reactive power compensation capability of the inverter is able to control the voltage in the system output. Two main kind of tests have been carried out: the first one takes into account the general specifications with 80kW in discharging mode (around 75kW expected on the grid) and 40kW in charging mode. The depth of discharge (DoD) is going to be set up from 75% till 15% because these are the values to take into account for the full cycle. The other kind of test carried out is based on small cycles around 75% with several values of active power and combinations of reactive power and harmonic mitigation.

3.1 P, kW + Q, kvar + ITHD, A

In this test the reactive power (Q) compensation and higher order current harmonics filtration (ITHD) functions are both turned on. The PQF has been set to achieve a dynamic capacitance with cosfi=1 and all the harmonic components that the PQFI BESS converter is able to filter out from the grid have been selected. The maximum parameters in terms of reactive power compensation with the set-point of cosfi=1 are the following:

- Charging mode: 90kVAr.
- Discharging mode: 66kVAr

3.1.1 Test procedure

The test procedure has been carried out as follows:

a) Cycling at high SOC:

- Charge or discharge the battery to SOC=75% with standard cycle (80kW for discharging or 40kW for charging) if the SOC differs from 75%. Rest time until battery has cooled down.
- Discharge the battery to SOC=74% with power set to 80 kW DC constant power, which will correspond to an approximate C-rate of (80)/135 = 0,592.
- Charge the batteries up to SOC=75% with 80 kW constant power.
- Discharge the battery to SOC=74% with power set to 60 kW DC constant power, which will correspond to an approximate C-rate of (60)/135 = 0,44.
- Charge the batteries up to SOC=75% with 60 kW constant power.
- Discharge the battery to SOC=74% with power set to 40 kW DC constant power, which will correspond to an approximate C-rate of (40)/135 = 0,296.
- Charge the batteries up to SOC=75% with 40 kW constant power.
- Discharge the battery to SOC=74% with power set to 20 kW DC constant power, which will correspond to an approximate C-rate of (20)/135 = 0,148.
- Charge the batteries up to SOC=75% with 20 kW constant power.
- Rest time until battery has cooled down. 30min minimum resting time.

b) Full cycle considering normal operation:

- Discharge down the batteries with 80 kW constant power during 1 hour. Setting output AC power at 80 kW ac will give approx. 77 kW discharge on the battery (because of the losses in the PQF, approx. 3 kW), corresponding to an approximate C-rate of 77/135 = 0.57.
- Rest time until battery has cooled down. 1 hour minimum resting time.
- Charge up the battery with 40kW for 2 hours, which will correspond to an approximate C-rate of (40)/135 = 0,296.
- Rest time until battery has cooled down. 1 hour minimum resting time.

3.1.2 Test results

As it can observed in Fig. 2 and Fig. 3, respectively, the inverter output voltage is higher in the case of discharging mode than in charging mode. This is due to the modulation of the inverter. The variations observed for the same mode and depending on the active power level, cannot be taken into consideration as they appear randomly caused but the grid voltage variation.

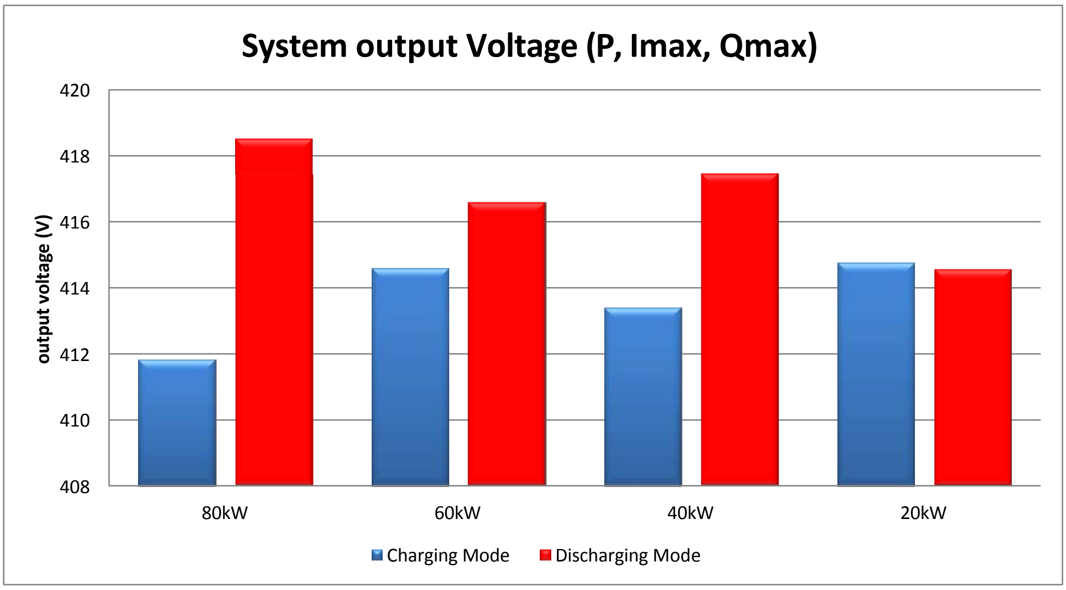

Figure 2: Voltage variation for different levels of discharge and charge active powers for the case of maximum harmonic filtration and reactive compensation in the case of cycling at high SOCs.

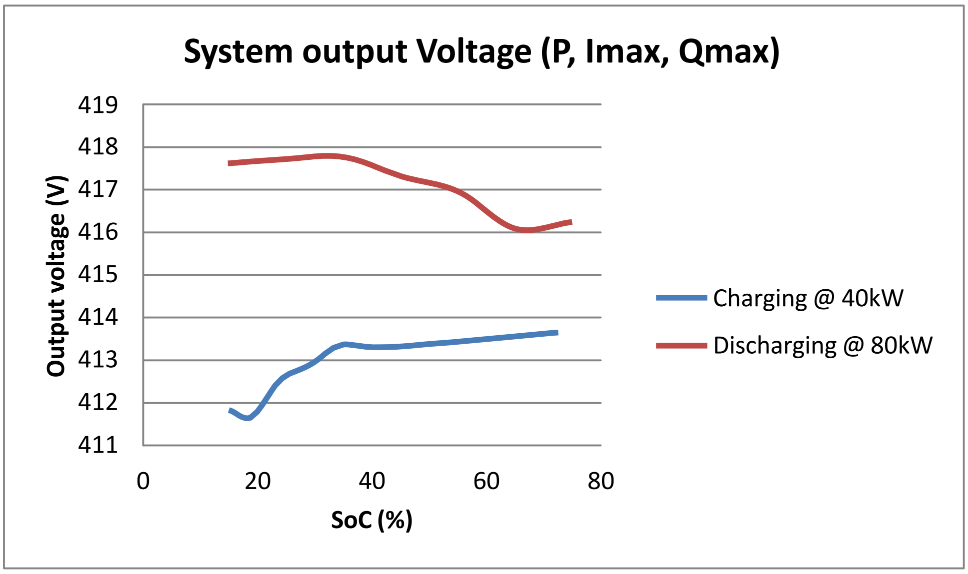

Figure 3. Voltage variation with the SoC for different levels of discharge and charge active powers for the case of maximum harmonic filtration and reactive compensation in the case of full cycles.

3.2 P, kW + Q, kvar

In this test the reactive power (Q) is turned on. The PQF has been set to achieve a dynamic capacitance with cosfi=1. The maximum parameters in terms of reactive power compensation with the set-point of cosfi=1 are the following:

- Charging mode: 90kVAr.
- Discharging mode: 66kVAr

3.2.1 Test procedure

The test procedure has been carried out as follows:

a) Cycling at high SOC:

- Deselect all the harmonics in the PQF Manager and set the reactive compensation in Dynamic capacitance with the target of cosfi=1.
- Charge or discharge the battery to SOC=75% with standard cycle (80kW for discharging or 40kW for charging) if the SOC differs from 75%. Rest time until battery has cooled down.
- Discharge the battery to SOC=74% with power set to 80 kW DC constant power, which will correspond to an approximate C-rate of (80)/135 = 0,592.
- Charge the batteries up to SOC=75% with 80 kW constant power.

- Discharge the battery to SOC=74% with power set to 60 kW DC constant power, which will correspond to an approximate C-rate of (60)/135 = 0,44.
- Charge the batteries up to SOC=75% with 60 kW constant power.
- Discharge the battery to SOC=74% with power set to 40 kW DC constant power, which will correspond to an approximate C-rate of (40)/135 = 0,296.
- Charge the batteries up to SOC=75% with 40 kW constant power.
- Discharge the battery to SOC=74% with power set to 20 kW DC constant power, which will correspond to an approximate C-rate of (20)/135 = 0,148.
- Charge the batteries up to SOC=75% with 20 kW constant power.
- Rest time until battery has cooled down. 30min minimum resting time.

b) Full cycle considering normal operation:

- Discharge down the batteries with 80 kW constant power during 1 hour. Setting output AC power at 80 kW ac will give approx. 77 kW discharge on the battery (because of the losses in the PQF, approx. 3 kW), corresponding to an approximate C-rate of 77/135 = 0.57.
- Rest time until battery has cooled down. 1 hour minimum resting time.
- Charge up the battery with 40kW for 2 hours, which will correspond to an approximate C-rate of (40)/135 = 0,296.
- Rest time until battery has cooled down. 1 hour minimum resting time.

3.2.2 Test results

As in the previous test the test, the voltage is higher when the system is discharging batteries due to the modulation in the inverter (see Fig. 4 and Fig. 5).

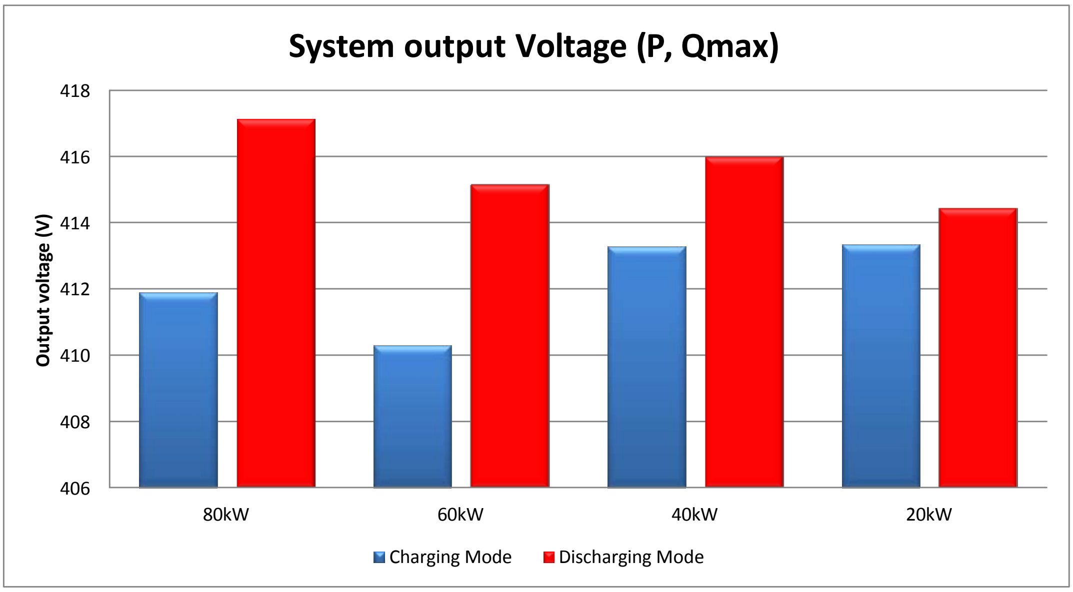

Figure 4. Voltage variation for different levels of discharge and charge active powers for the case of reactive compensation in the case of cycling at high SOCs.

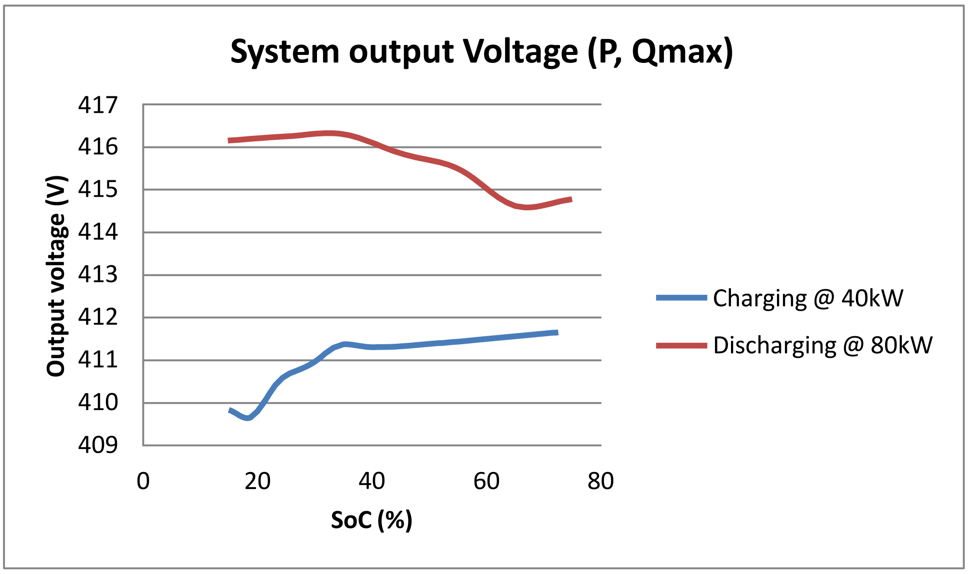

Figure 5. Voltage variation with the SoC for different levels of discharge and charge active powers for the case of reactive compensation in the case of full cycles.

3.3 P, kW

In this test the reactive power (Q) and the harmonic filtration are both turned off.

3.3.1 Test procedure

The test procedure has been carried out as follows:

a) Cycling at high SOC:

- Switch-off the reactive power compensation function and select all possible harmonic components that could be filtered out in the PQF Manager.
- Charge or discharge the battery to SOC=75% with standard cycle (80kW for discharging or 40kW for charging) if the SOC differs from 75%. Rest time until battery has cooled down.
- Discharge the battery to SOC=74% with power set to 80 kW DC constant power, which will correspond to an approximate C-rate of (80)/135 = 0,592.
- Charge the batteries up to SOC=75% with 80 kW constant power.
- Discharge the battery to SOC=74% with power set to 60 kW DC constant power, which will correspond to an approximate C-rate of (60)/135 = 0,44.
- Charge the batteries up to SOC=75% with 60 kW constant power.
- Discharge the battery to SOC=74% with power set to 40 kW DC constant power, which will correspond to an approximate C-rate of (40)/135 = 0,296.
- Charge the batteries up to SOC=75% with 40 kW constant power.

- Discharge the battery to SOC=74% with power set to 20 kW DC constant power, which will correspond to an approximate C-rate of (20)/135 = 0,148.
- Charge the batteries up to SOC=75% with 20 kW constant power.
- Rest time until battery has cooled down. 30min minimum resting time.

b) Full cycle considering normal operation:

- Discharge down the batteries with 80 kW constant power during 1 hour. Setting output AC power at 80 kW ac will give approx. 77 kW discharge on the battery (because of the losses in the PQF, approx. 3 kW), corresponding to an approximate C-rate of 77/135 = 0.57.
- Rest time until battery has cooled down. 1 hour minimum resting time.
- Charge up the battery with 40kW for 2 hours, which will correspond to an approximate C-rate of (40)/135 = 0,296.
- Rest time until battery has cooled down. 1 hour minimum resting time.

3.3.2 Test results

In this test results (Fig. 6 and Fig. 7), it can be observed that, as before, the voltage is higher when batteries are being discharged. On the other side, the voltage level in the system output is smaller than in the both cases shown above due to basically the disconnection of the reactive compensation.

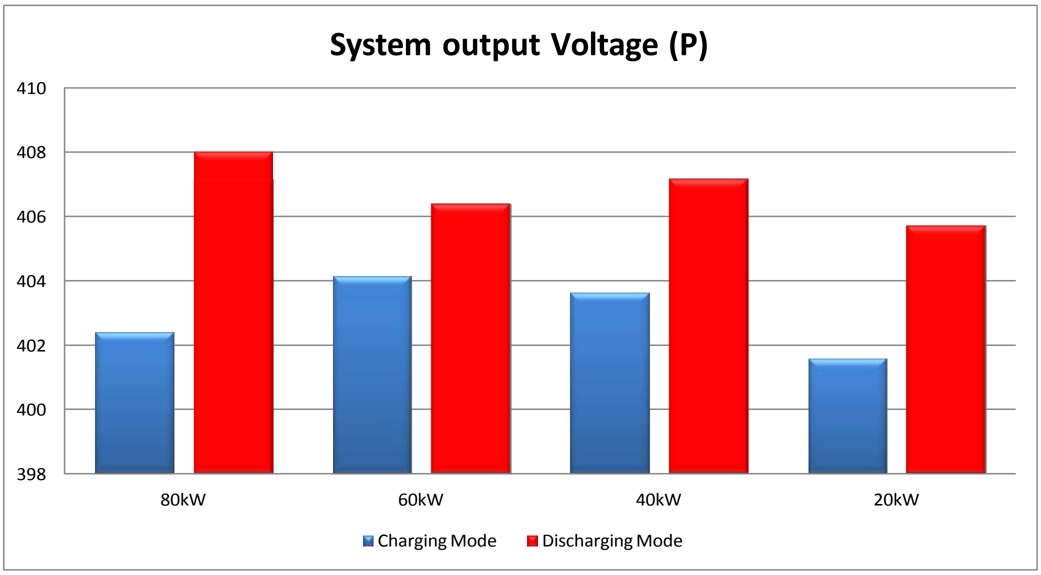

Figure 6. Voltage variation for different levels of discharge and charge active powers in the case of cycling at high SOCs.

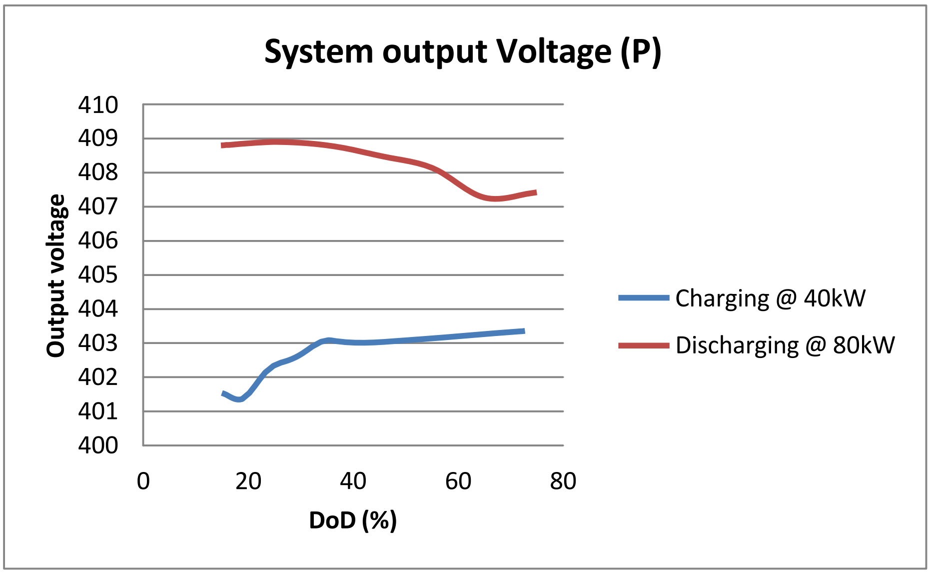

Figure 7. Voltage variation with the SoC for different levels of discharge and charge active powers in the case of full cycles.

3.4 Comparison of the three tests

This is a comparison of the tests shown in epigraphs 3.1, 3.2 and 3.3 in order to compare them in terms of voltage variation for the same conditions.

3.4.1 Charging Mode

As it can be seen in Fig. 8, when the system is compensating reactive power, the voltage in the output increases in approximately 8V when only the reactive power compensation is switched on. Also it is important to remark that in the moment that the harmonic filtration is set to compensate the harmonics, the voltage in the system output also increases, in this case with around 2V compared with the case that it is not.

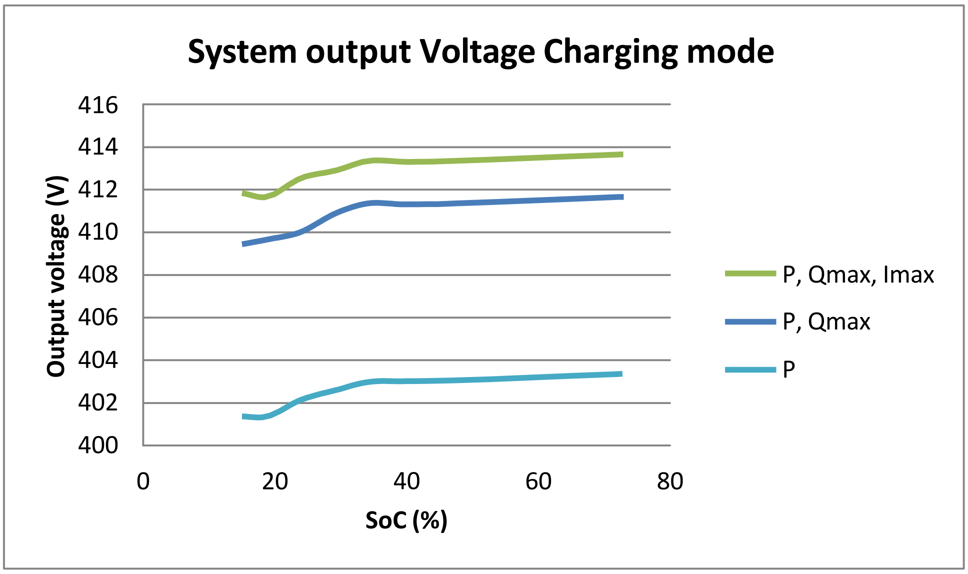

Figure 8. Voltage variation with the SoC for different levels of discharge and charge active powers in the case of full cycles.

3.4.2 Discharging Mode

As it can be seen in Fig. 9, and happened during charging mode, when the system is compensating reactive power, the voltage in the output increases in approximately 9V when only the reactive power compensation is switched on. Also it is important to remark that in the moment that the harmonic filtration is set to compensate the harmonics, the voltage in the system output also increases, in this case with around 2V compared with the case that it is not.
Comparing the discharging mode with the charging mode, it can be observed that as mentioned before the voltage is higher when discharging the batteries.

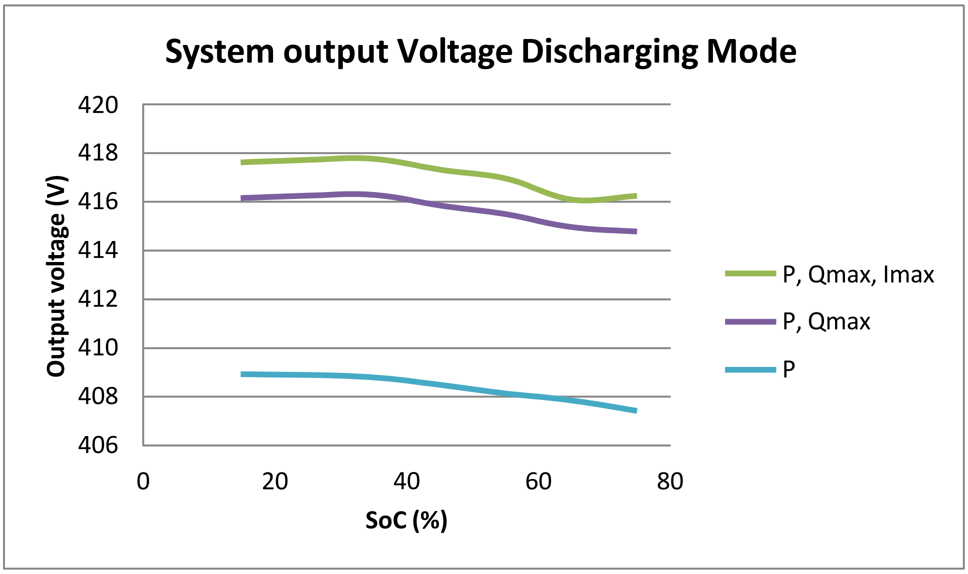

Figure 9. Voltage variation with the SoC for different levels of discharge and charge active powers in the case of full cycles.

4 Conclusions

After the tests done in the ESM and evaluated the data, the main conclusions are the following.

- The voltage increase due to reactive compesation is around 8V in charge and discharge mode.
- When the system is mitigating harmonics in the same time is compensating reactive, the output voltage is increased by additional 2V.
- The system present higher output voltage when the batteries are discharging than when they are charging.
- The voltage variation could be used to control the voltage and support it in the node where the ESM is connected.
- Further analysis are reccomended for the case that the ESM is not charging or discharging the batteries.
- It is important to notice that the voltage has been measured in the inverter output with transformer and then this voltage has been calculated in the secondary side of the transformer.

ABB AS

Main office:
Aruküla tee 59
75301 Jüri, Rae vald, Harjumaa. Estonia
Tel: +372 6801 800
Fax: +372 6801 810
E-mail: info@ee.abb.com
Internet: www.abb.ee

Manufacturing site:
Aruküla tee 83
75301 Jüri, Rae vald, Harjumaa. Estonia
Tel: +372 634 9295
Fax: +372 6349299
E-mail: css.orders@ee.abb.com

REDUCTION OF TRANSFORMER LOSSES

April 3, 2012

PÖYRY
Engineering balanced sustainability™

Preface

Contact

P.O. box 1002
Gullbergs Strandgata 8
SE-405 21, Gothenburg
Sweden
E-mail: SwedPower@poyry.com
Tel. +46 (0) 10 474 0000
Fax +46 (0) 10 474 0999
Business ID: 556850-0515
www.poyry.se

Pöyry SwedPower AB

Summary

An initial estimation of the reduction of the losses in the 20/0,4 kV transformer is presented. The estimation is based on the measurement data during the period of 2012-01-09 to 2012-02-21 and the no load and load losses of the actual transformer.

The losses are presented for an example day (2012-01-09) with during while the daily reduction is presented for each day during the period presented above. The mean daily loss reduction for the daily cycle including the charging/discharging cycle is 3,65 kWh which gives a total yearly reduction of losses in the transformer of 1350 kWh.

Also the reduction of losses due to only reactive power compensation is investigated. The mean daily loss reduction for the daily cycle excluding the charging/discharging cycle is 3,12 kWh which gives a total yearly reduction of losses in the transformer of 1300 kWh. The mean daily loss reduction for the daily cycle where the charging/discharging cycle is replaced by reactive power compensation is 4,01 kWh which gives a total yearly reduction of losses in the transformer of 1450 kWh.

Contents

Preface

Summary

1 BACKGROUND

As a part of project 2 an initial investigation of the reductions of losses in the 20/0,4 kV transformer. The calculation is based on a simple model of transformer.

Two studies were also done to investigate the reduction of the losses when only reactive power consumption is compensation.

Assumed data for transformer is presented in table 1 and was received from Stefan Carlsson 2012-03-29.

Table 1. Assumed data fot the transformer

Nominal power	800 kVA
No-load losses	1006 W
Load losses at nominal power	6470 W

2 METHOD

The losses of the transformer are model as a constant no load losses and the load losses is dependent on the utilization rate in square. The case without storage is used as reference value. The load for the case without storage is calculated as the difference of the measurements of the transformer and the power consumption of the storage system while for the case with storage is measurements of transformer used, as described in eq. 1-4. The subscript trans. indicates that the measurements are made on the secondary side of transformer while the conv. indicates the measurements for the storage system.

$$P_{without\ storage} = P_{trans} - P_{conv} \quad (1)$$

$$P_{with\ storage} = P_{trans} \quad (2)$$

$$Q_{without\ storage} = Q_{trans} - Q_{conv} \quad (3)$$

$$Q_{with\ storage} = Q_{trans} \quad (4)$$

The utilization rate (x) is calculated according to eq. 5-6.

$$x_{without\ storage} = \frac{\sqrt{P^2_{without\ storage} + Q^2_{without\ storage}}}{800} \quad (5)$$

$$x_{with\ storage} = \frac{\sqrt{P^2_{with\ storage} + Q^2_{with\ storage}}}{800} \quad (6)$$

The losses P_{losses} are calculated according to eq. 7 where $P_{load\ losses}$ is the load losses at nominal power and $P_{load\ losses}$ is the no load losses of the transformer.

$$P_{losses} = x^2 \cdot P_{load\ losses} + P_{no\ load\ losses} \quad (7)$$

Not included in the study are the losses due to the internal losses of transformer and the auxiliary power consumption of the transformer. These would only have minor impact reduction of the losses but would increase reduction so the presented results are conservative.

2.1 Only reactive power compensation

The first method for estimation of the reduction of losses due to compensation of reactive power is based on that operation sequences when charging and discharging is excluded. This corresponds to an operation situation where the BESS is disconnected during the charging and discharging cycle.

The second methods is based on the simulated case where there charging and discharging cycles are replace with conditions like when on reactive power compensation is active. This was implemented by a fixed compensation rate of -97,9 kVAr and active losses of 5,2 kW.

3 RESULT

In figure 1 is the calculated losses (kW) of the transformer shown both for the case with and without the storage for an example day (2012-01-09). The reduction of the losses can also be seen. A negative reduction means an increase in losses.

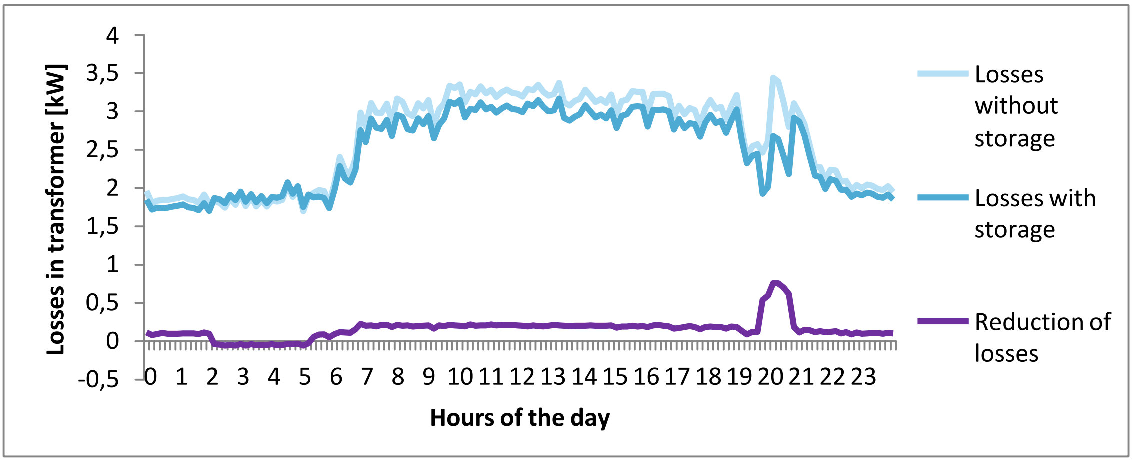

Figure 1. Estimated losses and reduction of losses for the 20/0,4 kV transformer for 2012-01-09. A negative reduction means an increase in losses.

Figure 2 shows the total reduction of losses (in kWh) during each day under the period 2012-01-09 to 2012-02-21.

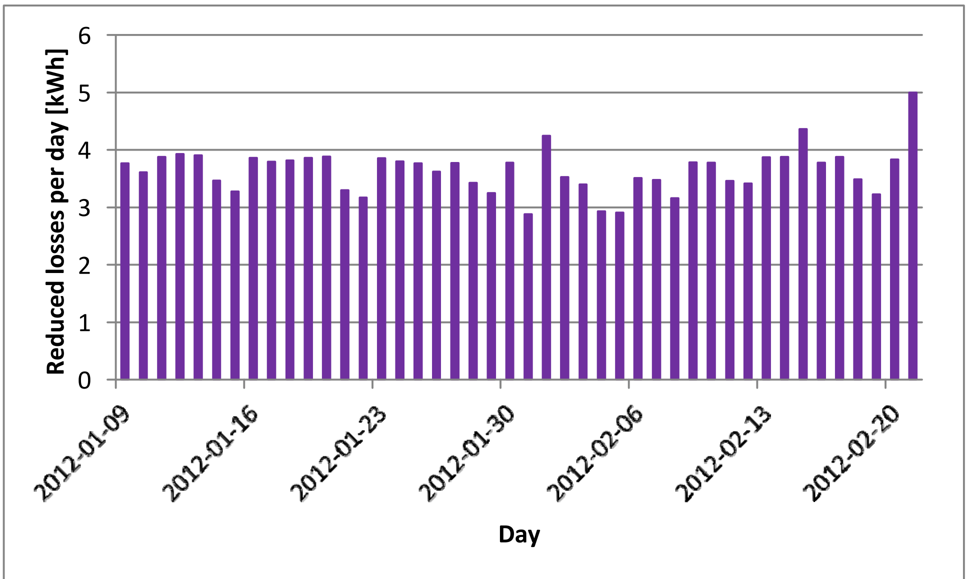

Figure 2. Reduced losses per day during the period 2012-01-09 to 2012-02-21.

3.1 Generalized loss estimations

The mean value of the loss reduction under the period 2012-01-09 to 2012-02-21 is 3,65 kWh/day. This means that the expected total yearly (365 days) reduction of losses is 1332 kWh/year.

3.2 Generalized loss estimation based on only reactive power compensation.

For the first method based only on the reduction of losses during no charging or discharging is the mean value of the loss reduction under the period 2012-01-09 to 2012-

02-21 is 3,12 kWh/day. This means that the expected total yearly (365 days) reduction of losses is 1138 kWh/year.

For the second method based on the reduction of losses during when the BESS is used only for reactive power compensation is the mean value of the loss reduction under the period 2012-01-09 to 2012-02-21 is 4,01 kWh/day. This means that the expected total yearly (365 days) reduction of losses is 1463 kWh/year.

Document number: 1VPD110001A0118	**Energy Storage Module** **Evaluation of losses**	

Dept.	Project	Status Date	Author	Status	Revision
PPMV	FEAB	24.07.2013	Carlos Nieto	Released	1

Rev.	Description	Modified by	Date/Initial
1	First version	Carlos Nieto	24.07.2013

Table of Contents

1 Introduction

1.1 Scope, purpose and extent

The scope of this document is to present a technical report about the evaluation of losses in the Energy storage Module (ESM) property of FEAB installed in Falköping (Sweden).

The purpose of the series of tests carried out in the ESM is the determination of all the components losses. These are given by the losses in the power circuit and the losses in the auxiliary power circuit.

The schematic of the FEAB ESM power circuit can be seen in the Figure 1. The main components of the power circuit are:

- Li-Ion battery system (+C);
- DC power breaker (+Q2);
- DC contactor (+K1);
- PQFI BESS converter (+TA);
- Isolation transformer (+T)
- AC power breaker (+Q1).

Definition of the indicated on Figure 1.1 measured parameters could be found in Appendix 1.

In addition to the losses throughout the power circuit, the energy consumed by the auxiliary equipment inside the ESM is taken into account. The main loads of the ESM auxiliary circuit are:

- Air-conditioning system;
- Internal lighting;
- ESM control system components.

For carrying out the tests, several combinations of active power and reactive power compensation and higher order current harmonics filtration have been tested in order to verify the contribution of each operation mode to the system losses.

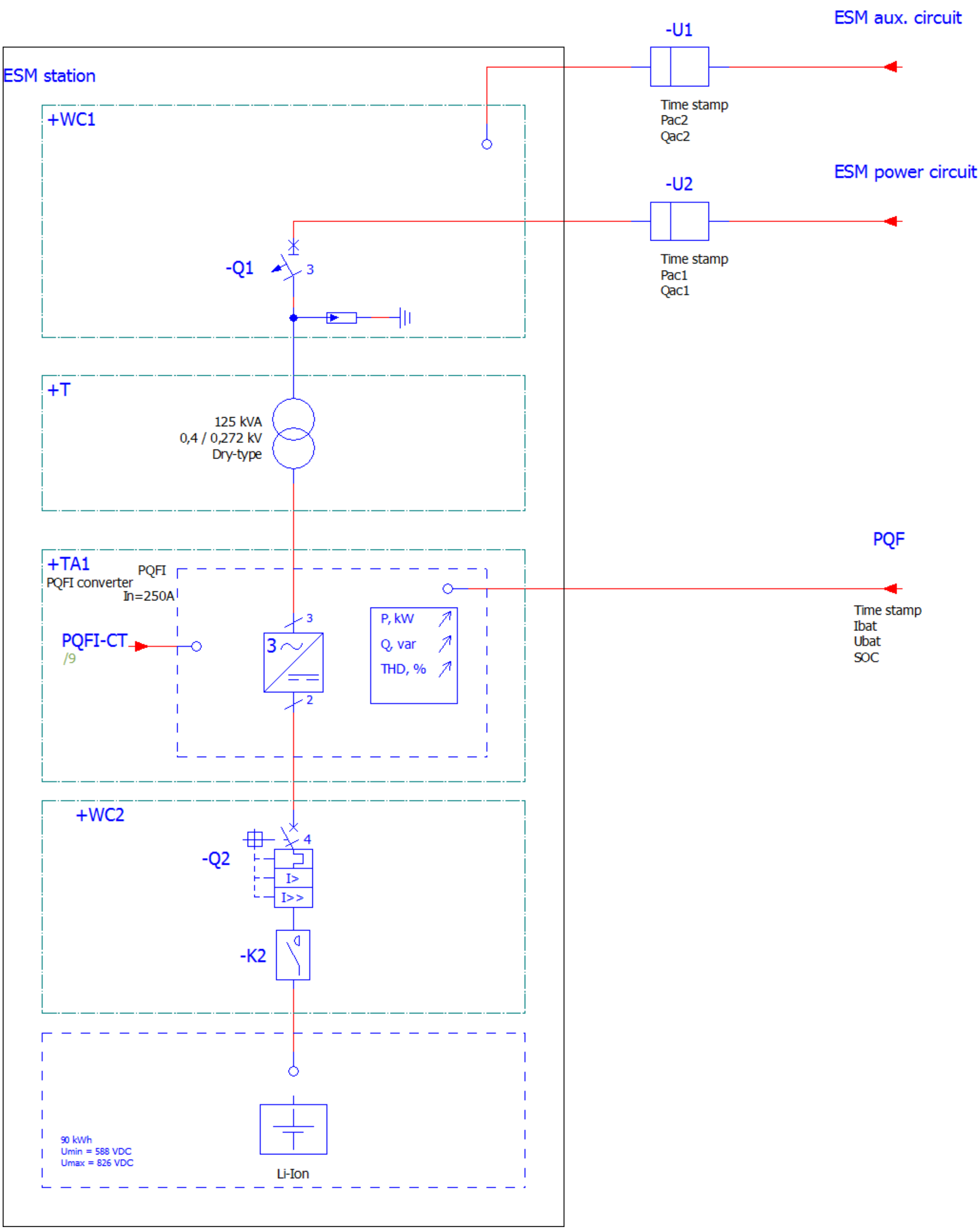

Figure 1. Energy storage system losses evaluation tests overall diagram

1.2 References

[Ref 1] Test Specification for Evaluation of losses in energy storage system.

1.3 Abbreviations

BESS Battery Energy Storage System

PQF Power Quality Filter (an active power quality filters platform based on which the power converter for energy storage system has been realized)

BMS Battery Management System

FEAB Falbygdens Energi AB

ESM Energy Storage Module

AC Alternating Current

DC Direct Current

2 General

2.1 Hardware

The hardware used to develop the test is the Energy storage Module (ESM) property of FEAB installed in Falköping (Sweden) and the meters from Metrum which monitors the operation of the ESM. All the configurations and the methods for testing are described in [Ref 1].

2.2 System Settings

The following settings have been modified during the tests:

- Active power, kW;
- Reactive power, kVar;
- Higher order harmonics filtration current, A.

2.2.1 Measurements and calculations

The time synchronization between the PQFI- and Metrum measuring system has been done after the tests when all the data were put together.

Based on the measurements, the power flow on different locations of the power circuit and the energy consumption of the auxiliary equipment have been analysed.

Based on the data acquired by the measurement equipment (see Fig. 1), the losses in the different components are given by the following expressions:

- Inverter losses:

$$Ploss\_inv = \left| Ibat \cdot Ubat - \sqrt{3} \cdot UnRSRMS \cdot IpRRMS \right|$$

- Transformer losses:

$$Ploss\_trafo = \left| Pac1 - \sqrt{3} \cdot UnRSRMS \cdot IpRRMS \right|$$

- Power circuit losses:

$$Ploss\_main = Ploss\_inv + Ploss\_trafo$$

- Auxiliary circuit consumption:

$$P\_aux = Pac2$$

- Total losses:

$$Ploss = Ploss\_main + P\_aux$$

The performance of the system can be calculated as:

$$\eta_{chg} = \frac{Ibat \cdot Ubat}{Pac1 + Pac2}$$ (in charging mode)

$$\eta_{dchg} = \frac{Pac1}{Ibat \cdot Ubat + Pac2}$$ (in discharging mode)

3 Tests

The aim of the following tests is to identify the losses of the system for each operation mode taking into account the general specifications with 80kW in discharging mode (around 75kW expected on the grid) and 40kW in charging mode. The depth of discharge (DoD) is going to be set up from 75% till 15% because these are the values to take into account for the full cycle. Also, as the losses in the system are higher for higher DC voltage due to the inverter (mostly based on switching losses), small cycles around 75% with several values of active power and combinations of reactive power and harmonic mitigation have been carried out. These small cycles have been done in the same time period in order to evaluate the losses under the same conditions (temperature and air conditioning).

3.1 P, kW + Q, kvar + ITHD, A

In this test the reactive power (Q) compensation and higher order current harmonics filtration (ITHD) functions are both turned on. The PQF has been set to achieve a dynamic capacitance with cosfi=1 and all the harmonic components that the PQFI BESS converter is able to filter out from the grid have been selected.

3.1.1 Test procedure

The test procedure has been carried out as follows:

a) Cycling at high SOC:

- Charge or discharge the battery to SOC=75% with standard cycle (80kW for discharging or 40kW for charging) if the SOC differs from 75%. Rest time until battery has cooled down.

- Discharge the battery to SOC=74% with power set to 80 kW DC constant power, which will correspond to an approximate C-rate of (80)/135 = 0,592.
- Charge the batteries up to SOC=75% with 80 kW constant power.
- Discharge the battery to SOC=74% with power set to 60 kW DC constant power, which will correspond to an approximate C-rate of (60)/135 = 0,44.
- Charge the batteries up to SOC=75% with 60 kW constant power.
- Discharge the battery to SOC=74% with power set to 40 kW DC constant power, which will correspond to an approximate C-rate of (40)/135 = 0,296.
- Charge the batteries up to SOC=75% with 40 kW constant power.
- Discharge the battery to SOC=74% with power set to 20 kW DC constant power, which will correspond to an approximate C-rate of (20)/135 = 0,148.
- Charge the batteries up to SOC=75% with 20 kW constant power.
- Rest time until battery has cooled down. 30min minimum resting time.

b) Full cycle considering normal operation:

- Discharge down the batteries with 80 kW constant power during 1 hour. Setting output AC power at 80 kW ac will give approx. 77 kW discharge on the battery (because of the losses in the PQF, approx. 3 kW), corresponding to an approximate C-rate of 77/135 = 0.57.
- Rest time until battery has cooled down. 1 hour minimum resting time.
- Charge up the battery with 40kW for 2 hours, which will correspond to an approximate C-rate of (40)/135 = 0,296.
- Rest time until battery has cooled down. 1 hour minimum resting time.

3.1.2 Test results

Both the inverter losses and the transformer losses obtained during the cycling at high SOC test are shown in Fig. 2 and Fig. 3, respectively. As it can be observed, the inverter and transformer losses are higher when the system is charging the batteries than when the system is discharging them. Also as higher active power, as higher the losses are. In the case of the inverter, this is due to the fact to the conduction losses of the IGBTs. For the transformer, this variation is due to ohmic losses.

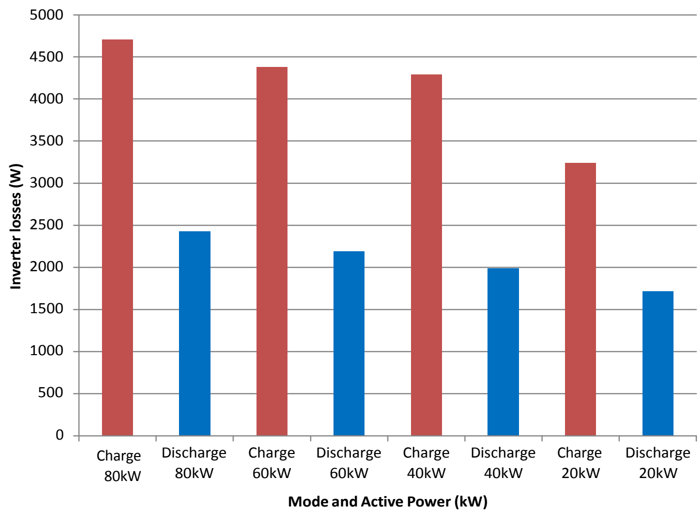

Figure 2. Inverter losses for the test when the system is charging and discharging the batteries and at the same time is compensating reactive power and mitigating harmonics.

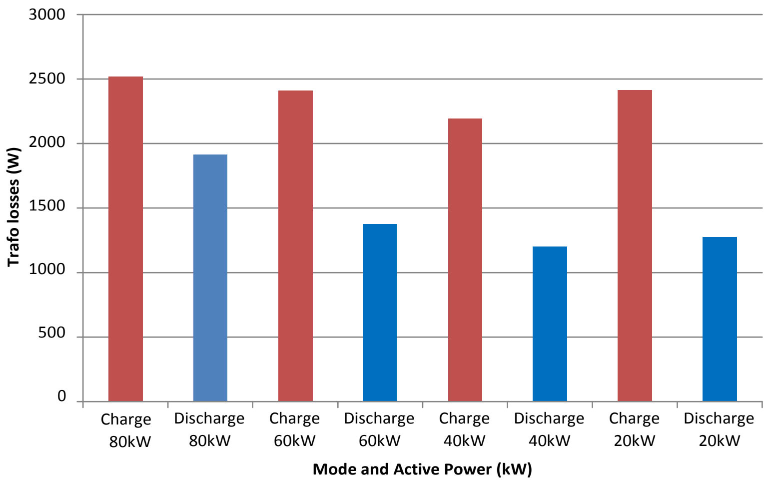

Figure 3. Transformer losses for the test when the system is charging and discharging the batteries and at the same time is compensating reactive power and mitigating harmonics

The performance of the power circuit is represented in Fig. 4, where it can be visualized how the performance is higher in discharging mode than in charging mode. Also the performance is higher for higher C-rate of the batteries. This is due to the fact that the ratio between the losses and the power absorbed (charging mode) or injected (discharging mode) from and to the grid is smaller for higher C-rates. The best performance has been obtained for the discharging mode at 80kW, while the lowest performance was in the case for charging mode at 20kW.

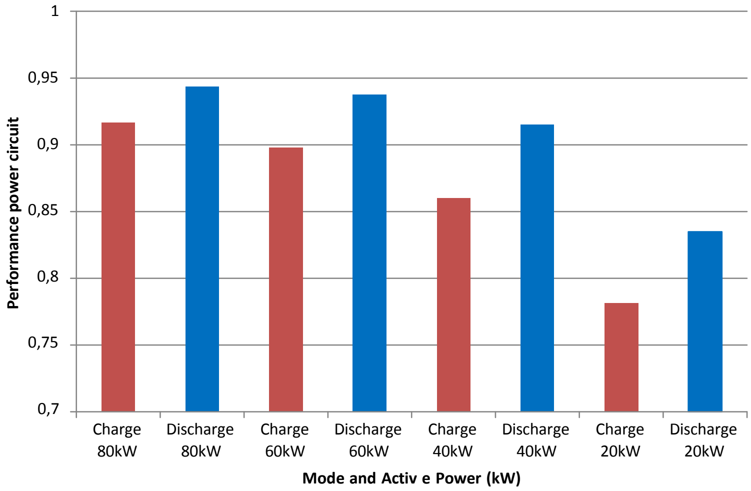

Figure 4. Performance of the main circuit for the test when the system is charging and discharging the batteries and at the same time is compensating reactive power and mitigating harmonics.

The auxiliary consumption of all the equipment of the system for each case as before is represented in Fig. 5, where the consumption is more or less constant for each case with a value approximately equal to 2.2kW. As the test has been done in a period of time with no variations in the external conditions (temperature), the consumption has remained quite constant. Therefore there is not any additional factor that affects the auxiliary consumption regarding the operation mode or the level of active power.

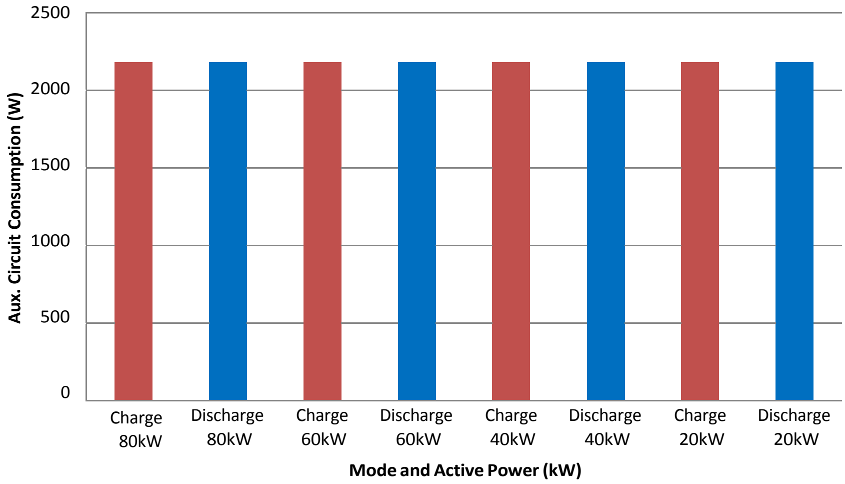

Figure 5. Consumption of the auxiliary circuit for the test when the system is charging and discharging the batteries and at the same time is compensating reactive power and mitigating harmonics.

Taking into consideration the losses of the main circuit and the consumption of the auxiliary circuit, the total losses of the system and the total performance are represented in Fig.6 and Fig. 7, respectively. The total losses of the system, as it can be observed in Fig. 6, are higher in charging mode than in discharging mode as expected having a look to the abovementioned losses in the inverter and transformer. The highest total performance of the system is for the case of discharging mode at 80kW with a value of 92% and the lowest is for charging mode at 20kW with a value of 72%.

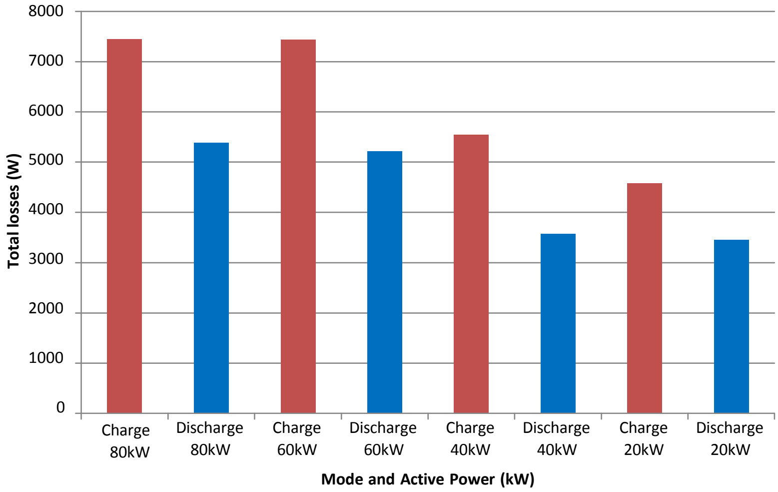

Figure 6. Total losses of the system for the test when the system is charging and discharging the batteries and at the same time is compensating reactive power and mitigating harmonics.

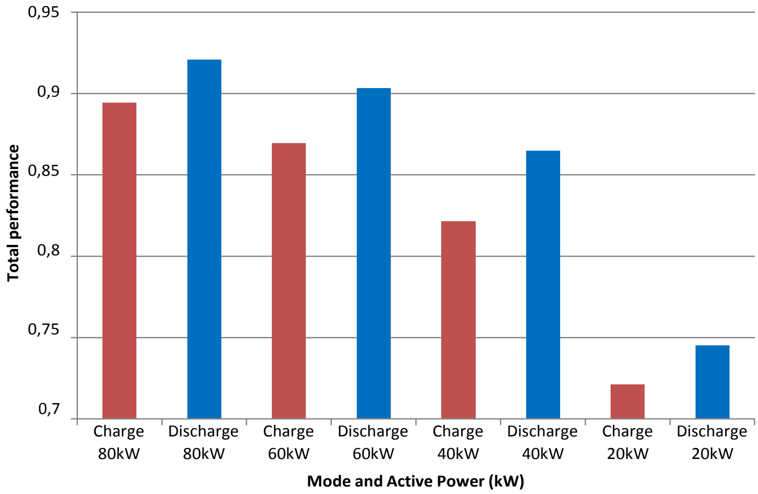

Figure 7. Total performance of the system for the test when the system is charging and discharging the batteries and at the same time is compensating reactive power and mitigating harmonics.

In the case of the full cycle considering normal operation of the system, discharging from 75%SOC until 15% at 80kW during 1 hour and charging till 75%SOC at 40kW during 2 hours, for the variation of the SOC, the inverter losses, transformer losses and total losses of the power circuit are represented in Fig. 8, Fig. 9 and Fig. 10, respectively.

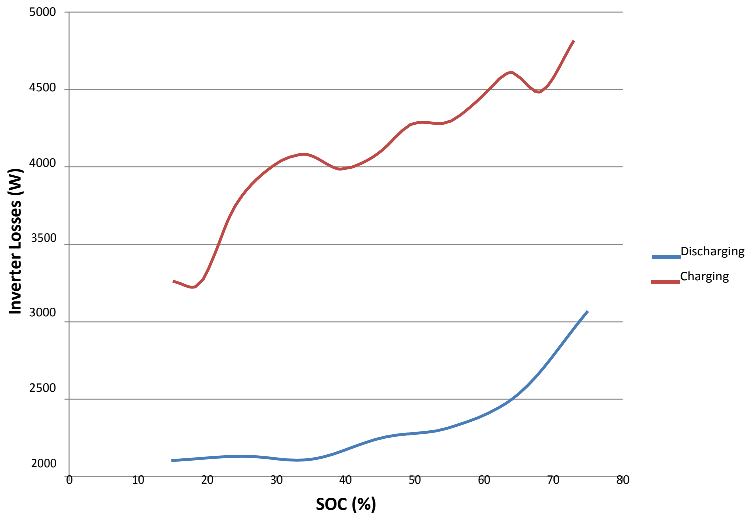

Figure 8. Inverter losses variation with the SOC for the test when the system is charging and discharging the batteries and at the same time is compensating reactive power and mitigating harmonics.

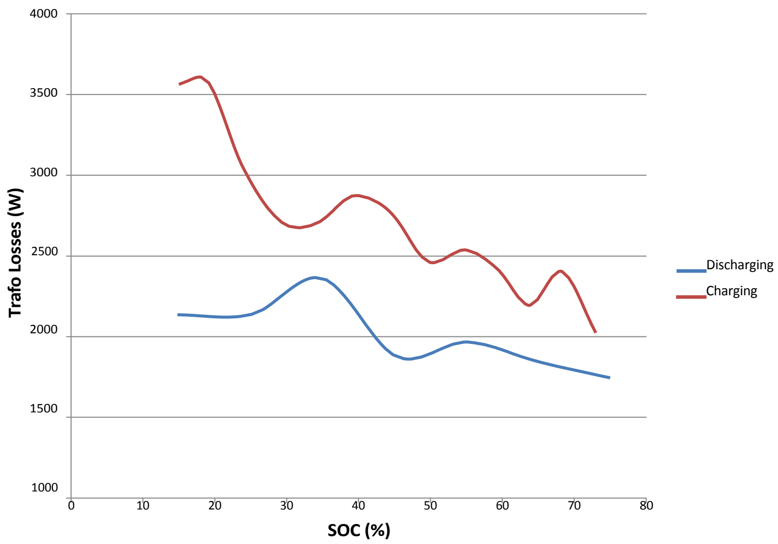

Figure 9. Transformer losses variation with the SOC for the test when the system is charging and discharging the batteries and at the same time is compensating reactive power and mitigating harmonics.

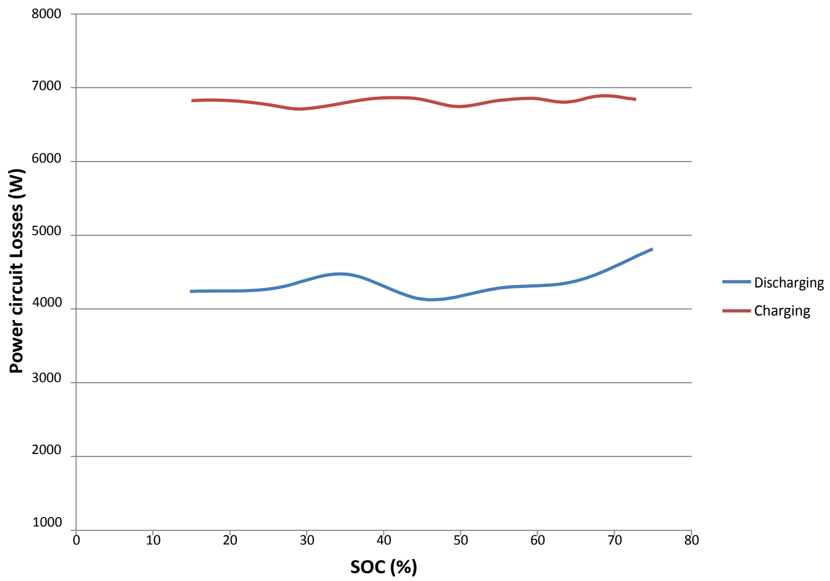

Figure 10. Main circuit losses variation with the SOC for the test when the system is charging and discharging the batteries and at the same time is compensating reactive power and mitigating harmonics.

As mentioned before, the inverter losses are higher for high SOC due to the switching losses, which are mainly based on the DC voltage applied to the inverter. For the case of the transformer, the losses are higher for low SOC due to ohmic losses. If one takes a look to the main circuit losses, it can be observed how the losses remain more or less constant for the discharging and charging processes.

If the system is charged during 2 hours, it can be observed that that SOC reaches 72% instead of 75% as the initial SOC before discharging. This is due to the round trip efficiency of the batteries. This value is higher than 96.5% as the battery manufacturer establishes.

As seen before, the auxiliary consumption is independent from the operation of the system. Therefore, considering the auxiliary consumption, the losses of the main circuit and the round trip efficiency for the full cycle, the performance of the system in the case this is compensating reactive power and harmonics at its full capacity, is 76%.

3.2 P, kW + Q, kvar

In this test the reactive power (Q) is turned on. The PQF has been set to achieve a dynamic capacitance with cosfi=1.

3.2.1 Test procedure

The test procedure has been carried out as follows:

a) Cycling at high SOC:

- Deselect all the harmonics in the PQF Manager and set the reactive compensation in Dynamic capacitance with the target of cosfi=1.
- Charge or discharge the battery to SOC=75% with standard cycle (80kW for discharging or 40kW for charging) if the SOC differs from 75%. Rest time until battery has cooled down.
- Discharge the battery to SOC=74% with power set to 80 kW DC constant power, which will correspond to an approximate C-rate of (80)/135 = 0,592.
- Charge the batteries up to SOC=75% with 80 kW constant power.
- Discharge the battery to SOC=74% with power set to 60 kW DC constant power, which will correspond to an approximate C-rate of (60)/135 = 0,44.
- Charge the batteries up to SOC=75% with 60 kW constant power.
- Discharge the battery to SOC=74% with power set to 40 kW DC constant power, which will correspond to an approximate C-rate of (40)/135 = 0,296.
- Charge the batteries up to SOC=75% with 40 kW constant power.
- Discharge the battery to SOC=74% with power set to 20 kW DC constant power, which will correspond to an approximate C-rate of (20)/135 = 0,148.
- Charge the batteries up to SOC=75% with 20 kW constant power.
- Rest time until battery has cooled down. 30min minimum resting time.

b) Full cycle considering normal operation:

- Discharge down the batteries with 80 kW constant power during 1 hour. Setting output AC power at 80 kW ac will give approx. 77 kW discharge on the battery (because of the losses in the PQF, approx. 3 kW), corresponding to an approximate C-rate of 77/135 = 0.57.
- Rest time until battery has cooled down. 1 hour minimum resting time.
- Charge up the battery with 40kW for 2 hours, which will correspond to an approximate C-rate of (40)/135 = 0,296.
- Rest time until battery has cooled down. 1 hour minimum resting time.

3.2.2 Test results

Both the inverter losses and the transformer losses obtained during the cycling at high SOC test are shown in Fig. 11 and Fig. 12, respectively. As for the test shown in 3.1, the inverter and transformer losses are higher when the system is charging the batteries than when the system is discharging them. Also as higher active power, as higher the losses are.

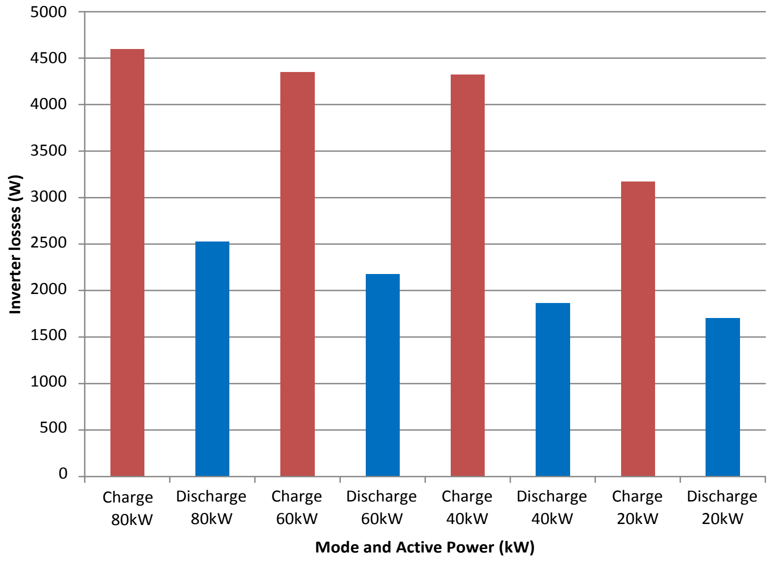

Figure 11. Inverter losses for the test when the system is charging and discharging the batteries and at the same time is compensating reactive power.

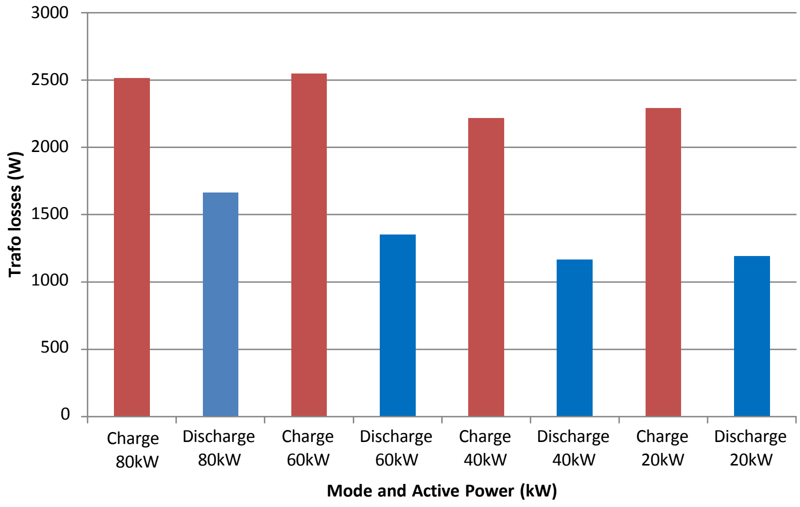

Figure 12. Transformer losses for the test when the system is charging and discharging the batteries and at the same time is compensating reactive power.

The performance of the power circuit is represented in Fig. 13, where it can be visualized how the performance is higher in discharging mode than in charging mode. Also the performance is higher for higher C-rate of the batteries. The best performance has been obtained for the discharging mode at 80kW (94%), while the lowest performance was in the case for charging mode at 20kW (77%).

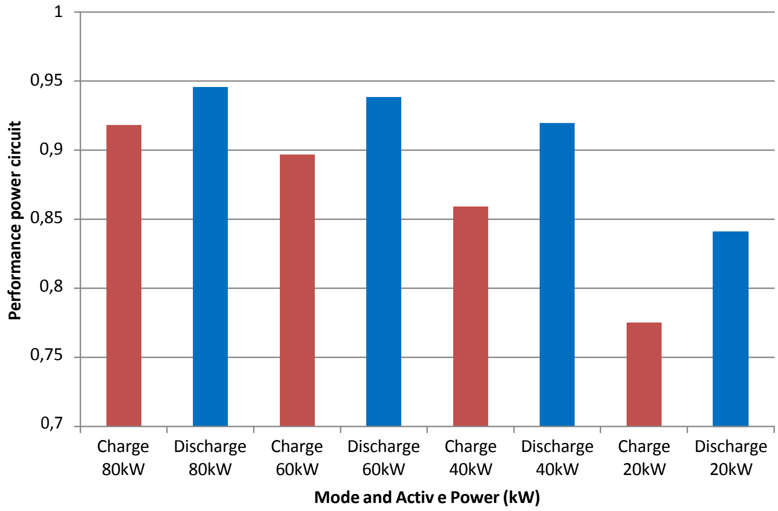

Figure 13. Performance of the main circuit for the test when the system is charging and discharging the batteries and at the same time is compensating reactive power.

The auxiliary consumption of all the equipment of the system for each case as before is represented in Fig. 14, where the consumption is more or less constant for each case with a value approximately equal to 1.8kW. In this test the auxiliary consumption is lower (400W less) than for above presented test with reactive and harmonic compensation. This might be due to the fact that the air conditioning were not working with the same power as before.

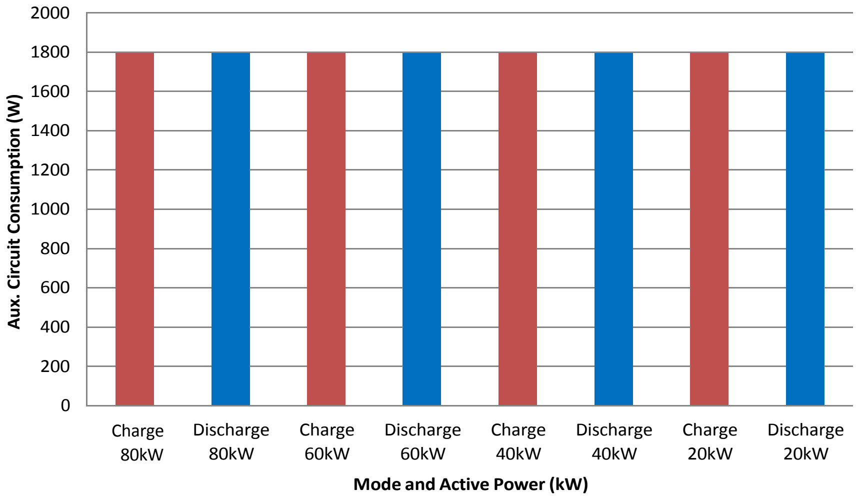

Figure 14. Consumption of the auxiliary circuit for the test when the system is charging and discharging the batteries and at the same time is compensating reactive power.

Taking into consideration the losses of the main circuit and the consumption of the auxiliary circuit, the total losses of the system and the total performance are represented in Fig.15 and Fig. 16, respectively. In this test, the total losses are 400W lower than the test done before and this difference is the same than the one in the auxiliary consumption. Therefore the losses are basically the same for the test presented here and the one in 3.1.

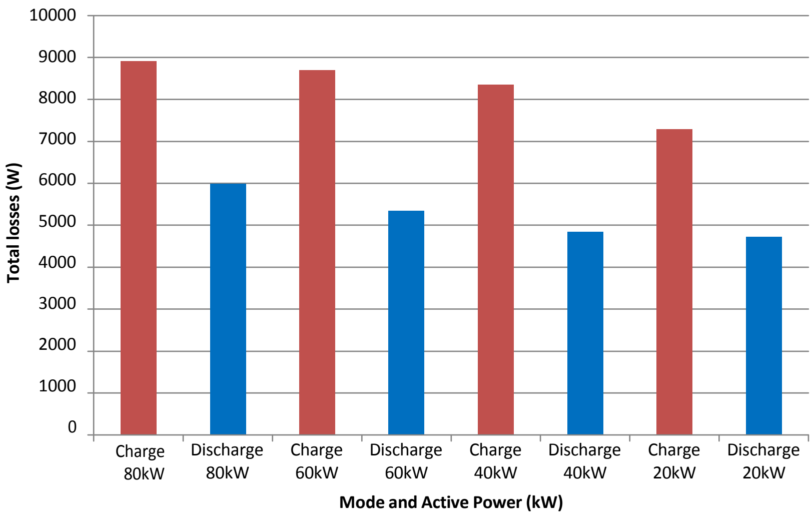

Figure 15. Total losses of the system for the test when the system is charging and discharging the batteries and at the same time is compensating reactive power and mitigating harmonics.

The highest total performance of the system is for the case of discharging mode at 80kW with a value of 92% and the lowest is for charging mode at 20kW with a value of 72%.

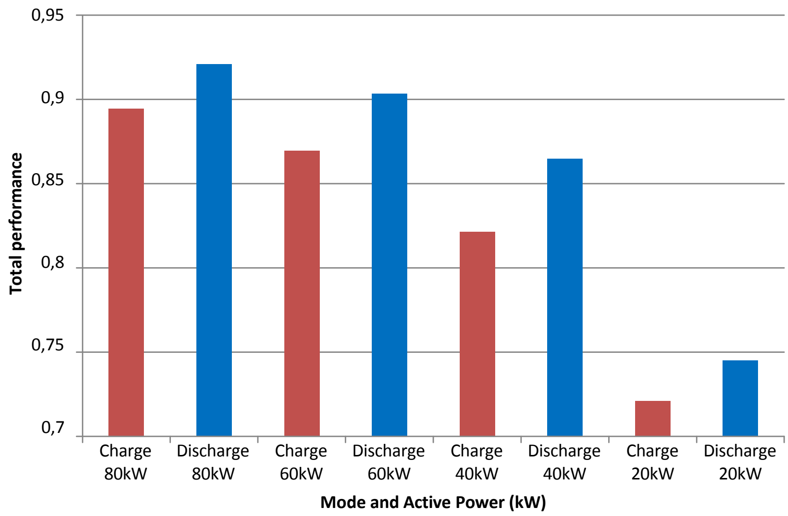

Figure 16. Total performance of the system for the test when the system is charging and discharging the batteries and at the same time is compensating reactive power and mitigating harmonics.

In the case of the full cycle considering normal operation of the system, discharging from 75%SOC until 15% at 80kW during 1 hour and charging till 75%SOC at 40kW during 2 hours, for the variation of the SOC, the inverter losses, transformer losses and total losses of the power circuit are represented in Fig. 17, Fig. 18 and Fig. 19, respectively.

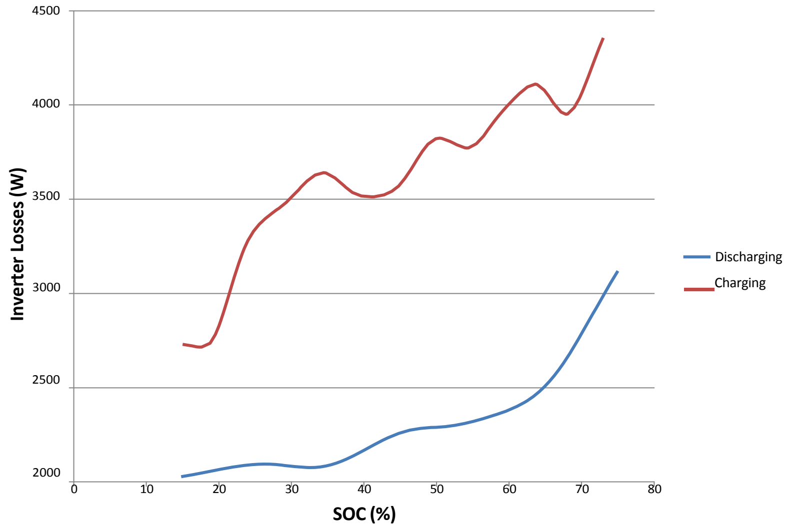

Figure 17. Inverter losses variation with the SOC for the test when the system is charging and discharging the batteries and at the same time is compensating reactive power.

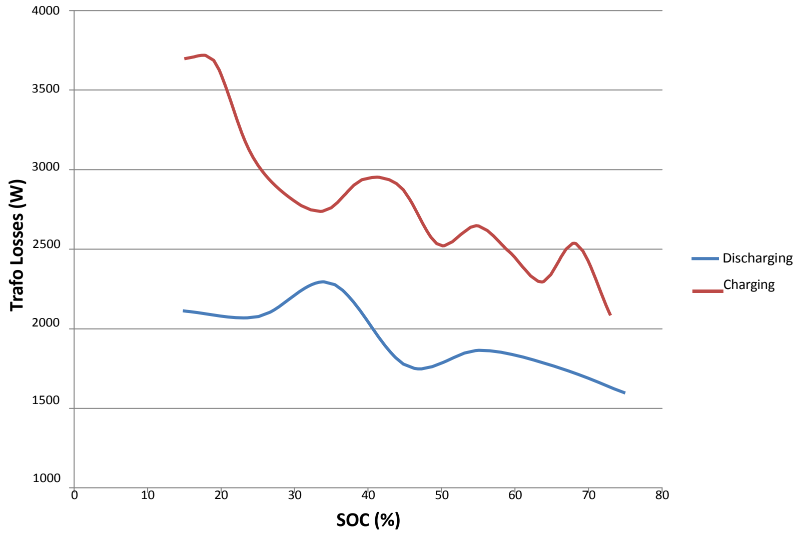

Figure 18. Transformer losses variation with the SOC for the test when the system is charging and discharging the batteries and at the same time is compensating reactive power.

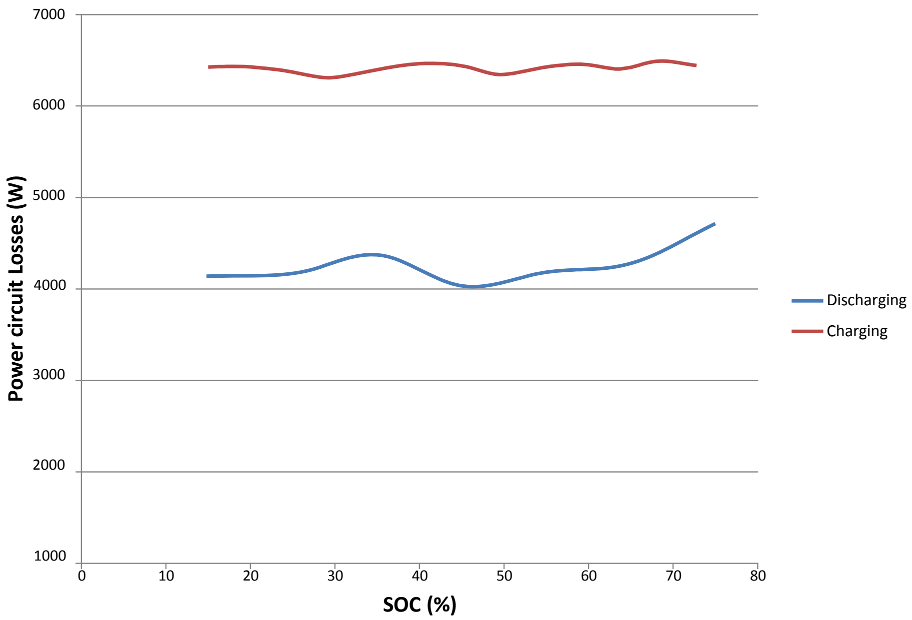

Figure 19. Main circuit losses variation with the SOC for the test when the system is charging and discharging the batteries and at the same time is compensating reactive.

As observed before, the inverter, transformer and therefore main circuit losses are higher for charging mode than for discharging mode.

If the system is charged during 2 hours, it can be observed that that SOC reaches 72% instead of 75% as the initial SOC before discharging. This is due to the round trip efficiency of the batteries. This value is higher than 96.5% as the battery manufacturer establishes.

As seen before, the auxiliary consumption is independent from the operation of the system. Therefore, considering the auxiliary consumption, the losses of the main circuit and the round trip efficiency for the full cycle, the performance of the system in the case when it is compensating reactive power, is 76.5%. The difference in performance around 0.5% is due to the difference in the auxiliary consumption above mentioned.

3.3 P, kW + ITHD, A

In this test the reactive power (Q) is turned off and the inverter is mitigating harmonics in order to cancel the present ones in the grid.

3.3.1 Test procedure

The test procedure has been carried out as follows:

a) Cycling at high SOC:

- Switch-off the reactive power compensation function and select all possible harmonic components that could be filtered out in the PQF Manager.
- Charge or discharge the battery to SOC=75% with standard cycle (80kW for discharging or 40kW for charging) if the SOC differs from 75%. Rest time until battery has cooled down.
- Discharge the battery to SOC=74% with power set to 80 kW DC constant power, which will correspond to an approximate C-rate of (80)/135 = 0,592.
- Charge the batteries up to SOC=75% with 80 kW constant power.
- Discharge the battery to SOC=74% with power set to 60 kW DC constant power, which will correspond to an approximate C-rate of (60)/135 = 0,44.
- Charge the batteries up to SOC=75% with 60 kW constant power.
- Discharge the battery to SOC=74% with power set to 40 kW DC constant power, which will correspond to an approximate C-rate of (40)/135 = 0,296.
- Charge the batteries up to SOC=75% with 40 kW constant power.
- Discharge the battery to SOC=74% with power set to 20 kW DC constant power, which will correspond to an approximate C-rate of (20)/135 = 0,148.
- Charge the batteries up to SOC=75% with 20 kW constant power.
- Rest time until battery has cooled down. 30min minimum resting time.

b) Full cycle considering normal operation:

- Discharge down the batteries with 80 kW constant power during 1 hour. Setting output AC power at 80 kW ac will give approx. 77 kW discharge on the battery (because of the losses in the PQF, approx. 3 kW), corresponding to an approximate C-rate of 77/135 = 0.57.
- Rest time until battery has cooled down. 1 hour minimum resting time.
- Charge up the battery with 40kW for 2 hours, which will correspond to an approximate C-rate of (40)/135 = 0,296.
- Rest time until battery has cooled down. 1 hour minimum resting time.

3.3.2 Test results

Both the inverter losses and the transformer losses obtained during the cycling at high SOC test are shown in Fig. 20 and Fig. 21, respectively. As for the test shown in 3.1 and 3.2, the inverter and transformer losses are higher when the system is charging the batteries than when the system is discharging them. Also as higher active power, as higher the losses are.

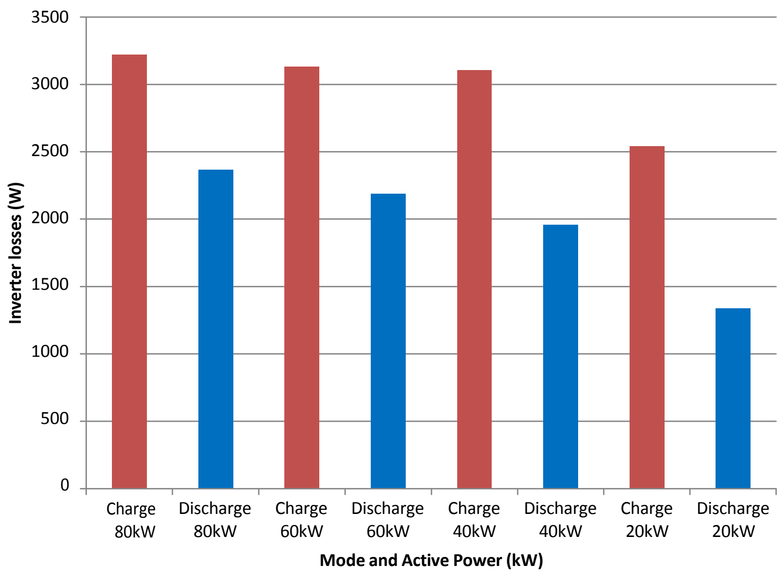

Figure 20. Inverter losses for the test when the system is charging and discharging the batteries and at the same time is compensating harmonics.

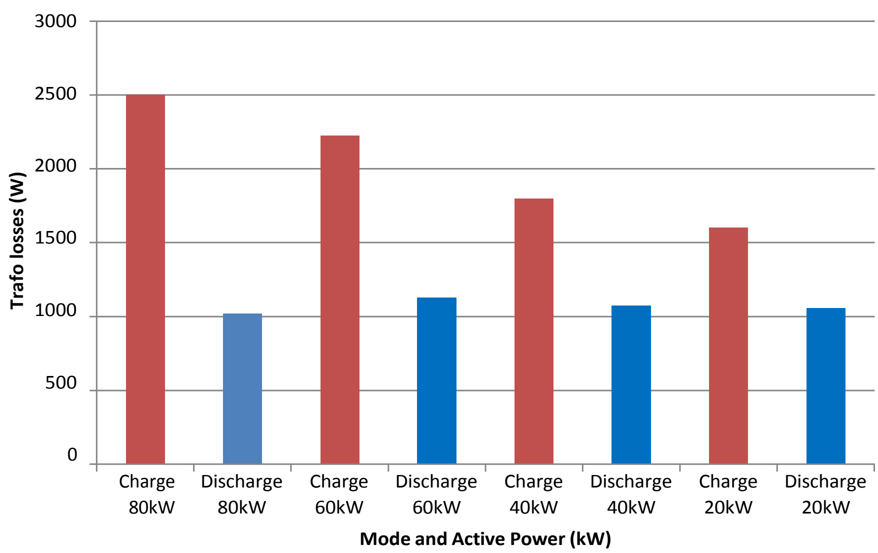

Figure 21. Transformer losses for the test when the system is charging and discharging the batteries and at the same time is compensating harmonics.

The performance of the power circuit is represented in Fig. 22, where it can be visualized how the performance is higher in discharging mode than in charging mode. Also the performance is higher for higher C-rate of the batteries. The best performance has been obtained for the discharging mode at 80kW (higher than 95%), while the lowest performance was in the case for charging mode at 20kW (83%).

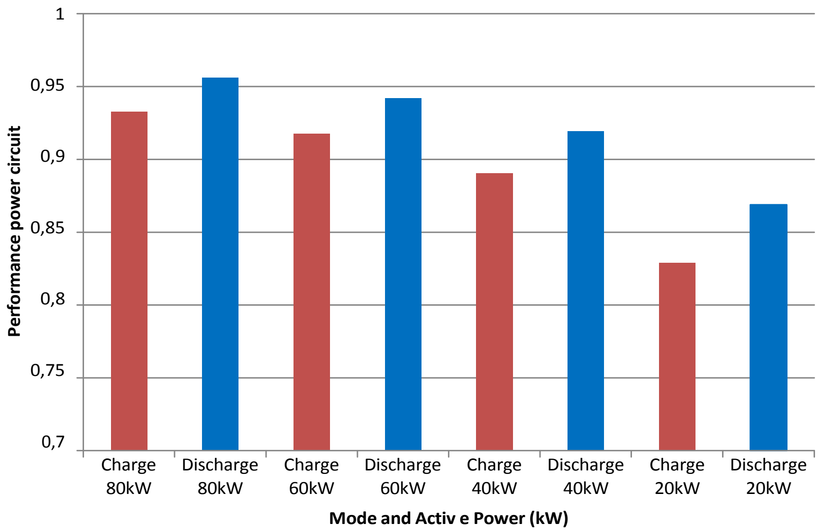

Figure 22. Performance of the main circuit for the test when the system is charging and discharging the batteries and at the same time is compensating harmonics.

The auxiliary consumption of all the equipment of the system for each case as before is represented in Fig. 23, where the consumption is more or less constant for each case with a value approximately equal to 2kW.

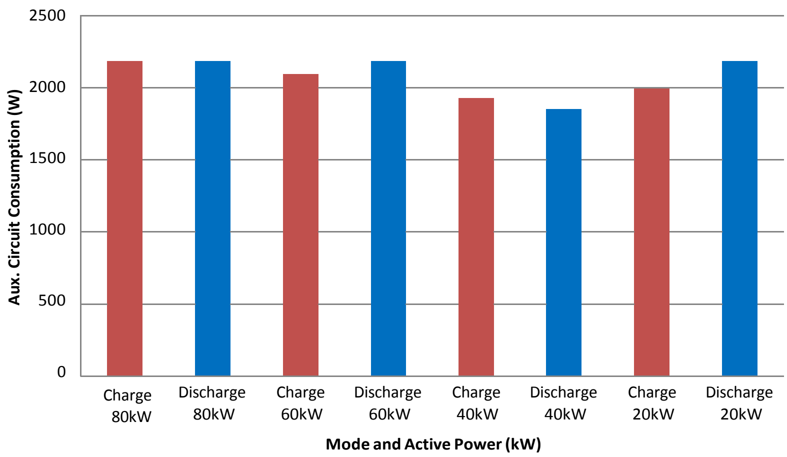

Figure 23. Consumption of the auxiliary circuit for the test when the system is charging and discharging the batteries and at the same time is compensating harmonics.

Taking into consideration the losses of the main circuit and the consumption of the auxiliary circuit, the total losses of the system and the total performance are represented in Fig.24 and Fig. 25, respectively. In this test, the total losses are 1kW lower than for the two test done before.

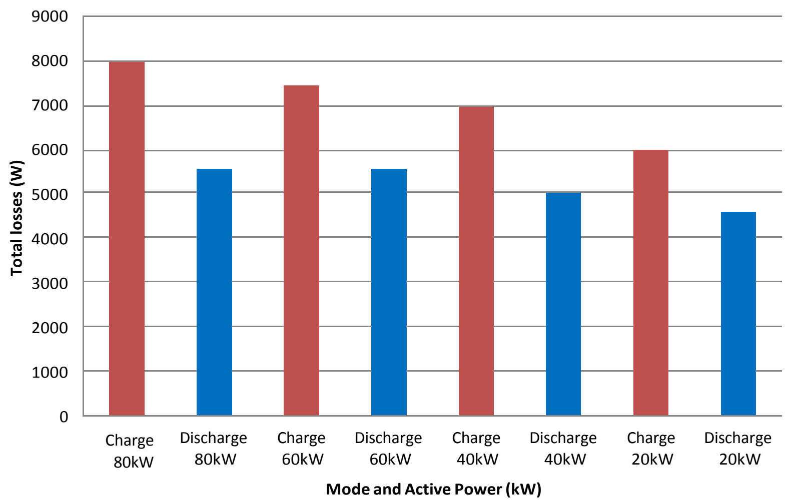

Figure 24. Total losses of the system for the test when the system is charging and discharging the batteries and at the same time is compensating reactive power and mitigating harmonics.

The highest total performance of the system is for the case of discharging mode at 80kW with a value of 93% and the lowest is for charging mode at 20kW with a value of 76%.

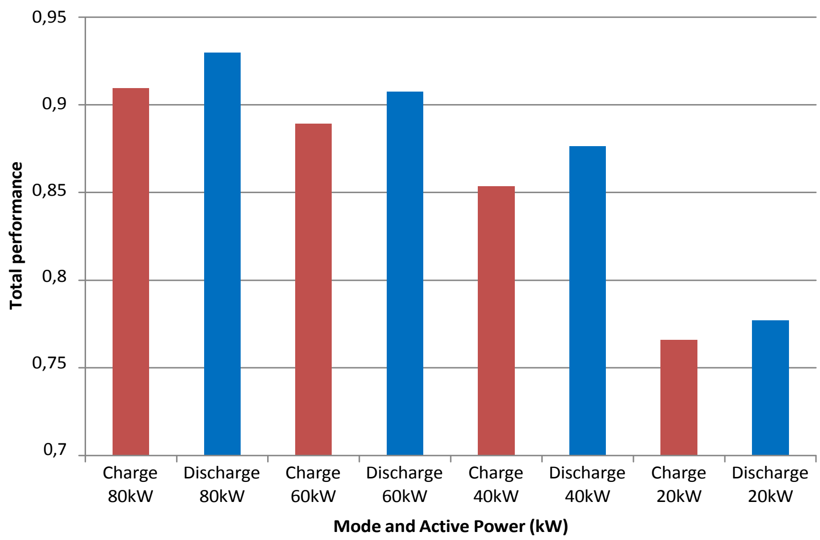

Figure 25. Total performance of the system for the test when the system is charging and discharging the batteries and at the same time is compensating reactive power and mitigating harmonics.

In the case of the full cycle considering normal operation of the system, discharging from 75%SOC until 15% at 80kW during 1 hour and charging till 75%SOC at 40kW during 2 hours, for the variation of the SOC, the inverter losses, transformer losses and total losses of the power circuit are represented in Fig. 26, Fig. 27 and Fig. 28, respectively.

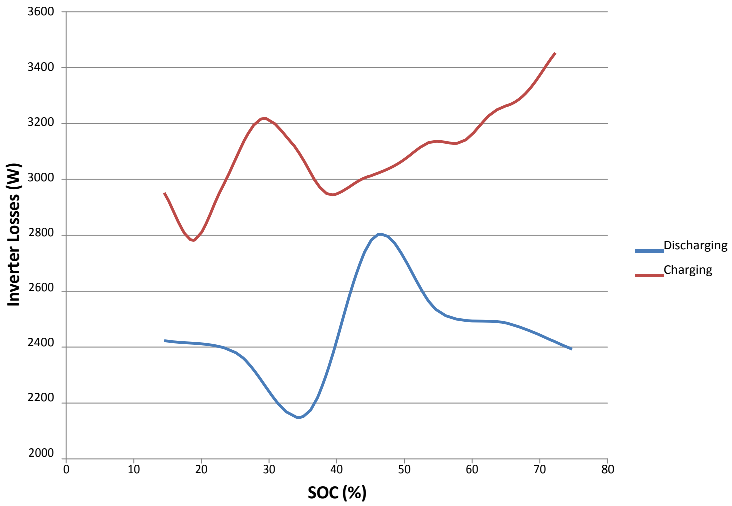

Figure 26. Inverter losses variation with the SOC for the test when the system is charging and discharging the batteries and at the same time is compensating harmonics.

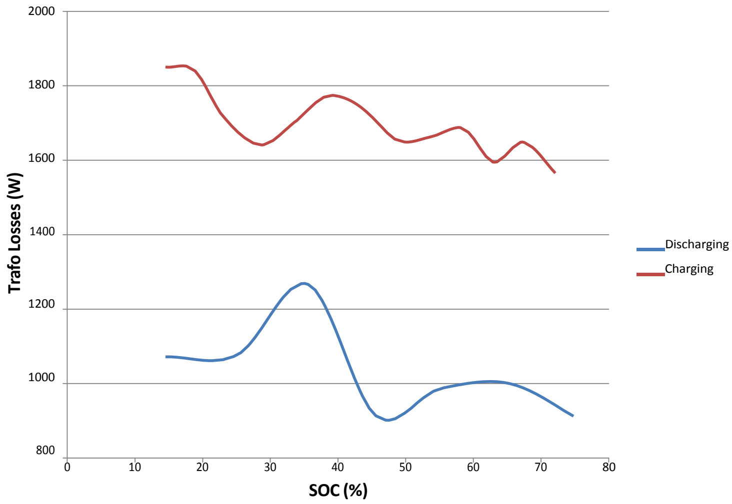

Figure 27. Transformer losses variation with the SOC for the test when the system is charging and discharging the batteries and at the same time is compensating harmonics.

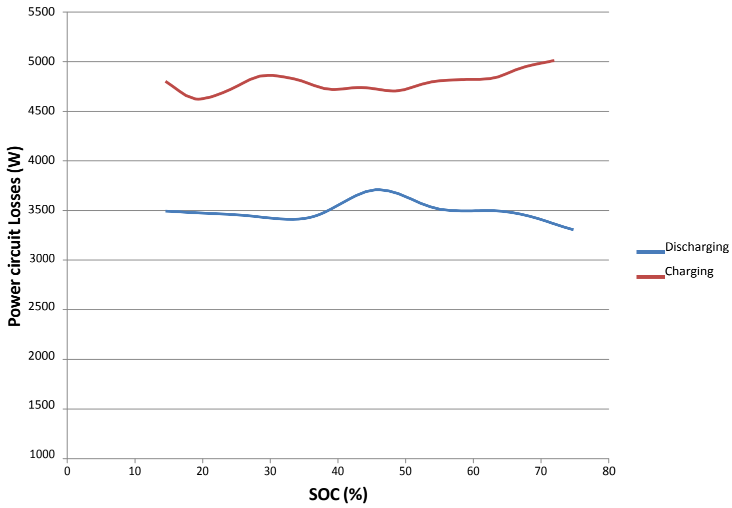

Figure 28. Main circuit losses variation with the SOC for the test when the system is charging and discharging the batteries and at the same time is compensating harmonics.

As observed before, the inverter, transformer and therefore main circuit losses are higher for charging mode than for discharging mode. For the inverter and transformer losses, it can be observed a wrong measurement for the state of charge of 30%, because the measure is not on the normal trend of the losses variation.

If the system is charged during 2 hours, it can be observed that that SOC reaches 73% instead of 75% as the initial SOC before discharging. This is due to the round trip efficiency of the batteries. This value is higher than 96.5% as the battery manufacturer establishes.

As seen before, the auxiliary consumption is independent from the operation of the system. Therefore, considering the auxiliary consumption, the losses of the main circuit and the round trip efficiency for the full cycle, the performance of the system in the case when it is compensating harmonics, is 80%. This value is higher than the obtained when the system is compensating reactive power.

3.4 P, kW

In this test the reactive power (Q) and the harmonic mitigation are both turned off. Therefore, the inverter is just charging and discharging the batteries without any other additional feautre.

3.4.1 Test procedure

The test procedure has been carried out as follows:

a) Cycling at high SOC:

- Switch-off the reactive power compensation function and the harmonic compensation in the PQF Manager.

- Charge or discharge the battery to SOC=75% with standard cycle (80kW for discharging or 40kW for charging) if the SOC differs from 75%. Rest time until battery has cooled down.
- Discharge the battery to SOC=74% with power set to 80 kW DC constant power, which will correspond to an approximate C-rate of (80)/135 = 0,592.
- Charge the batteries up to SOC=75% with 80 kW constant power.
- Discharge the battery to SOC=74% with power set to 60 kW DC constant power, which will correspond to an approximate C-rate of (60)/135 = 0,44.
- Charge the batteries up to SOC=75% with 60 kW constant power.
- Discharge the battery to SOC=74% with power set to 40 kW DC constant power, which will correspond to an approximate C-rate of (40)/135 = 0,296.
- Charge the batteries up to SOC=75% with 40 kW constant power.
- Discharge the battery to SOC=74% with power set to 20 kW DC constant power, which will correspond to an approximate C-rate of (20)/135 = 0,148.
- Charge the batteries up to SOC=75% with 20 kW constant power.
- Rest time until battery has cooled down. 30min minimum resting time.

b) Full cycle considering normal operation:

- Discharge down the batteries with 80 kW constant power during 1 hour. Setting output AC power at 80 kW ac will give approx. 77 kW discharge on the battery (because of the losses in the PQF, approx. 3 kW), corresponding to an approximate C-rate of 77/135 = 0.57.
- Rest time until battery has cooled down. 1 hour minimum resting time.
- Charge up the battery with 40kW for 2 hours, which will correspond to an approximate C-rate of (40)/135 = 0,296.
- Rest time until battery has cooled down. 1 hour minimum resting time.

3.4.2 Test results

The inverter losses and the transformer losses obtained during the cycling at high SOC test are shown in Fig. 29 and Fig. 30, respectively. As for the test shown in 3.1, 3.2 and 3.3, the inverter and transformer losses are higher when the system is charging the batteries than when the system is discharging them. Also as higher active power, as higher the losses are. In this case it can be observed how the losses in the transformer are higher for charging at 60kW than at 80kW. This can be due to a wrong measurement.

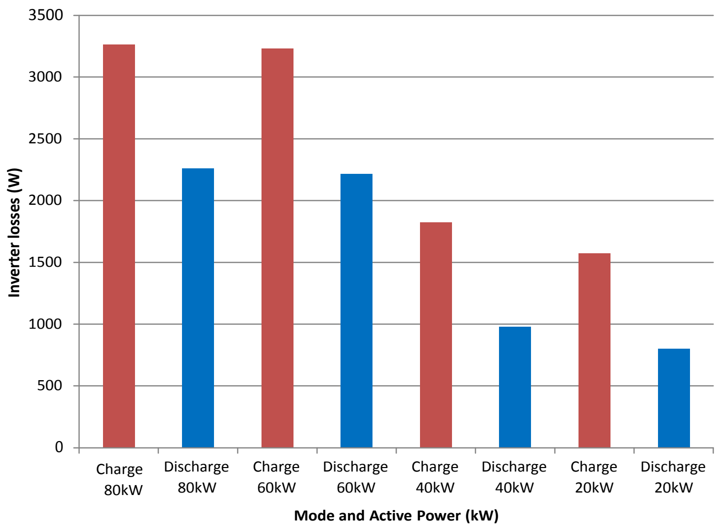

Figure 29. Inverter losses for the test when the system is charging and discharging the batteries.

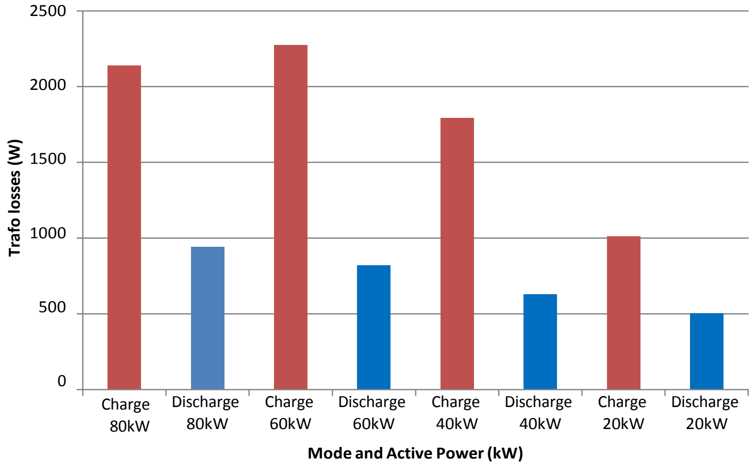

Figure 30. Transformer losses for the test when the system is charging and discharging the batteries.

The performance of the power circuit is represented in Fig. 31, where it can be visualized how the performance is higher in discharging mode than in charging mode. Also the performance is higher for higher C-rate of the batteries. The best performance has been obtained for the discharging mode at 80kW (almost 96%), while the lowest performance was in the case for charging mode at 20kW (88%).

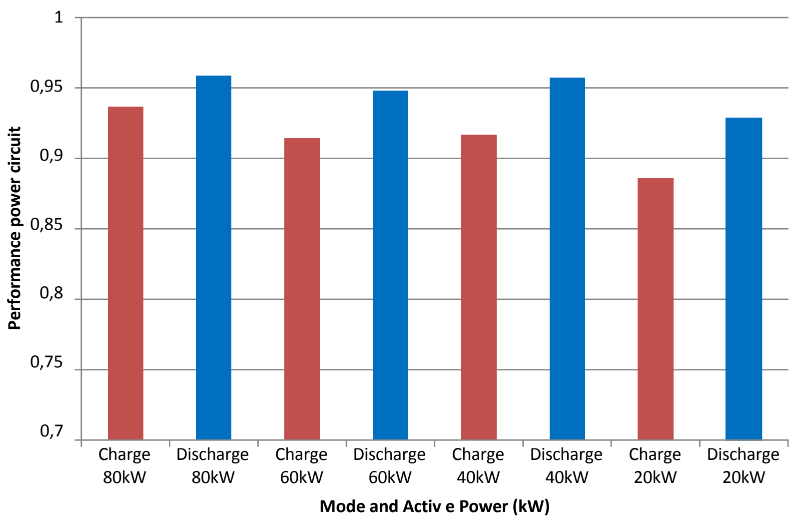

Figure 31. Performance of the main circuit for the test when the system is charging and discharging the batteries and at the same time is compensating harmonics.

The auxiliary consumption of all the equipment of the system for each case as before is represented in Fig. 32, where the consumption is more or less constant for each case with a value approximately equal to 2kW.

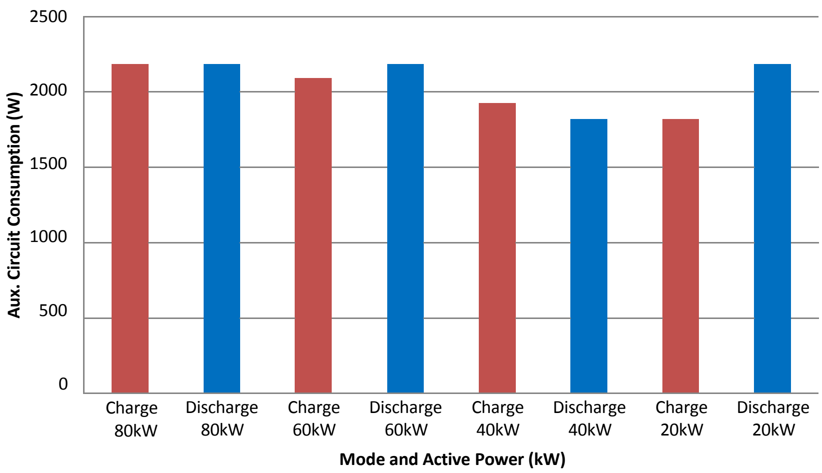

Figure 32. Consumption of the auxiliary circuit for the test when the system is charging and discharging the batteries.

Taking into consideration the losses of the main circuit and the consumption of the auxiliary circuit, the total losses of the system and the total performance are represented in Fig.33 and Fig. 34, respectively. In this test, the total losses are 1kW lower than for the two test shown in 3.1 and 3.2.

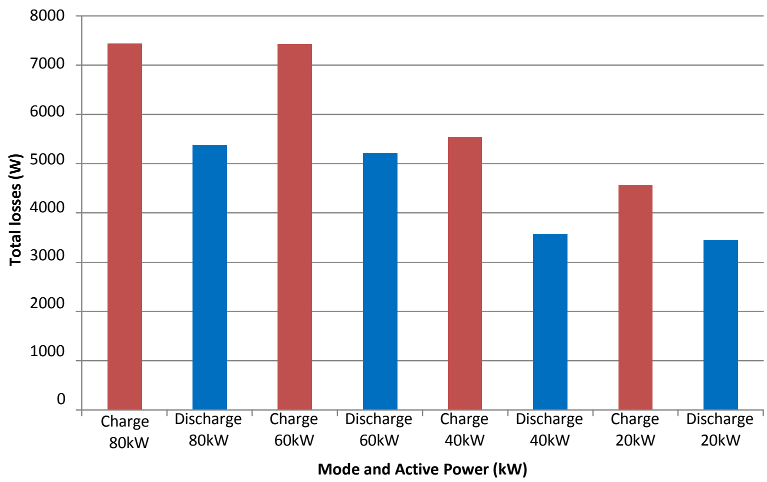

Figure 33. Total losses of the system for the test when the system is charging and discharging the batteries.

The highest total performance of the system is for the case of discharging mode at 80kW with a value of 93.2% and the lowest is for charging mode at 20kW with a value of 81.4%.

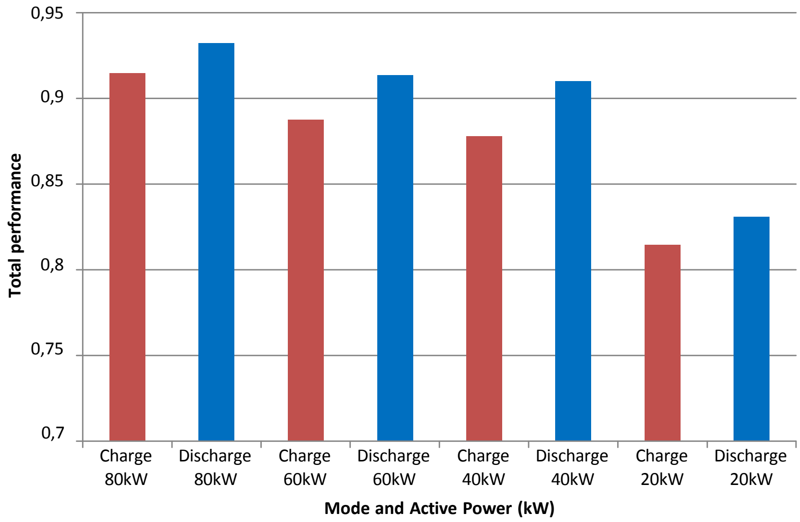

Figure 34. Total performance of the system for the test when the system is charging and discharging the batteries.

In the case of the full cycle considering normal operation of the system, discharging from 75%SOC until 15% at 80kW during 1 hour and charging till 75%SOC at 40kW during 2 hours, for the variation of the SOC, the inverter losses, transformer losses and total losses of the power circuit are represented in Fig. 35, Fig. 36 and Fig. 37, respectively.

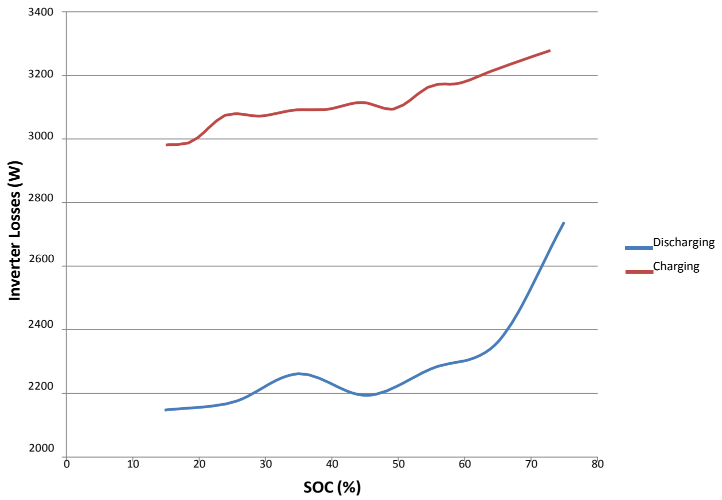

Figure 35. Inverter losses variation with the SOC for the test when the system is charging and discharging the batteries.

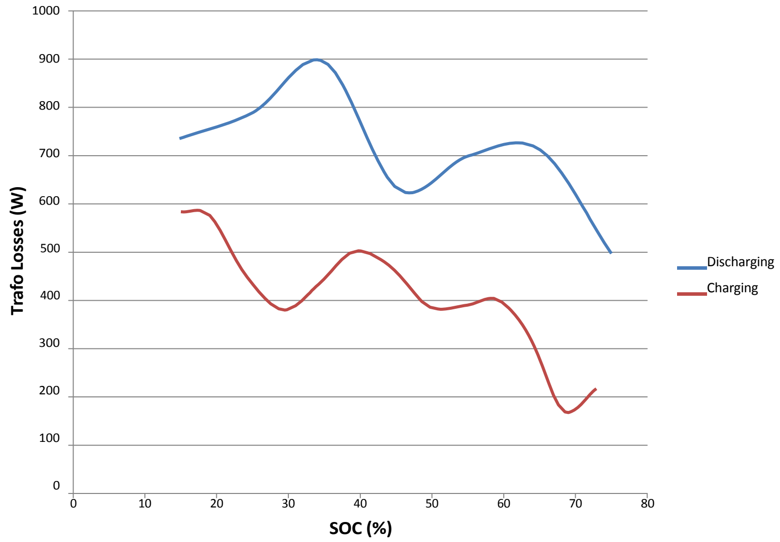

Figure 36. Transformer losses variation with the SOC for the test when the system is charging and discharging the batteries.

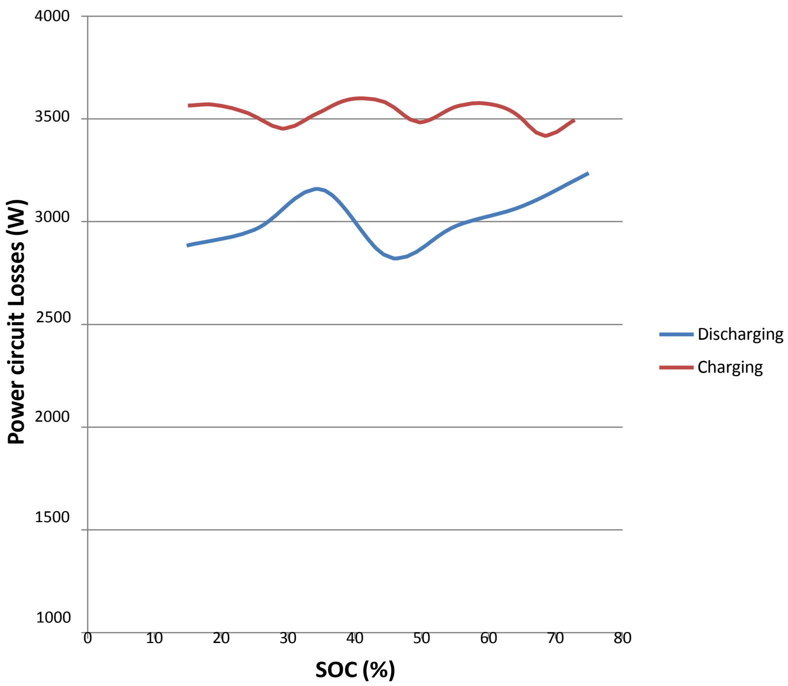

Figure 37. Main circuit losses variation with the SOC for the test when the system is charging and discharging the batteries.

As observed before, the inverter, transformer and therefore main circuit losses are higher for charging mode than for discharging mode.

If the system is charged during 2 hours, it can be observed that that SOC reaches 73% instead of 75% as the initial SOC before discharging. This is due to the round trip efficiency of the batteries. This value is higher than 96.5% as the battery manufacturer establishes.

As seen before, the auxiliary consumption is independent from the operation of the system. Therefore, considering the auxiliary consumption, the losses of the main circuit and the round trip efficiency for the full cycle, the performance of the system in the case when it is compensating harmonics, is 80.2%. This value is higher than the obtained when the system is compensating reactive power.

3.5 Q, kvar + ITHD, A

In this test the reactive power (Q) and the harmonic mitigation are both turned on. It is important to remark that no active power flow exits between the grid and the batteries and vice versa. This mode is the same mode as when the system is running in stand-by.

3.5.1 Test procedure

- Set up the I_{THD} to max in the PQF Manager.

- Change the Q set-point to 100 kVAr in the PQF Manager
- Run the system during predefined time period (e.g. 2 min) in order to store the data.
- Change the Q set-point to 90 kVAr in the PQF Manager.
- Run the system during predefined time period (e.g. 2 min) in order to store the data.
- Change the Q set-point to 66 kvar in the PQF Manager.
- Run the system during predefined time period (e.g. 2 min) in order to store the data.

3.5.2 Test results

As in this case there is not active power flow to and from the batteries, the active power consumed from the grid is based on the losses in the inverter and transformer in order to compensate reactive power and mitigate high order harmonics in the grid.

On Fig. 38, the total consumption from the grid can be observed for the three cases presented in the test procedure. As higher the level of reactive compensation, as higher the consumption on the system.

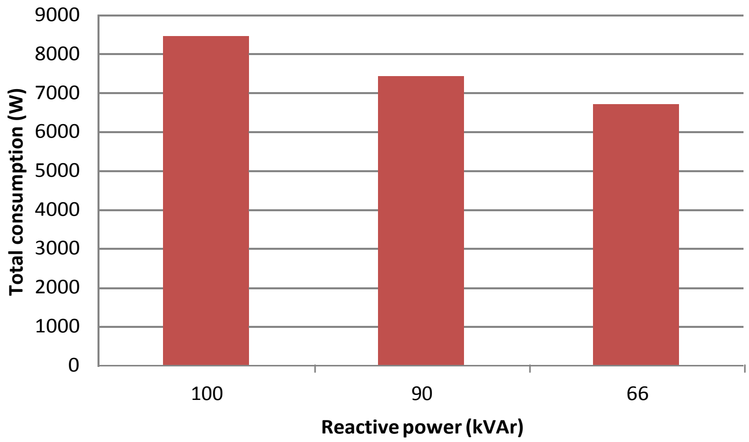

Figure 38. Total consumption for the test when the system is compensating reactive power and mitigating harmonics.

In Fig. 39, the performance of the system in terms of reactive power injected to the grid is shown. The maximum performance is higher than 99.2% for the case of injecting 66kVAr and 98.6% for the case of injecting 100kVAr.

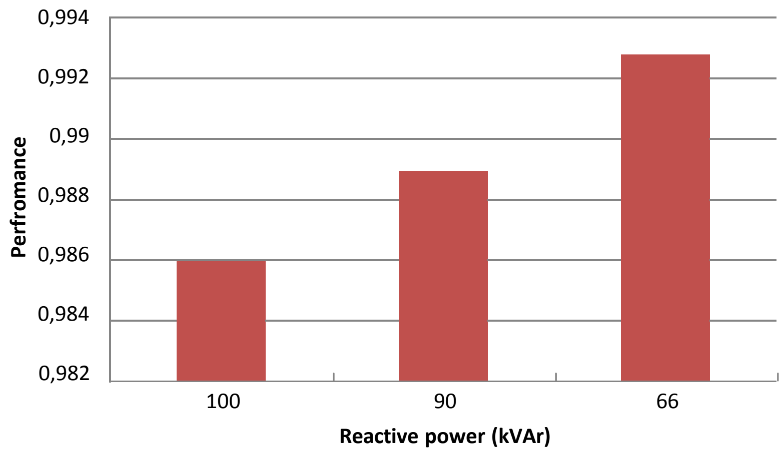

Figure 39. Performance of the system in terms of reactive power injected to the grid.

3.6 ITHD, A

In this test the harmonic mitigation is turned on. This mode will not be a normal operation mode of the system but it is important to evaluate the losses of the system in these conditions.

3.6.1 Test procedure

- Set up the I_{THD} to max in the PQF Manager.
- Run the system during predefined time period (e.g. 2 min) in order to store the data.

3.6.2 Test results

In Fig. 40, the inverter losses, the transformer losses and the auxiliary consumption are shown for this test.

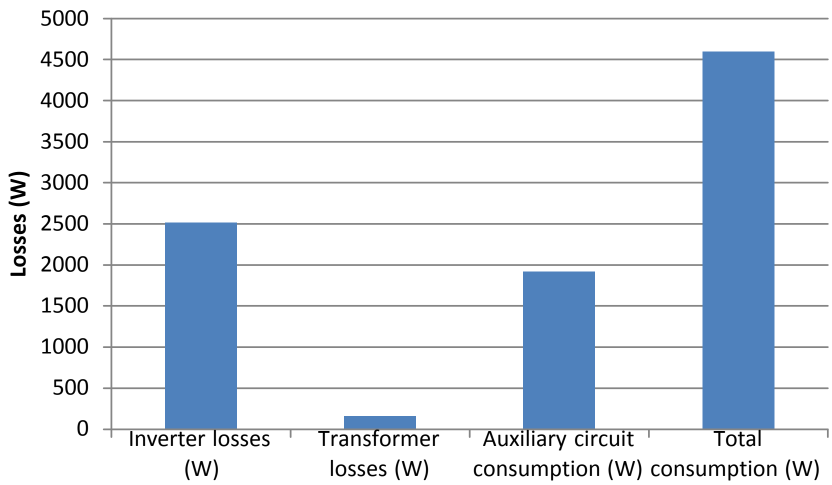

Figure 40. Inverter losses, transformer losses, auxiliary circuit consumption and total consumption for the test when the inverter is compensating harmonics.

4 Conclusions

After the tests done in the ESM and evaluated the data and all the cases, the main conclusions are the following.

- The losses in the system are higher in charging mode than in discharging mode.
- The total performance of the system is higher for higher C-rates. This is due to the fact that the auxiliary consumption has more impact when the active flow to and from the batteries is low and also because the losses in the inverter, which are the main losses in the system, are higher basically based on the switching losses. The best obtained total performance is for the case of discharging with only active power at 80kW with a value of 91%, while the lowest one is for the case of charging with reactive power compensation and harmonic mitigation at 20kW with a value of 72%.
- When the system is compensating reactive power, the losses are higher than in the case the system is only charging or discharging the batteries. The difference between the two tests with and without reactive power compensation is around 1.5kW.
- The impact of the harmonic mitigation in the system losses is around 100W when either charging or discharging modes are operating together with the capability of the inverter of mitigating harmonics.
- The efficiency of the system, considering all the losses and consumptions, taking into account both charging and discharging cycles (full cycle) are summarised in the following tables for each of the available operating conditions regarding active power, reactive compensation and harmonic mitigation:

	P, kW + Q, kVAr + ITHD, A			
Level of active power	Discharge 80kW	Discharge 60kW	Discharge 40kW	Discharge 20kW
Charge 80kW	0,823	0,808	0,773	0,666
Charge 60kW	0,800	0,785	0,752	0,648
Charge 40kW	0,756	0,742	0,710	0,612
Charge 20kW	0,664	0,651	0,624	0,537

Table 1: Total performances of the system for full cycles and inverter compensating reactive power and mitigating harmonics.

	P, kW + Q, kVAr			
Level of active power	Discharge 80kW	Discharge 60kW	Discharge 40kW	Discharge 20kW
Charge 80kW	0,831	0,818	0,789	0,687
Charge 60kW	0,807	0,794	0,766	0,667
Charge 40kW	0,764	0,752	0,726	0,632
Charge 20kW	0,666	0,656	0,633	0,551

Table 2: Total performances of the system for full cycles and inverter compensating reactive power.

	P, kW + ITHD, A			
Level of active power	Discharge 80kW	Discharge 60kW	Discharge 40kW	Discharge 20kW
Charge 80kW	0,845	0,825	0,797	0,707
Charge 60kW	0,827	0,807	0,779	0,691
Charge 40kW	0,794	0,775	0,748	0,681
Charge 20kW	0,712	0,695	0,671	0,595

Table 3: Total performances of the system for full cycles and inverter mitigating harmonics.

	P, kW			
Level of active power	Discharge 80kW	Discharge 60kW	Discharge 40kW	Discharge 20kW
Charge 80kW	0,853	0,808	0,832	0,760
Charge 60kW	0,828	0,785	0,808	0,737
Charge 40kW	0,818	0,742	0,799	0,729
Charge 20kW	0,759	0,651	0,741	0,677

Table 4: Total performances of the system for full cycles and no further capabilities of the inverter are in use.

Having a look to the below tables, the maximum performances are given for the discharge and charge process at 80kW and the low ones for the case of 20kW. This is due to the fact that the auxiliary consumption has big impact on the system performance (2kW against 20kW, 10%). Therefore, from the efficiency point of view, it is better to charge and discharge the batteries in one hour at 80kW.

- For the stand-by mode, e.g. when the system is only compensating reactive power and mitigating harmonics at its full capacity (100kVar), the losses of the system together with the auxiliary consumption are 8.5kW.
- The auxiliary consumption, for the same time and conditions in one day, is quite constant. Therefore it does not depend on the operation of the system. Only the air conditioning system will have impact on it due to the cooling or heating of the enclosure. The auxiliary consumption achieved during the test can be considered as 2kW.

ABB Document number: 1VPD110001A0118		Energy Storage Module Evaluation of losses			
Dept. PPMV	Project FEAB	Status Date 24.07.2013	Author Carlos Nieto	Status Released	Revision 1

ABB AS

Main office:
Aruküla tee 59
75301 Jüri, Rae vald, Harjumaa. Estonia
Tel: +372 6801 800
Fax: +372 6801 810
E-mail: info@ee.abb.com
Internet: www.abb.ee

Manufacturing site:
Aruküla tee 83
75301 Jüri, Rae vald, Harjumaa. Estonia
Tel: +372 634 9295
Fax: +372 6349299
E-mail: css.orders@ee.abb.com

ABB	ZCRD Corporate Research			SECRC/PT/LR-14/103
Issued by department ZCRD/SECRC/PT/EPS	Last edit date 2014-04-15	Lang. Eng	Revision 01	Page 1/19
Doc. Title	Field test 6 and 7: Capacity measurements on BESS at FEAB: Battery capacity, efficiency and pulse tests			
Project name/ID	Energy Storage: evaluation of FEAB BESS/crid 30163	Status of document	Final	
Creator name	Willy Hermansson			

9ADB1-003_ DocA4p_Portrait_Template_en.dot Rev 2.10

FEAB BESS.
Field test 6 and 7.
Measurements of Battery capacity, efficiency and pulse tests

Energy Storage: Evaluation of FEAB BESS installation

TABLE OF CONTENTS

1 ABSTRACT

This report covers measurements done in January 2014 of battery charge and discharge capacity, battery efficiency and pulsed power internal ohmic resistance and open cell voltage on the installed BESS at FEAB in Falköping. The system consists of an ABB PQFI inverter with L G Chem Li-ion batteries.

The measurements are done as part of a field test program performed to study the properties and performance of the system.

The measurements done in this report is part of the evaluation of the degradation properties of the battery system and are as such in this stage done at the beginning of the system operation to get its initial values. The intention is to repeat the measurements after a substantial period of operation in order to study the effect of battery ageing.

2 ABBREVIATIONS

BESS	Battery Energy Storage System
BMS	Battery Management System
ESM	Energy Storage Module
FEAB	Falbygdens Energi AB
OCV	The battery open cell voltage (at 0A battery current)
PLC	Programmable Logic Controller
PQF	Power Quality Filter (an active power quality filters platform based on which the power converter for energy storage system has been realized)
SOC	the battery state-of-charge
AC	Alternating Current
DC	Direct Current

3 BACKGROUND AND SCOPE

The scope of this report is to present measurements on the Energy storage Module (ESM) property of FEAB installed in Falköping (Sweden).

The report covers the following tests, see project plan [1] and test descriptions [2, 3]:

1) Field test 6: Capacity and round trip efficiency

2) Field test 7: Battery degradation.

The round trip efficiency test will charge the battery at a specific rate to a specific level. Thereafter the battery will be discharged at a specific rate to a specific level. The round trip efficiency based on the battery round trip efficiency gives a measure of the efficiency of the battery itself in the operation. By measuring the capacity at various times a general overall performance of the battery system can be defined.

During operation with charge/discharge cycling the battery cells will to some extent degrade because of ageing. This degradation is a function on operation cycle (e.g. number of discharge cycles, charge and discharge rates, depth of discharge etc.) and there is also a degradation because of calendar time.

This study aims to get some data on how much the battery system degrades under the operation. Therefore the test summarized in this report is the first measurements done when the battery system is quite new to give the starting value of the battery properties. To get some data of the battery degradation at long time operation the measurements are then planned to be repeated after several months of operation.

Similar tests were made earlier [4] on the FEAB BESS with a battery system from International Battery, but since the batteries were replaced with new from L G Chem in 2013 the measurements had to be repeated using the new system.

4 GENERAL AND TEST CONDITIONS

The hardware used for the tests is the Energy storage Module (ESM) property of FEAB installed in Falköping (Sweden), see system description in [5].

For the measurements the system was set in manual operation mode by the system PLC to give set-points for charge and discharge power of the batteries, [6].

For data acquisition a PC with the ABB script "BESS_Link 4.5.21" was used communicating with the PQFI inverter control through a RS232 – USB connection.

The following data were logged:

State of charge (%)
Battery voltage (V)
Min cell voltage (V)
Max cell voltage (V)
DC current (A)
Ambient temp (C)
Max cell temperature (C)
Min cell temperature (C)
Max charge current (A) (limit value given from BMS)
Max discharge current (A) (limit value given from BMS)
DC bus voltage (V)
AC power (kW)

Before the measurements the following parameters were set to 0.0 using the "Console" menue on the "BESS_Link 4.5.21"

Ib _fSloop
Ib _fOffsetLosses
Ib _fSloopQ
Ib _fOffsetLossesQ

This was done in order for the PQFI control to operate entirely on battery power without compensation for the inverter losses etc., i.e. to get the true operation for the battery itself.

The standard setting of the system is operation between SOC-levels 5 %<SOC<75 %. In order to be able to operate the battery in its full SOC range of 0 %<SOC<100 % the following parameters were set:

Ib _fSOC_EOC = 100.0
Ib _fSOC_EOD = 0.0

Also to get the true active power operation of the battery the reactor power compensation and harmonic filtering of the inverter was turned off.

All these changed settings were reset to the original values after the measurements.

During the measurements the PQFI control was set to follow the data on maximum allowed charge and discharge power given by the battery´s BMS. This then automatically means that the system´s own end-of-charge and end-of-discharge criteria is followed since the BMS will give a maximum power of 0 kW when end-of-charge at SOC close to 100 % or end-of-discharge close to 0 % is reached.

5 TESTS

5.1 Capacity test

The battery was first charged up to SOC=100% by a charge from SOC = 75% (which is the normal maximum value of the battery) with a charge by a power of 40 kW.

5.1.1 Discharge

A discharge was then made with a power of 80 kW down to the end-of-discharge level set by the BMS. This was reached at SOC = approx. 0.6 %.

Fig. 1 shows an overview of the battery discharge. Fig.2 shows a detail of the discharge at the end of discharge, where the control of the battery current follows the maximum allowed level (“Max discharge current (A)”) as given by the BMS.

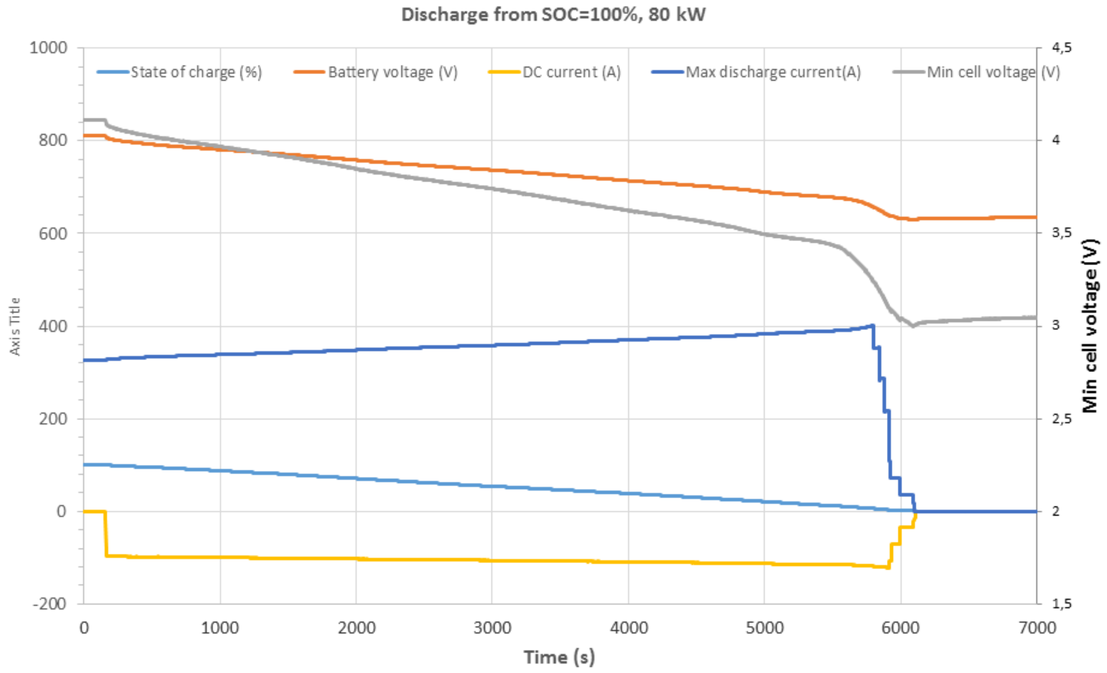

Fig.1 Battery discharge with 80 kW from SOC=100%.

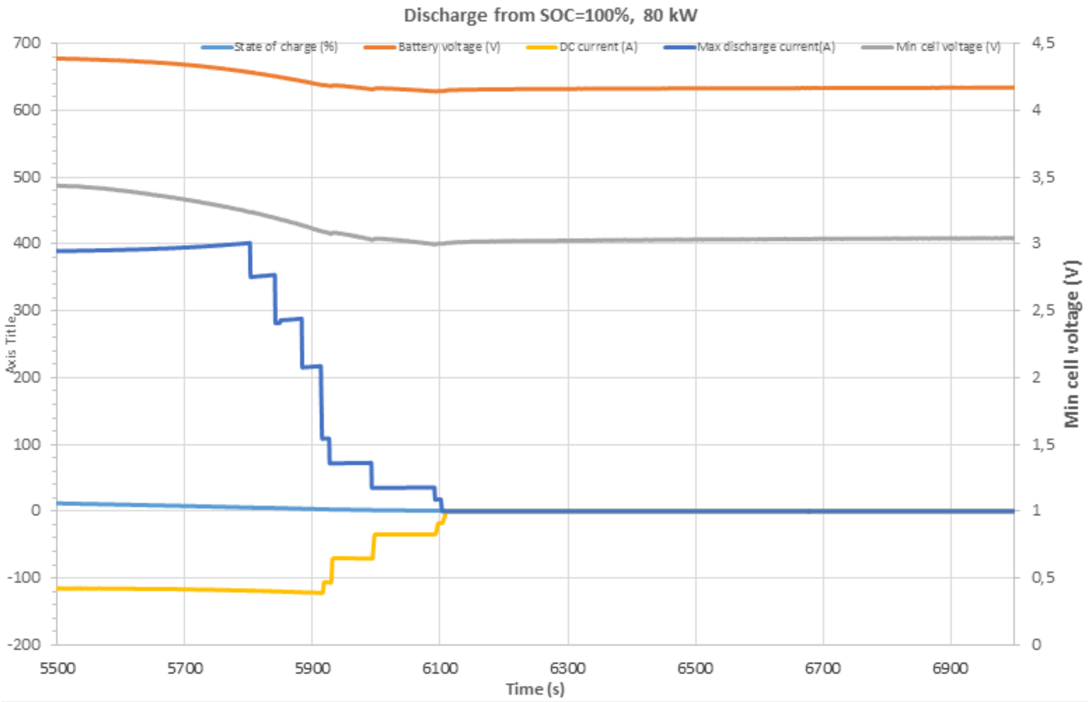

Fig.2 Detail of the battery discharge at end of discharge.

Fig. 3 shows in even more detail the performance at the end of discharge. Here we can see that at SOC < approx. 6 % the maximum allowed discharge current level as given from the BMS drops below the set point of the PQFI operation so the control of the system starts to reduce the battery current (since the control uses the “Max discharge current (A)” given from the BMS as the maximum control level) and at SOC = approx. 0.6 % the maximum allowed current is set to 0 A. This then corresponds to end-of-discharge.

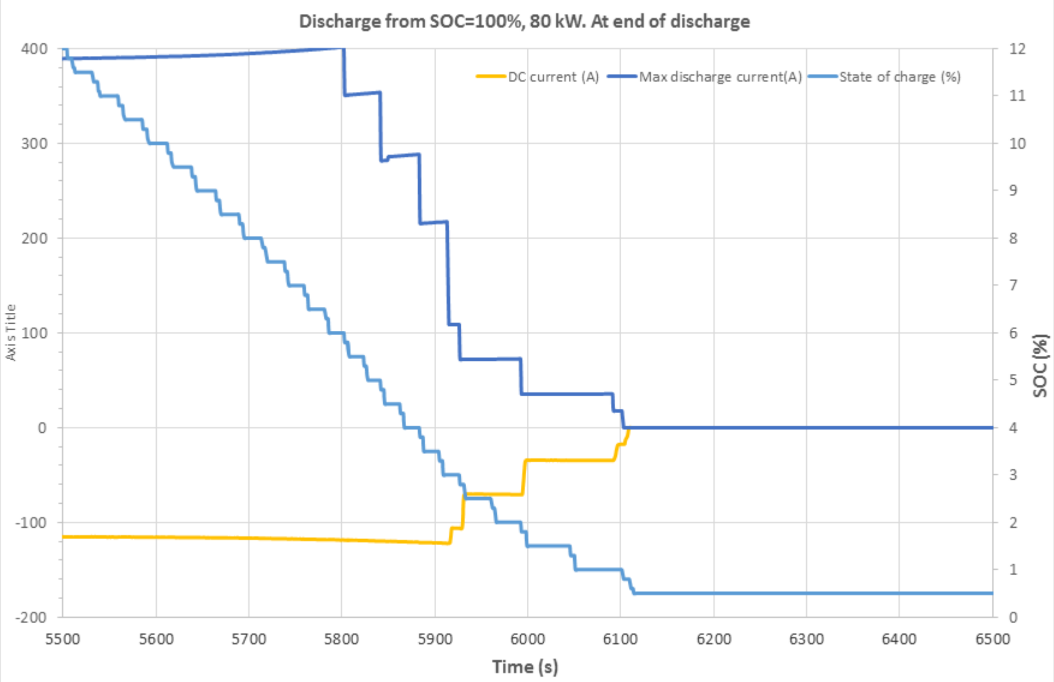

Fig. 3 Detail of the performance at end of discharge. The discharge stops at SOC = approx. 0.6 %.

Fig. 4 and 5 shows an overview of the recorded minimum and maximum cell voltages in the battery string during the discharge. It can be seen that the voltage difference is rather small, 25-30 mV, during most of the discharge period, but at the end of discharge it the difference is larger up to approx. 300 mV. This is what is expected and is normal.

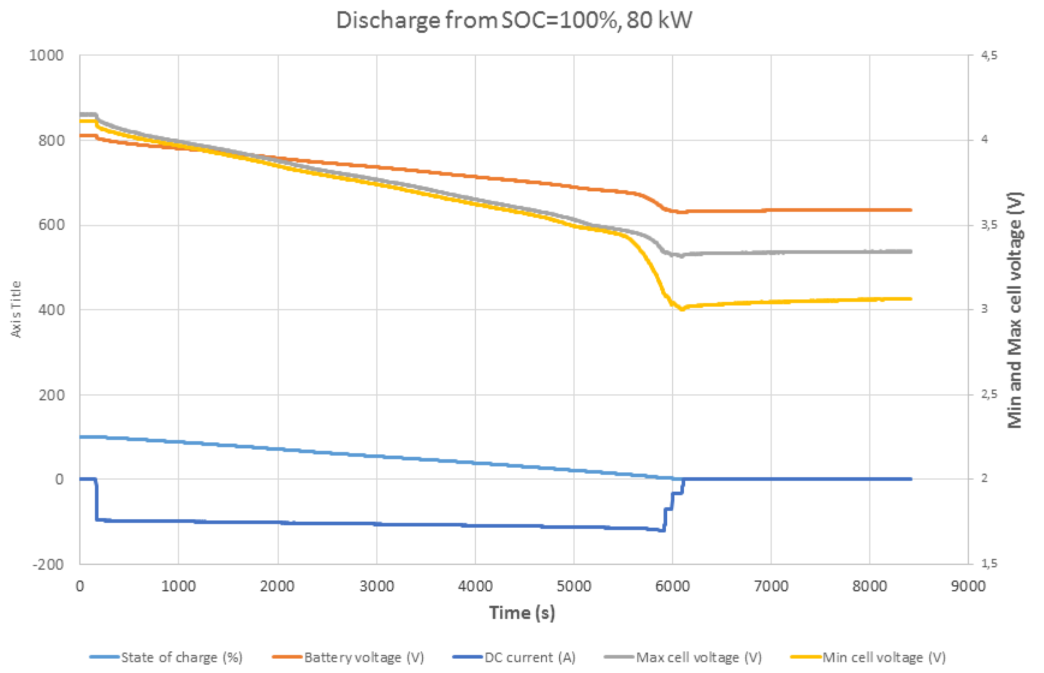

Fig. 4 Maximum and minimum cell voltages during the discharge.

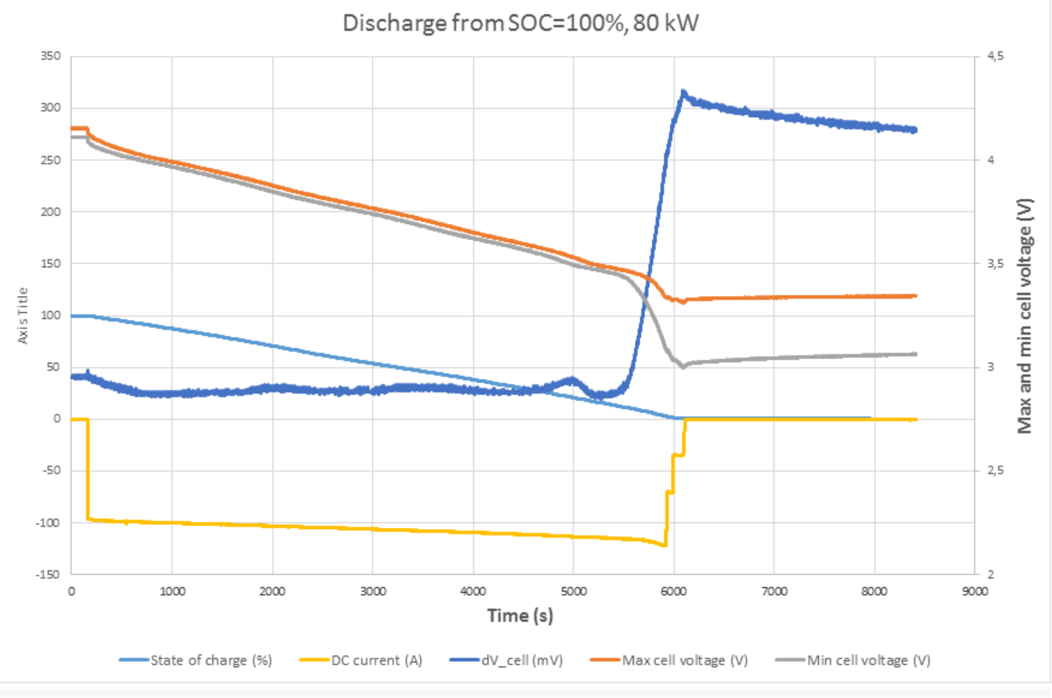

Fig. 5 Maximum and minimum cell voltages during the discharge and the difference dV between max and min cell voltages.

Fig. 6 shows the recorded minimum and maximum battery temperature during the discharge. The temperature at the start of the discharge was in the range 19.5 – 23 C and was at the end of the discharge in the range of 25 – 28 C, i.e. a temperature increase of approx. 5 C.
Finally Fig. 7 shows the achieved total discharged Ah and energy kWh in the test. The discharged capacity was approx. 173 Ah and 126.5 kWh.

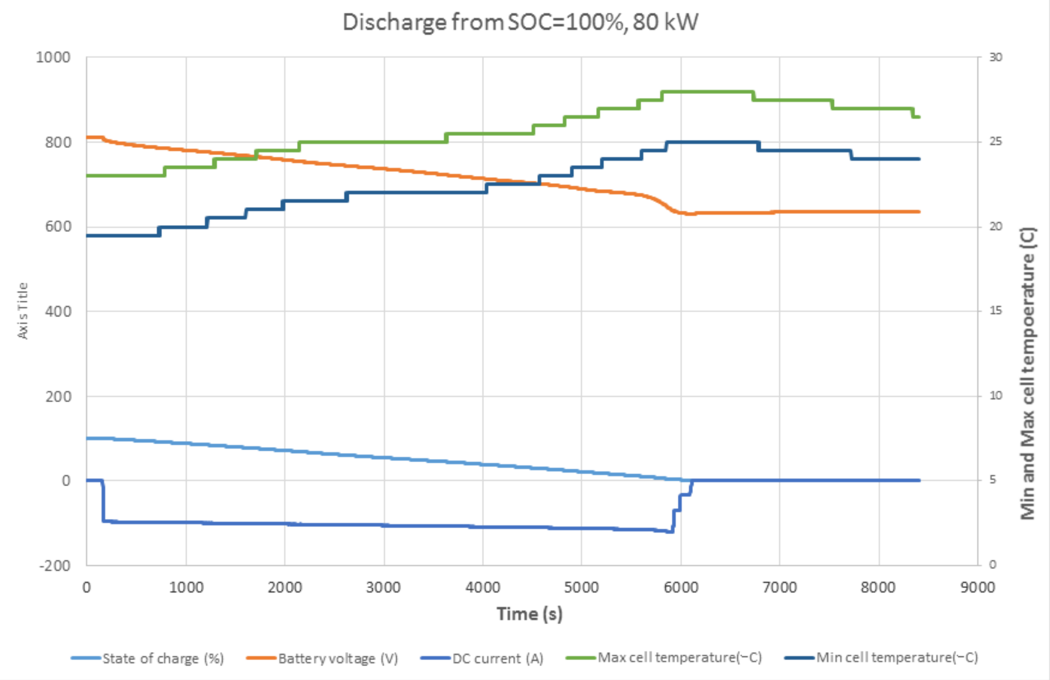

Fig. 6 Minimum and maximum battery temperature during the discharge.

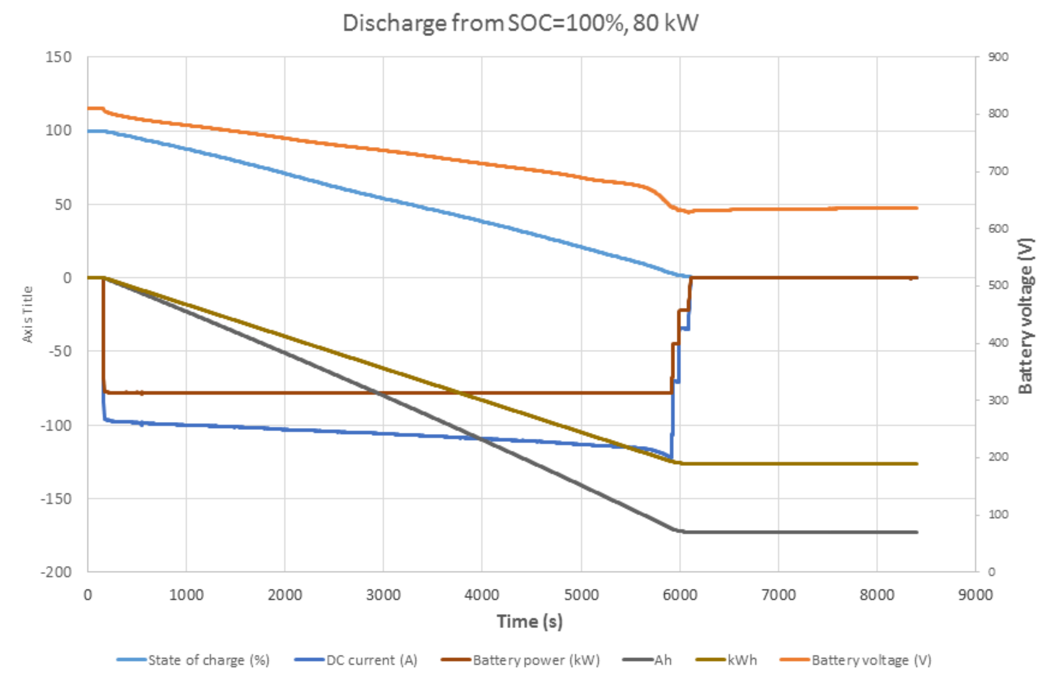

Fig. 7 Discharged capacity of approx. 173 Ah and 126.5 kWh.

5.1.2 Charge

After a rest time of approx. 30 min after the discharge the battery was charged with a power of 40 kW up to the end-of-charge level set by the BMS. This was reached at SOC=approx. 99.5 %.

Fig. 8 shows an overview of the battery charge and Fig. 9 shows a detail of the charge at the end of charge, where the control of the battery current follows the maximum allowed level (“Max charge current (A)”) as given by the BMS. Here we can see that at SOC > approx. 93 % the maximum allowed charge current level as given from the BMS drops below the set point of the PQFI operation so the control of the system starts to reduce the battery current (since the control uses the “Max charge current (A)” given from the BMS as the maximum control level) and at SOC = approx. 99.5 % the maximum allowed current is set to 0 A. This then corresponds to end-of-charge.

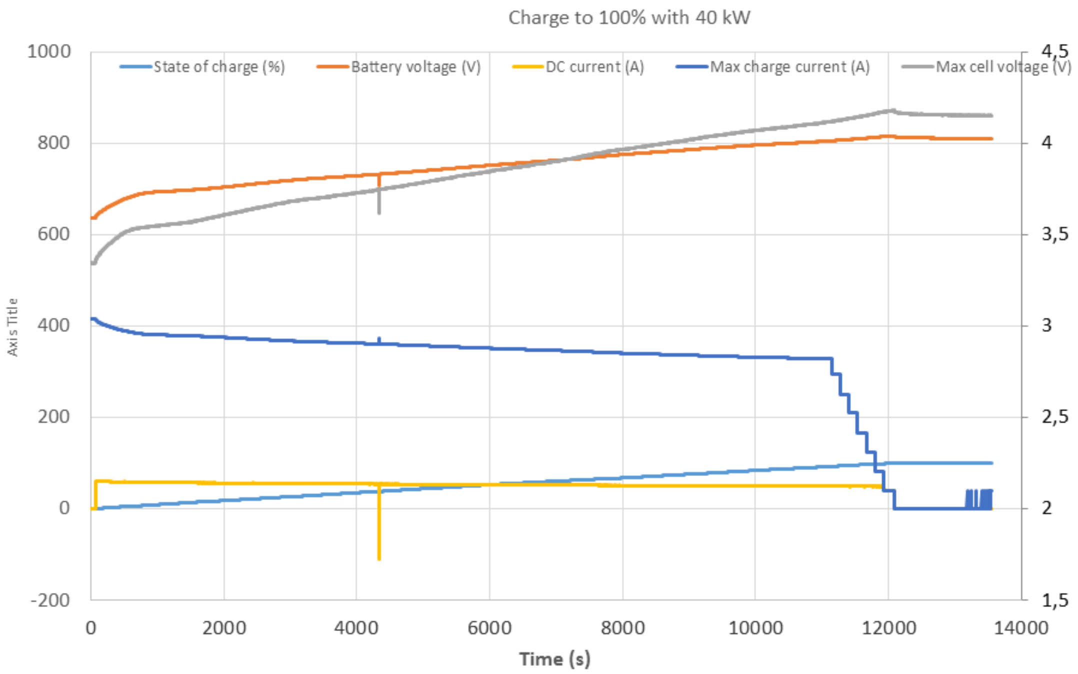

Fig. 8 Battery charge with 40 kW from SOC=0%.

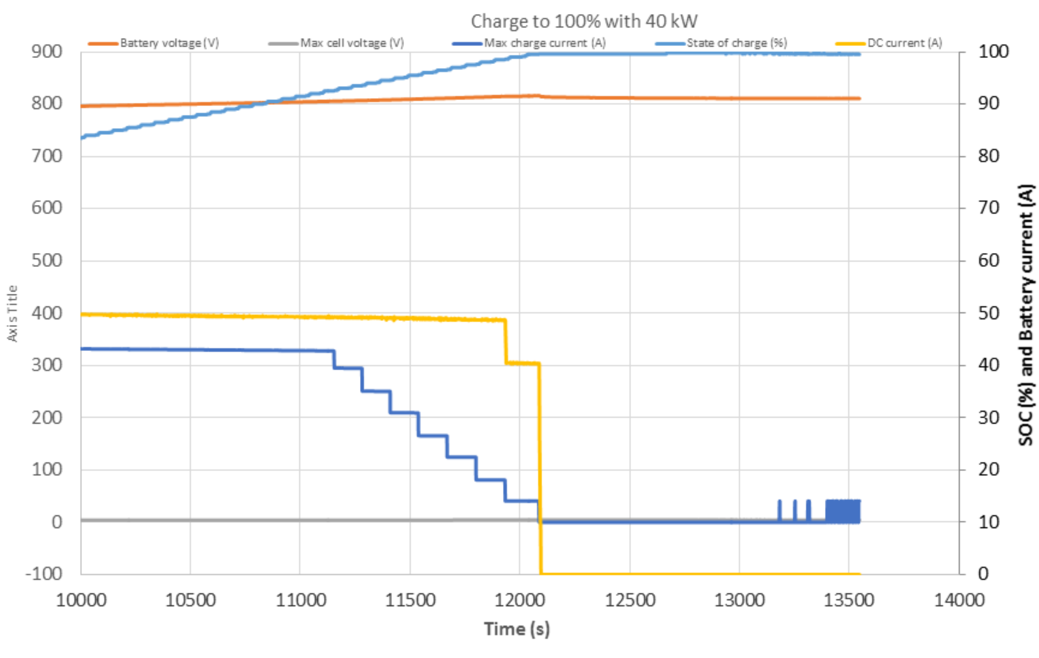

Fig. 9 Detail of the battery charge at end of charge.

To be noted in Fig. 8 at the time position of approx. 4500 s there is some disturbance in the recorded data. This does not seem to affect the charge process, but may be related to some noise in the BMS or the communication bus.

Fig. 10 shows an overview of the recorded minimum and maximum cell voltages in the battery string during the charge as well as the difference dV between max and min. It can be seen that the voltage difference is rather high, approx. 275 mV at the start of the charge and then drops to a rather small value, 19-33 mV, during most of the charge period. This is what is expected and is normal.
Fig. 11 shows the recorded minimum and maximum battery temperature during the charge. The temperature at the start of the charge was in the range 24 – 26 C and was at the middle of the charge in the range of 22.5 – 25.5 C and at the end in the range 23-26.5C. This means that at this charge power of 40 kW the temperature is almost stable.

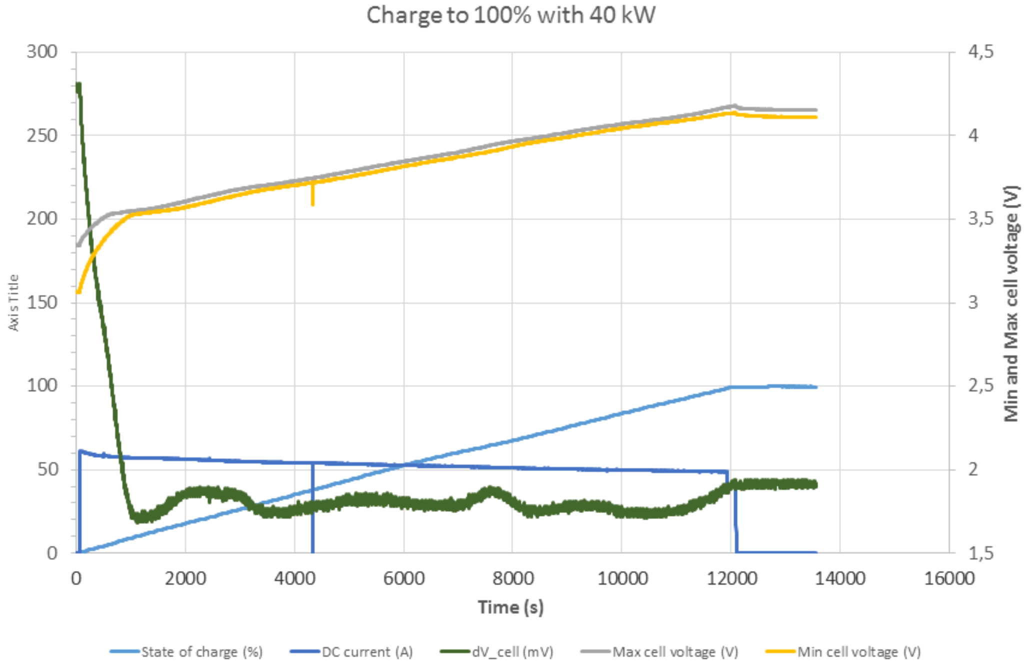

Fig. 10 Maximum and minimum cell voltages during the charge and the difference dV between max and min cell voltages.

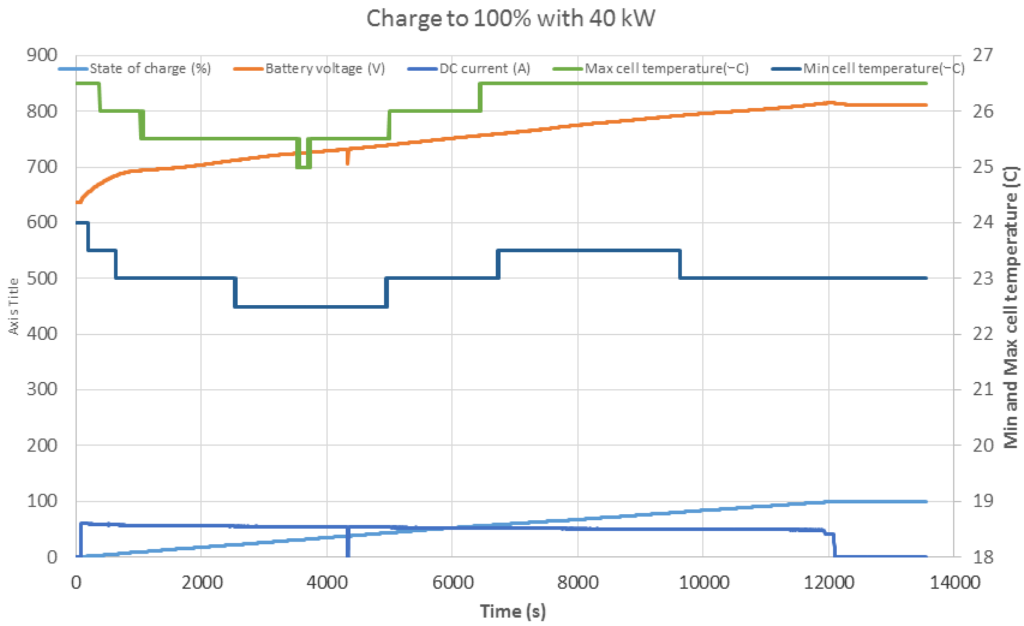

Fig. 11 Minimum and maximum battery temperature during the charge.

Finally Fig. 12 shows the achieved total charged Ah and energy kWh in the test. The charge capacity was approx. 175.9 Ah and 131.6 kWh.

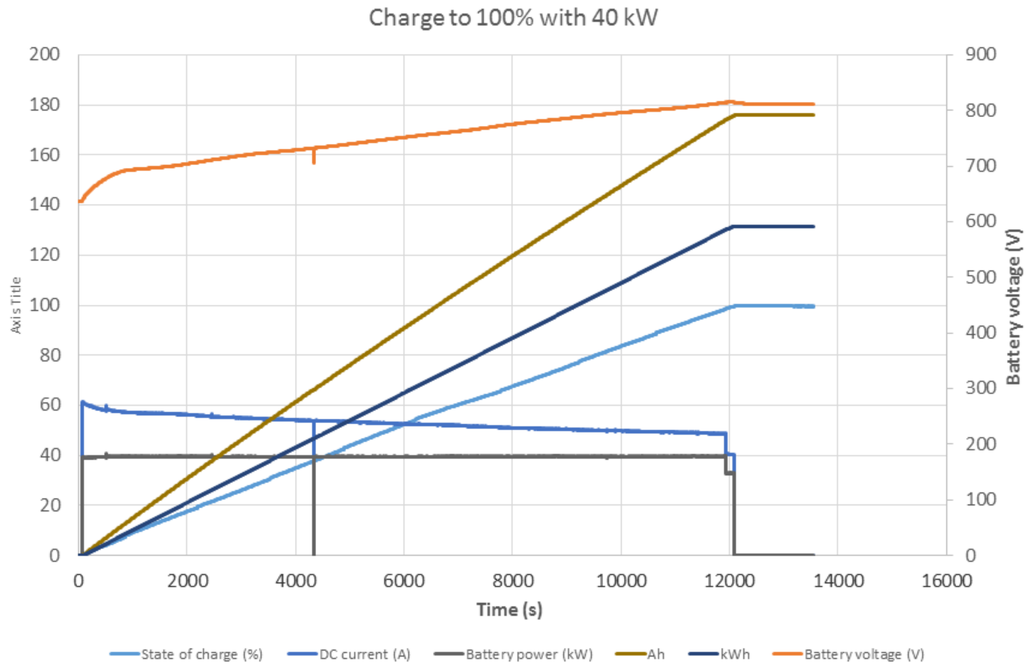

Fig. 12 Charge capacity of approx. 175.9 Ah and 131.6 kWh.

5.1.3 Summary of capacity test

The capacity test is summarized in the Table 1.

Table 1. Capacity and round trip efficiency of the battery

Discharge 99.8-0.5%		Charge 0-99.6%		Efficiency	
Ah	kWh	Ah	kWh	η_Ah_eff	η_kWh_eff
173	126.5	175.9	131.6	0.98	0.96

The efficiency values is defined as [2]:

η_Ah = Ah_dicharged/Ah_charged

η_kWh = kWh_dicharged/kWh_charged

5.2 Degradation test

The degradation test due to ageing during operation consists of two parts; 1) degradation of capacity and 2) degradation of internal resistance (i.e. increase of resistance) and from this a decrease of pulsed power capability.

Since this is a test that needs to be done after some time of operation the present measurements were made to get the status of the battery system at the beginning of its operation to get a starting reference value, see [3].

5.2.1 Capacity degradation

The start value for the battery capacity is given in the 5.1 “Capacity test” above.

5.2.2 Pulse tests and internal resistance

The internal resistance of the system was measured by a sequence of pulsed charge and discharge at various SOC-levels (90, 75, 50, 25 and 10 %), see [3]. The pulses were made with 30 s long pulses with a resting time of 30 s between each pulse in a sequence of increasing amplitudes of 20kW, 40kW, 60kW, 80kW and 100kW, as shown schematically in Fig. 13.

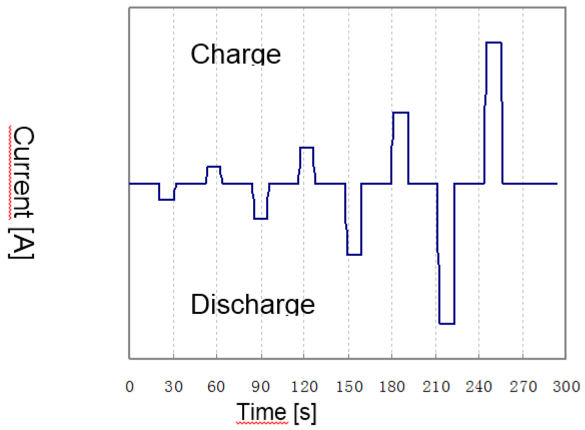

Fig. 13 Pulse testing according to the Dynamic Contrast Ratio Test Method for measurement of internal resistance [3]..

The current and battery voltage at the end of each of the 30 s charge/discharge pulses are recorded. Then a voltage/current curve can be plotted accordingly by curve fitting:

$$Ubatt = Ri_{SOC} \times Ibatt - OCV_{SOC}$$

The curve’s slope (Ri_{SOC}) is the DC internal resistance of the battery at the given SOC and OCV_{SOC} is the open circuit voltage of the battery at this specific SOC. Fig. 14 shows schematically the results for discharge pulses and Fig. 15 for charge pulses.

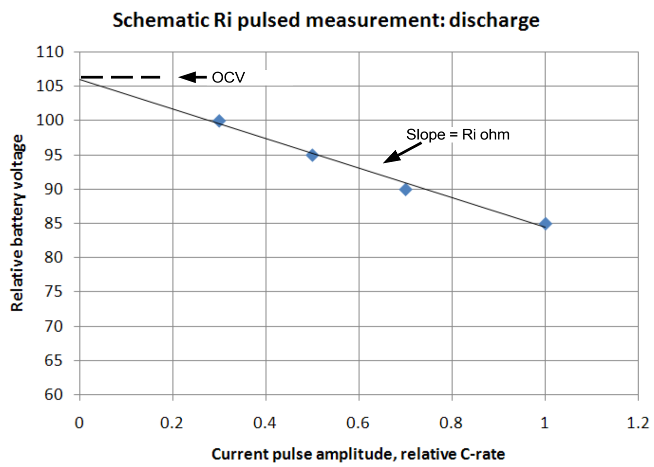

Fig. 14 Schematic principle R_i pulsed measurement at discharge

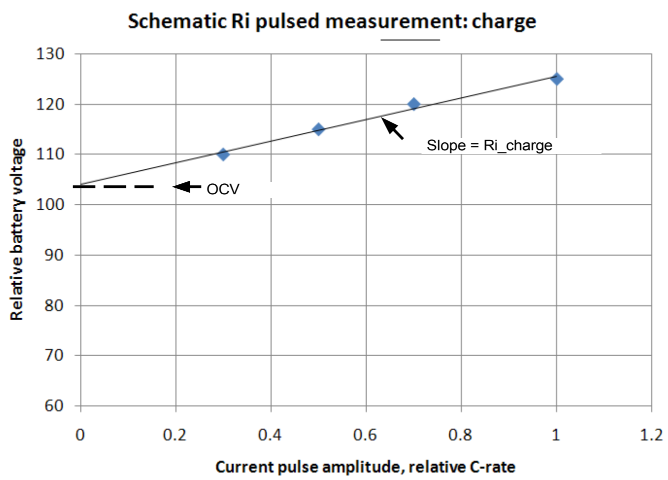

Fig. 15 Schematic principle R_i pulsed measurement at charge

Fig. 16 shows one example of a pulse sequence made on the system at SOC = 50 % and Fig. 17 shows the corresponding linear curve fitting to get the internal resistance and OCV value at discharge.

Fig. 16 Pulse sequence with 30s charge and discharge pulses of 20kW, 40kW, 60kW, 80kW and 100kW at SOC = 50 %.

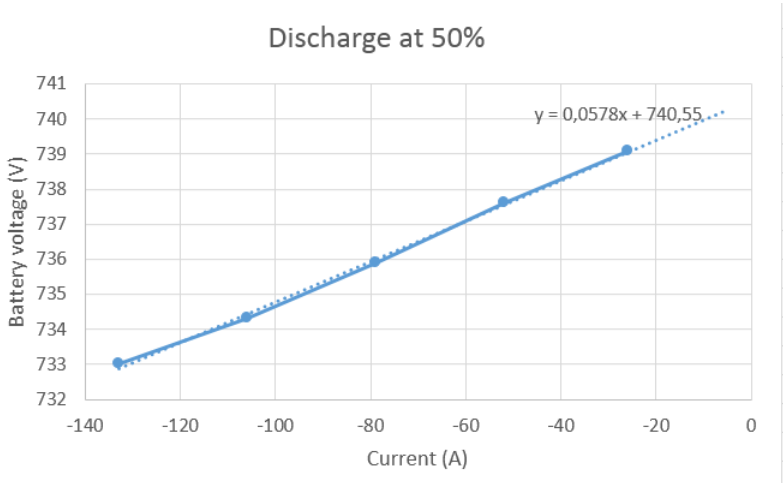

Fig. 17 Curve fitting to get internal resistance and OCV for discharge at SOC=50%.

Here the curve fitting gives a resistance R_i for discharge of 0.0578 ohm and an OCV of 740.6 V.

Fig. 18 shows the corresponding result for charge pulses at SOC=50%.

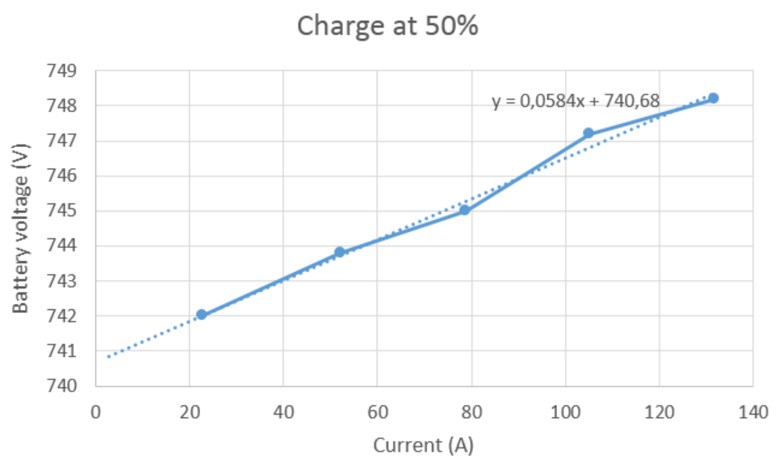

Fig. 18 Curve fitting to get internal resistance and OCV for charge at SOC=50%.

Here the curve fitting gives a resistance R_i for charge of 0.0584 ohm and an OCV of 740.7 V.

Fig. 19 shows the summary of the internal resistance and Fig. 20 shows the summary of the OCV at charge and discharge at the various SOC levels.

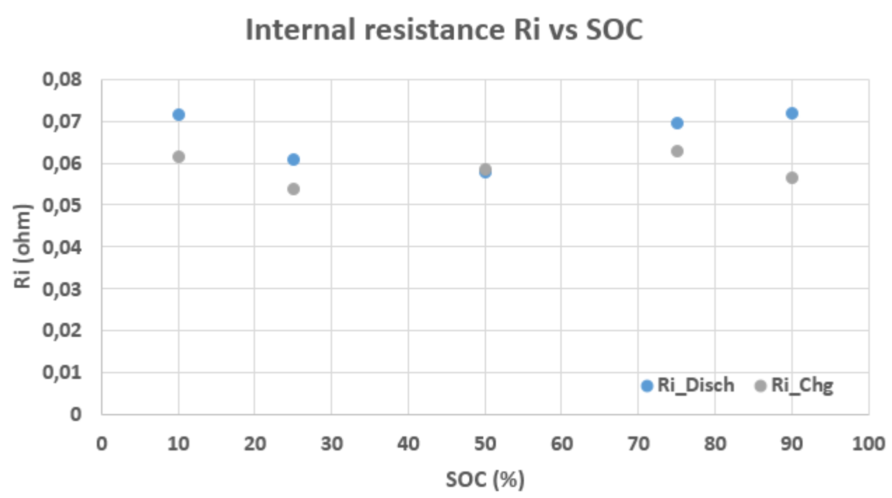

Fig. 19 Internal resistance vs. SOC from pulse measurement at charge and discharge.

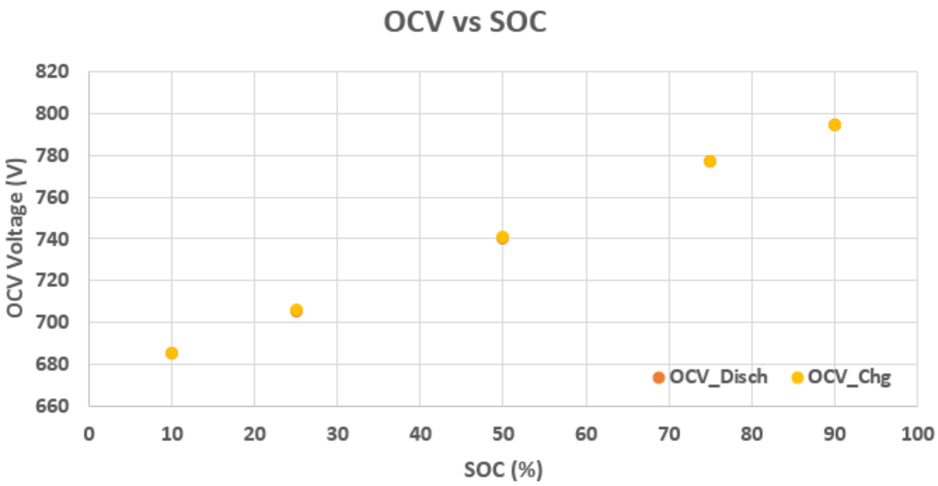

Fig. 20 OCV vs. SOC from pulse measurement at charge and discharge.

6 REFERENCES

[1] SECRC/PT/RM-11/356, Project Proposal 2012/2013, Field evaluation of grid connected energy storage.

[2] Test specification for Field Test No 6: Capacity and round trip efficiency, 2013-03-22

[3] Test specification for Field Test No 7: Battery degradation plus internal resistance and peak power capability, 2013-03-22.

[4] SECRC/PT/RM-12/115, Discharge/charge measurement on FEAB BESS installation 2012-01-31.

[5] 1VPD110001A0084, FEAB Energy Storage Module: System Description, 2013-05-20.

[6] DESS Operator´s Panel Manual, Tallinn 2011.

Change History

Rev.	Chapter	Description	Date / Dep. / Name
01	All	Initial document	<2014-04-22>/ SECRC/PT / W Hermansson

ABB	ZCRD Corporate Research			SECRC/PT/LR-14/243
Issued by department ZCRD/SECRC/PT/EPS	Last edit date 2014-09-20	Lang. Eng	Revision 01	Page 1/19
Doc. Title	Field test 7: Capacity measurements on BESS at FEAB: Evaluation of degradation. Measurements in Sept 2014			
Project name/ID	Energy Storage: evaluation of FEAB BESS/crid 30163	Status of document	Final	
Creator name	Willy Hermansson			

9ADB1-003_ DocA4p_Portrait_Template_en.dot Rev 2.10

FEAB BESS.
Field test 7.
Measurements of Battery capacity, efficiency and pulse tests, degradation

Energy Storage: Evaluation of FEAB BESS installation

TABLE OF CONTENTS

1 ABSTRACT

This report covers measurements done in September 2014 of battery charge and discharge capacity, battery efficiency and pulsed power internal ohmic resistance and open cell voltage (OCV) on the installed BESS at FEAB in Falköping. The system consists of an ABB PQFI inverter with L G Chem Li-ion batteries, [1].

The measurements are done as part of a field test program performed to study the properties and performance of the system.

The measurements done in this report are a repetition of measurements done in January 2014 [2] and the purpose is to study the degradation of the battery system. Since January 2014 the system has been operating approximately 230 full cycles of charge and discharge in the interval 15 % < SOC < 75 %, i.e. one cycle per day. Total number of cycles since the start in April 2013 was approximately 470 cycles [5].

2 ABBREVIATIONS

BESS	Battery Energy Storage System
BMS	Battery Management System
EOC	End of charge
ESM	Energy Storage Module
FEAB	Falbygdens Energi AB
OCV	The battery open cell voltage (at 0A battery current)
PLC	Programmable Logic Controller
PQF	Power Quality Filter (an active power quality filters platform based on which the power converter for energy storage system has been realized)
SOC	the battery state-of-charge
AC	Alternating Current
DC	Direct Current

3 BACKGROUND AND SCOPE

The scope of this report is to present measurements on the Energy storage Module (ESM) property of FEAB installed in Falköping (Sweden).

The report is part of the Field test No 7 for evaluating battery degradation, see project plan [3] and test description [4].

The round trip efficiency test will charge the battery at a specific rate to a specific level. Thereafter the battery will be discharged at a specific rate to a specific level. The round trip efficiency based on the battery round trip efficiency gives a measure of the efficiency of the battery itself in the operation. By measuring the capacity at various times a general overall performance of the battery system can be defined.

During operation with charge/discharge cycling the battery cells will to some extent degrade because of ageing. This degradation is a function on operation cycle (e.g.

number of discharge cycles, charge and discharge rates, depth of discharge etc.) and there is also a degradation because of calendar time.

This study aims to get some data on how much the battery system degrades under the operation. Therefore the test summarized in this report is the follow up measurements of the capacity and pulse measurements after approx. 230 charge/discharge cycles since the previous measurement in January 2014 [2]. The total number of operating cycles (charge/discharge between 15% < SOC < 75 %) since the start in April 2013 was approximately 470 cycles [5].

A summary evaluation of the battery degradation is given in [7].

4 GENERAL AND TEST CONDITIONS

The hardware used for the tests is the Energy storage Module (ESM) property of FEAB installed in Falköping (Sweden), see system description in [4].

For the measurements the system was set in manual operation mode by the system PLC to give set-points for charge and discharge power of the batteries, [6].

For data acquisition a PC with the ABB script "BESS_Link 4.5.21" was used communicating with the PQFI inverter control through a RS232 – USB connection.

The following data were logged:

State of charge (%)
Battery voltage (V)
Min cell voltage (V)
Max cell voltage (V)
DC current (A)
Ambient temp (C)
Max cell temperature (C)
Min cell temperature (C)
Max charge current (A) (limit value given from BMS)
Max discharge current (A) (limit value given from BMS)
DC bus voltage (V)
AC power (kW)

Before the measurements the following parameters were set to 0.0 using the "Console" menu on the "BESS_Link 4.5.21"

Ib _fSloop
Ib _fOffsetLosses
Ib _fSloopQ
Ib _fOffsetLossesQ

This was done in order for the PQFI control to operate entirely on battery power without compensation for the inverter losses etc., i.e. to get the true operation for the battery itself.

The standard setting of the system is operation between SOC-levels 15 %<SOC<75 %. In order to be able to operate the battery in its full SOC range of 0 %<SOC<100 % the following parameters were set:

Ib _fSOC_EOC = 100.0
Ib _fSOC_EOD = 0.0

Also to get the true active power operation of the battery the reactor power compensation and harmonic filtering of the inverter was turned off.

All these changed settings were reset to the original values after the measurements.

During the measurements the PQFI control was set to follow the data on maximum allowed charge and discharge power given by the battery´s BMS. This then automatically means that the system´s own end-of-charge and end-of-discharge criteria is followed since the BMS will give a maximum power of 0 kW when end-of-charge at SOC close to 100 % or end-of-discharge close to 0 % is reached.

5 TESTS

5.1 Capacity test

The battery was first charged up to SOC=100% by a charge from SOC = 75% (which is the normal maximum value of the battery, when operating in the automatic mode) with a charge by a power of 40 kW.

5.1.1 Discharge

A discharge was then made (starting from SOC = 99.5 %) with a power of 80 kW down to the end-of-discharge level set by the BMS. This was reached at SOC = approx. 0.5 %.

Fig. 1 shows an overview of the battery discharge. To be noted is a “spike” in the recorded data at the time position of approx. 3200s which seems to be caused by some disturbance on the CAN bus communication or in the BMS. However this does not seem to have any effect on the overall performance of the system.
Fig.2 shows a detail of the discharge at the end of discharge, where the control of the battery current follows the maximum allowed level (“Max discharge current (A)”) as given by the BMS.

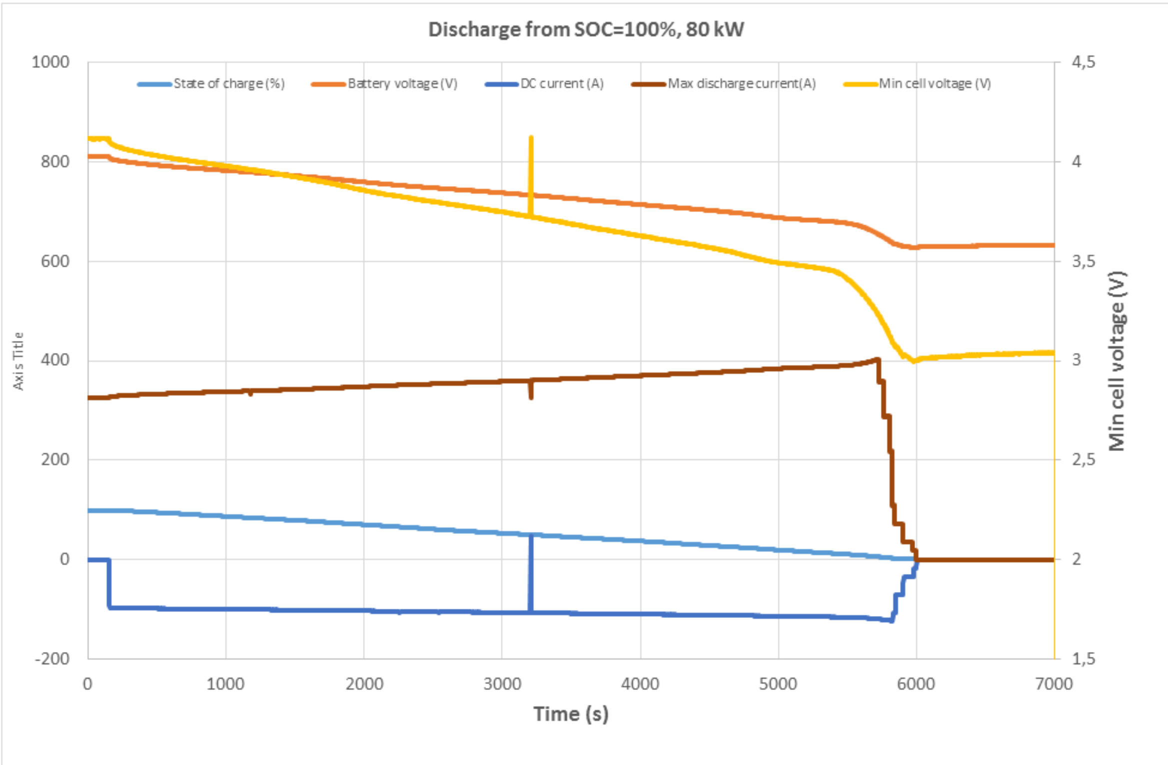

Fig.1 Battery discharge with 80 kW from SOC=99.5 %.

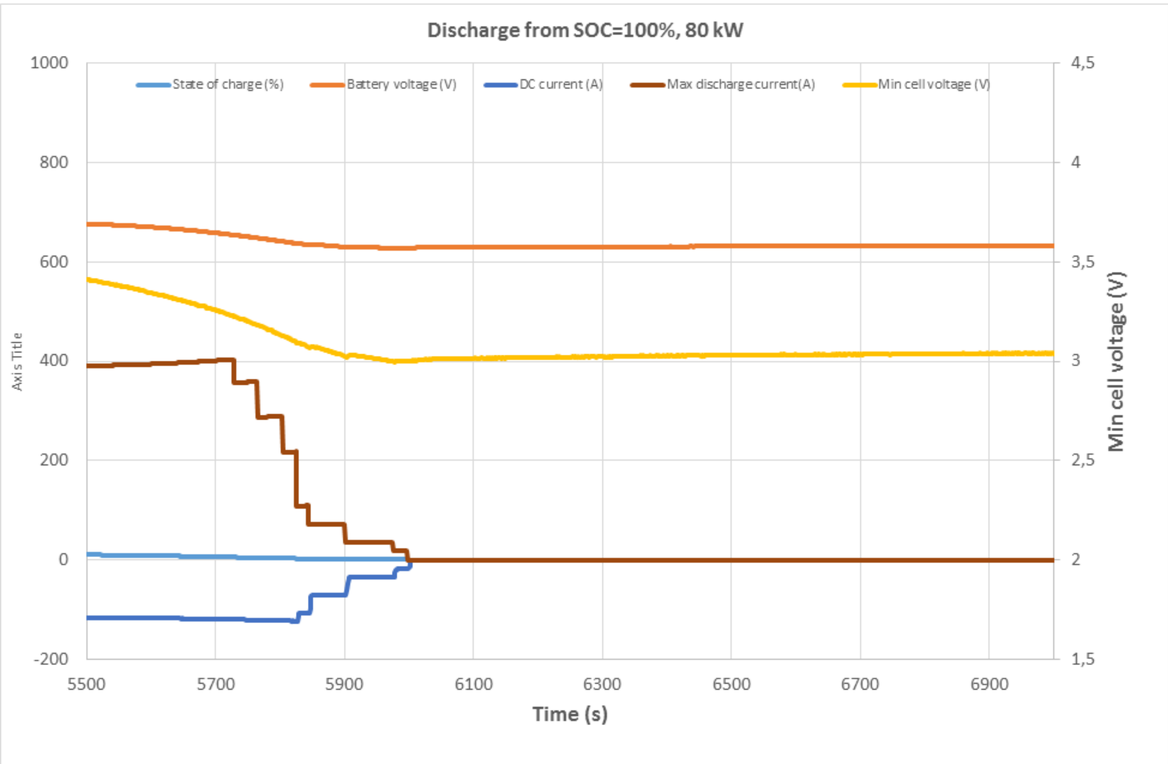

Fig.2 Detail of the battery discharge at end of discharge.

Fig. 3 shows in even more detail the performance at the end of discharge. Here we can see that at SOC < approx. 6 % the maximum allowed discharge current level as given from the BMS starts to drop and at SOC < approx. 3.5 % it drops below the set point of the PQFI operation so the control of the system starts to reduce the battery current (since the control uses the “Max discharge current (A)” given from the BMS as the maximum control level) and at SOC = approx. 0.5 % the maximum allowed current is set to 0 A. This then corresponds to end-of-discharge.

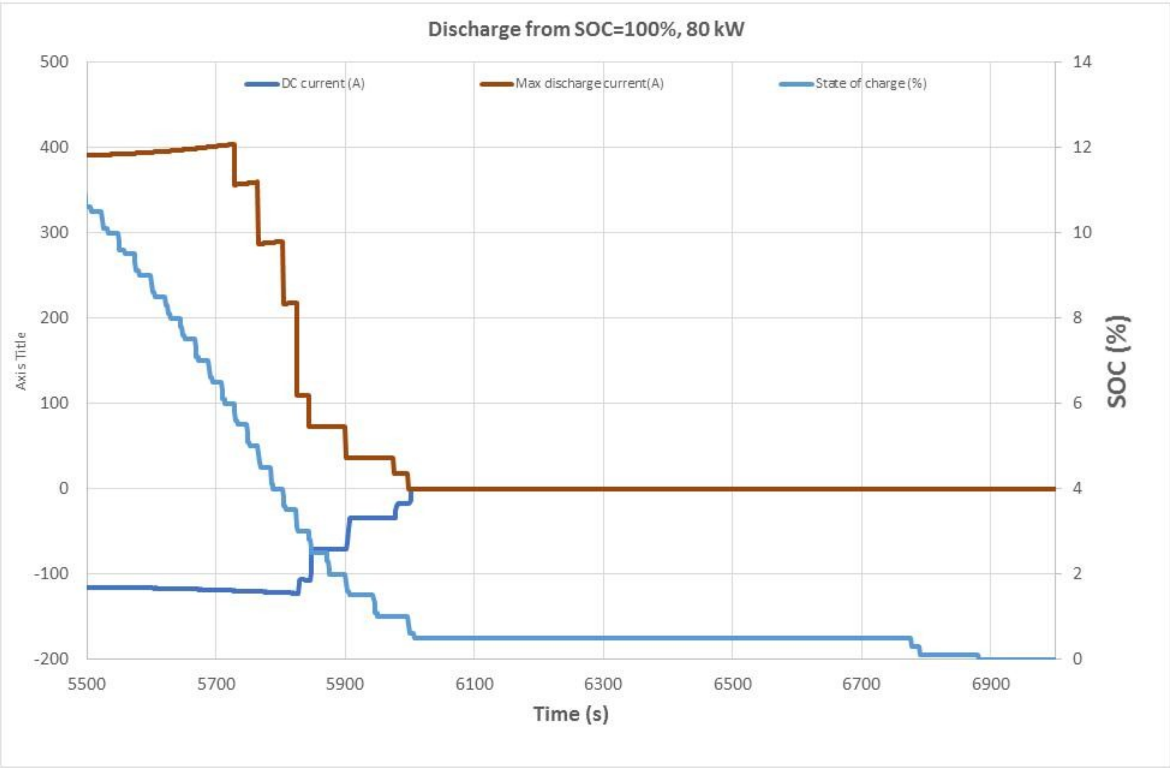

Fig. 3 Detail of the performance at end of discharge. The discharge stops at SOC = approx. 0.5 %.

Fig. 4 and 5 shows an overview of the recorded minimum and maximum cell voltages in the battery string during the discharge. It can be seen that the voltage difference is rather small, 25-40 mV, during most of the discharge period, but at the end of discharge the difference is larger up to approx. 380 mV. This is what expected and is normal.

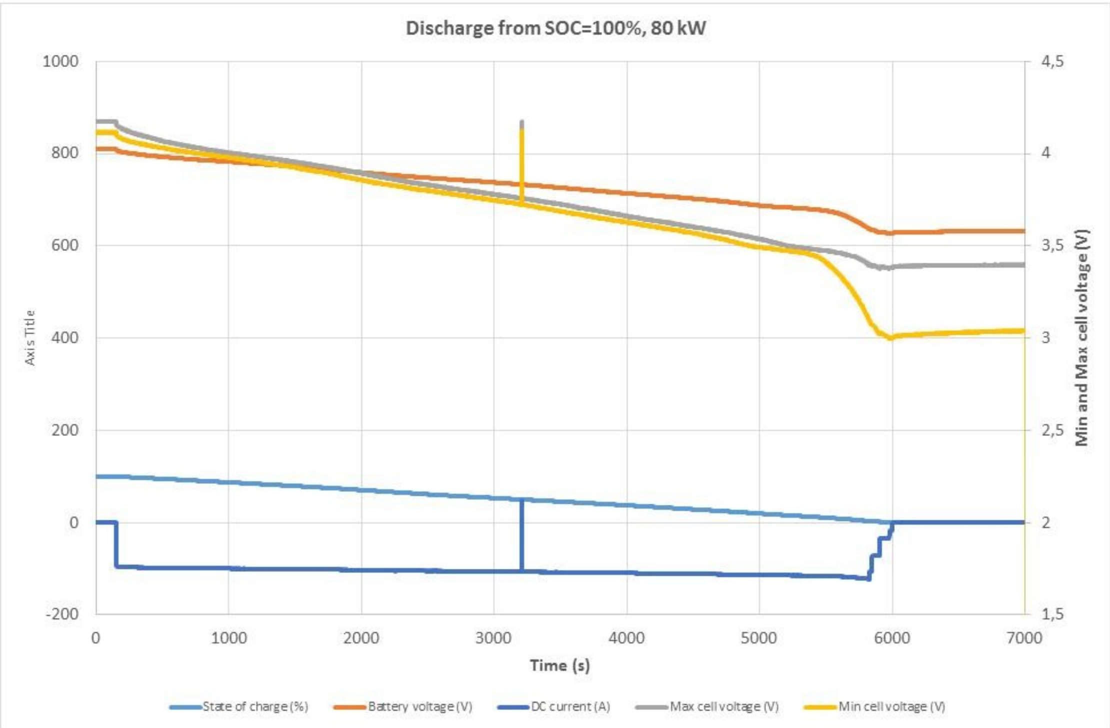

Fig. 4 Maximum and minimum cell voltages during the discharge.

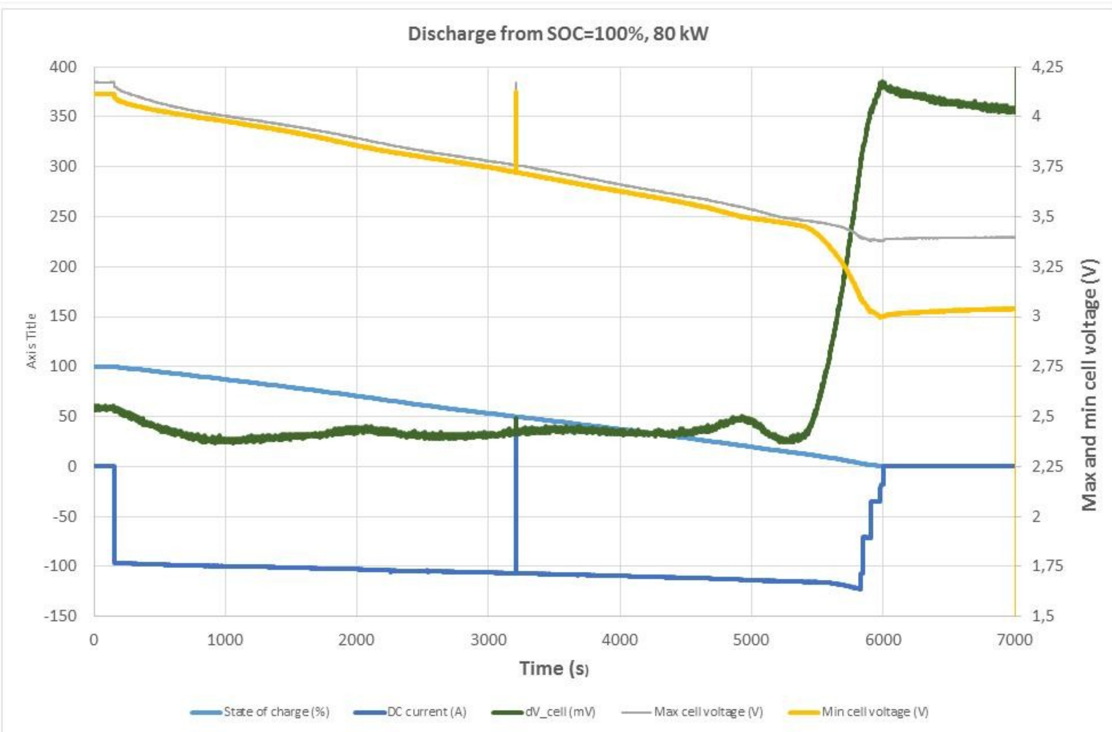

Fig. 5 Maximum and minimum cell voltages during the discharge and the difference dV between max and min cell voltages.

Fig. 6 shows the recorded minimum and maximum battery temperature during the discharge. The temperature at the start of the discharge was in the range 23 – 25.5 C and was at the end of the discharge in the range of 28 – 30 C, i.e. a temperature increase of approx. 5 C.
Finally Fig. 7 shows the achieved total discharged Ah and energy kWh in the test. The discharged capacity was approx. 170 Ah and 124.5 kWh for the discharge from SOC=99.5 % down to 0.5%.

To coincide with the charge interval of 1.5 % < SOC < 99 %, see below in 5.1.2, the discharged capacity from the data was 168.4 Ah and 123.3 kWh in this interval.

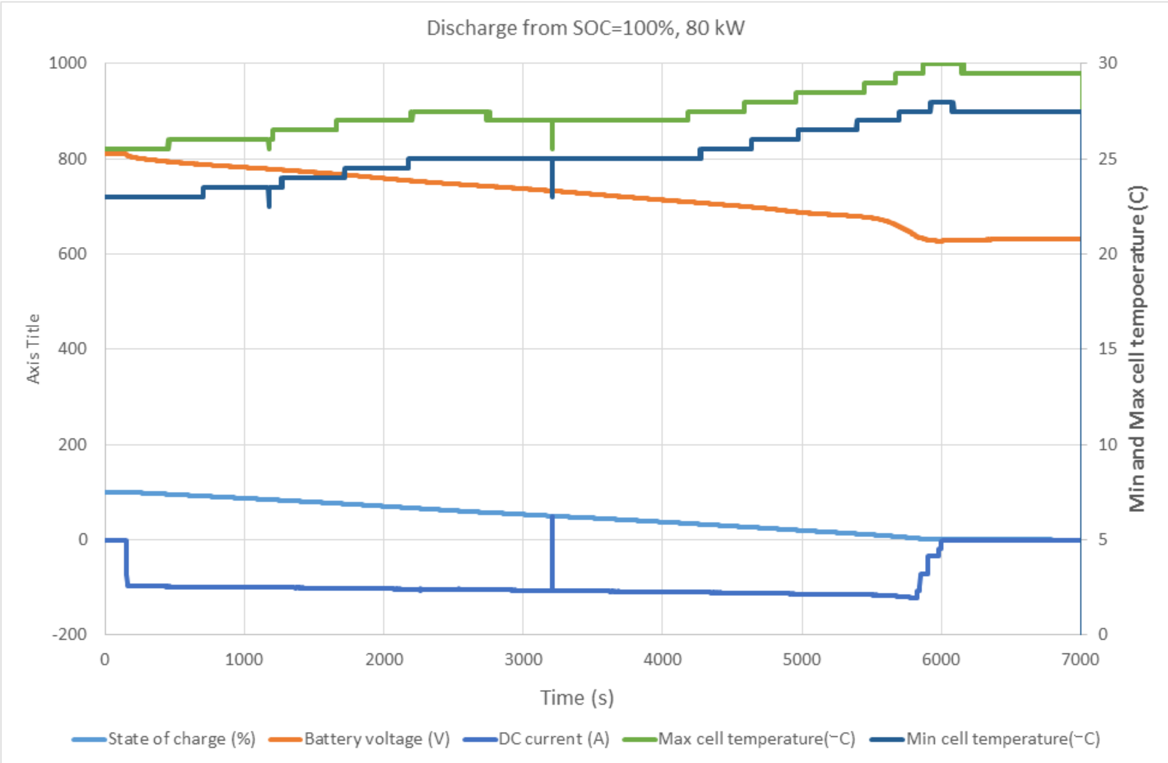

Fig. 6 Minimum and maximum battery temperature during the discharge.

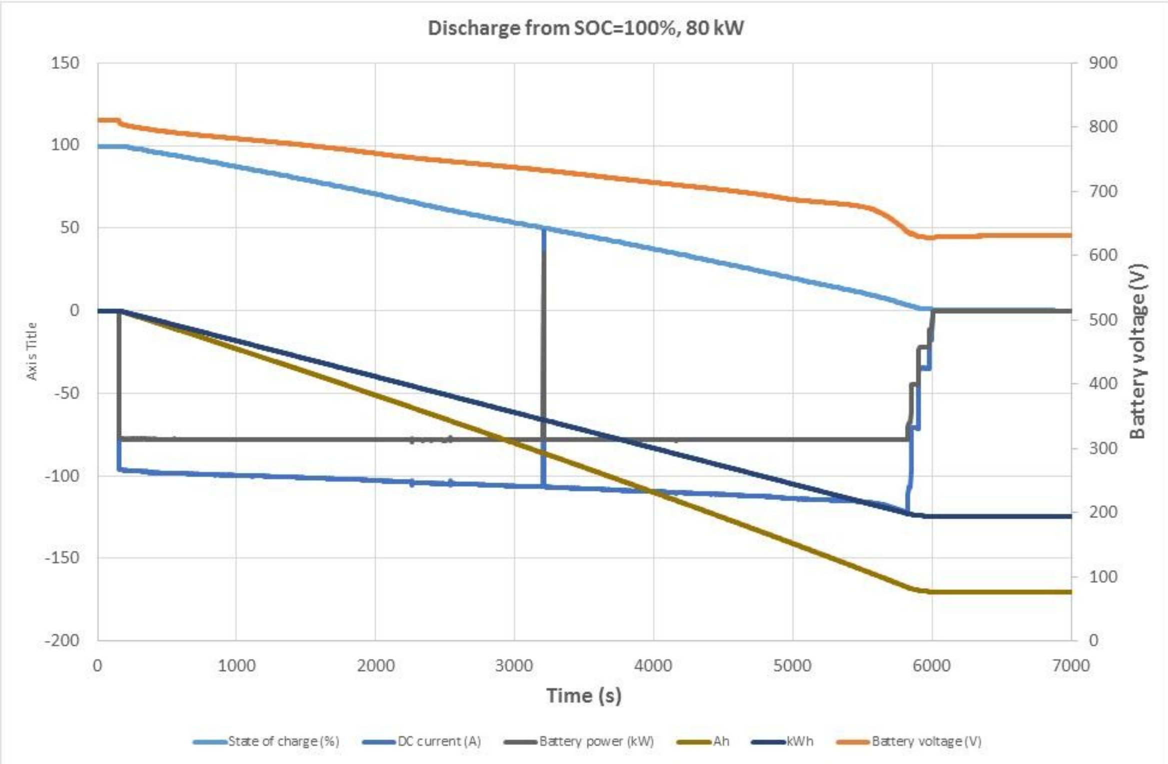

Fig. 7 Discharged capacity of approx. 170 Ah and 124.5 kWh with a discharge between 99.5%>SOC>0.5%.

5.1.2 Charge

After a rest time over night after the discharge the battery was charged with a power of 40 kW up to the end-of-charge level set by the BMS.

To be noted is that due to the performance of the BMS the charge needed to be started at SOC=1.5 %, and not 0%. With the present version of the BMS-script, made by LG Chem, the BMS is “locked-up” if the SOC goes down to 0% and also up to 100%. Therefore also the EOC set point was defined to SOC=99%, in order to avoid the “locking up” of the BMS.

Fig. 8 shows an overview of the battery charge and Fig. 9 shows a detail of the charge at the end of charge, where the control of the battery current follows the maximum allowed level (“Max charge current (A)”) as given by the BMS. Here we can see that at SOC > approx. 93 % the maximum allowed charge current level as given from the BMS start to drop down and becomes below the set point of the PQFI operation at SOC>98.8% so the control of the system starts to reduce the battery current (since the control uses the “Max charge current (A)” given from the BMS as the maximum control level) and at SOC = approx. 99 % the maximum allowed current is set to 0 A defined by the set point for EOC. This then corresponds to end-of-charge.

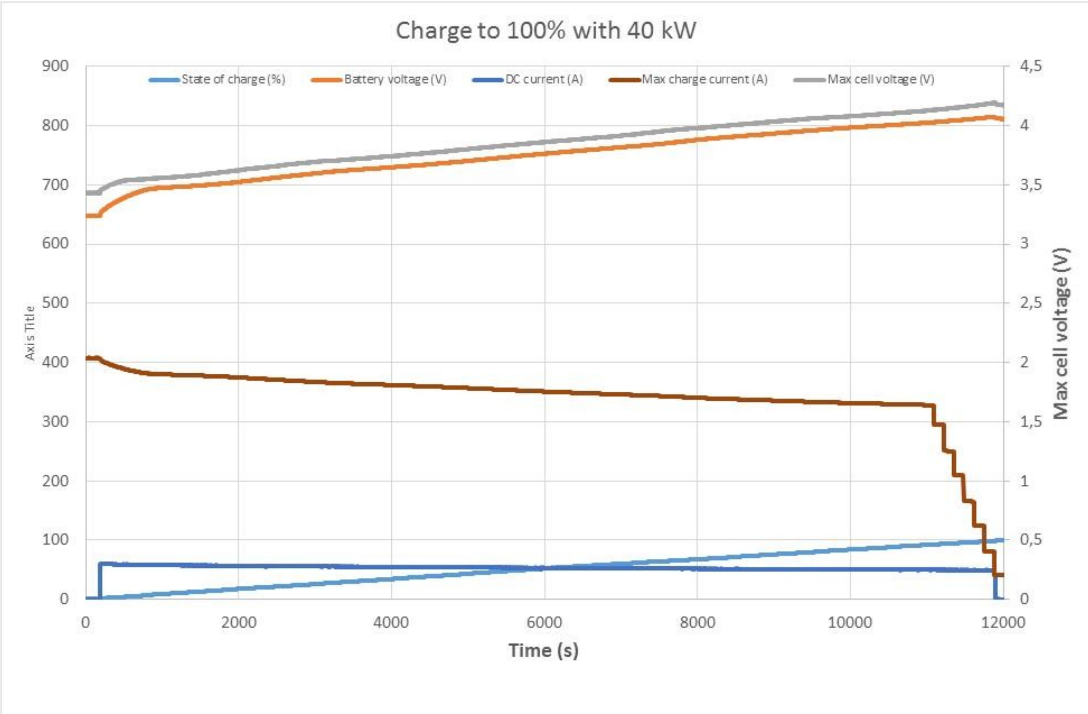

Fig. 8 Battery charge with 40 kW from SOC=1.5% up to 99%

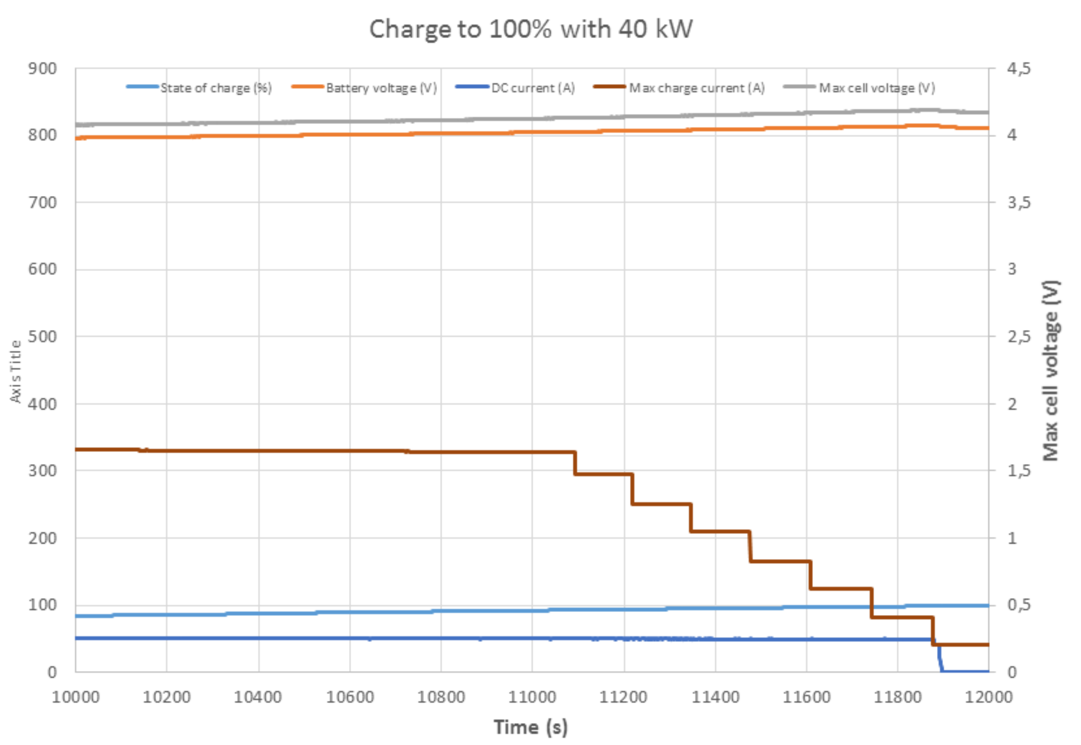

Fig. 9 Detail of the battery charge at end of charge.

Fig. 10 shows an overview of the recorded minimum and maximum cell voltages in the battery string during the charge as well as the difference dV between max and min. It can be seen that the voltage difference is rather high, approx. 260 mV at the start of the charge and then drops to a rather small value, 20-45 mV, during most of the charge period. This is what is expected and is normal.
Fig. 11 shows the recorded minimum and maximum battery temperature during the charge. The temperature at the start of the charge was in the range 24 – 26 C and was at the middle of the charge in the range of 21 – 22 C and at the end in the range 23.5-24.5C. This means that at this charge power of 40 kW the temperature is almost stable.

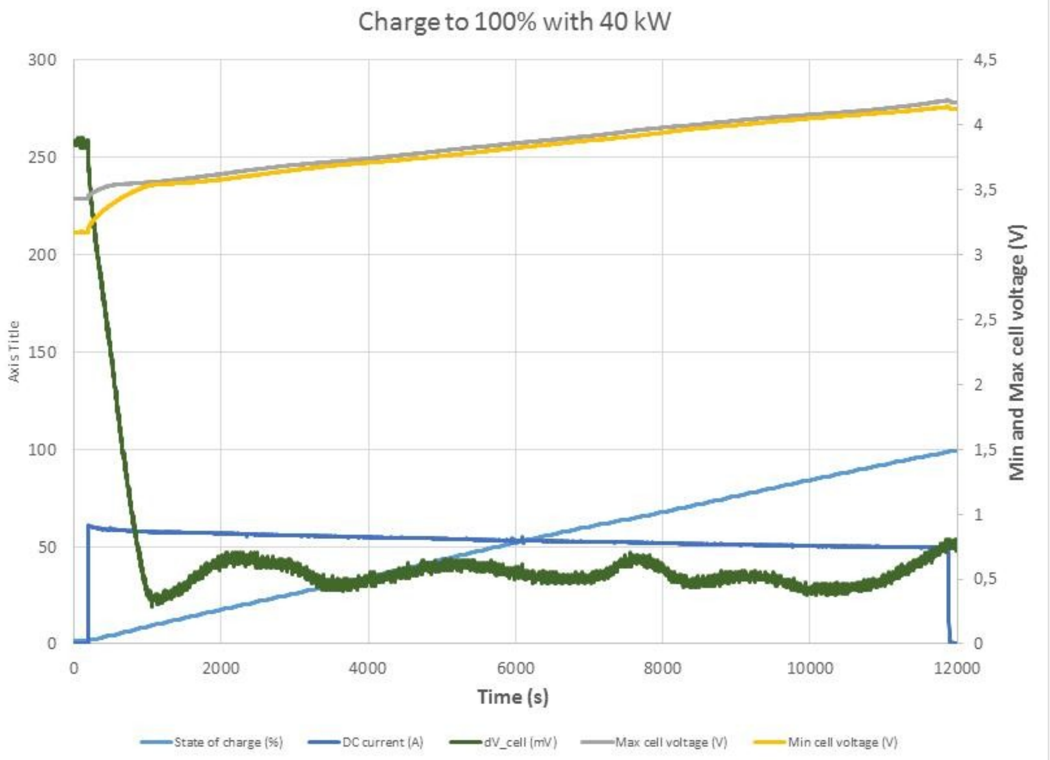

Fig. 10 Maximum and minimum cell voltages during the charge and the difference dV between max and min cell voltages.

Finally Fig. 12 shows the achieved total charged Ah and energy kWh in the test. The charge capacity was approx. 173.7 Ah and 130.2 kWh when charging between 1.5% < SOC < 99%.

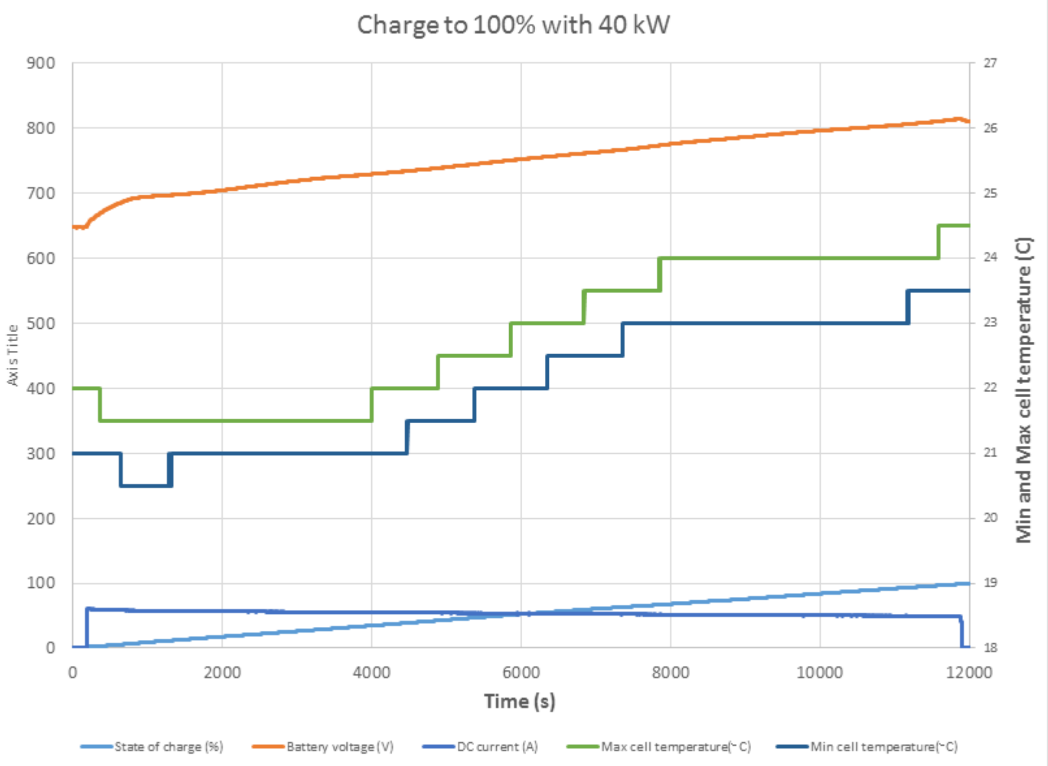

Fig. 11 Minimum and maximum battery temperature during the charge.

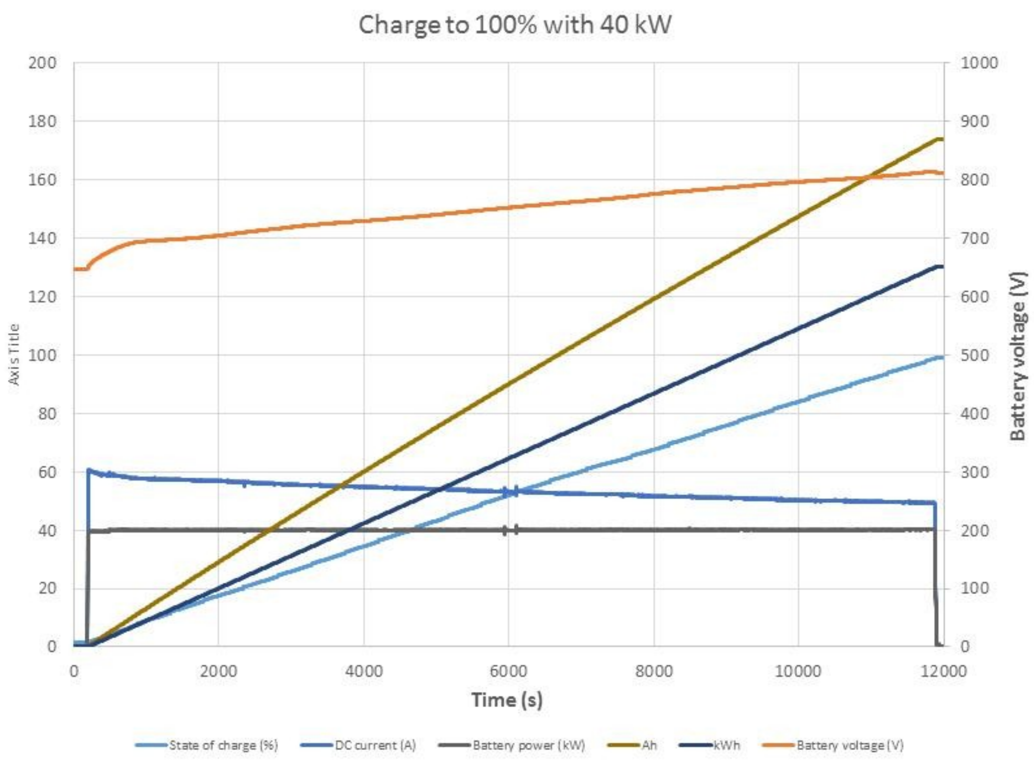

Fig. 12 Charge capacity of approx. 173.7 Ah and 130.2 kWh when charging between 1.5%<SOC<99%

5.1.3 Summary of capacity test

The capacity test is summarized in the Table 1.

Table 1. Capacity and round trip efficiency of the battery

Discharge 99-1.5%		**Charge 1.5-99%**		**Efficiency**	
Ah	**kWh**	**Ah**	**kWh**	**η_Ah_eff**	**η _kWh_eff**
168.4	123.3	173.7	130.2	0.97	0.95

Note: For discharge between 99.5 %>SOC>0.5% the discharged capacity was 170.0 Ah and 124.5 kWh.

The efficiency values is defined as [2]:

η_Ah = Ah_dicharged/Ah_charged

η_kWh = kWh_dicharged/kWh_charged

5.1.4 Pulse tests and internal resistance

The internal resistance of the system was measured by a sequence of pulsed charge and discharge at various SOC-levels (90, 75, 50), see [4]. Note: in this case measurements were not made at SOC-levels 25% and 10%. The pulses were made with 30 s long pulses with a resting time of 30 s between each pulse in a sequence of increasing amplitudes of 20kW, 40kW, 60kW, 80kW and 100kW, as shown schematically in Fig. 13.

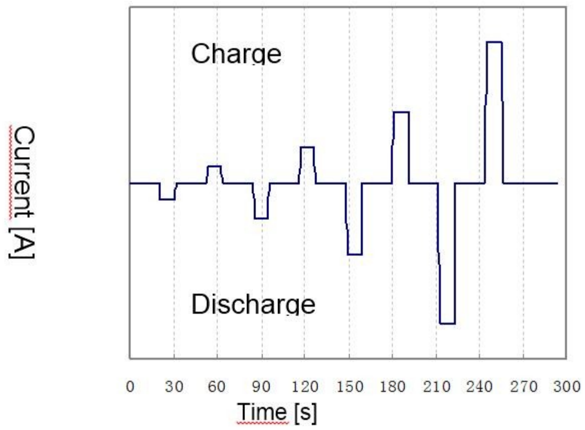

Fig. 13 Pulse testing according to the Dynamic Contrast Ratio Test Method for measurement of internal resistance [4].

The current and battery voltage at the end of each of the 30 s charge/discharge pulses are recorded. Then a voltage/current curve can be plotted accordingly by curve fitting:

$$Ubatt = Ri_{SOC} \times Ibatt - OCV_{SOC}$$

The curve's slope (*Ri_{SOC}*) is the DC internal resistance of the battery at the given SOC and *OCV_{SOC}* is the open circuit voltage of the battery at this specific SOC. Fig. 14 shows schematically the results for discharge pulses and Fig. 15 for charge pulses.

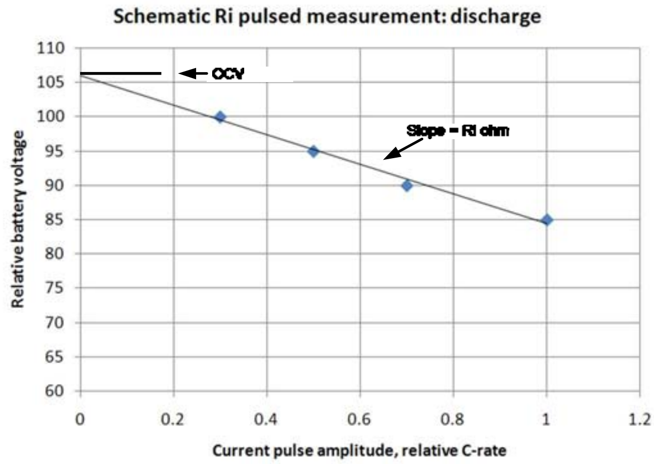

Fig. 14 Schematic principle R_i pulsed measurement at discharge

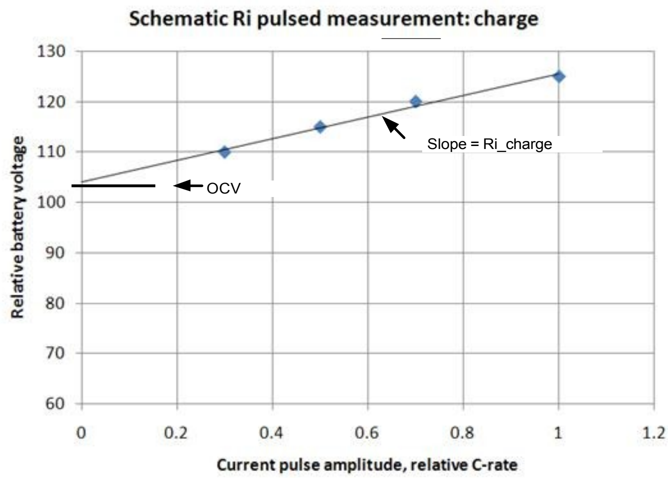

Fig. 15 Schematic principle R_i pulsed measurement at charge

Fig. 16 shows one example of a pulse sequence made on the system at SOC = 50 % and Fig. 17 shows the corresponding linear curve fitting to get the internal resistance and OCV value at discharge.

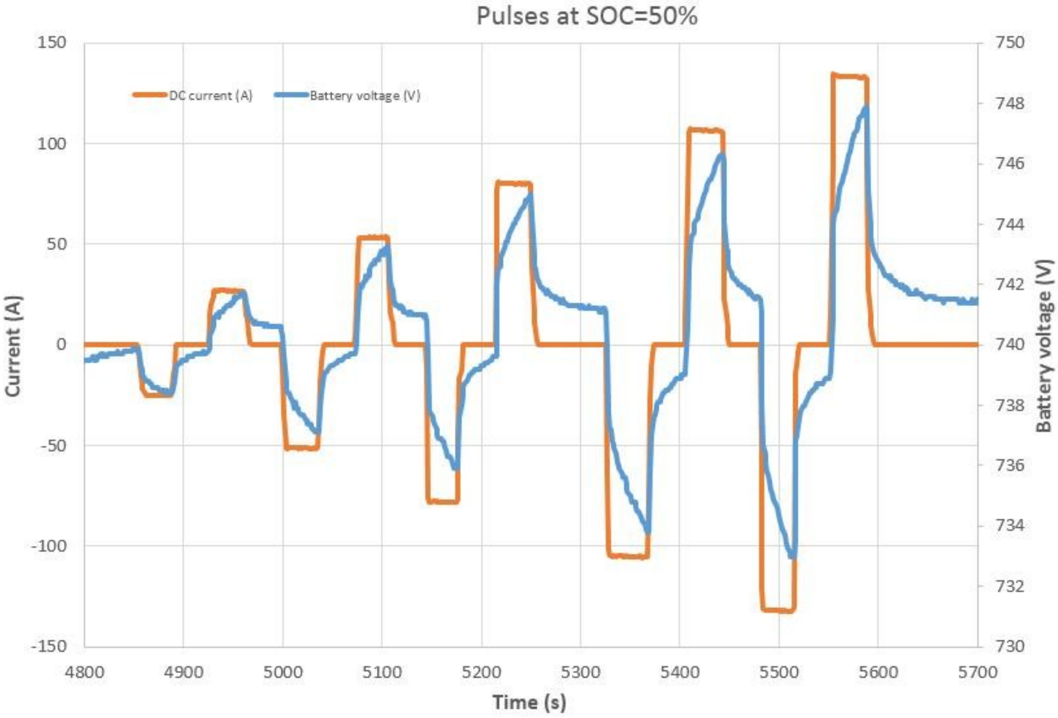

Fig. 16 Pulse sequence with 30s charge and discharge pulses of 20kW, 40kW, 60kW, 80kW and 100kW at SOC = 50 %.

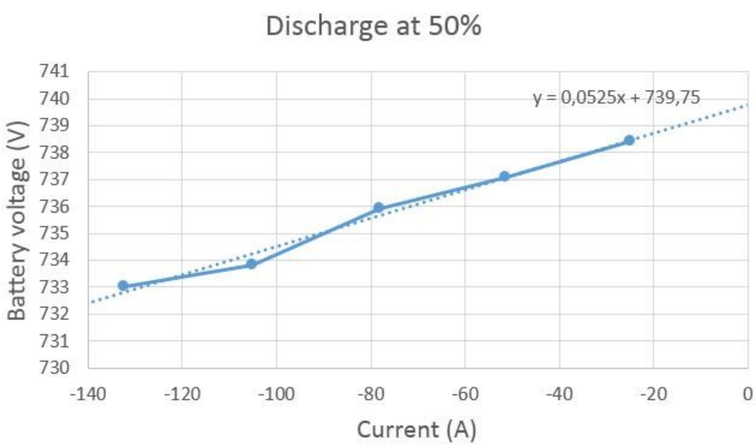

Fig. 17 Curve fitting to get internal resistance and OCV for discharge at SOC=50%.

Here the curve fitting gives a resistance R_i for discharge of 0.0525 ohm and an OCV of 739.8 V at SOC = 50 %.

Fig. 18 shows the corresponding result for charge pulses at SOC=50%.

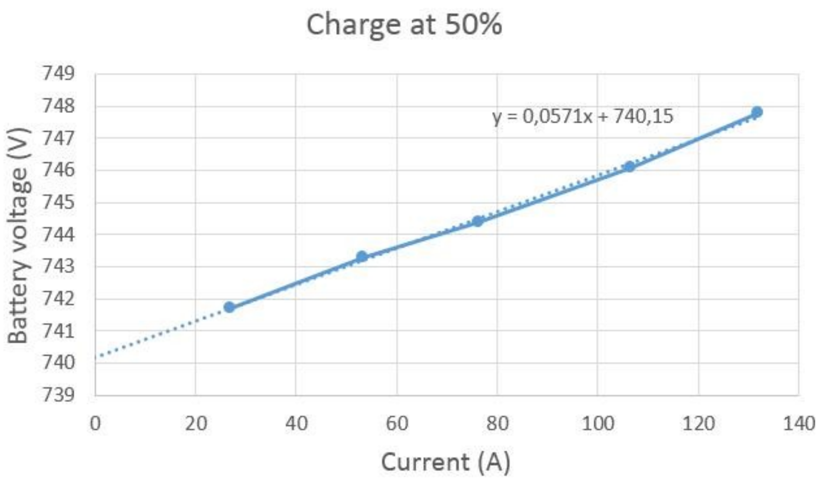

Fig. 18 Curve fitting to get internal resistance and OCV for charge at SOC=50%.

Here the curve fitting gives a resistance R_i for charge of 0.0571 ohm and an OCV of 740.2 V at SOC=50 %.

Fig. 19 shows the summary of the internal resistance and Fig. 20 shows the summary of the OCV at charge and discharge at the various SOC levels. As seen in the graph the OCV for both charge and discharge are almost identical, as it should be since the OCV measures the battery voltage with zero current.

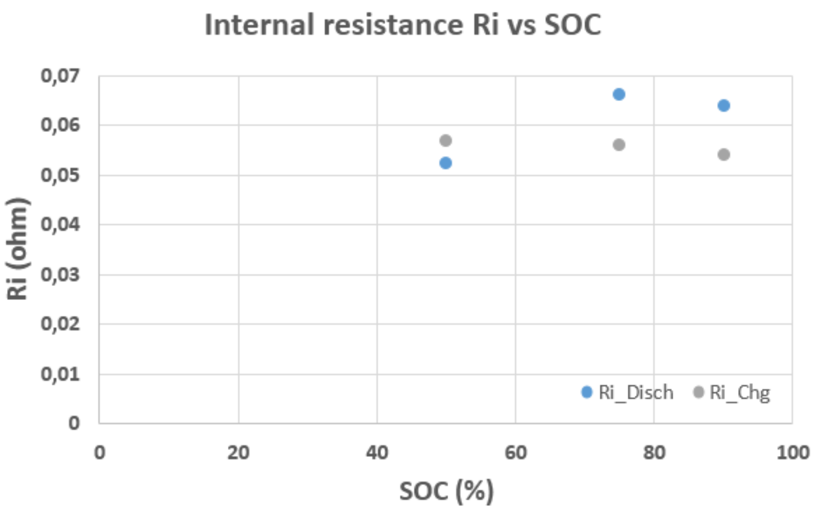

Fig. 19 Internal resistance vs. SOC from pulse measurement at charge and discharge.

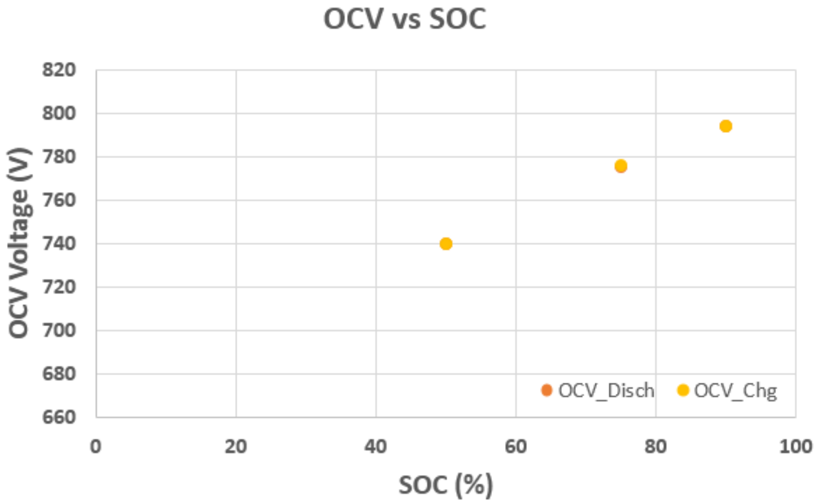

Fig. 20 OCV vs. SOC from pulse measurement at charge and discharge.

6 REFERENCES

[1] 1VPD110001A0084, FEAB Energy Storage Module: System Description, 2013-05-20.

[2] SECRC/PT/LR-14/103, Field test 6 and 7: Capacity measurements on BESS at FEAB: Battery capacity, efficiency and pulse tests, 2014-04-15.

[3] SECRC/PT/RM-11/356, Project Proposal 2012/2013, Field evaluation of grid connected energy storage.

[4] Test specification for Field Test No 7: Battery degradation plus internal resistance and peak power capability, 2013-03-22.

[5] DESS Operator´s Panel Manual, Tallinn 2011.

[6] Funktionstest: Testrapport av tillgänglighet och tillförlitlighet, FEAB, 2014-09-22.

[7] SECRC/PT/LR-14/244, Evaluation of battery degradation after 1 year operation of the FEAB BESS.

Change History

Rev.	Chapter	Description	Date / Dep. / Name
01	All	Initial document	<2014-09-22>/ SECRC/PT / W Hermansson

Issued by department	Last edit date	Lang.	Revision	Page
ZCRD/SECRC/PT/EPS	2014-09-22	Eng	01	1/10

Doc. Title	Evaluation of battery degradation after 1 year operation of the FEAB BESS, Field test 7.
Project name/ID	Energy Storage: evaluation of FEAB BESS/crid 30163 — Status of document: Final
Creator name	Willy Hermansson

9ADB1-003_ DocA4p_Portrait_Template_en.dot Rev 2.10

FEAB BESS.
Field test 7.
Evaluation of degradation

Energy Storage: Evaluation of FEAB BESS installation

TABLE OF CONTENTS

1 ABSTRACT AND SUMMARY

This report covers evaluation of the battery degradation after approximately 1 year of operation of the BESS at FEAB in Falköping. The system consists of an ABB PQFI inverter with L G Chem Li-ion batteries [1].

The evaluation is done as part of a field test program [2] performed to study the properties and performance of the system.

The evaluation is based on measurements done after 240 and 470 cycles of operation with one charge/discharge cycle between 15 % < SOC< 75 % (charge at 40 kW, and discharge at 80 kW).

Between the two measurements the battery capacity has decreased from 126.5 kWh to 124.5 kWh, and from 173 Ah to 170 Ah. Based on these data a linear extrapolation up to 10 years of operation (3650 cycles) indicates a remaining capacity of 95 – 100 kWh and 130 Ah. The design target for the battery system by LG Chem is a remaining capacity of 90 kWh, which means that the FEAB system seems to fulfill the requirement. However this estimation is very uncertain because of the limited amount of data and the long extrapolation.

Pulse tests with 30 s pulses have also been made at various SOC-levels after 170 and 410 cycles to determine the battery internal ohmic resistance and the open cell voltage (OCV = the battery voltage at zero current). The tests indicate a small decrease of the internal resistance and no change in the OCV. However the differences may be within the accuracy of the test so it is too early to draw any clear conclusions at this point. More measurements after longer time of operation should be done to get more clear answers.

2 ABBREVIATIONS

BESS	Battery Energy Storage System
ESM	Energy Storage Module
FEAB	Falbygdens Energi AB
OCV	Battery open cell voltage (at 0A battery current)
PQF	Power Quality Filter (an active power quality filters platform based on which the power converter for energy storage system has been realized)
SOC	Battery state-of-charge

3 BACKGROUND AND SCOPE

The scope of this report is to summarize the evaluation of the degradation (ageing) of the battery system in the Energy storage Module (ESM) property of FEAB installed in Falköping (Sweden) after approximately 1 year of operation.

The report covers the degradation of the battery capacity as described in project plan [2] and test description [3]:

During operation with charge/discharge cycling the battery cells will to some extent degrade because of ageing. This degradation is a function on operation cycle (e.g.

number of discharge cycles, charge and discharge rates, depth of discharge etc.) and there is also a degradation because of calendar time.

The BESS with the LG Chem batteries was started in April 2013. Capacity measurements of the system was made in January 2014 [4] after approximately 240 cycles of operation and then repeated in September 2014 [5] after another 230 cycles, i.e. after a total of approximately 470 cycles, [6]. During operation of the BESS one full cycle is made per day of a charge/discharge between 5 % < SOC < 75 %.

The analysis of the degradation is made for battery capacity, efficiency and also looking at the internal resistance during pulsed operation and the OCV [3].

4 GENERAL AND TEST CONDITIONS

Test conditions and how the tests were made are reported in [4] and [5].

5 CAPACITY DEGRADATION

The nominal starting capacity of the system as given by LG Chem was 180 Ah, 135 kWh. Taking into account the calendar ageing and cycle ageing (one cycle per day between 15% < SOC < 75%) LG Chem has designed for a remaining capacity of approx. 90 kWh after 10 years of operation.

From the measurements, [4, 5] we have the capacity data shown in Table 1.

Table 1 Summary of capacity measurements

Time	**No of cycles 2)**	**Discharge capacity**		**Efficiency**		
		Ah	**kWh**	**η_Ah_eff**	**η _kWh_eff**	
Original1)	0	180	135	--	--	
Jan. 2014	240	173	126.5	0.98	0.96	
Sept. 2014	470	170	124.5	0.97	0.95	

1) Nominal values as given from LG Chem.

2) One cycle per day between 15 % < SOC < 75 %. Charge 40 kW, discharge 80 kW.

Fig.1 shows the kWh capacity vs. number of operating cycles from the measurements and Fig. 2 shows an attempt to make an extrapolation up to 10 years of operation (i.e. 3650 number of cycles).

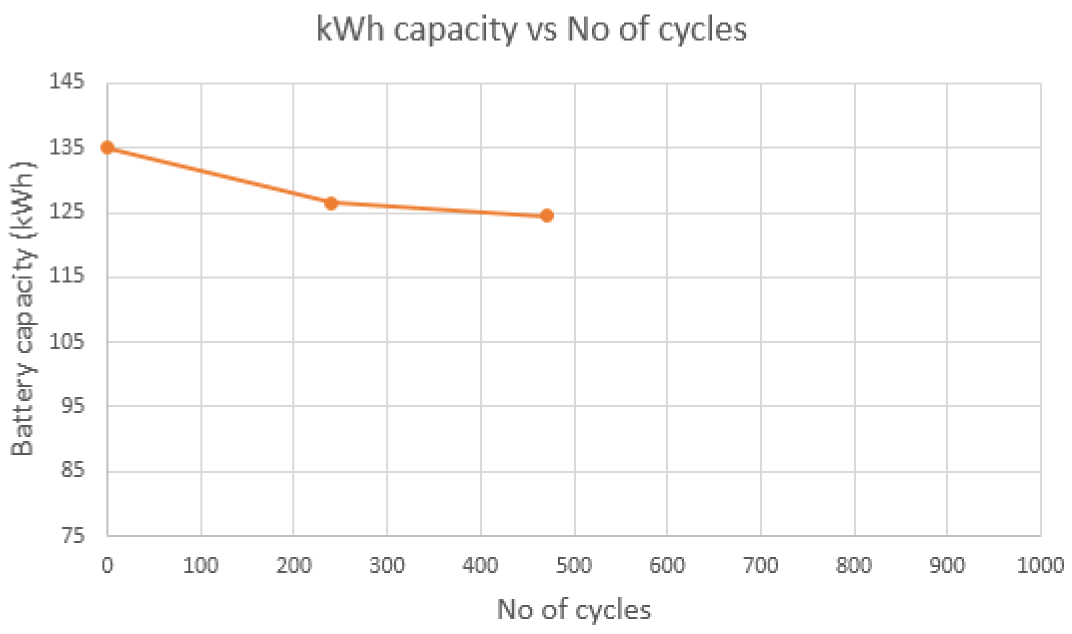

Fig.1 Battery capacity vs number of cycles of operation.

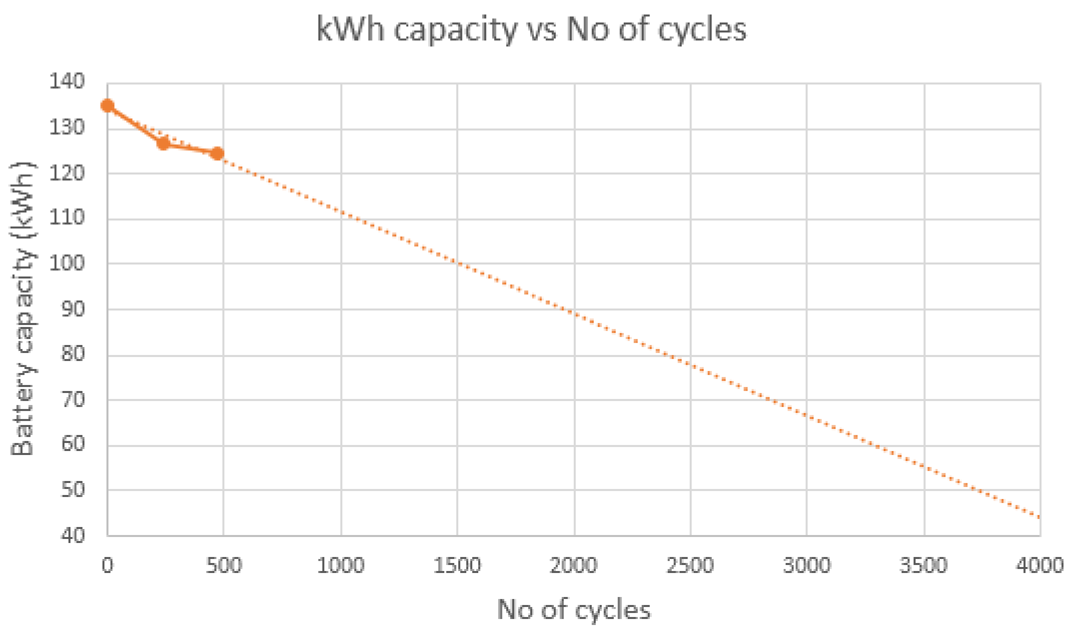

Fig.2 Extrapolation of battery capacity up to 10 years of operation.

If we just make a simple linear extrapolation of all data (including the nominal starting value) it seems that we after 10 years would have a remaining capacity of only 55 kWh. However this way of extrapolating may not be relevant due to several reasons, e.g. we do not know exactly under what conditions the nominal starting value of 135 kWh was measured, and also since the degradation is the sum of the calendar and cycle ageing how old the battery was at start is also important to know. Usually also there may be a faster degradation during the first cycles and that the ageing process after that are more slow, so a simple linear extrapolation might not be correct.

Looking at only the measured data after 240 and 470 cycles Fig. 3 shows the corresponding result. Here we can see that a simple linear extrapolation indicates a remaining capacity of 95-100 kWh after 10 years of operation, i.e. close to the design target of 90 kWh and also well above the promised battery capacity of 75 kWh.

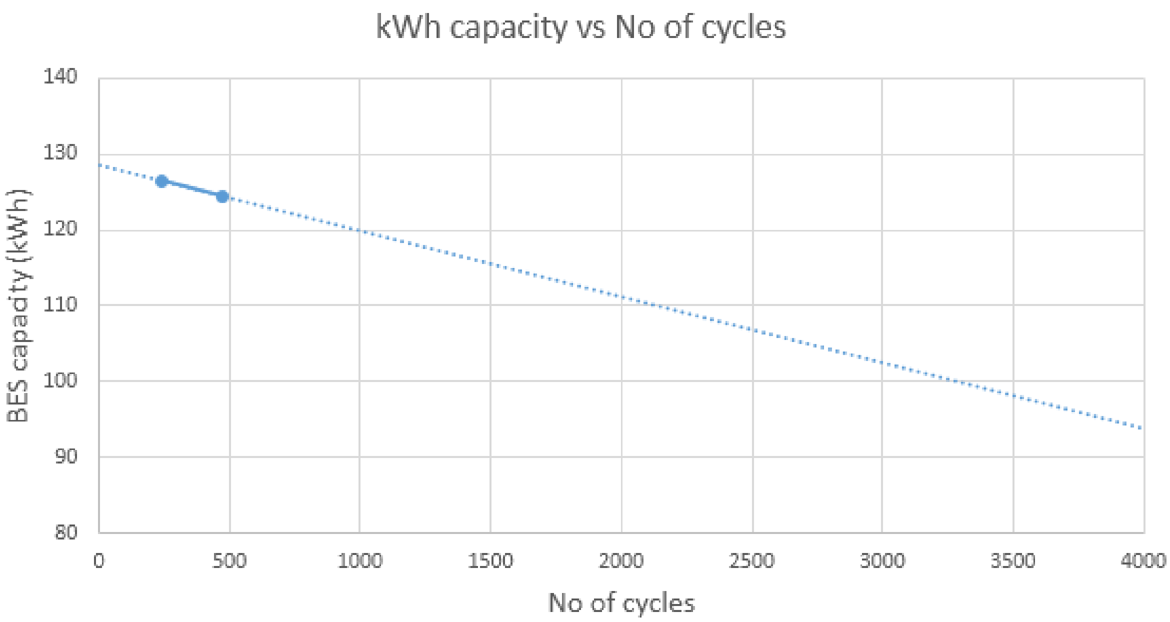

Fig. 3 Extrapolation of battery kWh capacity based on measured data after 240 and 470 cycles.

It should however be remarked that it is difficult to make any perfect extrapolated estimation based only on the very limited data we have at the moment. For that we would need at least another measurement under the same conditions after a longer time of operation.

Fig. 4 shows the corresponding result for the battery Ah-capacity, indicating a remaining capacity of approx. 130 Ah after 10 years of operation.

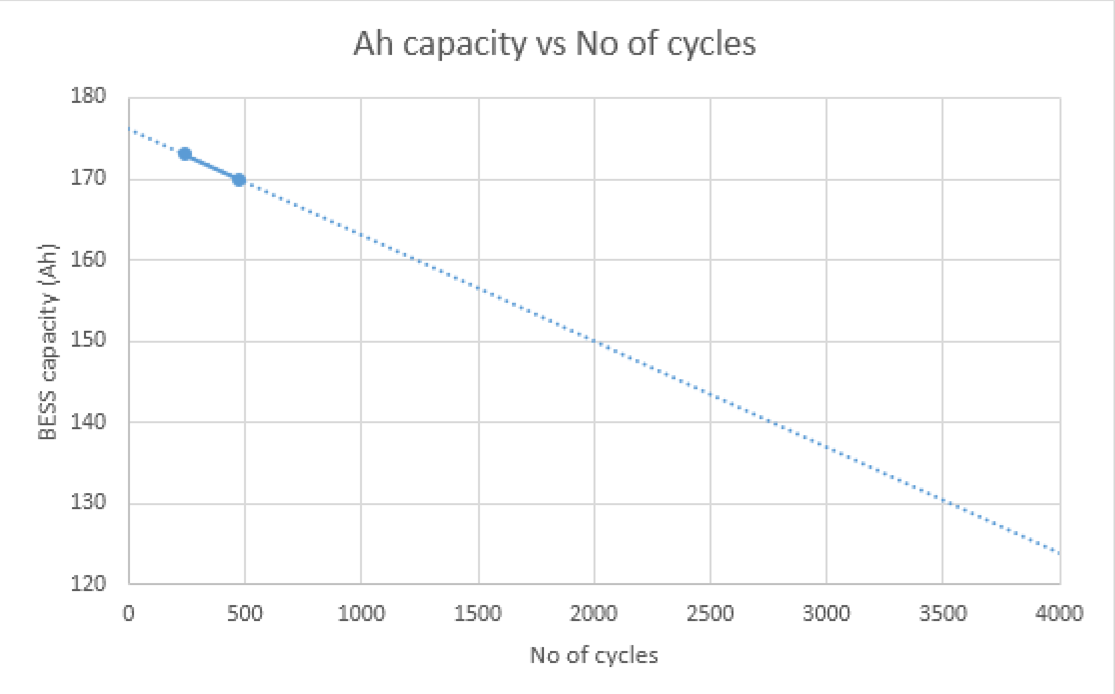

Fig. 4 Extrapolation of battery Ah capacity based on measured data after 240 and 470 cycles.

6 PULSE TESTS AND INTERNAL RESISTANCE

Table 2 shows the measured internal battery resistance at pulsed discharge operation with 30 s pulses for various SOC-levels, taken from [4, 5].

Table 2. Internal resistance at discharge for 30s pulses

Time	No of cycles [1)]	Internal resistance at discharge (ohm)				
		SOC=10%	SOC=25%	SOC=50%	SOC=75%	SOC=90%
Jan. 2014	240	0.0716	0.0609	0.0578	0.0696	0.0718
Sept. 2014	470			0.0525	0.0662	0.064

1) One cycle per day between 15 % < SOC < 75 %. Charge 40 kW, discharge 80 kW.

The amount of data is very limited so it is difficult to draw any large conclusions. However there seem to be a trend of decreasing resistance with time, although this effect may be within the accuracy of the test.

Table 3 shows the measured internal battery resistance at pulsed charge operation with 30 s pulses for various SOC-levels, taken from [4, 5].

Table 3. Internal resistance at charge for 30s pulses

Time	No of cycles [1)]	Internal resistance at charge (ohm)				
		SOC=10%	SOC=25%	SOC=50%	SOC=75%	SOC=90%
Jan. 2014	240	0.0614	0.0537	0.0584	0.0628	0.0564
Sept. 2014	470			0.0571	0.056	0.0541

1) One cycle per day between 15 % < SOC < 75 %. Charge 40 kW, discharge 80 kW.

The amount of data is also here very limited so it is difficult to draw any large conclusions. However there seem to be a trend of decreasing resistance with time also here, but this effect may be within the accuracy of the test.

The measured OCV (=battery voltage at zero current) for various SOC-levels during the pulse measurements, taken from [4, 5], are shown in Table 4 and 5.

Table 4. OCV measured at discharge

Time	No of cycles [1)]	OCV (V)				
		SOC=10%	SOC=25%	SOC=50%	SOC=75%	SOC=90%
Jan. 2014	240	685	705	741	777	795
Sept. 2014	470			740	776	794

1) One cycle per day between 15 % < SOC < 75 %. Charge 40 kW, discharge 80 kW.

Table 5. OCV measured at charge

Time	No of cycles [1)]	OCV (V)				
		SOC=10%	SOC=25%	SOC=50%	SOC=75%	SOC=90%
Jan. 2014	240	685	706	741	777	794
Sept. 2014	470			740	776	794

1) One cycle per day between 15 % < SOC < 75 %. Charge 40 kW, discharge 80 kW.

To be noted is that the OCV is the same for both discharge and charge, which is as expected since the OCV is the battery voltage in stand-by mode at zero current.

Also OCV values are identical (within the measurement accuracy) at the two occasions after 240 and 470 cycles of operation, i.e. no clear change can be seen.

7 REFERENCES

[1] 1VPD110001A0084, FEAB Energy Storage Module: System Description, 2013-05-20

[2] SECRC/PT/RM-11/356, Project Proposal 2012/2013, Field evaluation of grid connected energy storage.

[3] Test specification for Field Test No 7: Battery degradation plus internal resistance and peak power capability, 2013-03-22.

[4] SECRC/PT/LR-14/103, Field test 6 and 7: Capacity measurements on BESS at FEAB: Battery capacity, efficiency and pulse tests, 2014-04-15.

[5] SECRC/PT/LR-14/243, Capacity measurements on BESS at FEAB: Evaluation of degradation. Measurements in Sept 2014, 2014-09-20.

[6] Funktionstest: Testrapport av tillgänglighet och tillförlitlighet, FEAB, 2014-09-22.

Change History

Rev.	Chapter	Description	Date / Dep. / Name
01	All	Initial document	<2014-04-23>/ SECRC/PT / W Hermansson

Funktionstest: Testrapport av Tillgänglighet och Tillförlitlighet

Innehållsförteckning

1. Inledning

Den här testrapporten ingår i projektet *Test och utvärdering av energilager*. Testet *Tillgänglighet och Tillförlitlighet* innebär en utvärdering av energilagret och systemet över en längre tid i en verklig driftsituation. Om energilagret ska kunna användas för en mer kommersiell drift och delta på någon typ av marknad för att sälja tjänster, så krävs det även att man har kontroll över att det fungerar och att det levererar tjänsten som tänkt. Det finns många av energilagrets olika egenskaper och funktioner som skulle vara relevanta att testa. Exempelvis driftsäkerhet, robusthet, säkerhet, prestanda men också användbarhet, tillgänglighet, skalbarhet, livscykeleffektivitet osv. Vissa av funktionerna har utvärderats i några av de andra testerna i projektet, men i det här testet har fokus varit att analysera tillgängligheten och tillförlitligheten hos energilagret.

1.1 Bakgrund

En hög tillförlitlighet är en egenskap som nästan alla elnäten i världen har och framför allt i Sverige. Avbrott i strömförsörjningen påverkar kunderna negativt och långa omfattande avbrott kan även bli samhällsfarligt.
En hög tillförlitlighet av elnätet får man genom en hög tillförlitlighet av alla komponenter i elnätet. Det är därför viktigt att de olika komponenterna i elnätet, i framtiden också batterilagret, har en hög tillförlitlighet.

1.1.1 Tillförlitlighet

En viktig tillförlitlighetsegenskap hos energilagret är dess driftsäkerhet.

”Driftsäkerhet är förmågan hos en enhet att kunna utföra krävd funktion under angivna förhållanden vid ett givet tidsintervall under antagandet att erforderliga externa underhållsresurser tillhandahålls[1]*”.*

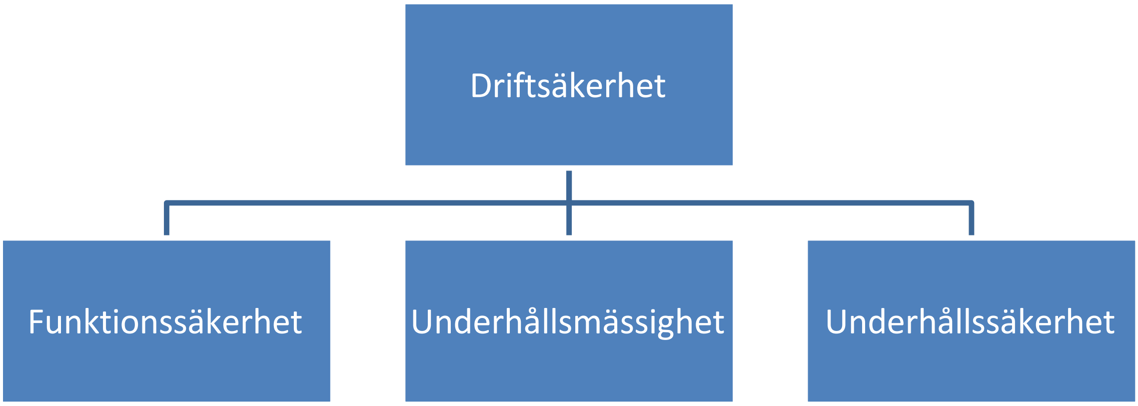

Figur 1. Driftsäkerhet

En enhets driftssäkerhetsegenskaper bestäms av:

- *Funktionssäkerhet*, som är en produkts förmåga att utföra krävd funktion under givna förhållanden.
- *Underhållsmässighet*, som är ett mått på hur lätt det är att upptäcka, lokalisera och avhjälpa fel på produkten.

[1] Bo Bergman, Bengt Klefsjö, Kvalitet från behov till användning, Studentlitteratur, 2008, sid 149-150

- U*nderhållssäkerhet*, som är underhållsorganisationens förmåga att tillhandahålla de resurser som erfordras för underhållet.

De två förstnämnda egenskaperna är knutna till produkten, medan underhållssäkerheten är ett mått på underhållsorganisationens effektivitet. [2]

1.1.2 Tillgänglighet

Tillgänglighet är ett driftsäkerhetsmått som går att mäta på flera olika sätt. De faktorer som man får ta hänsyn till är exempelvis momentant värde, medelvärde och asymptotiskt värde, nedan några exempel.

- *Allmän metod för mått på tillgänglighet*. Denna tillgänglighetsmetod tar hänsyn till total tid och är lämplig för system som alltid är i drift.
- *Inre tillgänglighet*. Som enbart beror på det tekniska systemet. Med den metoden tas endast hänsyn till avhjälpande underhåll.
- *Systemtillgänglighet*. Som enbart beror på det tekniska systemet och på det underhållstekniska systemet.
- *Drifttillgänglighet*. Som beror på det tekniska systemet, det underhållstekniska systemet och ledningssystemet för drift.[3]

1.2 Omfattning

Tre nyckeltal har valts ut för att analyseras (två för tillförlitlighet och en för tillgänglighet) i rapporten. Testperioden har varit från 2013-04-30 till 2014-08-30 (16 månader).

Mått som ingår:

1. *Funktionssäkerhet*, som ingår i tillförlitlighet, är förmågan hos en enhet att utföra en krävd funktion under givna förhållanden under ett givet tidsintervall. Ett vanligt mått som användes för funktionssäkerhet är *felfrekvens*, dvs antal fel per tidsenhet.
2. *Underhållsmässighet* är förmågan hos en enhet att utföra krävd funktion under givna förhållanden under ett angivet tidsintervall. Dvs ”hur lätt är det att göra underhåll?” och mäts i det här fallet som *medelreparationstiden (återställningstid).*
3. *Tillgängligheten* mäts som totaldriftstid minus stopptid genom totaldriftstid. Denna tillgänglighetsmetod tar hänsyn till den totala tiden och är vald för systemet alltid är i drift.

1.2.1 Avgränsningar

Underhållssäkerhet som också ingår begreppet Driftsäkerhet har inte testats. Ursprungsidén var att genomföra en FMEA (Failure Modes and Effects Analysis) som är en systematisk metod för att förutsäga möjliga fel och konsekvenser. Men detta fall hade det endast varit ABBs leveranstider av olika komponenter som hade utvärderats och inget som en underhållsorganisation hos Feab kan påverka.

[2] Bo Bergman Bengt Klefsjö, Kvalitet från behov till användning, Studentlitteratur, 2008, Sid 149 -150
[3] http://sv.wikipedia.org/wiki/Drifts%C3%A4kerhet#M.C3.A5tt_f.C3.B6r_tillg.C3.A4nglighet, 2014-09-18

1.3 Dokumenthistorik:

Utgåva	Datum	Utfärdare	Kommentar
0.1	2014-09-16	Pia Borg	Första version, utkast
0,2	2014-10-09	Pia Borg	Justering av tiden för testperioden
0,3	2014-10-14	Pia Borg	Uppdaterad efter granskning

1.4 Refererade dokument

Alla dokument som omnämns i sluttestrapporten:

[Ref 1] Testspecifikation Tillgänglighet och Tillförlitlighet
[Ref 2] Systembeskrivning 1
[Ref 3] Testmiljöbeskrivning 1
[Ref 4] Testprotokoll Tillgänglighet och Tillförlitlighet

1.5 Förkortningar och begrepp

Nedan förklaras alla begrepp och förkortningar som används i dokumentet.

Feab	Falbygdens Energi AB
LG	Lucky- Goldstar
RTU	Remote Terminal Units
MODBUS – TCP	Seriell kommunikationsprotokoll
IEC 61850	Standard för konstruktion av elektrisk transformator automation mm

2. Översikt

Sen 2013-08-30 har Feab:s underhållspersonal registrerat alla stillestånd av energilagret i en ärendehanteringslista. Den innehåller uppgifter som datum och tid när energilagret stannade och återstartades, felkod, prioriteringsgrad av händelsen, möjlig orsak till att energilagret löste ut osv.

Innan testperioden pågick 4 månader med inkörning av de nya batterierna, se diagram 1. Det första stilleståndet under perioden orsakades av att energilagret störde ut avläsningen av fjärrvärmemätare. När det upptäcktes stannades energilagret. Det visade sig att i samband med batteribytet från International Battery till LG hade en mellantransformator kopplats bort. Man åtgärdade problemet med att koppla in transformatorn igen. Det andra stilleståndet berodde på att batterienheten gick sönder och behövde därför bytas ut. ABB (Estland) löste och åtgärdade bägge problemen.

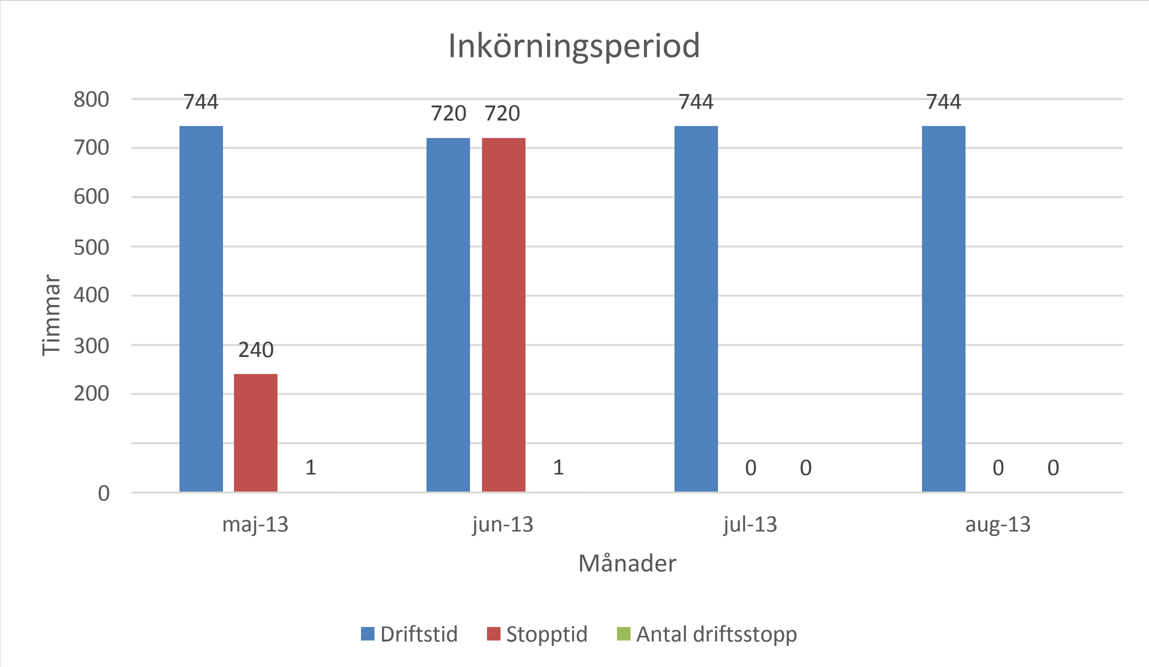

Diagram 1. Driftstid och stopptid under inkörningsperioden.

Under den 12 månader långa testperioden stannade energilagret totalt 9 gånger, se diagram 2. Samtliga fel orsakades av händelser i det överliggande nätet. Energilagret var från början inte utrustad med något externt övervakningssystem som larmar vid driftstopp eller fel. Då upptäcks endast störningar i energilagret vid ronderingen en gång per vecka. Det innebar att det inte fanns någon tillräcklig kontroll över driften och att driftstoppen varade därför längre än nödvändigt.

Energilagret har nu integrerades med distributionsnätets *Micro Scada* och övervakas sen juni 2014 på samma sätt som de övriga komponenterna i elnätet. Man har anslutit energilagret via en signalkabel från närliggande transformatorstation så att ett samlingslarm går in i *Micro Scada*. Vid utlöst brytare går ett larm till *Micro Scada* som sedan skickar det vidare till servicepersonalens Mini Call. Integreringen har skett genom en implementering av RTU och standardiserat protokoll och inte som först var tänkt, genom MODBUS-TCP och IEC 61850. Funktionen är dock den samma.

Efter installationen av larmet har driftstoppstiderna minskat något. Som minst varade ett driftstopp nästan 2 timmar. Då samtliga fel under sommaren 2014 har berott på åskoväder och elavbrott har energilagrets återstart prioriterats lägre än elleveransen till övriga kunderna. Även då man har haft informationen om att energilagret stått stilla har det inte funnits resurser att återstarta det förrän efter 1 – 2 dagar. Vid några tillfälle har avbrottet inträffat under helger (endast jourpersonal tillgänglig) vilket har inneburit att energilagret inte kunnat startas om förrän under måndagen när ordinarie personal återigen har varit i tjänst. Att energilagret står stilla i dagsläget påverkar ingen annan elkund. Prioriteringsordningen skulle däremot behöva vara annorlunda om energilagret levererade någon typ av tjänst till kund där driftstopp skulle innebära bortfall av både inkomst eller elleverans.

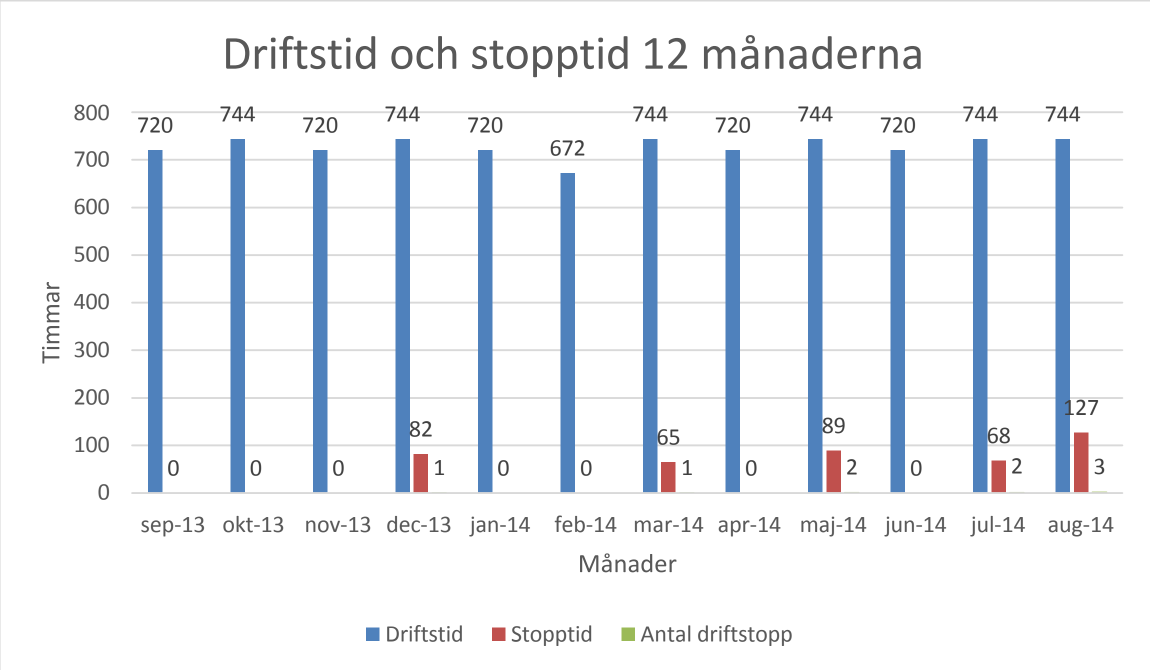

Diagram 2. Driftstid och stopptid under 12 månaderna i energilagret.

Under det första halvåret inträffade det endast ett driftstopp, se diagram 2. Händelsen upptäcktes vid veckoronderingen. Det enda man har kunnat se är att driftstoppet men all sannolikhet orsakades av spänningsfall på överliggande nät. Det har antingen varit för låg spänning eller för långt (tidsmässigt) spänningsbortfall.

Under de senaste 6 månaderna som energilagret har utvärderat har det förekommit fler driftstopp än tidigare. Orsaken till det är (som tidigare nämnts i rapporten) alla de åskoväder med bla efterföljande elavbrott som har förekommit under sommaren 2014. I maj skedde 2 driftstopp, ett på 2 dagar och 4 timmar respektive ett på nästan 1 dag och 13 timmar.

I juli inträffade nästa två driftstopp, ett på 2 dagar och 18 timmar respektive ett på nästan 2 timmar. Vid det senare driftstoppet fick underhållspersonalen på Feab larm om stilleståndet.

Testperioden för augusti innehöll (flest till antalet) tre driftstopp. Första stoppet varade 1 dag och 3 timmar, det andra 2 dagar och 1 timme medan det sista pågick 2 dagar och 3 timmar. Anledningen till de långa driftstoppen, trots inkopplat larm, är som tidigare nämnts att energilagret inte har haft någon hög prioritet för återstart vid elavbrott.

3. Utförda beräkningar

3.1 Felfrekvens (Funktionssäkerhet)

Funktionssäkerhet som ingår i tillförlitlighet är förmågan hos en enhet att utföra en krävd funktion under givna förhållanden under ett givet tidsintervall. Ett vanligt mått som kan användes för se på funktionssäkerhet är felfrekvens, dvs antal fel per tidsenhet (exempelvis fel/år).

3.1.1 Formel

Felfrekvens = $\frac{\text{[illegible]}}{\text{[illegible]}}$

Driftsperiod = 12 månader
Antalet fel under driftsperioden = 0 stycken
Antal indirekta fel under driftsperioden = 9 stycken

<u>Felfrekvensen för energilagret</u> = $\frac{0}{12}$ = 0 fel/månaden
<u>Felfrekvensen för systemet</u> = $\frac{9}{12}$ = 0,75fel/månaden

3.1.2 Analys av resultat

Ingen utav de 9 stopptillfällena har orsakats av något direkt fel i energilagret. Resultatet för energilagret blir därför hög funktionssäkerhet med en *Felfrekvens = 0 fel/månaden*. Om man däremot beräknar indirekta fel som har orsakats av yttre händelser blir felfrekvensen i genomsnitt 0,75 fel/månaden för hela anläggningen.

3.2 Medelreparationstid (Underhållsmässighet)

Underhållsmässighet är förmågan hos en enhet att utföra krävd funktion under givna förhållanden under ett angivet tidsintervall. Populär förklaring av underhållsmässighet är ”hur lätt är det att göra underhåll?”. Här har underhållsmässighet utvärderats genom medelreparationstiden (MTTR) som i detta fall är lika med återställningstiden av energilagret.

3.2.1 Formel

MTTR = $\frac{\text{[illegible]}}{\text{[illegible]}}$

Summa återställningstid (reparationstid) = 431 timmar (12 månader)
- Antalet återstarter (reparationer) = 9 stycken

Summa reparationstid under de första 6 månaderna = 82 timmar
- Antalet reparationer = 1 stycken

Summa reparationstid under de sista 6 månaderna = 349 timmar
- Antalet reparationer = 8 stycken

Summa reparationstid efter att larm hade kopplats in = 195 timmar (2 månader)
- Antalet reparationer = 5 stycken

Under den tiden som testet genomfördes var medelreparationstiden följande vid olika utvärderingsperioder:

<u>Under 12 månader.</u> <u>MTTR</u>= $\frac{431}{9}$ = 47,88… 47,9 timmar.

<u>De första 6 månaderna</u>. <u>MTTR</u>= $\frac{82}{1}$ = 82,0 timmar.

<u>De sista 6 månaderna.</u> <u>MTTR</u>= $\frac{349}{8}$ = 43,62… 43,6 timmar.

<u>Efter att larm hade kopplats in.</u> <u>MTTR</u>= $\frac{195}{5}$ = 39,0 timmar.

3.2.2 Analys av resultat

I detta fall är reparationstiden samma som återställningstiden. Det är tiden från att energilagret har löst ut och stannat tills att Feab:s personal har återställt och startat upp energilagret igen. Trenden är att återställningstiden gradvis sjunker. I slutet av juni 2014 kopplades ett larm från energilagret till Scada vilket kan förklara varför medelreparationstiden har minskat ytterligare under de sista 2 månaderna trots att det är ett relativt högt antal avbrott. Fortfarande har övriga elkunder högre prioritet vid elavbrott än energilagret. Vilket också är naturligt då anläggningen fortfarande är en prototyp och inte används för något kommersiellt syfte samt att inga andra elkunder har berörts av att energilagret har stått stilla.

3.3 Tillgänglighet

Det finns flera sätt att mäta tillgänglighet på. Det finns olika faktorer som man kan ta hänsyn till exempelvis momentant värde, medelvärde osv. Enhet är i procent Tillgänglighet = 1-otillgänglighet i procent. Denna tillgänglighetsmetod tar hänsyn till total tid och är vald för systemet då det alltid är i drift. Drifttid + otillgänglighet(summa väntetid + summa åtgärdstid)= total tid Ttot.

3.3.1 Formel

$$Tillgänglighet = \frac{T[illegible] - [illegible]i[illegible]ä[illegible]ih[illegible]}{T[illegible]}$$

Summa totaldriftstid = 8 760 timmar (12 månader)

- Reparationstid = 431 timmar (12 månader)

Driftstid 6 månader = 4380 timmar

- Reparationstid de första 6 månaderna = 82 timmar
- Reparationstid de sista 6 månaderna = 349 timmar

Driftstid 2 månader = 1488 timmar

- Reparationstid efter inkopplat larm = 195 timmar

<u>Tillgänglighet (12 månader)</u> = $\frac{8760-431}{8760}$ = 0,950… = 95 %

<u>Tillgänglighet (första 6 månader)</u> = $\frac{4380-82}{4380}$ = 0,981…= 98 %

Tillgänglighet (sista 6 månader) = $\frac{4380-349}{4380}$ = 0,920…= 92 %

Tillgänglighet (inkopplat larm) = $\frac{1488-195}{1488}$ = 0,868…= 87 %

3.3.2 Analys av resultatet

Resultatet visar att tillgängligheten för energilagret har totalt sett varit 95 % under de 12 månader som utvärderingsperioden har pågått. De olika stopptiderna har varierat mellan ca 2 timmar (efter att larmet hade kopplats in) till drygt 82 timmar. En anledning till de långa stopptiderna har varit att från första början upptäcktes felen endast vid rondering av energilagret (1 gång/vecka). En annan orsak är att alla andra elkunder prioriteras vid elavbrott framför återstart av energilagret. Under de senaste 4 månader har samtliga stopp inträffat vid åskoväder och sannolikt orsakats av spänningsfall, antingen för låg spänning eller för långt spänningsbortfall. Samtliga stopp och fel har orsakats av händelser i överliggande nät. Energilagret har ingen automatisk återstart i dag och ingen funktion för att särskilja olika typer fel. Att det löser ut och stannar vid olika händelser i överliggande nät kan vara ett problem.

4. Diskussion

Energilagret i Falköping är inte utrustad med omriktare som klarar att hålla frekvensen själv och man klarar inte utlösningsvillkoren hos kunderna i det aktuella nätet. Som det är konstruerat nu kan energilagret inte användas för ”ö-drift”, vilket heller inte är tillåtet. Men ska det användas för någon typ av reservkraft bör det inte vara lika känsligt för händelser i överliggande nät. Det borde vara utrustad med någon form av automatisk återstart som träder in om det inte är något fel på energilagret som har orsakat stoppet. Det skulle vara intressant att analysera störningstålighet av energilagret. För framtiden är det även viktigt att det definieras krav på störningstålighet av energilager.

Document number: 1VPD110001A0118	**Energy Storage Module** **Evaluation of ambient conditions**				
Dept.	Project	Status Date	Author	Status	Revision
PPMV	FEAB	19.08.2013	Carlos Nieto	Released	1

Rev.	Description	Modified by	Date/Initial
1	First version	Carlos Nieto	19.08.2013

Table of Contents

1 Introduction

1.1 Scope, purpose and extent

The scope of this document is to present a technical report about the evaluation of ambient conditions in the Energy storage Module (ESM) property of FEAB installed in Falköping (Sweden).

The purpose of the series of tests is to check the noise level outside the enclosure and the temperature inside the enclosure.

1.2 References

[Ref 1] Test Specification for Evaluation of ambient conditions in energy storage system.
[Ref 2] Test environment description for evaluation of ambient conditions - Audible noise 20130405.
[Ref 3] Test environment description for evaluation of ambient conditions - Temperature 20130405

1.3 Abbreviations

BESS Battery Energy Storage System

PQF Power Quality Filter (an active power quality filters platform based on which the power converter for energy storage system has been realized)

FEAB Falbygdens Energi AB

ESM Energy Storage Module

AC Alternating Current

DC Direct Current

2 General

2.1 Hardware

The hardware used to develop the test is the Energy storage Module (ESM) property of FEAB installed in Falköping (Sweden) a sound level meter and the data logger installed inside the enclosure. All the configurations and the methods for testing are described in [Ref 1].

2.2 System Settings

The following settings have been modified during the tests:

- System switched off;
- System running in normal conditions.

3 Tests

The aim of the following tests is to identify the temperature inside the enclosure during normal operation of the ESM and the audible noise outside the enclosure.

3.1 Temperature

3.1.1 Test procedure

The temperature test has been carried out through the readings of the data logger installed inside the ESM. The data logger received the information from four temperature sensors allocated in different points of the enclosure, such as close to the doors, battery room, inverter room and also outside the ESM. The measurements have been recorded during May and June, 2013.

3.1.2 Test results

Figure 1 shows the temperature variation during May and June, 2013. As it can be seen, the temperature in the hottest sensor does not exceed 45°C. It should be remarked that the temperature sensors are allocated in close to the ceiling of the enclosure, thus they are measuring the highest temperature of the air.

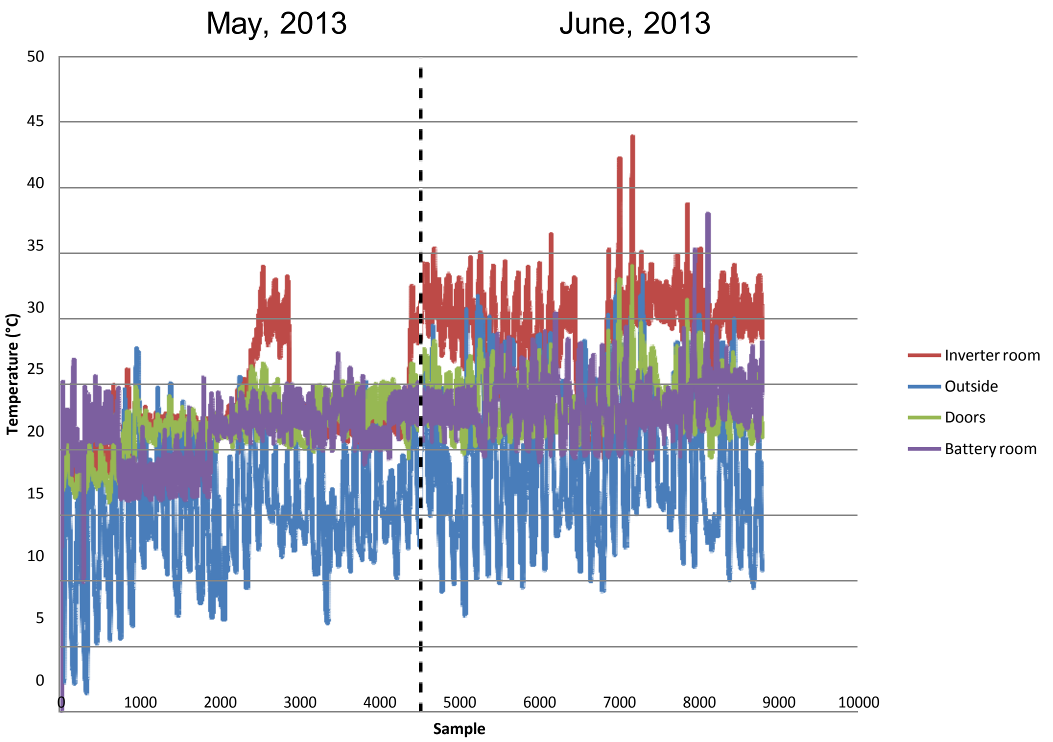

3.2 Audible noise

3.2.1 Test procedure

The audible noise test has been carried out by means of a sound level meter measuring the noise outside the enclosure with the system switched off and running in normal operation at both night and day time in order to compare results. The measurements have been taken in the points depicted in Figure 1 which are separated from the enclosure 1 meter.

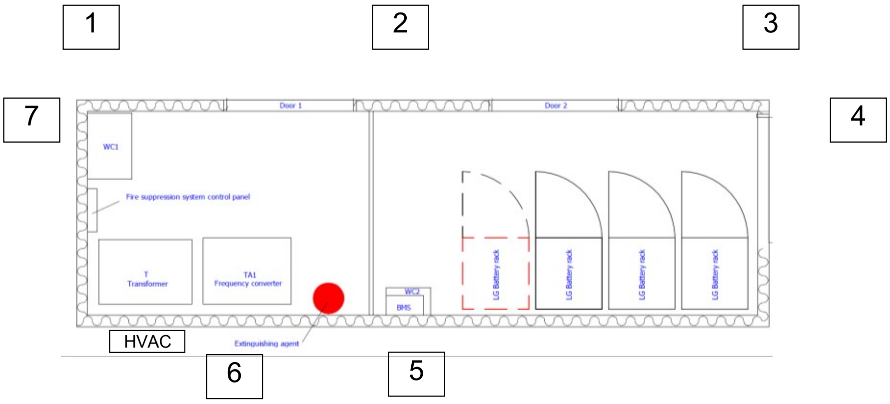

Figure 1: Measurements points for audible noise.

3.2.2 Test results

Table 1 shows the results of the test for day and night time with system running and switched off.

Sound Level (dBA)		Point 1	Point 2	Point 3	Point 4	Point 5	Point 6	Point 7	Mean Value
Day time	ESM OFF	58	59	57	58	55	56	57	57,14
	ESM ON	59	60	58	57	56	57	57	57,71
Night time	ESM OFF	47	46	46	46	47	47	46	46,43
	ESM ON	47	47	46	46	48	48	47	47,00

Table 1: Audible noise in dBA in different conditions for the measurement points of Figure 1.

As it can be observed in Table 1, the contribution of the operation of the ESM to the audible noise is minimum, with an approximate value of 0,6dBA.

The noise during day time was very influenced by cars passing by the ESM installation. At night time with no cars, the ambient noise was significantly reduced.

4 Conclusions

After the tests done in the ESM and evaluated the data, the main conclusions for the ambient conditions are the following.

- The maximum temperature achieved in the enclosure is 45°C in the hottest point close to the inverter.
- The contribution of the ESM to the audible noise is 0,6dBA when the ESM is running.

ABB Document number: 1VPD110001A0118	**Energy Storage Module** **Evaluation of ambient conditions**				
Dept. PPMV	Project FEAB	Status Date 19.08.2013	Author Carlos Nieto	Status Released	Revision 1

ABB AS

Main office:
Aruküla tee 59
75301 Jüri, Rae vald, Harjumaa. Estonia
Tel: +372 6801 800
Fax: +372 6801 810
E-mail: info@ee.abb.com
Internet: www.abb.ee

Manufacturing site:
Aruküla tee 83
75301 Jüri, Rae vald, Harjumaa. Estonia
Tel: +372 634 9295
Fax: +372 6349299
E-mail: css.orders@ee.abb.com

Brief Report Corporate Research			SECRC/PT/2012	
Issued by department SECRC	Last edit date 2012-11-28	Lang. Eng	Revision 01	Page 1/25
Customer		Classification	Normal	
Doc. title	**Magnetic Fields at Fälköpings battery energy storage installation**			
Project name/ID		Status of document	Draft	
Main Author	Ener Salinas	Project ID (CRID) or Order no		
Additional Author(s)		CR Program		
Distribution				
Keywords	Magnetic field, DC, energy storage, converters, battery, substation, , EMC.			

ABSTRACT:

A set of magnetic field measurements were performed inside and outside the battery energy storage installation at Falköping. At the same time, the magnetic field in the vicinity of the adjacent substation as well as the nearby walking path was also measured.

Measurements outside the installations at the public walking path as well as the regions towards a children's playground in the vicinity the magnetic field values were well below the recommended values given by well-established organizations (WHO, ICNIRP).

The inner measurements were made in standby and in discharge model. The main fields produced in this facility supposed to be DC. Yet, surprisingly, the detected magnetic fields for both modes consisted mainly of high values (e.g. 30 μT) and high frequencies (up to 3 kHz).

Moreover, since previously there were some unexplained tripping in the system, this main finding is expected to help understanding the nature of those failures.

TABLE OF CONTENTS

1 BACKGROUND

On the one hand, in the past decade, the systems related to the insertion of renewable energies to the main grid, as well as DC transmission and storage have become more and more commonplace. On the other hand, encompassing this development, the use of modern devices can sometimes generate issues concerning magnetic fields generated by the installation components and the cause of this issue is twofold. One reason is related with the long debated health effects and the other is the electromagnetic compatibility (EMC) issues.

With respect to **EMC**, there are immunity standards for sensitive equipment that can be affected by the facility magnetic fields and the designers have to comply with them to keep the functioning of the installation running smoothly. Although careful design consideration are made in installations design and implementation, whenever new equipment is installed, especially converters or any semiconductor in combination with inductor and capacitors based devices, sometimes, surprisingly high magnetic fields are generated and high frequency currents are found stray. Often these issues require a rethinking of the design. Fortunately in most cases there are solutions and cost-effective measures that solve the problem.

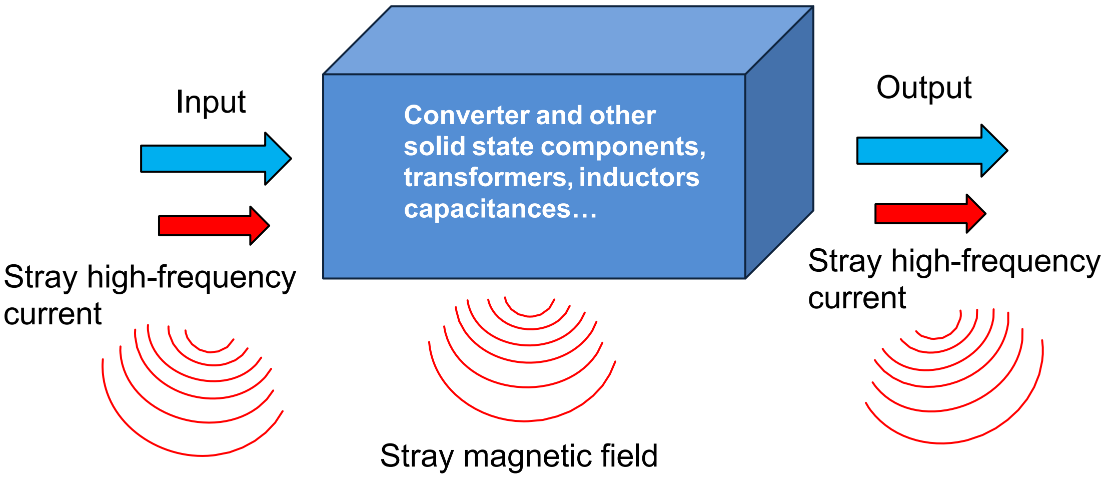

Figure 1 *Modern equipment installations can sometimes show unexpected EMC issues.*

In contrast, the health issues are not that tangible, especially the ones related to low AC magnetic field values and long-term exposure, which after more than two decades of studies there has not been found a mechanism accountable for the suspected harmful effects – consisting mainly in results of epidemiological studies. Various countries have given regulations and posed some limits. For example in Switzerland the official field value limit for 50Hz is 1 µT. In Sweden there are no official values, but most building organization and electrical companies try to keep magnetic field values for public long-term exposure **around or under 1 µT range**. To this it can be added that the 1 µT range seems to be a threshold under which the cost of magnetic field mitigation techniques increase significantly. Say, if we want the magnetic field of an installation that originally emitted an average of 20 µT to be reduced it is technically possible

For health effects related to acute exposure to high values of magnetic fields, there are recommendations of the organization ICNIRP which in its latest version (2011) gives the following recommended values (for 50/60Hz):

- **For electric workers: 1000 µT**
- **For general public: 200 µT**

For other frequencies, higher and lower than power frequencies the ICNIRP recommendations are generalized in the Figure 2, from 1 Hz to 100 kHz.

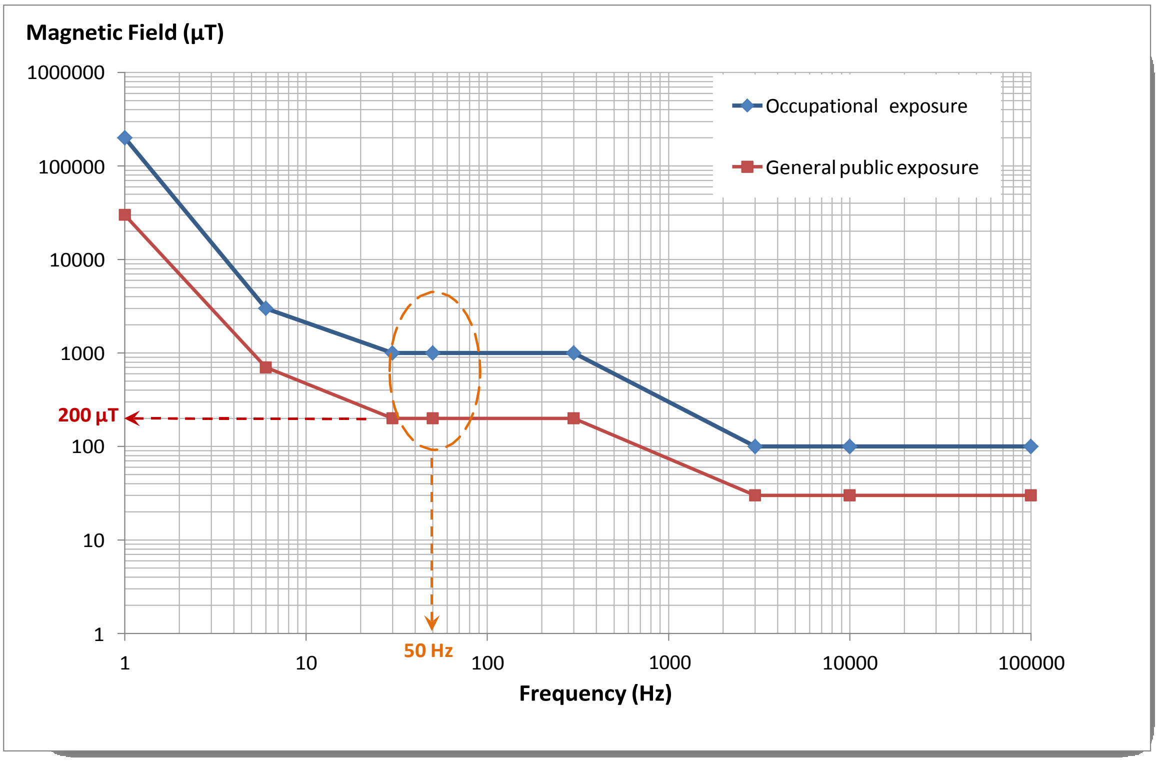

***Figure 2** ICNIRP recommendations for exposure to different frequencies.*

However, as pointed out above, these are only recommendations; the responsible organization for the installation may decide to implement smaller values, or to use some other criteria. Especially if it finds a cost-effective way to keep the magnetic field at even lower values (following the precautionary principle).

2 BATTERY ENERGY STORAGE INSTALLATION AT FALKÖPING

The battery energy storage installation (Figure 3a- left) is located in the city of Falköping adjacent to a secondary substation (Figure 3a- right) and connected to it's LV 0.4 kV bus-bars. Its footprint is: Length = 6260 mm; Width = 2060 mm; Height = 2689 mm.

These installations are nearby the Falbygden Energi (FEAB) building (see Appendix 1)

The installation consists of a battery storage room and a control room. Figure 3b-left shows the battery storage room and Figure 3b-right shows a view from the control room.

The battery set is of the type Lithium-Ion and has the following characteristics:

Nominal discharge power:	92 kW
Nominal Energy:	92 kWh
DC voltage span:	450…648 VDC
Number of modules in string:	20 PC
Battery rack dimensions LxHxD:	1626 x 1849 x 984 mm

The control room is shown in Figure 4-left. It consists of a connection to the battery room, a PQF BESS converter on the right of that figure followed by a coupling transformer. The energy converter has the following characteristics:

Type:	ESI-I - V1 - M250 - IP21
Rated current:	250 A
Voltage:	208…480 VAC
Working voltage :	272 VAC
Frequency:	50/60 Hz
Dimensions WxDxH:	800 x 600 x 2150 mm

Figure 3a *Battery energy storage installation (left) connected to a secondary substation (right).*

Figure 3b *Left: battery storage room; right: view from the control room.*

Figure 4 *Control room (left) and detail of the converter panel (right).*

4 THE AREA OF INTEREST/PATHS FOR MEASURING MAGNETIC FIELDS

It is necessary to measure the magnetic in specific locations. The interest is to measure inside and outside the installation. **Inside the installation** is mainly for determining EMC issues. On the other hand, the reason for measurements **outside the substation** is for determining how the emission values are with respect to public exposure to magnetic fields. In Figure 5 the internal square grid is shown, as well as the external paths around the storage installation and the adjacent substation. In addition, measurements were also taken along a pedestrian's walking path nearby the substation and in the upper left corner it is also shown a measurement path for the boundary fence of a kindergarten located in the vicinity of the installation.

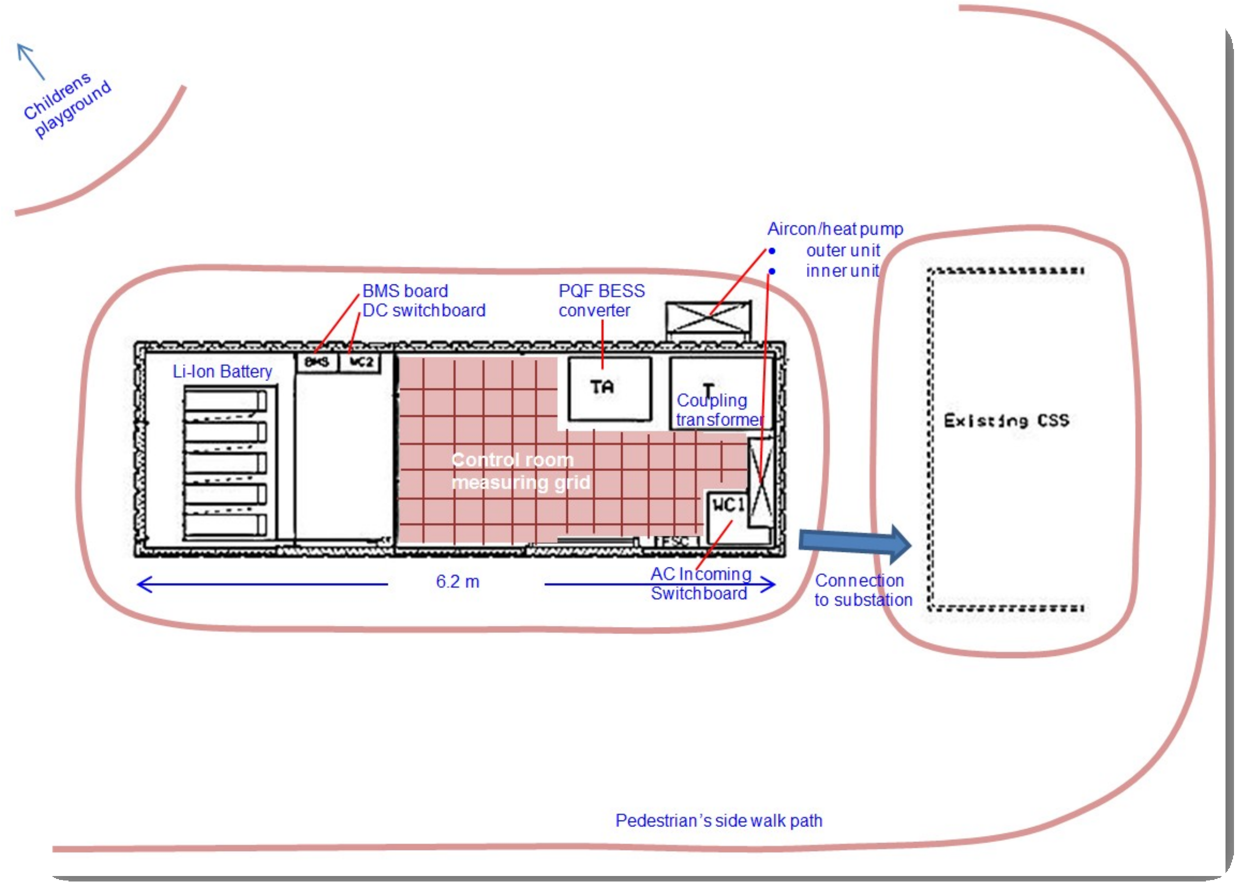

Figure 5 *Area of interest in dark pink. A grid was depicted on the floor* ***indoors*** *and some paths were designed to take measurements* ***outside*** *the installations.*

5 INSTRUMENTATION

The instrument used to measure the rms value of the magnetic field (or magnetic flux density) was a 3-axis gaussmeter model ***BMM 3000*** manufactured by the Swedish company Environmentor It is shown in Figure 6 and its characteristics are:

- Measurement Range: 5nT-2mT. Frequency range: 5Hz-2kHz (-3dB).
- Fixed band filters of 16.7, 50, 100 and 150Hz.
- Power: 4 x 1.5 C Cells. Dimensions: 180mm x 190mm x 100mm.

Figure 6 *Gaussmeter BMM 3000 and its 3-axis sensor.*

The sensor is based on the Faraday induction principle therefore it only measures AC magnetic fields and is unable to measure DC values. We measured in all its available spectrum range, namely 5Hz up to 2 kHz.

6 MEASUREMENTS INSIDE THE STORAGE INSTALLATIONS

An indoors 30-cm square grid was depicted on the floor of the control room. Two types of measurements were taken in:

1) discharge mode and,

2) standby mode

In each set three measurements levels were considered

a) H = 0 near floor level. Actually it was taken at 20 cm above the floor to match the height of suspected conductors

b) H = 1m above

c) H = 2m above

The results from indoors measurements is shown in Table 1 and the next figures. The red and the shaded values represent peak values.

***Table 1** Magnetic fields (in microtesla) indoors with frequencies up to (2 kHz) in **discharging** mode.*

H = 0		1	2	3	4	5	6	7	8	9	10	11	12
	1												
	2	2,9	4	3,7	4,5	5,7							
	3	1,3	1,6	1,8	2,8	5,25		300					
	4	1,07	1,2	1,26	1,57	4,01							402
	5	0,8	1,1	1,1	1,83	1,85	2,6	3,8	6,5	6	7,5		
	6	1,1	1,1	1,3	1,55	1,55	1,6	2,5	2,5	4,3	3,2		
H = 1 m		1	2	3	4	5	6	7	8	9	10	11	12
	1	1,4	1,7	2	3,1	3,7							
	2	1,4	1,3	1,8	2,8	5,6							
	3	1,42	1,32	1,7	2,58	5,7							
	4	1,32	1,18	1,31	1,81	3,21	7,2						
	5	1	1,04	1,16	1,81	2,23	3	4,5	5	5,3	7,9		
	6	1,7	0,94	1,3	1,26	1,52	1,7	2,5	2,6	3,7	4,5		
H = 2m		1	2	3	4	5	6	7	8	9	10	11	12
	1	0,7	1,3	1,4	2	2,1	4,8						
	2	0,8	1	1,3	1,9	2,6	4,7						
	3	0,8	0,92	1,44	1,85	2,64	4,66						
	4	0,71	0,85	1,04	1,47	2,08	2,8	3,2	4,6	5	4	3,1	2,5
	5	0,6	0,76	1,08	1,3	1,65	2	2,6	3,6	3,4	3,5		
	6	0,73	0,77	1,1	1,2	1,3	1,6	2,1	2,9	2,9	3,1		

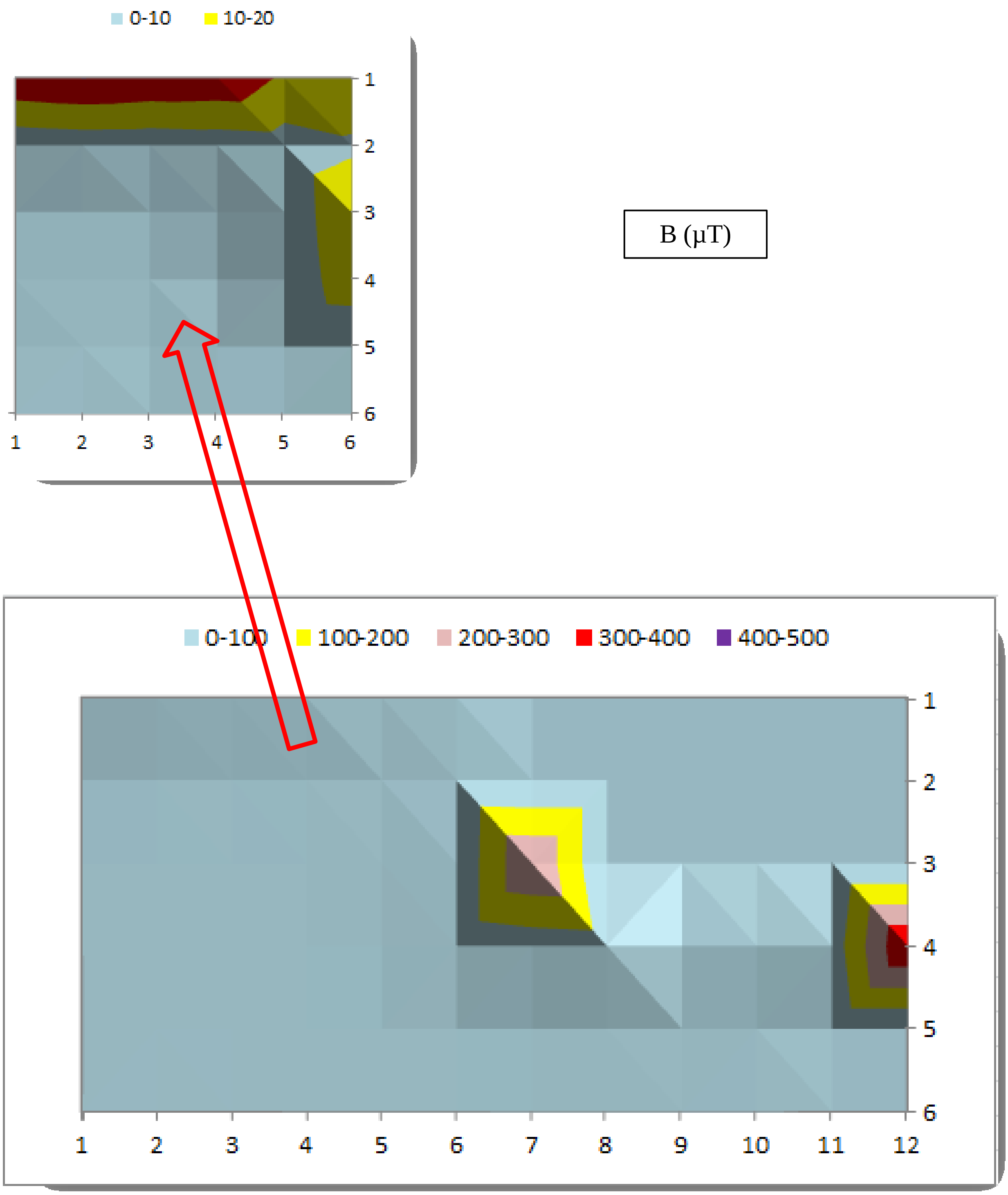

***Figure 7** Plots of the magnetic field values at the floor level in the control room corresponding **H=0** in Table 1. The upper frame represents, in more detail, field values in the region in front of the DC cables.*

For H=1m and H= 2m, we can see the Figures 8 and 9.

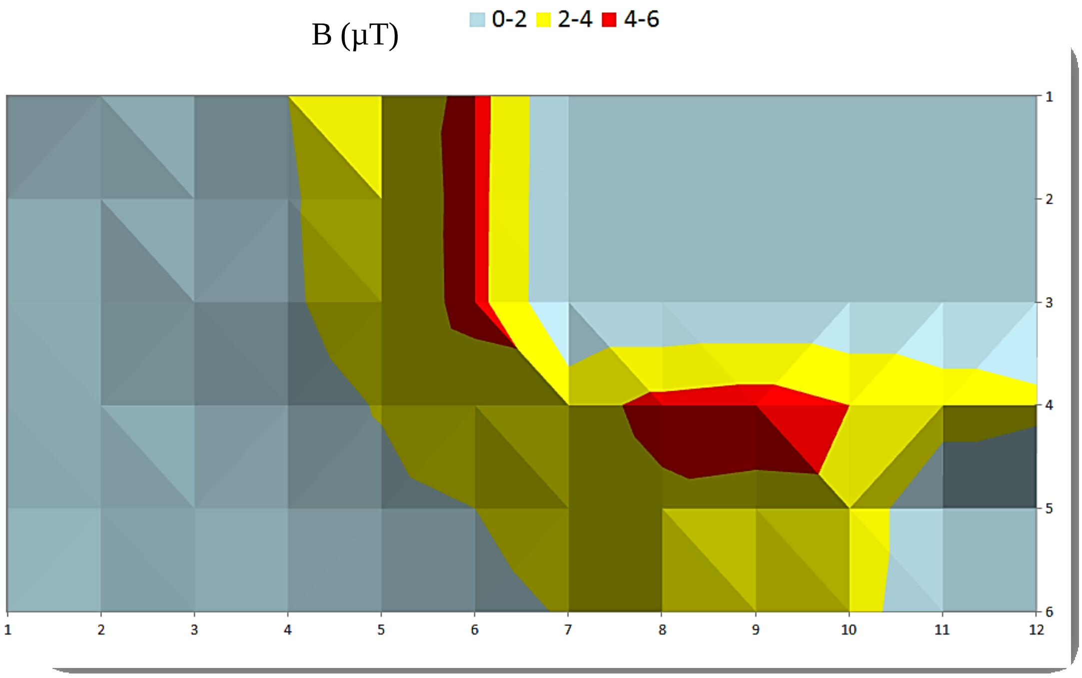

Figure 8 *Magnetic field values in the control room at* ***H=1 m****, corresponding to Table 1.*

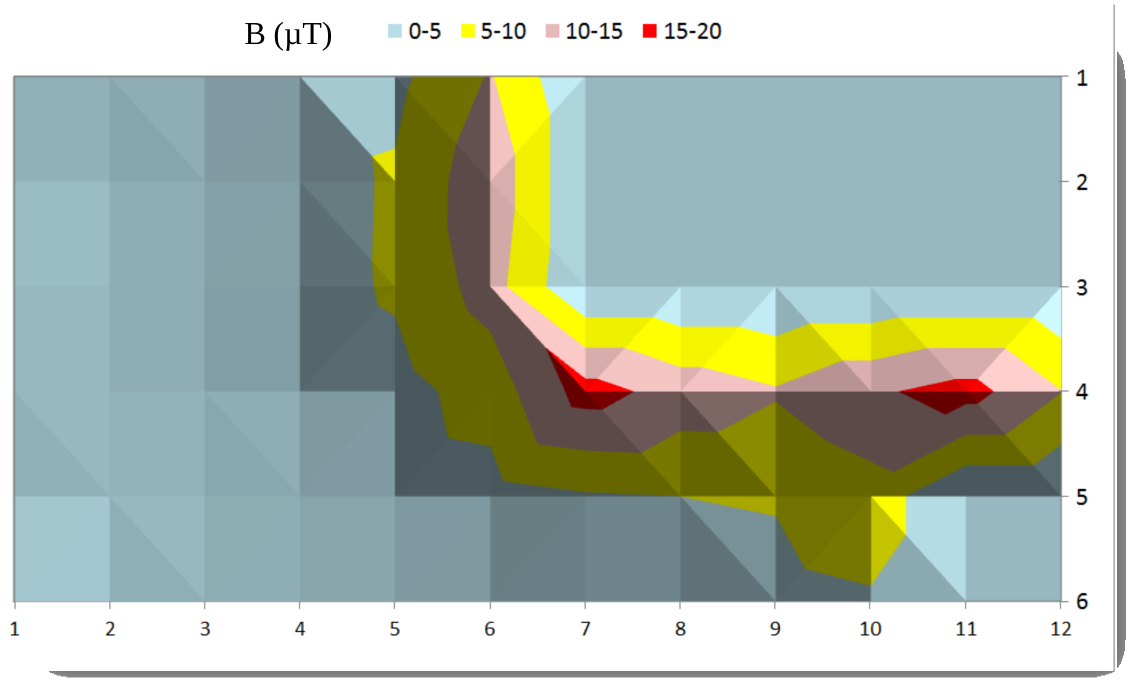

Figure 9 *Magnetic field values in the control room at* ***H = 2 m****, corresponding to Table 1.*

The second set of data was obtained for standby mode, at different heights (see Table2). The shaded areas represent peak values. To follow better the field distribution we plot the data at the floor level in different ranges.

***Table 2** Magnetic fields (in microtesla) indoors with frequencies up to (2 kHz) in **standby** mode.*

H=0

	1	2	3	4	5	6	7	8	9	10	11	12
1	26	29	23	18		14						
2	2,5	5,8	3,8	4,5	7,2	9,6						
3	3,5	1,8	2,7	4,5	6,1	20,3						
4	1,1	1,5	1,2	6,2	5	12,9	45	65	42,5	36,6	54,9	
5	2,2	1,2	4,6	2,4	2	4,2	9,8	6,3	7,4	8,2		
6	1,1	1,2	4,5	1,8	1,6	5,6	2,1	3,1	4,8	4,8		

H=1m

	1	2	3	4	5	6	7	8	9	10	11	12
1	3,2	4	2,6	3		15						
2	1,8	4	2,2	3,3	6,5	10						
3	6,2	2	2,2	5,8	5,5	9,4						
4	1,4	1,4	1,6	6,4	4,5	7,7	22	19,4	32,8	26,8	18,8	27,8
5	1,8	1,1	4,2	2,1	2,5	4,7	9,3	5,1	12	6,6		
6	1,2	1,6	3,2	1,4	1,6	5,8	2,3	3	4,1	5,3		

H=2m

	1	2	3	4	5	6	7	8	9	10	11	12
1	1	4,7	2	2,5		7,2						
2	1	2	1,5	3,6	3,5	6,1						
3	2,7	2,5	1,8	5,7	4	5,1						
4	0,8	1	2,8	5	2,5	3,7	4,2	10,1	7,5	6,1	4,5	6,2
5	0,8	1,8	3	1,8	2,2	2,8	4,7	4,2	7,4	4		
6	1	2,1	1,7	1,2	2,1	4,7	2,9	3,3	3,7	3,9		

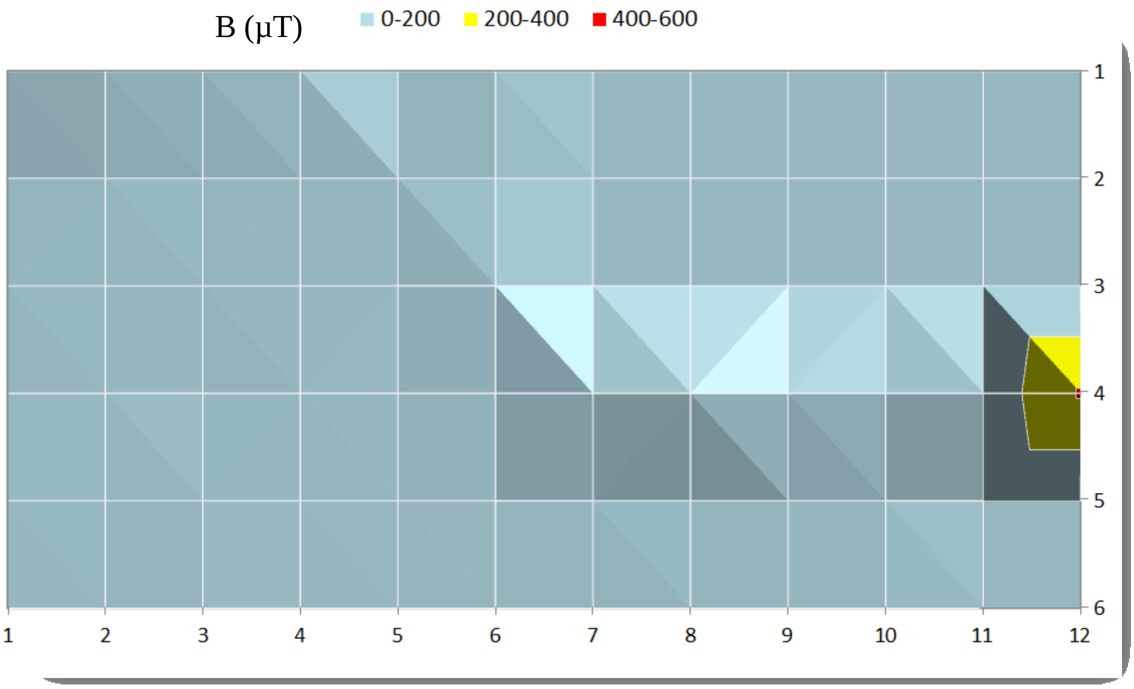

***Figure 10** Standby mode H=0 including high values.*

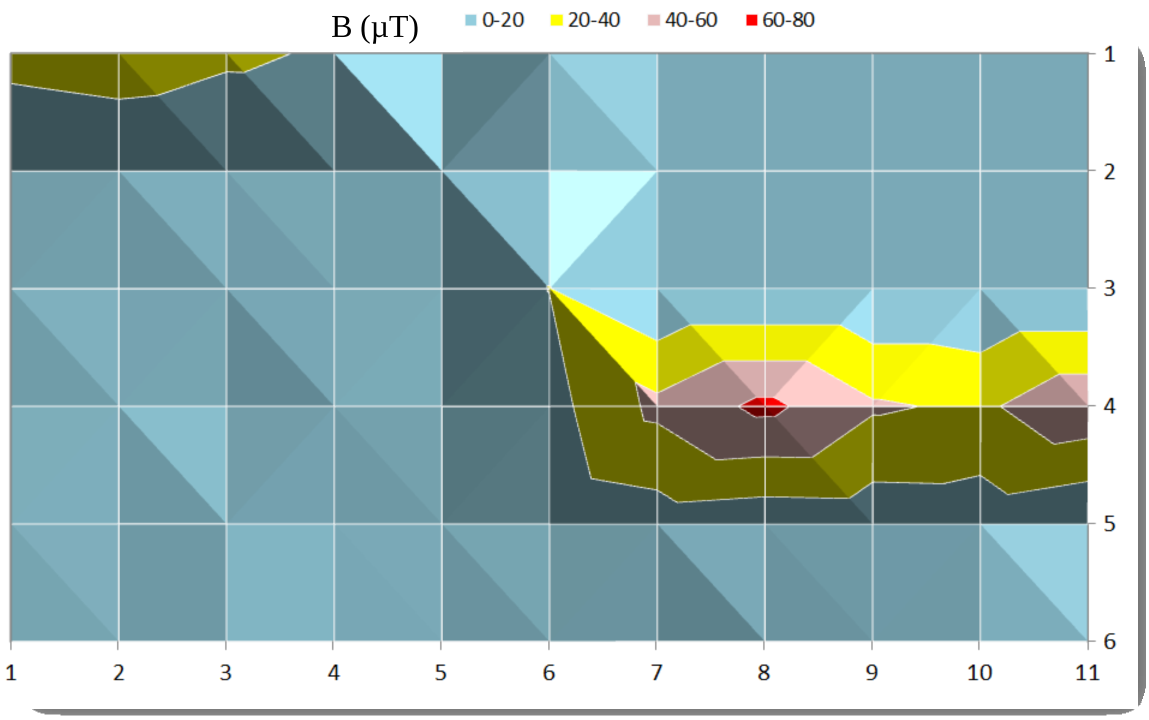

***Figure 11** Standby mode H=0, only values under 80 µT are plotted.*

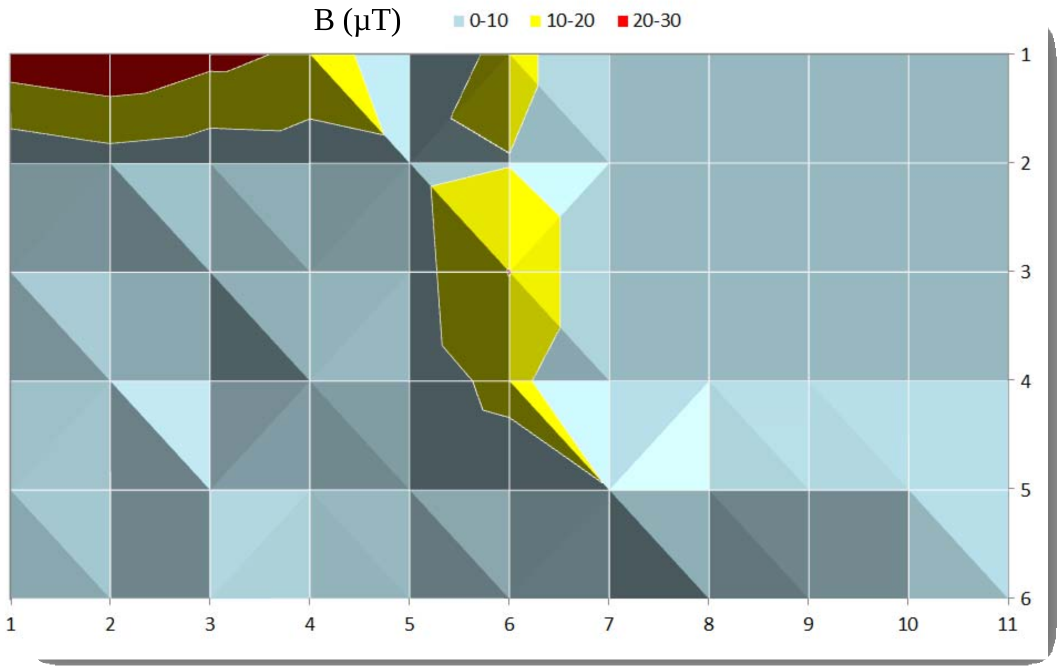

Figure 12 *Standby mode H=0, values under 30 µT are plotted.*

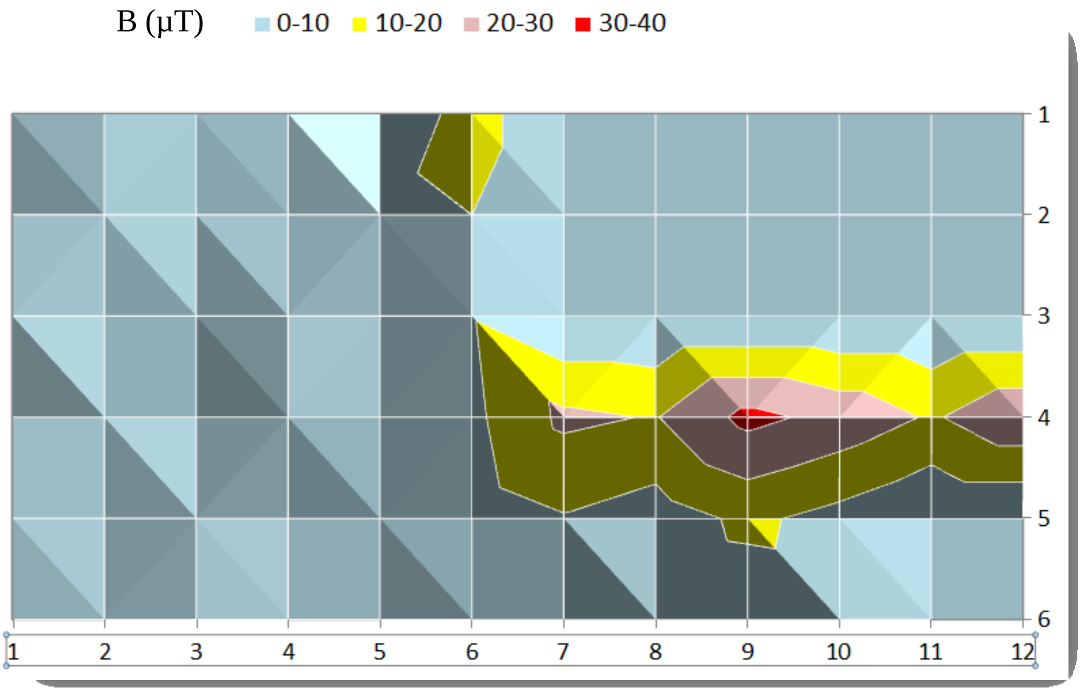

Figure 13 *Standby mode H=1m, all values included.*

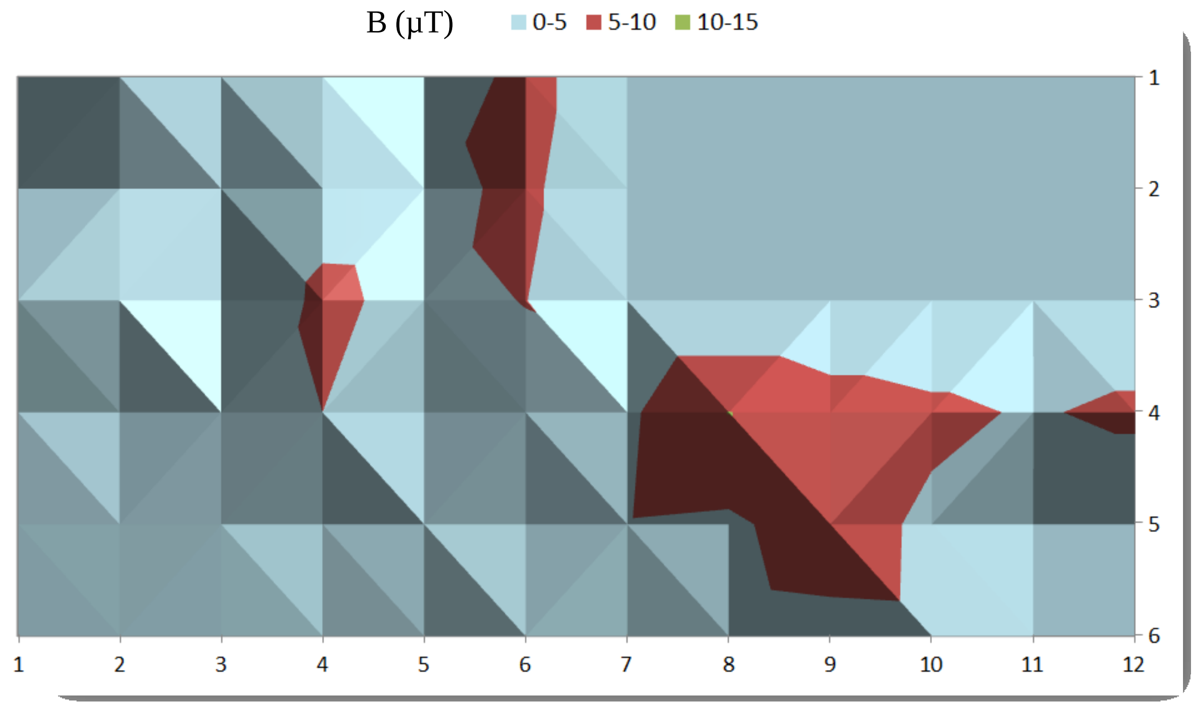

Figure 14 *Standby mode H=2m all values included.*

7 OUTDOORS MEASUREMENTS

Following the paths illustrated in Figure 5, the magnetic field was measured around the DC storage installations and control building as well as around the adjacent substation and a pedestrian path in the vicinity.

In **discharging mode**, the obtained values are given in Table 3. The field measuring distance to the installations is about 1 meter from the wall and 1m above the floor.

Maximum values were registered near the 3-phase AC power conductor going from the switchgear to the transformer and were measured on the external wall. These are depicted beside the 1m in Table 3 and Figure 15, namely 14μT and 15μT; in fact the later are closer to the wall and are at the right of the 1.4μT and 1.5μT values.

The other relatively high value 3 μT was taken along the path between the two installations, to register the presence of the cables going from the DC storage facility to the adjacent substation.

In Figure 16, low values of the magnetic field (lower than 3 μT) are shown.

A similar procedure was followed by the measurement in **standby mode** as shown in Table 4 and Figures 15 and 17.

Table 3 *Data from outdoors magnetic field measurements in discharge mode.*

B (µT)

	1	2	3	4	5	6	7	8	9	10	11	12	13	14	15	16	17	18	19
1						0,03													
2					0,03											0,1			
3				0,03													0,1		
4			0,05															0,1	
5		0,05																	0,1
6	0,03																		0,2
7																			0,3
8																			0,2
9					0,1	0,15	0,2	0,37	0,85	1,7	1,4	1,1							0,3
10					0,15							1,3		1,5	1,3	1,2	1,3		0,2
11					0,25						14	1,4		1,7			0,6		0,2
12					0,25						15	1,5		1,8			1		0,2
13					0,15							0,87		1,8			1,3		0,2
14					0,25	0,3	0,25	0,16	0,23	0,4	0,6	0,7	3	1,7			1,2		0,2
15														1,8			1,1		0,15
16														1,6			0,9		0,2
17														0,8	0,7	1,3	1,6		0,5
18																			0,3
19																			0,6
20																		0,8	
21																		0,9	
22																	0,95		
23							0,8										0,98		
24						0,8	1,6	0,9	0,9	1	1,1	0,6	0,4	0,5	0,5	0,9			
25							0,7												

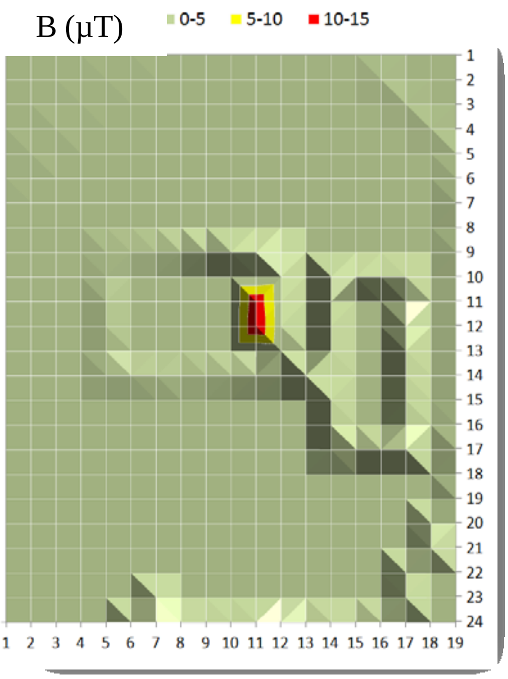

Figure 15 *Plot from field values in discharge mode shown in Table 3.*

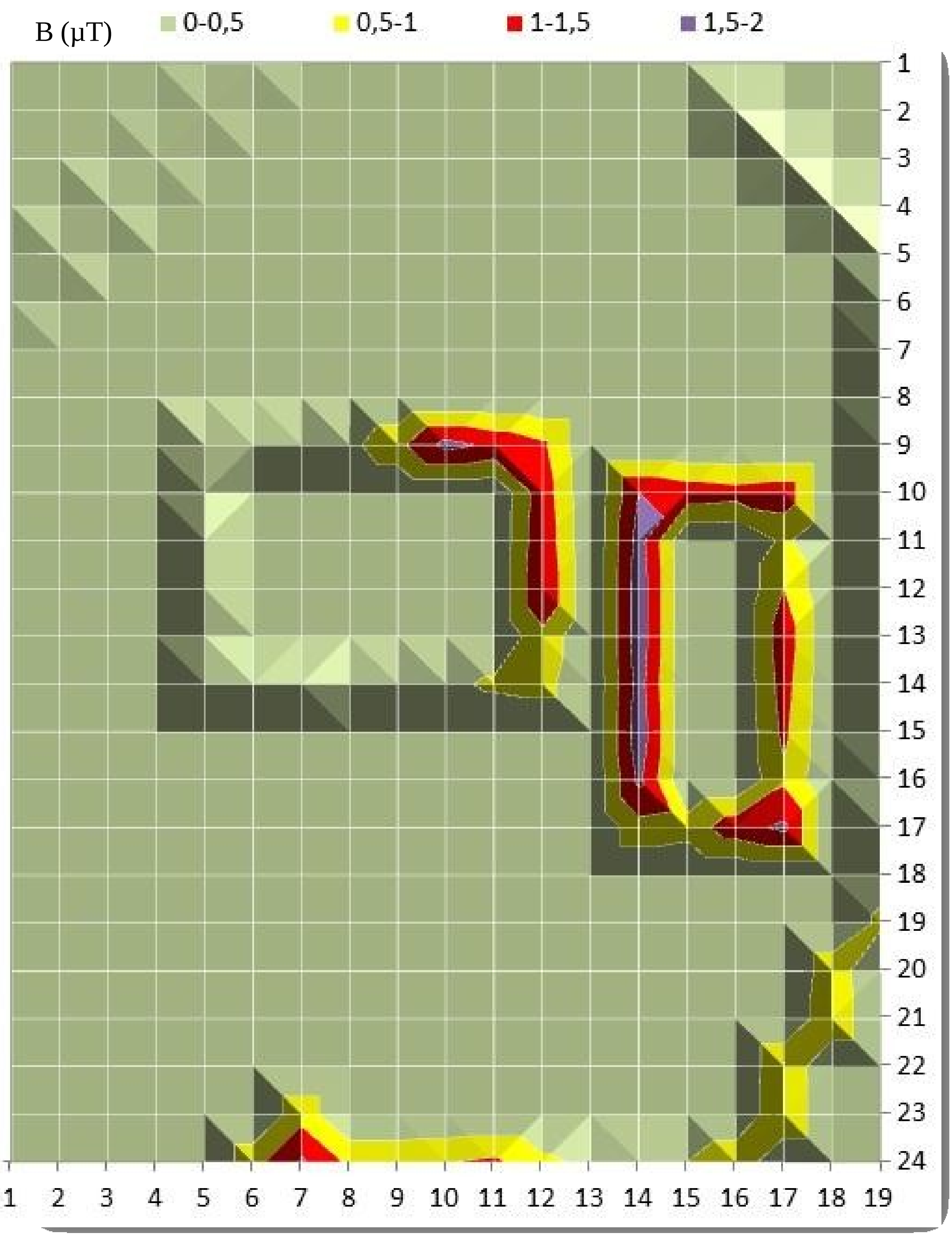

***Figure 16** Detailed field values in discharge mode, only values under 3 microtesla are shown.*

***Table 4** Data from outdoors magnetic field measurements (in microtesla) in standby mode.*

	1	2	3	4	5	6	7	8	9	10	11	12	13	14	15	16	17	18	19
1						0,03													
2					0,03							B (µT)							
3				0,03															
4			0,03																
5		0,05																	0,05
6	0,05																		0,04
7																			0,1
8																			0,1
9					0,1	0,15	0,23	0,43	0,3	0,7	1,3	0,8							0,2
10					0,15							0,7		1,5	0,8	0,7	0,5		0,27
11					0,12						11	0,95		0,84			0,3		0,2
12					0,2						12	2,2		1,7			1,5		0,19
13					0,27							1,2		1,6			1,3		0,1
14					0,2	0,25	0,23	0,16	0,2	0,67	0,6	1,05	2,6	2,3			1,2		0,1
15														1,8			1,5		0,1
16														1,6			0,9		0,1
17														0,7	1,7	2,3	1,5		0,3
18																			0,4
19																			0,4
20																		0,6	
21																		0,5	
22																	0,6		
23							0,9										0,5		
24							2,2	0,9	0,8	0,8	0,7	0,7	0,7	0,7	0,6	0,6			
25							1,1												
26																			

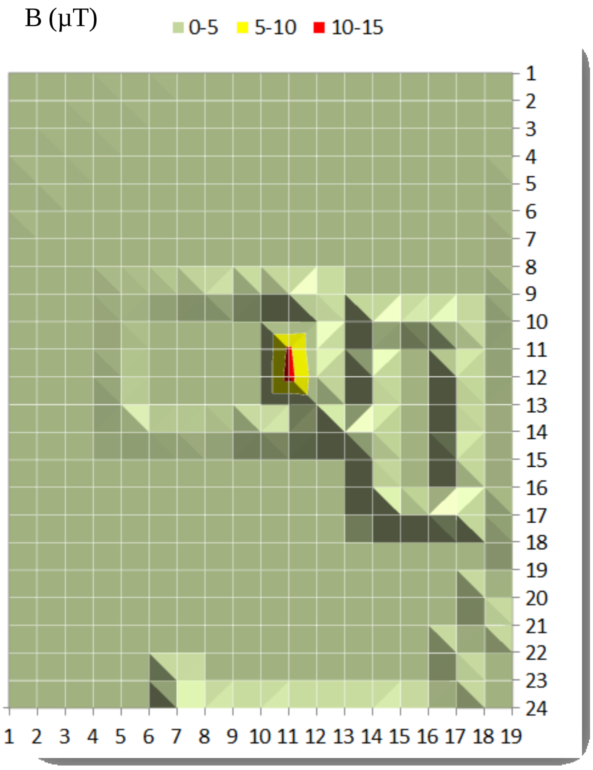

***Figure 17** Plot from field values in standby mode according to Table 4.*

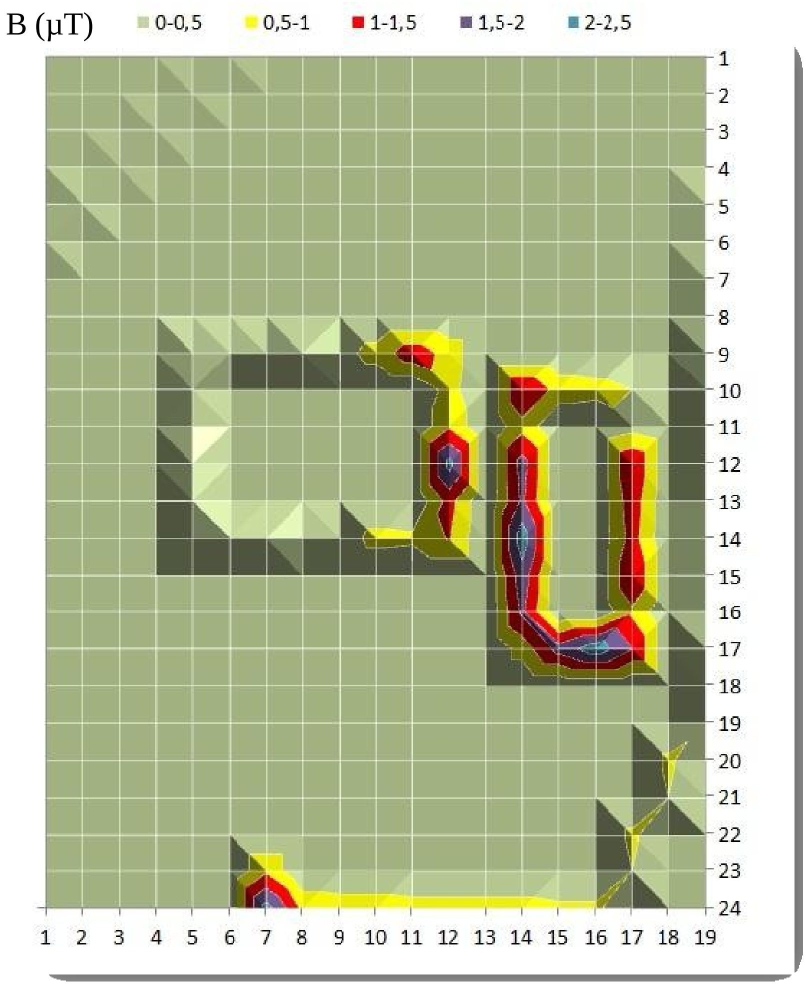

Figure 18 *Detailed field values in standby mode, only values under 3 microtesla are shown.*

Figures 15 and 17 look very similar to each other. The same can be said about Figures16 and 18. As it can be expected, the large magnetic field values indoors as in tables 1 and 2 (>400 μT) reflect peak outdoors values that can be observed in Figures 15 and 17. The connection storage installation-to-substation that transmits the power is made under the ground; thus the values 3μT and 2.6μT in tables 3 and 4 were measured near the level of the floor.

In the low-field range, Figures 16 and 18, the field values outside the installations are mainly distributed around the two installations and more in the two adjacent walls. In the same figures it can be observed that the pedestrian path has mainly values under 1μT except on one location were values up to 1.6 and 2.2 μT were registered. It was found out that the reason for this sudden increase was due to an underground power cable as we could track its direction.

On the upper left corner of Tables 3 and 4 and Figures 16 and 18 it is shown the field values around the fence of a neighboring kindergarten, the measured field values were field values are minimal (under 0.1μT).

8 OBSERVATIONS CONCLUSIONS AND RECOMMENDATIONS

- Indoors and outdoors measurements of the AC magnetic field were performed at the interior of the Falköping's energy storage facility control room and its surroundings including the adjacent substation. The AC field values at the pedestrians walk located at a few meters from these installations was also measured.
- The motivation was twofold: 1) to find out suspected EMC issues that were tripping the energy storage and 2) to investigate the magnetic field levels outside both installations mainly at a pedestrian path and at the fence of a neighbouring kindergarten.
- The measuring equipment was a 3-axis gaussmeter BMM 3000 with a range of frequencies 5 Hz to 2 kHz.
- The measured magnetic field values inside the control room show unusual AC values in both modes, namely standby and discharge. Peak values were detected in the following locations:
    - o nearby the pair of DC cables connecting the converter panel to the battery
    - o in front of the converter panel
    - o on the AC connections to the transformer
- The first location supposed not to carry any AC current in both modes. However, the intense field nearby that location indicates the presence of a high current. Let us take the standby mode values in Table 2 (a clip is shown in Figure 19 with values at the plane perpendicular to the middle of the cables).

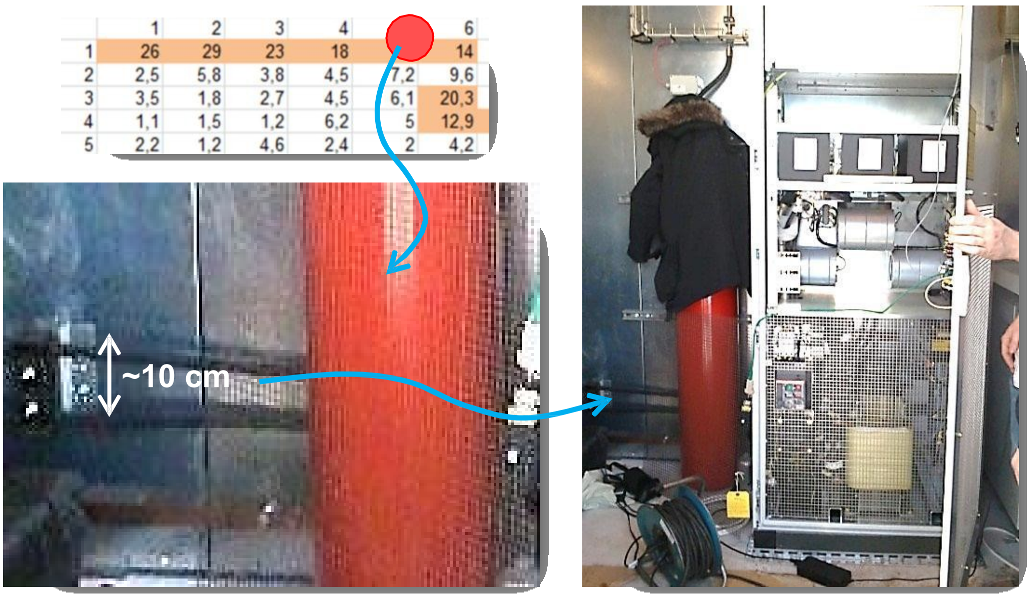

	1	2	3	4		6
1	26	29	23	18		14
2	2,5	5,8	3,8	4,5	7,2	9,6
3	3,5	1,8	2,7	4,5	6,1	20,3
4	1,1	1,5	1,2	6,2	5	12,9
5	2,2	1,2	4,6	2,4	2	4,2

Figure 19 *High AC magnetic field values near the "DC cables" in the control room.*

In Figure 19 it can be observed that the separation of cables is around 10 cm but it decreases as we move to the right. The consequence of this is that the field is larger at the left than at the right. This can be verified in the clip of Table2 in Figure 19; the values 26μT and 29 μT are larger than 23μT and 18μT.

- Moreover, the current responsible for the fields shown in Figure 19 can be computed from the fields using the formula (see Appendix 2):

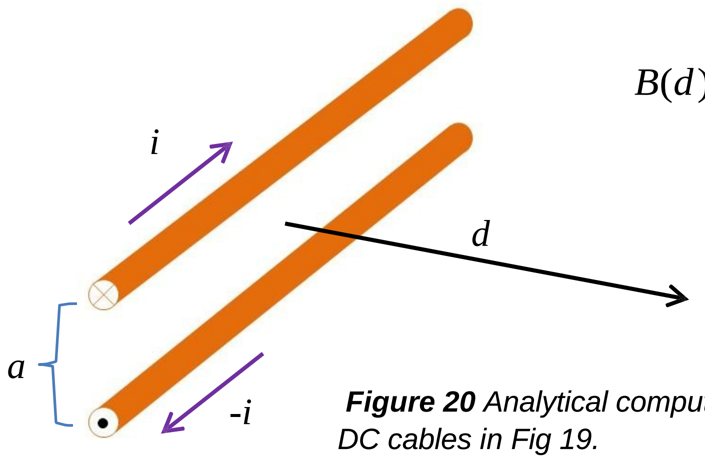

$$B(d) = \frac{\mu_0 i}{2}\left[\frac{a}{(a/2)^2 + d}\right]$$

Figure 20 *Analytical computation of the field around the DC cables in Fig 19.*

For a=10cm, we obtain: B[μT] = 8i [A]/(1+4n^2), where n = d/a;
then i [A] = (1+4n^2) B[μT]/8

Adjusting for the field values in the third column in Figure 19, we obtain that the current is approximately i = 10 A.

- In fact the total current measured <u>with a clamp meter</u> in the range of frequencies 50Hz to 2kHz was 11 A (rms).

Also, from a numerical simulation using numerical simulations (Figure 20), we obtain a similar variation for values of d = 5, 10, 20 and 30 cm respectively.

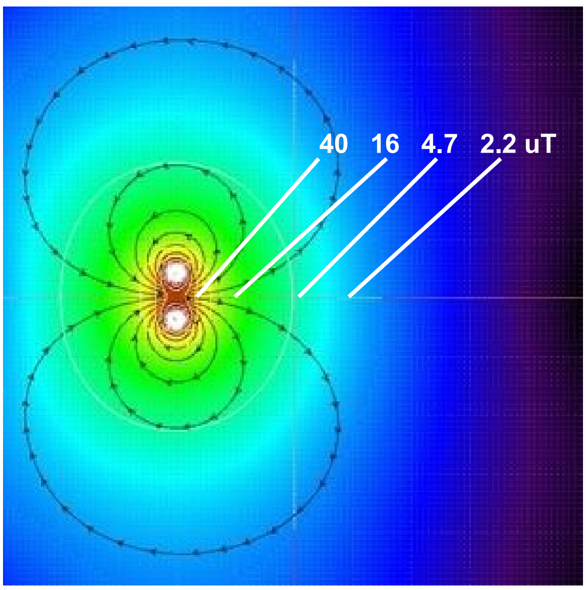

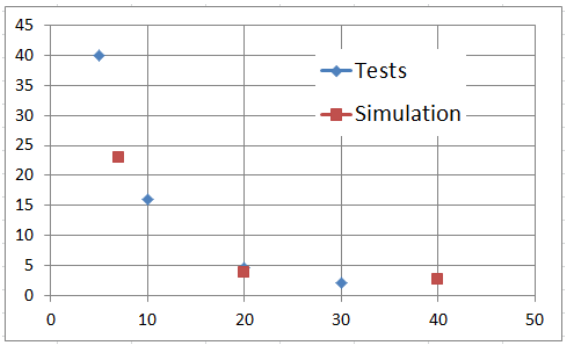

Figure 21*The numerical simulations (right) and their comparison (above) with the field measurement gives good results validating the assumption of the 11A AC source.*

- It is then recommended to check the possible sources of AC current which points out to the inverter panel (Figure 22), search for resonances, loops, stray currents, and in general non-linear phenomenon that can abruptly amplify a current carrying a manifold of frequencies. This circuit may also be causing the tripping of the DC system, via its control at the battery storage room, which is susceptible to the 11 amps EMC disturbances.

***Figure 22** The circuitry responsible for the high currents and magnetic fields may be located in this panel.*

- Other sources of magnetic fields can be found in the lower part of this panel. The field in front of the transformer is also high, as shown in Table 2 (for H=0)
- The connection between the AC incoming switchgear and the coupling transformer produces the highest registered fields (up to 402 μT).

Figure 23 *Up to 402 μT are produced near the cables connecting the AC incoming switchgear (right) with the coupling transformer (left).*

- External field values were moderately high also just on the external side of the wall where cables (Figure 23) were located. Except these locations most the field values at 1m from the DC storage facility were below 1 microtesla. On the other hand, on the surrounding of the AC substation several values were above 1μT, yet all below 2μT.
- In most measurements we did not find significant differences in the values of discharge or standby modes.
- The side walk for general public was located at a few meters from the installations, closer to the AC substation and a few meters more from the DC storage facility. As shown in Tables 3 and 4 all registered values are under 1 microtesla except on a few locations that it was measured above 1 microtesla. It was identified that electric cables were below those points.
- The children's playground and kindergarten located in the direction of upper-right corner in Table 3, is not affected by the magnetic fields of the two installations, as the measured values on the boundary were all under 0.05 microtesla, a very low value indeed.

9 APPENDIX 1

LOCATION OF THE BATTERY ENERGY STORAGE INSTALLATION

Figure 24

10 APPENDIX 2

Computation of the magnetic field of two parallel wires

The aim is to compute the magnetic field (and its dependence with the distance) of two parallel wires carrying a single phase current *i* (one wire carrying a current *i* and the other the return current –*i*). The field of one finite wire (segment with length *L*) is first evaluated:

$$\boldsymbol{B}(x,y,z) = \frac{\mu_0 i}{4\pi}(y\boldsymbol{e}_x - x\boldsymbol{e}_y) f(x,y,z) \quad (1)$$

where,

$$f(x,y,z) = \frac{1}{(x^2+y^2)}\left[\frac{L/2+z}{\sqrt{x^2+y^2+(L/2+z)^2}} + \frac{L/2-z}{\sqrt{x^2+y^2+(L/2-z)^2}}\right] \quad (2)$$

For a two-wire configuration with a separation *a* (Figure 25) both field contributions will superimpose

$$\boldsymbol{B} = \frac{\mu_0 i}{4\pi}\left\{[(y_1 f(x_1,y_1,z_1) - y_2 f(x_2,y_2,z_2)]\boldsymbol{e}_x + [(-x_1 f(x_1,y_1,z_1) + x_2 f(x_2,y_2,z_2)]\boldsymbol{e}_y\right\} \quad (3)$$

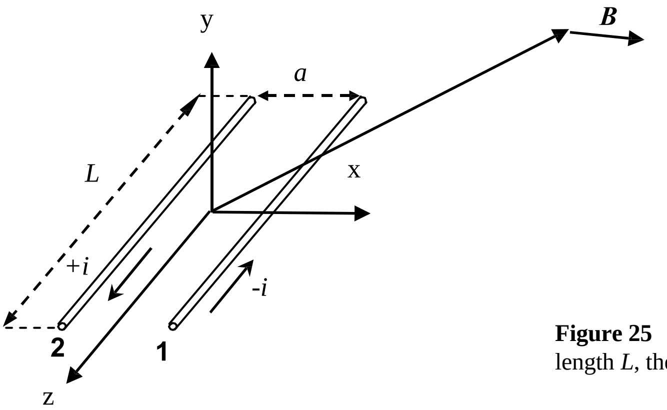

Figure 25 Magnetic field of two parallel finite wires of length *L*, the instantaneous currents are also shown.

The following relations hold: $x_1 = x - a/2;\ x_2 = x + a/2;\ y_1 = y_2 = y;\ z_1 = z_2 = z.$

In order to study the field decay with distance, e.g. along the y-axis, the calculation is made for $z = 0$ and $x = 0$. In that case, the field component along the x-axis vanishes, leaving a simple expression for the field of two parallel wires of finite length

$$\boldsymbol{B}(0,y,0) = \frac{\mu_0 i}{4\pi}\left\{\frac{aL}{[(a/2)^2+y^2]\sqrt{(a/2)^2+y^2+(L/2)^2}}\right\}\boldsymbol{e}_y \quad (4)$$

Furthermore, for long wires *y* << *L* the formula reduces to:

$$\boldsymbol{B}(0,y,0) = \frac{\mu_0 i}{2\pi}\left\{\frac{a}{(a/2)^2+y^2}\right\}\boldsymbol{e}_y \quad (5)$$

CHANGE HISTORY

Rev.	Chapter	Description	Date / Dep. / Name
01	All	Initial document	<yy-mm-dd>/ <dep.> / <name>

REVIEW HISTORY

Rev.	Chapter	Reviewer(s)	Date
01	All	<name> / <dep.>	<yy-mm-dd>

Upprättad av (namn / roll / enhet)	Produkt/System/Delsystem	Version
Viktor Weidenmo, Pöyry SwedPower	Frekvensreglering	0.3
	Ansvarig	Datum
	Lars Ohlsson	2014-09-12

Funktionstest: Testrapport, av Frekvensreglering

Innehållsförteckning

1. Inledning

1.1 Omfattning

Funktionstesterna inom Elforskprojektet "Test och utvärdering av energilager" är tänkta att genomföras i tre steg. I steg ett har grundläggande funktioner, såsom i- och urladdning, undersökts medan testerna i steg två fokuserar på automatisk styrning där olika händelser kan trigga i- och urladdningsförloppet. Detta kan jämföras med tidigare styrsystem där i- och urladdning kontrollerats enligt förinställda tidsscheman. Generell bakgrund till funktionstestet är [Ref 4].

Testerna i steg två är uppdelade i ytterligare tre steg där steg A, däribland frekvensreglering, utvärderar grundläggande applikationer som krävs för att gå vidare med mer tillämpade applikationer i steg B och kombinerade applikationer i steg C.

I detta steg, steg A, har adaptivitet testas där energilagrets aktiva effekt styrs av elnätets frekvens.

Testet genomfördes av FEAB, Metrum, ABB och Pöyry SwedPower enligt Testspecifikationen [Ref 2] med godkänt resultat 2014-06-25.

1.2 Dokumenthistorik:

Utgåva	Datum	Utfärdare	Kommentar
0.1	2014-07-02	Viktor Weidenmo	Första version, utkast
0.2	2014-08-29	Viktor Weidenmo	Andra version, utkast
0.3	2014-09-12	Viktor Weidenmo	Tredje versionen, lagt till text kring byte av effektriktning

1.3 Refererade dokument

Alla dokument som omnämns i sluttestrapporten:

[Ref 1] Systembeskrivning
[Ref 2] Testspecifikation_Frekvensreglering_rev4_2014-07-03
[Ref 3] Testmiljöbeskrivning
[Ref 4] Projektbeskrivning Test och utvärdering av energilager 2013-10-14
[Ref 5] Metrum_FrequencyReg_2014-06-25_DataLogg
[Ref 6] BMS_PQFI_201401625 frekv regl2

1.4 Förkortningar och begrepp

Nedan förklaras alla begrepp och förkortningar som används i dokumentet.

FEAB Falbyggden Energi AB
FT Funktions Testfall
PT Prestanda Testfall
ST Stabilitets Testfall
PL ProjektLedare
TL TestLedare
SOC State-of-Charge
PLC Programmable Logic Controller
AC Alternating Current

DC	Direct Current
f	frekvens
PQFI	Apparat som kontrollerar energilagret
BMS	Battery Management System
BESS	Battery Energy Storage System

2. Översikt

2.1 Utförda tester

2.1.1 FT nr 1, Frekvensreglering

Testet skulle visa att energilagrets aktiva effekt kan styras utifrån elnätets frekvens.

Under testet sattes gränsvärdet för start av urladdning av energilagret till 49.97 Hz i Metrums PQ-instrument. Urladdning av energilagret skedde med konstant effekt så länge frekvensen i elnätet var under gränsvärdet. Om frekvensen gick över gränsvärdet stoppades urladdningen.

Gränsvärde för start av laddning av energilagret sattes till 50.01 Hz i Metrums PQ-instrument. Laddning av energilagret skedde med konstant effekt så länge frekvensen i elnätet var över gränsvärdet. Om frekvensen gick under gränsvärdet stoppades laddningen.

Om frekvensen befann sig emellan de båda gränsvärdena (det vill säga inom frekvensdödbandet) skulle energilagret inte utbyta någon aktiv effekt.

Anledningen till att dessa gränsvärden valdes var att frekvensen under den aktuella tidpunkten för testet pendlade kring dessa värden vilket möjliggjorde att aktivering av både upp- och nedreglering skulle ske.

2.2 Defektstatus

Innan testet kunde genomföras åtgärdades ett antal defekter, se testprotokoll. Sedan kunde testet genomföras på ett godkänt sätt.

Det är ingen kritisk defekt men då ca var 5:e-ensekundsmätvärde från ABBs mätning i BMS/PQFI inte loggades försvårade det analysen av testresultatet.

3. Utförda tester

Testet har utförts och godkänts enligt Testspecifikationen [Ref 2] vilket även fungerat som testprotokoll.

3.1 FT nr 1, Frekvensreglering

3.1.1 Mätdata från testet

Mätdata från testet finns sparade i [Ref 5] och [Ref 6].

3.1.2 Testresultat

I Figur 1-4 visas testresultatet.

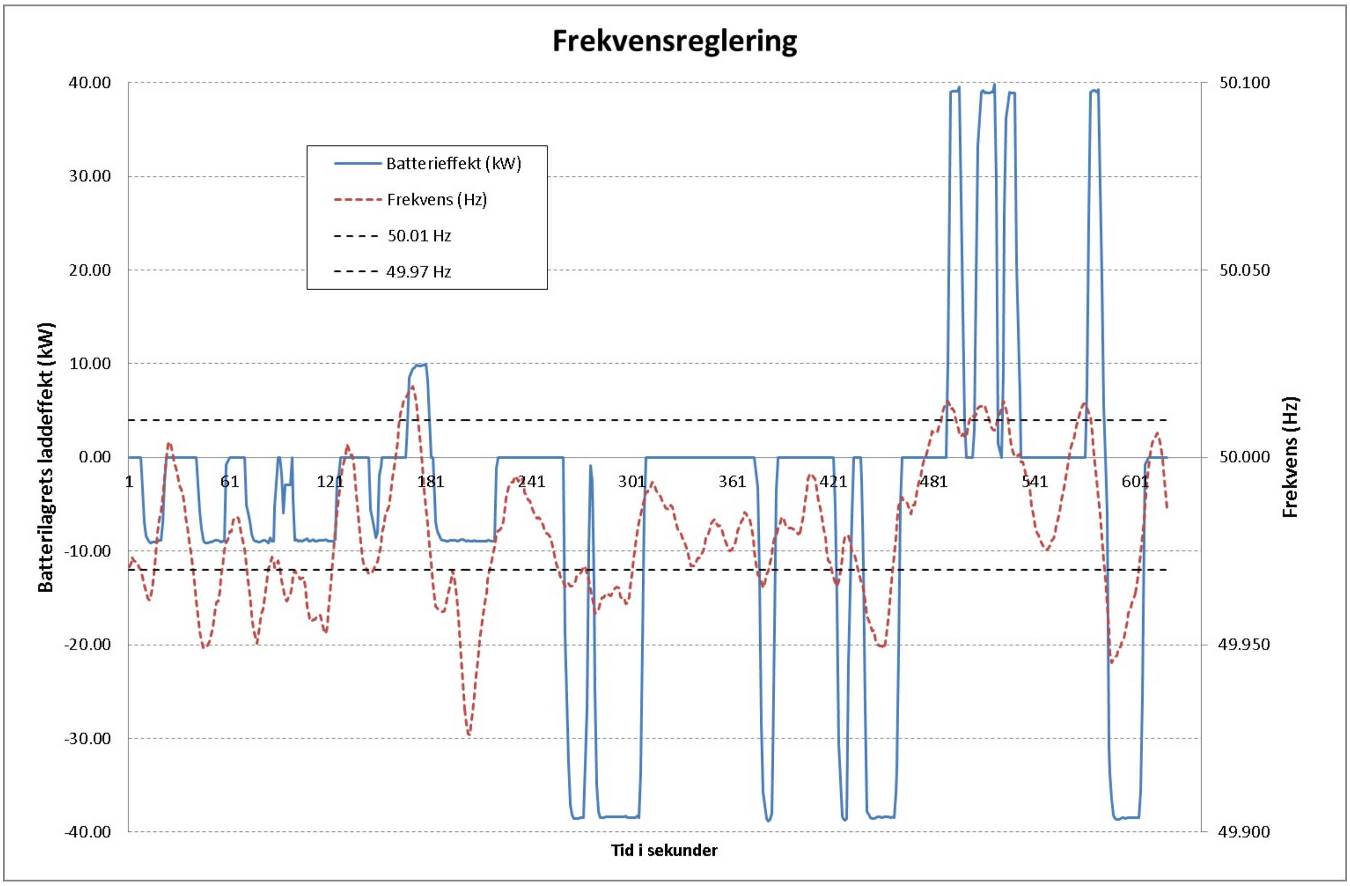

Figur 1. Frekvensreglering, utzoomad frekvens. Under testet var gränsvärdet för start av urladdning 49.97 Hz och gränsvärdet för start av laddning 50.01 Hz. Energilagrets effektbörvärde är först 10 kW och sedan 40 kW.

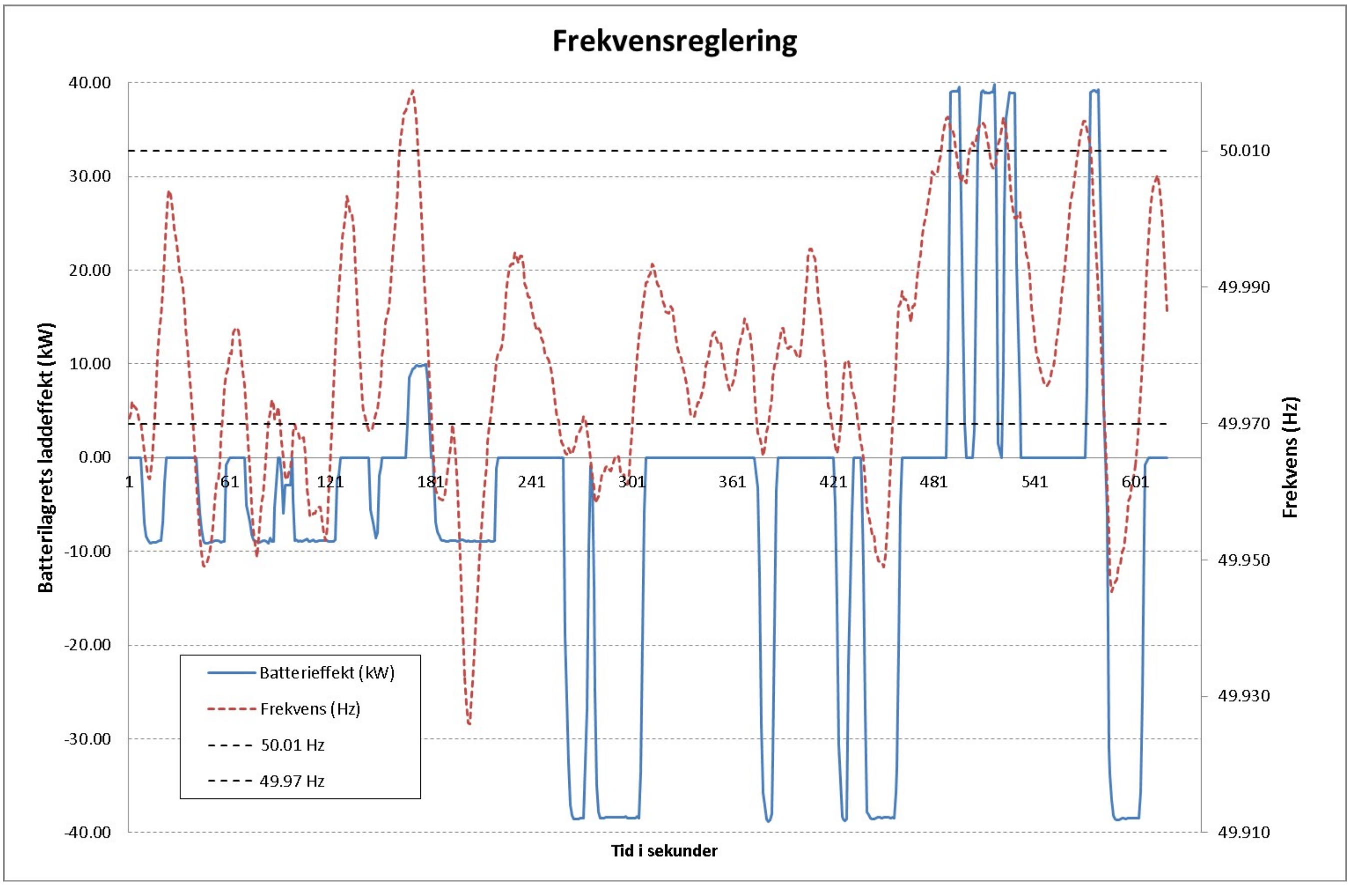

Figur 2. Frekvensreglering, inzoomad frekvens. Under testet var gränsvärdet för start av urladdning 49.97 Hz och gränsvärdet för start av laddning 50.01 Hz. Energilagrets effektbörvärde är först 10 kW och sedan 40 kW.

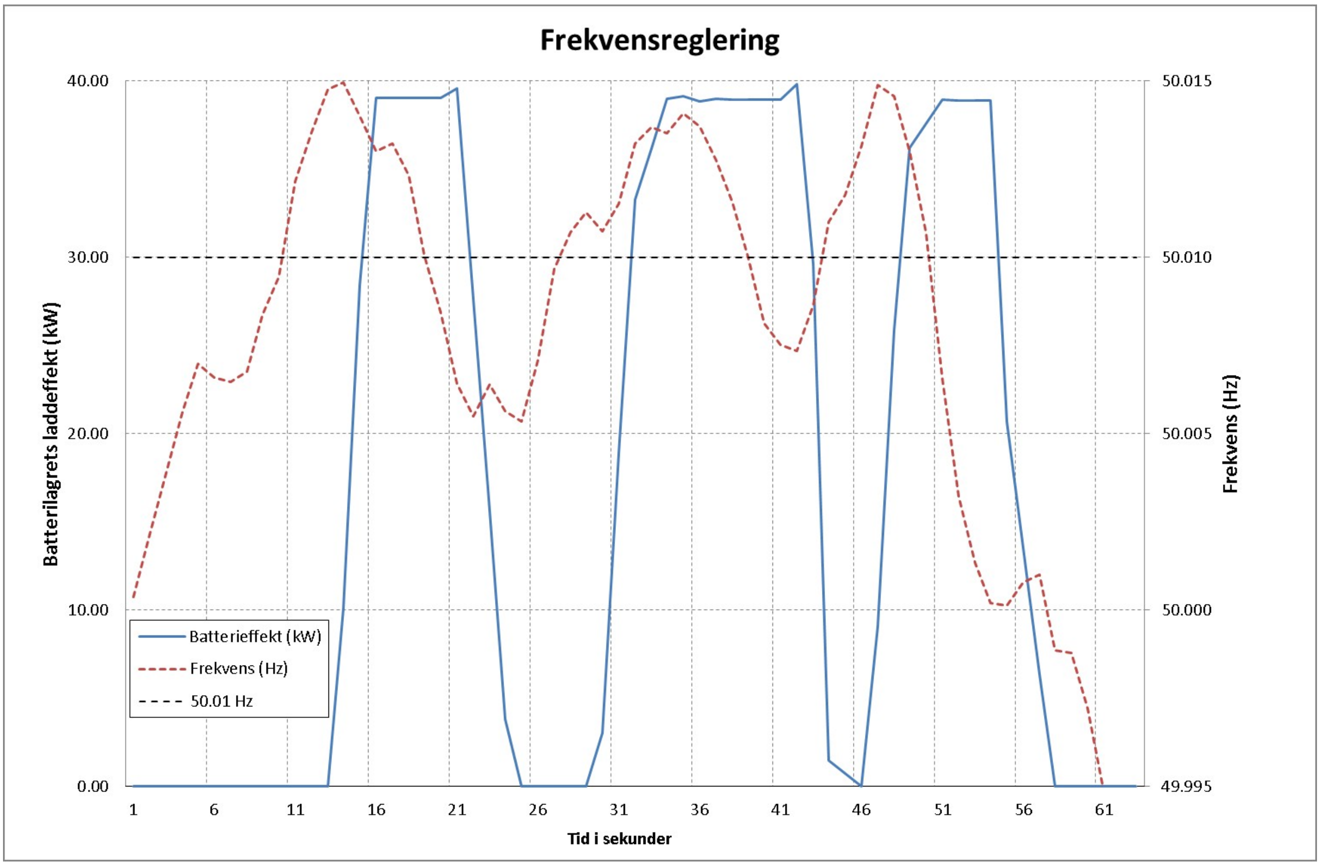

Figur 3. Frekvensreglering, inzoomat kring upprepade laddningar. Under testet var gränsvärdet för start av urladdning 49.97 Hz och gränsvärdet för start av laddning 50.01 Hz. Energilagrets effektbörvärde är först 10 kW och sedan 40 kW.

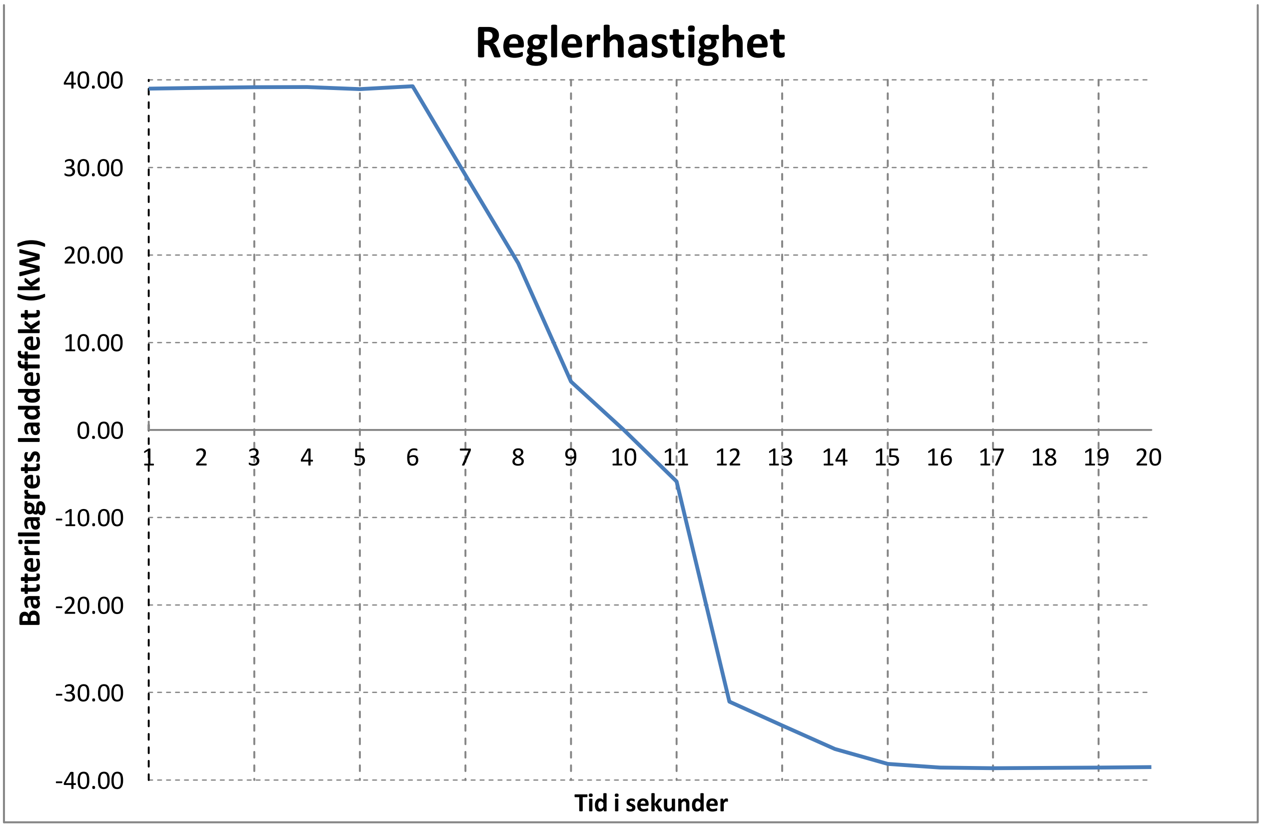

Figur 4. Reglerhastighet hos energilagret från 40 kW laddning till 40 kW urladdning.

3.1.3 Diskussion av testresultat

I Figur 1-3 ovan visas det att:

- urladdning av energilagret ha aktiverats då elnätets frekvens understiger det definierade gränsvärdet i Metrums PQ-instrument, samt
- laddning av energilagret ha aktiverats då elnätets frekvens överstiger det definierade gränsvärdet i Metrums PQ-instrument.

Frekvensregleringstestet har därmed visat att det går att styra energilagret utifrån externa händelser i nätet och inte enbart via förutbestämda tider som tidigare. Denna adaptiva styrning ger ett ökat antal användningsområden och möjliggör fler affärsmodeller som kan bidra till att förstärka intäktströmmen hos ett energilager. Detta är ett steg mot ett smartare och mer flexibelt system där ett energilager i varje givet ögonblick avgör vilken tjänst som ska erbjudas utifrån status i elnätet, väderförhållanden och kundbehov. Kommunikation med kunder och aktörer skulle kunna ske via SMS vid meddelande om förändrade prioriteringar av energilagringstjänster.

Utifrån testerna kan det observeras att det finns en fördröjning på ett par sekunder innan energilagret börjar utbyta den efterfrågade effekten. Detta kan ses i Figur 3 där det framgår att fördröjningen från det att triggningshändelsen sker, dvs frekvensen överstiger gränsvärdet, till dess att energilagret börjar utbyta effekt är ca 2-3 sekunder och ytterligare ca 3-4 sekunder innan full effekt uppnås (i Figur 3 med ett effektbörvärde på 40 kW). Fördröjningen i omriktarens respons består sannolikt av tre eller flera delar, t.ex:

- Fördröjning i Metrums utrustning och script från det att t.ex. frekvensen går över eller under gränsvärdet tills order ges till PLC:ns digitala ingång

- Fördröjningen från ingången på PLC:n tills order ges till PQF-kontrollen att ge effekt
- Fördröjningen internt i PQF-kontrollen från det att den får order tills ordern börjar verkställas
- Hur snabbt önskad maxeffekt ut/från nätet erhålls beror på reglerparametrarna i PQG kontrollen, bl.a. en parameter ”_fRamping”, som anger hur snabbt effekten rampas. Under testet användes standardinställningen på 10 kW/s, vilket är ganska långsamt.

I Figur 4 visas det hur energilagret byter effektriktning och går ifrån att laddas med 40 kW till att laddas ur med 40 kW. Bytet av effektriktning orsakades av att frekvensen i elnätet gick ifrån att vara över 50.01 Hz till under 49.97 Hz vilket kan ses i Figur 2 efter ungefär 580 sekunder. Att byta effektriktning tog för energilagret ca 8-9 sekunder vilket kan ses i Figure 4. Detta ger en uppmätt ramphastighet på ca 10 kW/s. Eftersom styrningen skett via en frekvensförändring som registrerats hos Metrums utrustning, och därmed orsakat viss fördröjning, är det sannolikt en anledning till att det inte blev precis 10 kW/s. Att energilagret kan styras från en effektnivå till en annan, däribland att byta effektriktning, är viktigt för att energilagret ska vara flexibelt och användbart. En snabb effektstyrning möjliggör för energilagret att verka på flera marknader och utöka antalet användningsområden då energilagret på kort tid kan gå från en reglerfunktion till en annan. Detta ökar nyttan och effektiviteten hos att en framtida optimeringsfunktion, som vid varje ögonblick kan välja att energilagret ska erbjuda den mest lönsamma tjänsten.

Responstiden och ramphastigheten är viktigt att känna till och bör i detta fall förbättras om energilagret skall användas för aggregering, se kap 5 Rekommendation. För att små energilager ska kunna assistera *Demand Respons* hos kunderna måste energilagren kunna reagera snabbt på en extern styrsignal, t.ex. ett effektflöde.

3.1.4 Testets koppling till frekvensreglering i Norden

För att styra frekvensen används i Norden flertalet vattenkraftstationer där en regulator ser till att om frekvensen sjunker under 50 Hz så ökar vattenkraftverket sin produktion av aktiv effekt. På samma sätt minskas produktionen om frekvensen stiger över 50 Hz. Dagens reglermarknader i Norden som främst syftar till att upprätthålla frekvensen är, i fallande aktionshastighet, primär-, sekundär- och tertiärregleringen, se Figur 5.

Då energilagret i Falköping är för litet för att kunna påverka frekvensen har ingen frekvensförändring i nätet att kunna uppmätas som direkt kan kopplas till energilagrets effektutbyte. Faktum är att det krävs en effektförändring i storleksordningen 100 MW eller mer för att på ett tydligt och direkt sätt kunna påverka frekvensen i det Nordiska elnätet. Det viktiga är istället att säkerställa att effektutbytet med nätet fungerar som planerat. Genom att utveckla funktionaliteten hos ett mindre energilager har steget minskats för att senare installera ett större enerilager som har större möjlighet att uppfylla de villkor som Svenska Kraftnät ställer på aktörer på reglermarknaden. I dagsläget accepteras reglerkapacitet i storleksordningen kW på primärregleringsmarknaden, dock måste effektnivån kunna upprätthållas under minst en timme. För ett energilager på 80 kW och 80 kWh med en initial laddnivå (SOC) på 50 % skulle man alltså kunna bidra med 40 kW i primärreglingsmarknaden under en given timme. Inom primärregleringen bör effektutbytet med nätet även variera proportionellt mot frekvensavvikelsen vilket ännu inte implementerats i energilagret. Det finns dock inga tekniska hinder för att implementera en sådan styrning.

Kravet på en timmes uthållighet kan i framtiden komma att minskas till exempelvis 15 minuter, mycket beroende på de stora last- och produktionsavvikelser som i dagsläget uppkommer vid timskiftena men även för att kunna underlätta för andra typer av frekvensregleringsresurser än storskalig vattenkraft.

Den största fördelen hos ett energilager är dess potential att reagera på förändringar betydligt snabbare än konventionella produktionsenheter vilka är beroende av fysiska förändringar, t.ex. ett ändrat vattenflöde. Just snabbheten kan komma att bli betydligt än viktigare om några år då nätets inbyggda rotationströghet minskar då fler generatorer och laster ansluts via frekvensomriktare. Detta medför att en frånkoppling av produktion eller konsumtion kan komma att ge en snabbare och kraftigare frekvensförändring jämfört med en liknande händelse i dagens system. Här kan frekvensreglerande energilager komma att spela en viktig roll med en snabb reaktionsförmåga, som kan nå ner mot millisekunder, och beroende på dimensionering upprätthållas i minst 15 minuter. Som det visas i Figur 4 har energiläget i dagsläget inte möjlighet att nå ned emot en reglerhastighet på några millisekunder, men om en framtida anläggning dimensioneras enligt det kravet är det tekniskt möjligt.

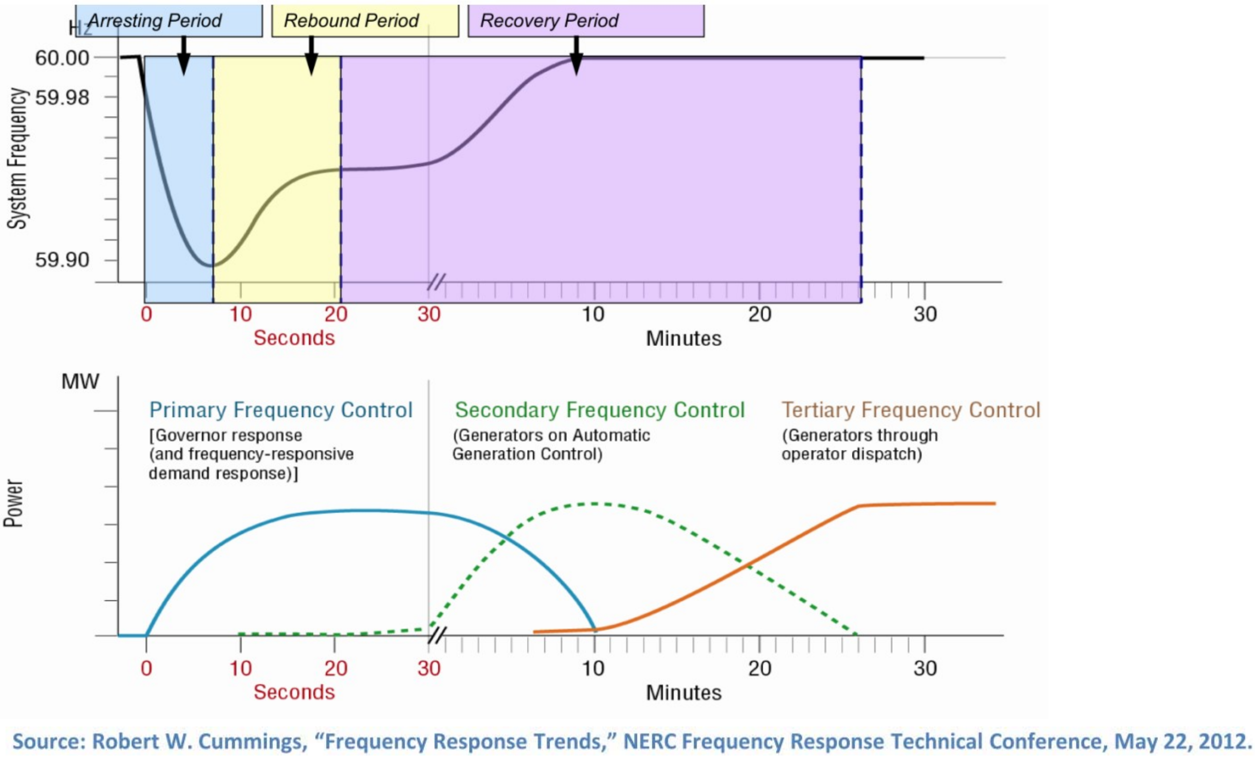

Figur 5. Frekvensregleringens olika delar.

4. Defektstatus

Totalt antal defekter = 0
Antal öppna defekter = 0
Defekter kvar att hantera (ej stängda) = 0

5. Risker, hot, problem

Testet har genomförts och godkänts enligt testspecifikationen [Ref 2] och inga risker kvarstår.

6. Rekommendationer

Testet har genomförts med godkänt resultat men det bör undersökas vad som kan göras för att få systemet att agera snabbare när frekvensen passerar satta gränsvärden och varför reaktionshastigheten hos energilagret verkar variera, se diskussion i 3.1.3. För att undersöka storleken på de olika fördröjningarna kan ett nytt test genomföras med separat mätning där bidraget från de olika komponenterna loggas (om det går att komma åt och mäta detta).

Ett sätt att öka reglerhastigheten är att ändra gränsvärdet för effektförändringar. Under testet användes standardinställningen för effektrampning på 10 kW/s, vilket är ganska långsamt, tidigare har tester på upp till ca 40 kW/s genomförts. För att öka hastigheten ytterligare måste sannolikt vissa parametrar för PI-regleringen i PQF:ens kontroll (t.ex. proportionalitet och dämpning) ändras för att inte få alltför mycket överslängar under regleringen. För att göra detta bör en dag avsättas för tester med support av ABBs enhet i Belgien som ansvarar för PQF-omriktaren.

Vid nya tester bör det göras så att både frekvensen och effekten som energilagret utbyter med nätet mäts i samma mätsystem för att underlätta analysen av resultatet och minimera felkällorna.

Vidare bör det undersökas varför ca var 5:e-sekundvärde från ABBs mätning i BMS/PQFI inte har loggats. Sannolikt orsakades detta av att ett för stort antal parametrar loggades i BMS/PQFI under testet, genom att minska antalet parametrar bör det gå att eliminera detta problem.

Möjliga tilläggstest, som kräver ett mer avancerat styrsystem men som ger en mer avancerad och automatisk styrning av energilagret, är till exempel:

- Kapacitetsförändring. Undersöka hur energilagrets tillgängliga kapacitet (SOC) förändras under tiden som energilagret deltar i frekvensregleringen. Detta är av stort intresse eftersom ett energilager som deltar på frekvensregleringsmarknaden är beroende av att alltid ha tillgängligt reglerkapacitet både uppåt och nedåt. Efter att ha deltagit på frekvensregleringsmarknaden ett eller flera dygn är det inte säkert att energilagret har kvar sin initiala laddnivå, dvs ca 50 %.
- Kapacitetsåterställning. Visa hur energilagrets tillgängliga kapacitet kan styras tillbaka till ca 50 % av maximal kapacitet vid behov, i syfte att kunna reagera till lika stor grad på uppreglering som nedreglering. Detta är en viktig funktion för att få till ett automatiskt styrsystem.
- Verifiera Droop-kontroll. Visa att energilagret utbyter aktiv effekt med nätet proportionellt mot en frekvensavvikelse.
- Spänningsstyrning. Visa att energilagret kan påverka spänningen i nätet, med hjälp av reaktiv effektreglering, samtidigt som energilagret frekvensreglerar.

Funktionstest: Testrapport, av Effektstyrning

Innehållsförteckning

1. Inledning

1.1 Omfattning

Funktionstesterna inom Elforskprojektet ”Test och utvärdering av energilager” är tänkta att genomföras i tre steg. I steg ett har grundläggande funktioner, såsom i- och urladdning, undersökts medan testerna i steg två fokuserar på automatisk styrning där olika händelser kan trigga i- och urladdningsförloppet. Detta kan jämföras med tidigare styrsystem där i- och urladdning kontrollerats enligt förinställda tidsscheman. Generell bakgrund till funktionstestet är [Ref 5].

Testerna i steg två är uppdelade i ytterligare tre steg där steg A, däribland frekvensreglering, utvärderar grundläggande applikationer som krävs för att gå vidare med mer tillämpade applikationer i steg B och kombinerade applikationer i steg C.

I detta steg, steg B, har Lagring av solel och Elmacken testats där energilagrets aktiva effekt styrs av ett effektflöde i nätet.

Testet genomfördes av FEAB, Metrum, ABB och Pöyry SwedPower enligt Testspecifikationen [Ref 2] med godkänt resultat 2014-06-25.

1.2 Dokumenthistorik:

Utgåva	Datum	Utfärdare	Kommentar
0.1	2014-07-03	Viktor Weidenmo	Första version, utkast
0.2	2014-08-29	Viktor Weidenmo	Andra version, utkast

1.3 Refererade dokument

Alla dokument som omnämns i sluttestrapporten:

[Ref 1] Systembeskrivning
[Ref 2] Testspecifikation_Effektstyrning_rev2_2014-07-03
[Ref 3] Testmiljöbeskrivning
[Ref 4] Projektbeskrivning Test och utvärdering av energilager 2013-10-14
[Ref 5] Metrum_Elmacken_2014-06-25_DataLogg
[Ref 6] Metrum_Solel_2014-06-25_DataLogg
[Ref 7] BMS_PQFI_201401625 elmacken
[Ref 8] BMS_PQFI_201401625 solpanel
[Ref 9] Funktionstest: Testrapport, av Effektstyrning

1.4 Förkortningar och begrepp

Nedan förklaras alla begrepp och förkortningar som används i dokumentet.

FEAB Falbyggden Energi AB
FT Funktions Testfall
PT Prestanda Testfall
ST Stabilitets Testfall
PL ProjektLedare
TL TestLedare
PLC Programmable Logic Controller
AC Alternating Current

DC	Direct Current
f	frekvens
PQFI	Apparat som kontrollerar energilagret
BMS	Battery Management System
SOC	State-of-charge
BESS	Battery Energy Storage System

2. Översikt

2.1 Utförda tester

2.1.1 FT nr 1, Lagring av solel

Visa att laddning av energilagret kan startas om ett uppmätt effektflöde går under ett visst värde.

Gränsvärde för start av laddning av energilagret sattes till 330 kW effektflöde genom nätstationstransformatorn vid Marknadsgatan i Metrums PQ-instrument. Laddning av energilagret skedde med konstant effekt så länge effektflödet genom nätstationstransformatorn var under gränsvärdet. Om effekten gick över gränsvärdet stoppades laddningen.

2.1.2 FT nr 2, Elmacken

Visa att energilagret kan stötta nätet med aktiv effekt om ett uppmätt effektflöde överskrider ett visst värde.

Gränsvärde för start av urladdning av energilagret sattes till 360 kW effektflöde genom nätstationstransformatorn vid Marknadsgatan i Metrums PQ-instrument. Urladdning av energilagret skedde med konstant effekt så länge effektflödet genom nätstationstransformatorn var över gränsvärdet. Om effektflödet gick under gränsvärdet stoppades urladdningen.

2.2 Defektstatus

Innan testet kunde genomföras åtgärdades ett antal defekter, se testprotokoll i [Ref 2]. Sedan kunde testet genomföras på ett godkänt sätt.

Det är ingen kritisk defekt men då ca var 5:e-ensekundsmätvärde från ABBs mätning i BMS/PQFI inte loggades försvårade det analysen av testresultatet.

3. Utförda tester

Testet har utförts och godkänts enligt Testspecifikationen [Ref 2] vilket även fungerat som testprotokoll.

3.1 FT nr 1, Lagring av solel

3.1.1 Mätdata från testet

Mätdata från testet finns sparade i [Ref 6] och [Ref 8].

3.1.2 Testresultat

I figurerna nedan visas testresulatet.

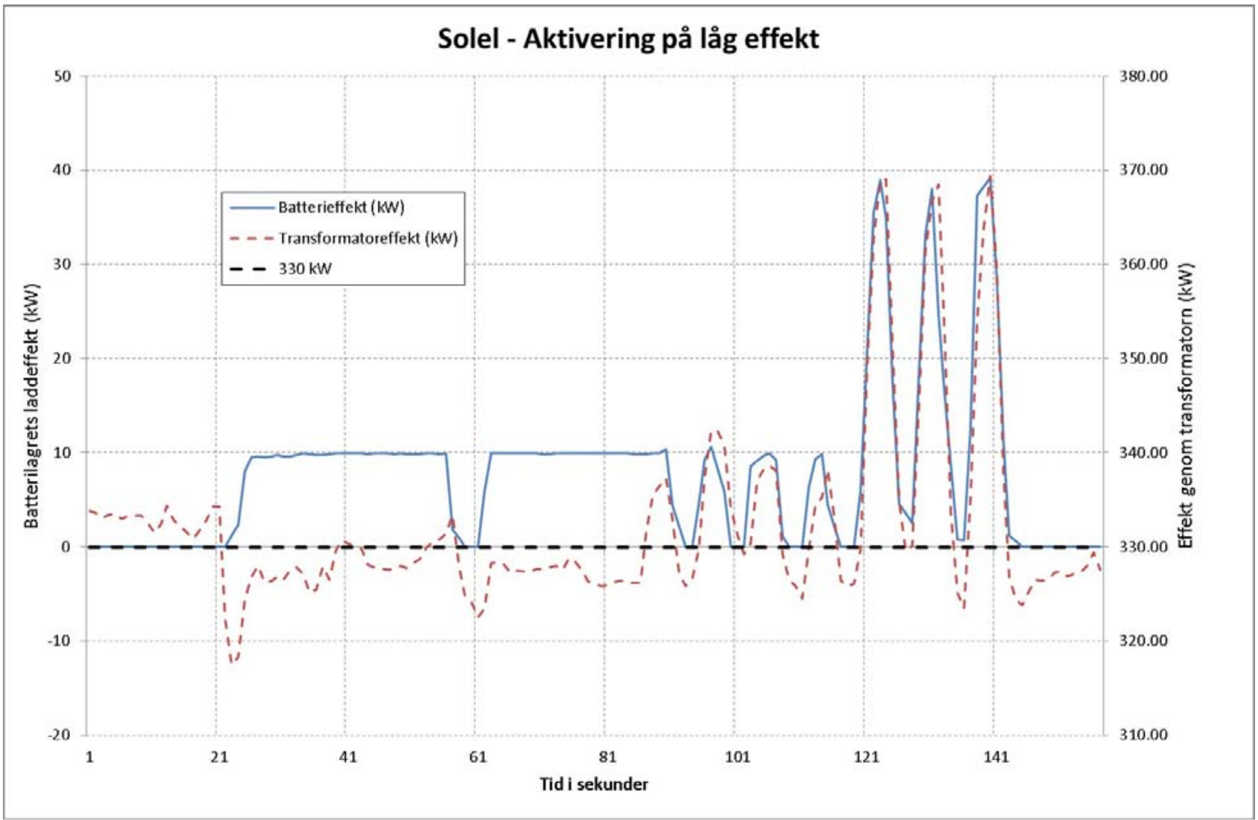

Figur 1. Lagring av Solel, energilagret börjar laddas om effekten genom nätstationstranformatorn understiger 330 kW. Energilagrets effektbörvärde är först 10 kW och sedan 40 kW.

3.1.3 Diskussion av testresultat

I figuren ovan visas det att:

- laddning av energilagret har aktiverats när den aktiva effekten genom transformatorn i Marknadsgatan går under det definierade gränsvärdet i Metrums PQ-instrument.

Testresultatet visar att energilagret skulle kunna användas för att lagra överskottsproduktion från solceller även om det krävs en viss vidarutveckling för att få ett automatiskt och säkert styrsystem. Denna adaptiva styrning ger ett ökat antal användningsområden och möjliggör fler affärsmodeller som kan bidra till att förstärka intäktströmmen hos ett energilager. Detta är ett steg mot ett smartare och mer flexibelt system där ett energilager i varje givet ögonblick avgör vilken tjänst som ska erbjudas utifrån status i elnätet, väderförhållanden och kundbehov. Kommunikation med kunder och aktörer skulle kunna ske via SMS vid meddelande om förändrade prioriteringar av energilagringstjänster.

Utifrån testerna kan det observeras att det finns en fördröjning på ett par sekunder innan energilagret börjar utbyta den efterfrågade effekten. Detta kan ses i Figur 1 ovan men är tydligare visat i Figur 3 i [Ref 9] där det framgår att fördröjningen från det att triggningshändelsen sker, dvs frekvensen överstiger gränsvärdet, till dess att energilagret börjar utbyta effekt är ca 2-3 sekunder och ytterligare ca 3-4 sekunder innan full effekt uppnås (i Figur 3 i [Ref 9] med ett effektbörvärde på 40 kW). Fördröjningen i omriktarens respons består sannolikt av tre eller flera delar, t.ex:

- Fördröjning i Metrums utrustning och script från det att t.ex. frekvensen går över eller under gränsvärdet tills order ges till PLC:ns digitala ingång
- Fördröjningen från ingången på PLC:n tills order ges till PQF-kontrollen att ge effekt
- Fördröjningen internt i PQF-kontrollen från det att den får order tills ordern börjar verkställas
- Hur snabbt önskad maxeffekt ut/från nätet erhålls beror på reglerparametrarna i PQG kontrollen, bl.a. en parameter ”_fRamping”, som anger hur snabbt effekten regleras. Under testet användes standardinställningen på 10 kW/s, vilket är ganska långsamt.

För att små energilager ska kunna assistera *Demand Respons* hos kunderna måste energilagren kunna reagera snabbt på en extern styrsignal, t.ex. ett effektflöde. I Figur 4 i [Ref 9] kan det ses att den uppmätta reglerhastigheten är ca 10 kW/s eftersom energilagret går ifrån att laddas med 40 kW till att laddas ur med 40 kW på ca 8-9 s. Eftersom styrningen skett via en frekvensförändring som registrerats hos Metrums utrustning, och därmed orsakat viss fördröjning, är det sannolikt en anledning till att det inte blev precis 10 kW/s. Just responstiden och reglertiden är viktigt att känna till och bör i detta fall förbättras om energilagret skall användas för aggregering och tex kunna assistera *Demand Respons* hos kunderna.

3.2 FT nr 2, Elmacken

3.2.1 Mätdata från testet

Mätdata från testet finns sparade i [Ref 5] och [Ref 7].

3.2.2 Testresultat

I figurerna nedan visas testresulatet.

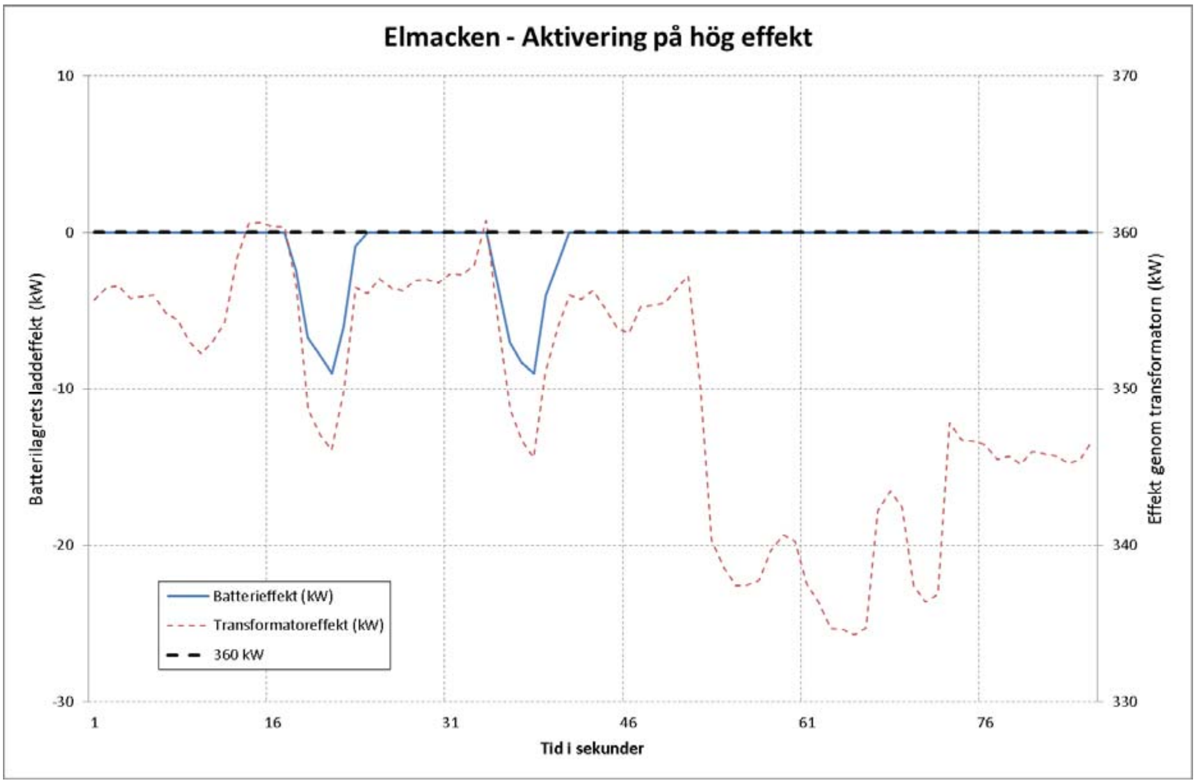

Figur 2. Elmacken, energilagret börjar laddas ur om effekten genom nätstationstranformatorn överstiger 360 kW. Energilagrets effektbörvärde är 10 kW

3.2.3 Diskussion av testresultat

I figuren ovan visas det att:

- urladdning av energilagret har aktiverats om den aktiva effekten genom transformatorn i Marknadsgatan överskrider det definierade gränsvärdet i Metrums PQ-instrument.

Testresultatet visar att energilagret kan användas för att stötta nätet vid höga effektuttag under kort tid, t.ex. vid laddning av elfordon även om det krävs en viss vidarutveckling för att få ett automatiskt och säkert styrsystem. Denna adaptiva styrning ger ett ökat antal användningsområden och möjliggör fler affärsmodeller som kan bidra till att förstärka intäktströmmen hos ett energilager. Detta är ett steg mot ett smartare och mer flexibelt system där ett energilager i varje givet ögonblick avgör vilken tjänst som ska erbjudas utifrån status i elnätet, väderförhållanden och kundbehov. Kommunikation med kunder och aktörer skulle kunna ske via SMS vid meddelande om förändrade prioriteringar av energilagringstjänster.

Utifrån testerna kan det observeras att det finns en fördröjning på ett par sekunder innan energilagret börjar utbyta den efterfrågade effekten. Se vidare diskussion i avsnitt 3.1.3 för detaljer.

4. Defektstatus

Totalt antal defekter = 0
Antal öppna defekter = 0
Defekter kvar att hantera (ej stängda) = 0

5. Risker, hot, problem

Testet har genomförts och godkänts enligt testspecifikationen [Ref 2] och inga risker kvarstår.

6. Rekommendationer

Testerna har genomförts med godkänt resultat men det bör undersökas vad som kan göras för att få systemet att agera snabbare när effekten passerar satta gränsvärden och varför reaktionshastigheten hos energilagret verkar variera, se diskussion i 3.1.3 och 3.2.3. För att undersöka hur stora de olika fördröjningarna kan ett nytt test genomföras med separat mätning där bidraget från de olika komponenterna loggas (om det går att komma åt och mäta detta).

Ett sätt att öka reglerhastigheten är att ändra gränsvärdet för effektförändringar. Under testet användes standardinställningen på 10 kW/s, vilket är ganska långsamt, tidigare har tester på upp till ca 40 kW/s genomförts. För att öka hastigheten ytterligare måste sannolikt vissa parametrar för PI-regleringen i PQF:ens kontroll (t.ex. proportionalitet och dämpning) ändras för att inte få alltför mycket överslängar under regleringen. För att göra detta bör en dag avsättas för tester med har support av ABBs enhet i Belgien som ansvarar för PQF-omriktaren.

Vid nya tester bör det göras så att både effekten som energilagret utbyter med nätet och effekten genom nätstationstransformatorn mäts i samma mätsystem för att underlätta analysen av resultatet och minimera felkällorna.

Vidare bör det undersökas varför ca var 5:e-sekundvärde från ABBs mätning i BMS/PQFI inte har loggats. Sannolikt orsakades detta av att ett för stort antal parametrar loggades i BMS/PQFI under testet, genom att minska antalet parametrar bör det gå att eliminera detta problem.

Möjliga tilläggstest, som kräver ett mer avancerat styrsystem men som ger en mer avancerad och automatisk styrning av energilagret, är till exempel:

- Visa att energilagret både kan laddas och utbyta reaktiv effekt för att motverka spänningsförändringar som uppkommer av överskottsproduktion av solel.
- Visa att energilagret både kan bidra med aktiv effekt och utbyta reaktiv effekt för att motverka spänningsförändringar som uppkommer vid höga effektuttag under kort tid.

Filnamn:	Bilaga 2 Testrapporter.docx
Katalog:	G:\Gemensam\Rapporter\Elforsks_rapporter\2014_original\14_58
Mall:	H:_MSOfficeMallar\Normal.dotm
Rubrik:	
Ämne:	
Författare:	Pia
Nyckelord:	
Kommentarer:	
Datum:	2014-10-23 15:11:00
Version:	3
Senast sparad:	2014-11-19 11:47:00
Senast sparad av:	KMO
Total redigeringstid:	2 minuter
Senast utskrivet:	2014-11-19 11:50:00
Vid senaste fullständiga utskrift	
Antal sidor:	223
Antal ord:	38 391 (cirka)
Antal tecken:	203 477 (cirka)